Studies in the Application of Group Theory

A THESIS
SUBMITTED FOR THE DEGREE
OF
DOCTOR OF PHILOSOPHY IN PHYSICS
IN THE
UNIVERSITY OF CANTERBURY
by

Luke Francis M^{c}Aven

University of Canterbury
April 1998

ABSTRACT

This thesis presents several developments in the mathematical tool of symmetry, group theory. In addition to studies calculating transformation coefficients in the Racah–Wigner calculus, we present several applications of such coefficients to physical systems.

We investigate the calculation of transformations between particular symmetric group bases. We discuss symmetric group bases adapted to subgroup factors of the form $S_a \times S_b$. We call these particular bases split bases.

A special case of transforming from standard to split bases is considered. We generalise that result and describe a simple method for relating permuted bases. We present the block–selective conjecture for calculating transformations between general standard and split bases.

We intensively examine a particular neglected multiplicity case, as part of obtaining algebraic solutions for transformations from the standard basis to the split basis adapted to $S_{n-3} \times S_3$. We prove that the Littlewood–Richardson rule does not fix the choice of multiplicity separation.

We use continuous groups to study the double delta function model of correlation crystal fields. We obtain an explicit expression for the transformation coefficients which relate terms in the model to physical operators. This allows us to improve the understanding of why only some terms contribute in this model.

In the last major study, we use point groups to study magneto–optical effects (Kerr rotation) in chromium trihalides. We discuss how the Racah–Wigner algebra is used by the computer programme RACAH to calculate spin–orbit coupling coefficients. Those coefficients are then used in the analysis of the reflectance spectra of chromium trihalides. We provide support for the recently proposed reassignment of the transitions contributing to the Kerr rotation of chromium tribromide.

Several minor investigations complement the major studies. Possible lines of further investigation are discussed where appropriate.

Acknowledgements

I thank my supervisors, Assoc.Prof. Phil Butler and Dr. Mike Reid, for the support and assistance they have provided. I also appreciate the assistance of Dr. Hughan Ross, both in the early stages of my study and in the specific collaboration on some research. Dr. Angèle Hamel has been very helpful in collaborating on the symmetric group papers. I also thank Professors Shinagawa and Sato for their involvement in the chromium tribromide projects. Others, such as Dr. Barry Searle and Jonathon Whittle, are thanked for their input into ideas represented in the third appendix.

Thanks go to Janet, for supporting me and for helping with the editing. Finally, I would like to thank the rest of my family: Mum, Dad, Paul and Kim, for their support throughout both my doctoral and earlier study.

CONTENTS

LIST OF FIGURES

LIST OF TABLES

1. INTRODUCTION

Symmetry is immunity to a possible change [1]

The underlying aim of this thesis is to improve the use and understanding of group theory in applications, particularly applications in condensed matter or solid state physics. We have worked along two lines towards this aim:

- ◇ Making specific calculations requiring the use of group theory.
- ◇ Improving calculation of the group theoretical coupling and recoupling coefficients necessary for many applications.

There are three main parts to this thesis, but those may be further divided into a number of specific studies. We will list those studies before outlining the content of this thesis in more detail.

- We calculate transformation coefficients which relate permuted symmetric group bases.
- We describe a technique, which we call the block selective conjecture, for directly calculating split–standard symmetric group transformation coefficients from representation matrices in the standard basis.
- We present algebraic expressions for the coefficients which relate the standard S_n–basis, to the split S_n–$S_{n-3,3}$–basis.
- We discuss the choice of multiplicity separation in the previous expressions. We present criteria for choosing the separation.
- We give some selection rules for the product of basis functions (or Young tableaux), derived through the calculation of algebraic solutions.
- We use continuous groups to improve the understanding of why only some terms contribute in the double delta function model of correlation crystal fields.
- We present an analysis of the calculation of $CrBr_3$ spin–orbit coupling coefficients performed by the computer program RACAH.

[1] *Rosen (1995, p.2)*

- We carry out two independent studies to study the energy structure, and specifically the Kerr rotation, of chromium trihalide systems.
  - We use an USCF–X α–SW alpha method to calculate the electronic states, and make assignments to charge transfer transitions.
  - We use an LCAO method to calculate the energy structure, and combine this with a Gaussian fit of transitions to the reflectance data.

Because of the diverse range of those problems, it is necessary to provide separate background sections for each. However, some background material is relevant throughout and we use chapter 2 to introduce this material. Sections 2.1, 2.2, 2.3 and 2.4 contain brief discussions of group theory, vector spaces, group representation theory, and applications of group theory in physics. The latter includes an introduction to the Racah–Wigner calculus (also known as the Racah–Wigner algebra).

Chapters 3, 4 and 5 address the calculation of symmetric group transformation coefficients.

We begin, in sections 3.1 and 3.2, by providing background on the symmetric group and its representation theory. Particular emphasis is placed on details such as the identification and ordering of basis vectors in various bases. We introduce the split basis for an irrep of S_n. This is one adapted to both S_n and to a product subgroup $S_a \times S_b$, where $a + b = n$ and where we chose the standard (Young–Yamanouchi) basis for each of S_a and S_b. The transformation coefficients for S_n are introduced in section 3.3, including the split–standard coefficients upon which we concentrate. This section includes a review of techniques previously used to calculate the split–standard transformation coefficients. We discuss a general technique for transforming between bases, which has not been used in the context of split–standard basis transformations.

Section 3.4 contains a reproduction of our first published paper (Hamel et al. 1996). Initial stages of this investigation were largely carried out by Hamel and Butler, with Ross and myself providing significant input in the latter stages. In this work, we discuss a case of split–standard transformation coefficients. One can consider the standard basis to have basis functions adapted to a chain of subgroups, described at each level by a diagram obtained by removal of the highest labelled box in the diagram at the level above. The matrix elements of the adjacent permutations are particularly simple in this standard basis. It became apparent during our investigations that the matrix elements in another basis were also very simple. In this *dual* basis, the chain is obtained by removal of the lowest labelled box in each diagram. We were able to describe the transformation between the dual and standard bases. Since publishing this work, we have gained a fuller appreciation of the result. In particular, we describe in section 3.5 a generalisation which makes the result more lucid. Bases adapted to group chains differing in only one box, but any one box, from level to level, are made readily accessible

by transformation through this generalisation. We demonstrate that those transformations are trivial split–standard transformation coefficients.

Before turning our hand to the calculation of split–standard transformation coefficients, we find it useful to examine more fully the results of section 3.5. Section 4.1 naturally extends those results to the reordering of split bases. Thus, we consider the transformation from the S_n–$S_{a,b}$–basis to the S_n–$S_{b,a}$–basis. Rather than just considering the rearrangement of one box at a time, we are able to consider any number of boxes being moved around. The transformation matrix is shown to be a (permuted) representation matrix of a cycle permutation in a split basis.

Compared to the aim of obtaining the split–standard transformation coefficients, those rearrangement results may seem to be of limited use. However, they serve well the purpose of motivating our conjecture, which we introduce in section 4.2, for calculating split–standard transformation coefficients. The block selective conjecture also uses representations of cycle permutations, but in the standard basis, as a basic structure for the transformation matrix. The block selective name comes from the application to the representation matrix of a block binary matrix, to obtain the final result.

Although unproven, we have used our description to calculate split–standard transformation coefficients for all cases up to and including S_6. It fails in one case, the multiplicity case occurring in the decomposition of the irrep [3 2 1] to $[2\ 1] \times [2\ 1]$. We illustrate our technique with an example. We have gained some appreciation of why the block selective conjecture works and we can also understand some implications. The block selective conjecture needs more work before we submit it for publication.

The case for which the block selective conjecture fails is of particular interest, since it involves the first occurrence of multiplicity in split–standard transformation coefficients. Two previous calculations of this matrix (Chen, Collinson & Gao 1983, Pan & Chen 1993) gave different separations, therefore the problem clearly needed further investigation. Chapter 5 addresses the problem of multiplicity separation in split–standard transformation coefficients. Section 5.1 introduces product multiplicities and the Littlewood–Richardson rule.

In order to analyse the particular case above, [3 2 1] to $[2\ 1] \times [2\ 1]$, it is useful to consider it to be a special case of the transformation between the standard basis and the S_n–$S_{n-3,3}$–basis. In section 5.2, we reproduce the body of a paper, recently submitted for publication, on this general problem. We have derived algebraic expressions for those transformation coefficients, including in particular the general solution for the multiplicity case, before any choice of separation is made. We prove that the Littlewood–Richardson rule does not fix the choice of multiplicity separation. We then proceed to discuss the choice of separation and give criteria for simplicity of the solutions obtained.

Following the paper, we emphasise a feature of the transformation coefficients hitherto not considered in detail. In section 5.3, we present some selection rules

for the product of an arbitrary irrep with the basis vectors of the irrep [2 1]. Those results are independent of the Littlewood–Richardson rule, but are tied in with *jeu de taquin*, which is itself linked to the constructive steps of the Littlewood–Richardson rule.

Our discussion of symmetric groups is rounded off in section 5.4, with a discussion of more difficult multiplicity problems. We consider a general multiplicity two case arising in the transformation between the standard basis and the S_n–$S_{n-4,4}$–basis.

In chapter 6, we use group theory to study models of crystal correlation fields, in particular, the double–delta function model proposed by Judd. Correlation crystal fields improve the detailed description of features in the spectra of crystals, particularly those crystals containing lanthanide ions. We examine the transformation properties of Judd's model, known to improve spectroscopic fits for some lanthanide systems. Our analysis hinges upon calculating the coefficients which transform between two sets of two–body operators. Although the transformation coefficients have previously been calculated, we obtain explicit expressions which allow us to better understand the vanishing of some of terms in the model coefficients. We discuss the use of crystal correlation fields in section 6.1 and introduce the continuous groups in section 6.2. We describe some aspects of this research in section 6.3. The published results of our investigation (McAven, Reid & Butler 1996) are reproduced in appendix A.

Chapters 7 and 8 relate to the investigation of Kerr rotation in chromium trihalide systems.

The Racah–Wigner calculus is a sophisticated mathematical formalism, extremely useful for calculating the matrix elements required in chemistry and physics, particularly in spectroscopy. However, this calculus is not familiar to experimentalists and although extremely useful, calculations involving it are often unwieldy. The computer package, RACAH, which we introduce in section 7.1, is designed to simplify and unify the application of the Racah–Wigner calculus. We discuss the package, developed and developing, under the supervision of Assoc. Prof. P. H. Butler. We demonstrate the usefulness of RACAH by applying it to the calculation of spin–orbit coupling coefficients for chromium tribromide. This project was initiated by Dr. Ross, at the request of Prof. Shinagawa. Dr. Ross was responsible for much of this aspect of the RACAH development which made the calculations possible. I made significant contributions to the published research work in the middle to later stages. We reproduce the paper (Ross et al. 1996) in appendix B. It is significant to note that we take about five pages to outline the calculations which RACAH performs and which one would repeat if doing the calculation by hand. This does not even begin to include the tedium required to manually calculate all the $6j$, $3jm$ and $2j$ appearing in the final result. The input and output of RACAH on the other hand, can be presented in a page.

Prof. Shinagawa required those coupling coefficients for an investigation of Kerr rotation in chromium tribromide, and more generally, the electronic struc-

ture of chromium trihalides. I collaborated with Shinagawa, Sato, Ross and Butler in extending the earlier analysis of Shinagawa et al. (1995). Before describing those, we give some background information, useful in understanding the physical concepts involved with the Kerr rotation and electronic structure of the chromium trihalides. In section 7.2 we introduce point groups. Section 7.3 presents characteristics of the chromium trihalide systems, and a brief description of the Kerr rotation.

The first project using the coefficients was carried out mostly by Shinagawa and Sato and extends directly the earlier work of Shinagawa et al. (1995). Chromium trichloride and chromium triiodide systems are considered, in addition to the chromium tribromide of Shinagawa et al. (1995). The spin–orbit coupling coefficients, calculated in the project in appendix B, are used to study charge transfer transitions responsible for Kerr rotation in those systems. My contribution is mainly to the structure of the published paper (Shinagawa et al. 1996). The research is outlined in section 7.4 and the abstract of this paper is reproduced in appendix C.

The remaining part of chapter 7 is dedicated to an analysis of the chromium trihalide systems, independent of both Shinagawa et al. (1995) and Shinagawa et al. (1996). This project is mostly my work, with valuable contributions from Dr Ross throughout the early to middle stages. We have reproduced the paper, to be submitted, in chapter 8. But first, it is necessary to discuss the work undertaken in obtaining the results. In section 7.5, we profile the C program TB, which we have written to calculate energy levels for cluster systems. We proceed in section 7.6 with a discussion of how reflectance data for the chromium trihalides is analysed. We relate the various coefficients of interest and give the procedure for obtaining the elements of the dielectric constants from the reflectance data. The imaginary part of the dielectric constant can be fitted with Gaussians. We discuss some details of the process by which this is done in section 7.6.2.

We summarise the results of our research in chapter 9.

Appendices A, B and C have previously been discussed, and contain our publications on the delta function and chromium tribromide studies.

In order to analyse the split–standard transformation coefficients, we have developed a series of MATLAB scripts. We give a list of some of those scripts in appendix D.

Appendix E contains other projects I have been involved with, or am proposing as possible research topics. For example, section E.1 contains a brief review of an honours project undertaken by Jonathon Whittle and supervised by Dr. Reid and myself. We investigated bipolar expansions of delta functions and functions of the form $r_{12}^{(-j-1)}C_m^{(j)}$, in particular the case of the latter where $j = 0$.

2. BACKGROUND

This chapter gives some relevant background to the study of group theory in physics.

2.1 Group theory

Many texts are available on group theory and the applications of group theory in physics (Hamermesh 1962, Wybourne 1974, Elliott & Dawber 1979*b*, Elliott & Dawber 1979*a*, Cornwell 1984, Sternberg 1994, Mirman 1995*b*, Stancu 1996). We draw on those texts for the results presented in the next sections. In this section, we introduce some basic concepts and terms used in group theory.

Group theory is the mathematical language used to exploit symmetries. Formally, we can define a group in the following way:

> Consider a set A of objects and a binary operation on that set. The binary operation, often called the group product, describes a map $A \times A \rightarrow A$. If the set and operation satisfy certain structural constraints:
> - Associativity $(a_1 a_2)a_3 = a_1(a_2 a_3) \;\; \forall\, a_i \in A$
> - Identity existence $\exists e \;:\; ea = ae = a \;\; \forall\, a \in A$
> - Inverse existence $\forall a \in A \;\; \exists b \in A \;:\; ab = ba = e$,
>
> the set and operation form a group, G. The identity element is denoted here by e and the inverse of an element a will generally be denoted by a^{-1}.

For example, the set of numbers $\{1, -1, i, -i\}$ and ordinary multiplication form a group. We call the set and the group L. We express the product structure of a group as a group multiplication table (sometimes called a Cayley table). For $a, b \in L$, we have the multiplication table:

$L_a \backslash L_b$	1	-1	i	$-i$
1	1	-1	i	$-i$
-1	-1	1	$-i$	i
i	i	$-i$	-1	1
$-i$	$-i$	i	1	-1

(2.1)

A *subset* B of a set A is a set of elements, all of which are in A. The term *proper subset* is applied to all subsets of A, with the exception of A itself and the

subset containing the identity element only. If B is a proper subset of A, we write $B \subset A$, or $A \supset B$. For example, $\{1, i\} \subset L$. The set of objects in a group always contains subsets (including the set itself). If such a subset is closed under the binary operation which closes the set, then the subset and binary operation form a *subgroup* of the group. Thus the subset $\{1, i\}$ with ordinary multiplication is not a subgroup of L, but we see from (2.1) that $\{1, -1\}$ with ordinary multiplication is a subgroup L_1 of L. We use the term *proper subgroup* when the subset is a proper subset, as is $\{1, -1\} \supset L$.

The relationship between some groups and subgroups is particularly interesting. Consider a group G with two subgroups H and K. If $hk = kh$ for all $h \in H$ and $k \in K$, and every $g \in G$ can be written as a unique product hk, then G is a direct product of H and K. We write $G = H \times K$, and call G a direct product group.

If there are a finite number of elements in a group, the group is said to be finite (see section 7.2). The number of elements in a group is called the *order* of the group. A theorem bearing the name of Lagrange relates the order of groups and subgroups. (Although Euler and others gave this result prior to Lagrange (1771).) Since group theory was not developed by that stage, see section 3.1, the formulation of Lagrange was in a different context, but the result is nevertheless equivalent to the modern result found in most introductory group theory texts (Elliott & Dawber 1979*b*, Stancu 1996).

> *Lagrange's theorem*: the order of a subgroup divides into the order of a group.

We see that for our example above, $4/2 = 2$. There are two types of groups with an infinite order. The first has discrete or countable elements, for example the integers under addition. Because the elements are countable, the group elements can be parameterised by a single discrete parameter (each element in such a group can be labelled with an integer). Groups in the second infinite order type are called *continuous* groups (see section 6.2). Rather than varying discretely from element to element, the change is continuous, so the elements are not countable. These groups can be parameterised by a set of continuously varying parameters, for example, angles of rotation.

A significant feature of the group table of L, equation (2.1), is that the product a and b is equal to the product of b and a (so the table is symmetric about the main diagonal). Products and objects which satisfy this property are said to be *commutative* and groups with this property are called *Abelian* groups.

A less obvious feature of the group table for L is that every element can be expressed as a power of i ($i^0 = 1, i^1 = i, i^2 = -1, i^3 = -i$). We call i the generator of L. A group in which every element can be expressed as a power of one object is called a cyclic group (see section 7.2). Every cyclic group is abelian.

In general, not every element in a group can be expressed as the power of a single element, rather every element can be expressed as a product of generators.

For example (see section 3.1), the symmetric or permutation group has $n-1$ adjacent transposition generators. But the number of generators is not unique, since for example the $(1,2)$ interchange and the n–cycle also generate S_n.

The definition of a group is abstract, the nature of the elements and of the product in a group being immaterial. One may therefore have the same, but perhaps rearranged multiplication table for two groups, but different elements and a different product on the elements. This relationship (mapping) between the elements of the two groups is known as an *isomorphism*. We say two groups, G and H, are *isomorphic* if a one–to–one correspondence, $(g_i \in G) \leftrightarrow (h_i \in H)$ can be set up in such a way, that if $g_a g_b = g_c$, then $h_a h_b = h_c$. This equivalence relation is denoted $G \sim H$.

Consider the group R of rotations by $\pi/2$ in a plane, with the group product being the addition of the angles of rotation in the plane. The product of the group elements, $\{R(0), R(\pi/2), R(\pi), R(3\pi/2)\}$, is given in the multiplication table:

$R_a \backslash R_b$	$R(0)$	$R(\pi/2)$	$R(\pi)$	$R(3\pi/2)$
$R(0)$	$R(0)$	$R(\pi/2)$	$R(\pi)$	$R(3\pi/2)$
$R(\pi/2)$	$R(\pi/2)$	$R(\pi)$	$R(3\pi/2)$	$R(0)$
$R(\pi)$	$R(\pi)$	$R(3\pi/2)$	$R(0)$	$R(\pi/2)$
$R(3\pi/2)$	$R(3\pi/2)$	$R(0)$	$R(\pi/2)$	$R(\pi)$

(2.2)

It is easy to see that R is isomorphic to L, with the correspondence being $R(0) \leftrightarrow 1, R(\pi/2) \leftrightarrow i, R(\pi) \leftrightarrow -1, R(3\pi/2) \leftrightarrow -i$. In R, the rotation by $\pi/2$ is a generator.

One must always be careful however, to remember that although isomorphic groups describe the same abstract symmetry, the physics of the situations will generally be different and the groups should not be considered the same. Physicists and mathematicians would tend to use the word group differently at this level of abstraction. Physicists consider the abstract group and its action to be the group, whereas mathematicians need only the abstract group. We give some examples of particular clarity in the context of point groups (see section 7.2).

If one does not insist upon the one–to–one correspondence in an isomorphism, then we have a *homomorphism*, or *homomorphic* mapping. A group G is homomorphic to H if: to any $g_i \in G$ there corresponds an $h_i \in H$, and to each $h_i \in H$ at least one g_i, such that for $g_1 g_2 = g_i$, one has $h_1 h_2 = h_i$ (Stancu 1996, p.19). If G is homomorphic to H, we write $G \rightarrow H$. Homomorphic is not an equivalence relation, since $G \rightarrow H$ does not imply $H \rightarrow G$, that is the symmetry condition is not satisfied. Isomorphism is obviously a special case of homomorphism. In a homomorphism, the product structure of the group is retained, but several elements may be "lumped" together. When the mapping is not one–to–one, the homomorphic image is therefore smaller than the mapped group. Perhaps the best known example of a homomorphism is $SU_2 \rightarrow SO_3$ (see section 6.2). Rotations by 2π in SU_2 change signs (so space is double covered), whereas in SO_3, the rotation

by 2π is equivalent to the identity. The homomorphism $SU_2 \rightarrow SO_3$ reduces the double covering to a single covering.

A simple example of a homomorphism is $L \rightarrow L_1$. Consider the mapping (or morphism) of the elements in the group, L into the elements of the group, L_1: $1 \rightarrow 1, -1 \rightarrow 1, i \rightarrow -1, -i \rightarrow -i$.

The groups L and R have only four elements each and as such are easy to examine. They are some of the simplest groups however and in general, groups are much larger. Rather than describe the structure of groups element by element, it is usually much easier to consider collecting elements with similar properties together. One particularly useful type of collection is that of *conjugacy classes*.

Two elements, g_a and g_b of a group G, are *conjugate* (or similar) if there exists another element, g_i of G, such that,

$$g_a = g_i g_b g_i^{-1} . \tag{2.3}$$

If g_a and g_b are both conjugate to g_c, then they are also conjugate to each other. Elements that are conjugate to each other are put in the same conjugacy class, often simply called a class. Furthermore, since clearly no element belongs to more than one class, a group can be divided into distinct classes.

Another way of partitioning groups makes use of subgroups. If $H \subset G$ and $g \in G$, then we form a set of elements, gH, by multiplying g with each element of H. The set, gH is called a *left coset* of H. Every element of G belongs to either H, or to a coset of H. Similarly, one defines *right cosets* of H by the product Hg. We do not specifically make use of cosets in this thesis, but they are useful in defining the double cosets in section E.4.

Having introduced some group theoretical concepts, we can move towards the application of group theory to physics. We introduce group representation theory in section 2.3, but firstly discuss vector spaces.

2.2 Linear vector spaces

A symmetry is an invariance under a possible change or under a transformation. Group theory is a mathematical tool for studying symmetry abstractly. Group theory does not describe the objects or transformations themselves. The theory of vector spaces provides structure for studying the objects and transformations.

We are interested in linear vector spaces and in this section, give some key aspects relevant for our description of group representation theory.

We begin with a set of objects, $S = \{\mathbf{r}_1, \mathbf{r}_2 \ldots\}$. Consider a closed, commutative and associative addition defined on this set, such that a unique inverse exists for each element of the set and furthermore, the set contains an identity under this addition. Then construct a closed multiplication on this set, which satisfies for arbitrary complex numbers c and d,

$$(cd)\mathbf{r}_i = c(d\mathbf{r}_i) ,$$

$$(c+d)\mathbf{r}_i = c\mathbf{r}_i + d\mathbf{r}_i \ , \tag{2.4}$$
$$c(\mathbf{r}_i + \mathbf{r}_j) = c\mathbf{r}_i + c\mathbf{r}_j \ .$$

The set S, with the associated addition and multiplication, is then a linear vector space V. (If one insists that c and d are real, then one has a real linear vector space.)

A set of p vectors, $\mathbf{r}_i$ is said to be *linearly independent* if no member can be expressed in terms of the other members. Thus for a linearly independent set, the only solution to the equation,

$$\sum_{i=1}^{p} c_i \mathbf{r}_i = 0 \tag{2.5}$$

is $c_i = 0, \forall i$. The dimension, dim(V), $|V|$ or d_v of a vector space, is the greatest number of linearly independent vectors. Any set of d_g linearly independent vectors forms a basis for the vector space. Each element in a basis set is called a basis vector of that set. Every vector in the vector space can be generated from the basis vectors using addition and multiplication by numbers. We therefore say that the basis vectors *span* the space.

Since the choice of basis is not unique, one may make different choices for different uses of the same space. But then it is useful to know how to transform from one basis of a vector space to another basis of the same vector space. The transformation coefficients, which express the basis vectors of one basis in terms of another, will be discussed further later (see section 2.4), but let us look now at how a general vector is transformed into another general vector.

The *operator* T that carries the vector $\mathbf{r}$ to the vector $\mathbf{r}'$, can be defined by $T\mathbf{r} = \mathbf{r}'$. We are particularly interested in linear operators, which satisfy,

$$T(\mathbf{r}_1 + \mathbf{r}_2) = T\mathbf{r}_1 + T\mathbf{r}_2, \tag{2.6}$$
$$Tc\mathbf{r}_1 = cT\mathbf{r}_1 \ . \tag{2.7}$$

If $T\mathbf{r} = \mathbf{r}'$, $T\tilde{\mathbf{r}} = \tilde{\mathbf{r}}'$ and $S\mathbf{r} = \tilde{\mathbf{r}}$, then the operator transforming from $\mathbf{r}'$ to $\tilde{\mathbf{r}}'$ is,

$$S' = TST^{-1} \ . \tag{2.8}$$

We also want to consider transformations induced on functions ψ of the coordinate system, by the transformations of the coordinates themselves. Specifically, consider G to be a group of transformations of the coordinates $\mathbf{r}$. The induced transformation for $g \in G$ is denoted $T(g)$, and defined by

$$\psi'(\mathbf{r}) = T(g)\psi(\mathbf{r}) = \psi(g^{-1}\mathbf{r}) \ . \tag{2.9}$$

Thus a transformation in the vector space of the coordinates includes a transformation in the function space. The use of g^{-1} ensures that the ordering of operations is preserved in the induction of transformations between vector and function spaces.

An important concept from the theory of vector spaces is that of an *invariant subspace*. A subspace W of a space V is spanned by a subset of basis vectors of V. Thus if V is spanned by the set of basis vectors $\{\mathrm{v}_1, \mathrm{v}_2, \mathrm{v}_3\}$, then one subspace would be spanned by $\{\mathrm{v}_1, \mathrm{v}_3\}$, and another by $\{\mathrm{v}_2, \mathrm{v}_3\}$. A subspace is invariant with respect to an operator T, if for every vector w in the subspace W of V,

$$T\mathrm{w} = \mathrm{w}', \tag{2.10}$$

where $\mathrm{w}' \in W$.

Before moving on to group representation theory, let us introduce a type of vector space, used extensively in physics. A *ket space* is a vector space, the basis vectors or kets are written as $|i\rangle$. A ket space has an inner product defined on a pair of kets, $|i\rangle, |j\rangle$, so that the result $\langle i|j\rangle$ is always a complex number. Furthermore, the inner product of a ket with itself $\langle i|i\rangle$ is a positive definite real number. One often uses ket space to describe the eigenspaces of physical systems. Thus the eigenvectors of a Hamilton H are represented by eigenkets in the equation,

$$H|i\rangle = E_i|i\rangle \ . \tag{2.11}$$

One often sets up bases for ket spaces satisfying,

$$\langle i|j\rangle = \delta_{i,j} \ . \tag{2.12}$$

Such a basis is said to be orthonormal. We will use this notation in section 2.4.

2.3 Group representation theory

Although symmetries inherent in crystal structures influenced the development of group theory (see section 7.2), the essential role of group theory in physics only began to become clear during the 1920s and 1930s, as quantum mechanics developed. As we noted in the previous sections, the mathematicians definition of groups is abstract. The major breakthrough was to link physics and group theory using group representation theory, which serves to lift the abstraction. Classic texts by Weyl (1928,1946) and Wigner (1959), two figures central to the developments taking place, record the early infusion of group theory into physics. We shall return to the applications of group theory in section 2.4, but continue here with a description of the representation theory of groups.

Groups are mathematically abstract in the sense that the nature of the elements and of the product is immaterial. Many groups have abstract structures, if not physically, then mathematically. As such, they may be difficult to work with. It is therefore often useful to map the group structure into a well understood domain. When that domain is a vector space, we call the mapped–to structure in the vector space a representation of the group. Thus the abstract group theory describing the relations between objects, is united with a vector space describing the nature of the objects and transformations.

Formally, consider a group R of linear operators defined in a finite dimensional linear vector space V. This means that each $r \in R$ is an object in V. R is called a (linear) representation of an arbitrary group G on V if G is homomorphic to R on V. The homomorphic relation means, for example, that representations of SO_3 are also representations of SU_2. The vector space V is called the *representation space.*

Alternately one can consider the group of nonsingular linear transformations of a vector space V, sometimes denoted $GL(V)$, where GL stands for General Linear group. A representation of a group G on the vector space V is a homomorphism from G to $GL(V)$. Quantum mechanics is concerned with Hilbert spaces, and expresses symmetries using unitary or anti–unitary operators. We will not refer to this again, but the representations we are interested in are unitary representations in a Hilbert space.

We can consider each element of G to act as a linear transformation within the vector space,

$$R(g) : V \rightarrow V \;\; \forall \, g \in G \, , \tag{2.13}$$

where this action clearly ties the structure of R on V, to G. A representation specifies the group G, the vector space V and the action implicit in R. Incidentally, if $R \sim G$, then the representation is called *faithful.*

We are particularly interested in matrix representations, where the elements in the representation group R are matrices on the vector space V. The group product is simply matrix multiplication.

Let us return to the isomorphic groups L and R, introduced in section 2.1, to give an example of a matrix representation. We can specify the group R to rotate objects in the plane of a three dimensional space with orthogonal basis vectors x, y and z. Let us say the rotation is in the x–y plane. The action of $R(0)$ on those basis vectors gives the basis vectors themselves, so the matrix representation of $R(0)$ is,

$$M(R(0)) = \begin{pmatrix} 1 & 0 & 0 \\ 0 & 1 & 0 \\ 0 & 0 & 1 \end{pmatrix} \, . \tag{2.14}$$

Since the basis vectors x and y are orthogonal, the action of $R(\pi/2)$ is to rotate each into the other, with a change of sign in one. Handedness is used to determine which changes sign. Assuming a right handed system, the matrix representation of $(\pi/2)$ is,

$$M(R(\pi/2)) = \begin{pmatrix} 0 & -1 & 0 \\ 1 & 0 & 0 \\ 0 & 0 & 1 \end{pmatrix} \, . \tag{2.15}$$

Since $R(\pi/2)$ generates the group R, we easily find that in this representation,

$$M(R(\pi)) = \begin{pmatrix} -1 & 0 & 0 \\ 0 & -1 & 0 \\ 0 & 0 & 1 \end{pmatrix} \tag{2.16}$$

and

$$M(R(3\pi/2)) = \begin{pmatrix} 0 & 1 & 0 \\ -1 & 0 & 0 \\ 0 & 0 & 1 \end{pmatrix} . \tag{2.17}$$

In section 2.2, we discussed invariant subspaces. If a subspace W, of the representation vector space V, is invariant with respect to all operators of the group, we say that the representation V is reducible. A representation for which no such invariant subspaces exist is said to be an *irreducible representation*, usually shortened to *irrep*. The dimension of an irrep λ is denoted $|\lambda|$ and is equal to the dimension of the irrep space in which the irrep exists. The basis vectors of the irrep space are sometimes called the *partners* of the irrep. Only in Abelian groups is every irrep of dimension one. We sometimes write $\lambda(G)$ to indicate that λ is an irrep of the group G.

Any representation can be decomposed into irreps. Schur's Lemmas (Butler 1981, p.15) show that this decomposition is essentially unique. This decomposition is particularly useful since, while there are an infinite number of representations, there are finite numbers of *inequivalent* irreps for finite groups. Furthermore, the number of inequivalent irreps of a group is equal to the number of equivalence classes of the elements of a group. Representations T and T' are equivalent if all the operators of the representation are related by a mapping between the spaces the representations lie in. That is, for each $g \in G$,

$$T'(g) = AT(g)A^{-1} , \tag{2.18}$$

where A is a mapping from the space of T to the space of T'. Equivalent irreps will generally be denoted by lower case Greek letters in this thesis.

In decomposing representations into irreps, several copies of the same irrep may arise. This is particularly significant in the *direct product* of representations, which we shall consider now.

The direct product $(A \times B)$ of an $n \times n$ matrix A, with an $m \times m$ matrix B, is an $mn \times mn$ matrix with the elements given by,

$$(A \times B)_{ij,kl} = A_{ik}B_{jl} . \tag{2.19}$$

In analogy, we construct the direct product of two matrix representations. If P^a and P^b are representations of some group G, then the direct product of representation matrices for each $g \in G$,

$$P^{a\times b}_{ij,kl}(g) = P^a_{ik}(g)P^b_{jl}(g) , \tag{2.20}$$

also forms a representation of G. We call this the direct product representation, $P^a \times P^b = P^{a\times b}$. Let us consider an example to illustrate the decomposition into irreps. We shall use the group G_2 (see section 6.2).

The decomposition of the direct product of the irrep labelled (20), with itself, is

$$(20) \times (20) = (40) + (31) + (30) + (22) + 2(21) + 2(20) + (11) + (10) + (00) \,. \tag{2.21}$$

The 2 preceding (21) and (20) in the sum on the right, indicates that there are two copies of each of those irreps in the product. We call this number a multiplicity.

Let us now move on to discuss material relevant to the application of group theory.

2.4 *Applying group theory: The Racah–Wigner Calculus*

In this section, we give an introduction to some tools for applying group theory. We introduce the Racah–Wigner calculus for the manipulation of basis vectors. We also discuss the evaluation of matrix elements, and the Wigner–Eckart Theorem which utilises the symmetries to simplify those evaluations.

As we mentioned in section 2.3, the use of group theory in physics developed alongside the development of quantum mechanics. Chemistry and spectroscopy in particular built upon the existing interaction between group theory and crystallography and were early testing grounds of quantum mechanics. During the 1930s and 1940s, the use of group theory extended to nuclear and particle physics. Then later, in the 1960s and 1970s, to high energy physics, with particle zoos built from group theoretically based quark models.

The applications of group theory are now many, varied and widespread, see Coleman (1997) for example. We concentrate only on those concepts of particular relevance to spectroscopy. Such applications rely heavily on the use of the Racah–Wigner calculus, which we introduce later in this section.

So far, our discussion has concentrated on abstract concepts and the link to physics has been tenuous at best. In this section, we discuss symmetry as it applies to a quantum system and introduce the ideas of labelling states and operators by irreps of groups.

Earlier we discussed vector spaces (section 2.2) and in particular the transformations induced on a function space by a transformation of the coordinate system (see equation (2.9)). Now let us use those ideas to consider a system governed by a time–independent Hamiltonian $H(r)$. We denote an arbitrary wave function of this system by $\psi(\mathbf{r})$. Consider again a group G of coordinate transformations $g\mathbf{r} = \mathbf{r}'$, inducing a set of transformations $T(g)$ in the space of wavefunctions, through equation (2.9). The transformed Hamiltonian operator can also be found using equation (2.8),

$$H' = T(g)HT(g)^{-1} \,. \tag{2.22}$$

If $H' = H$ for all $g \in G$, then the Hamiltonian is invariant under these transformations, and G is a symmetry group of the Hamiltonian and therefore of the system itself. The group operators commute with the Hamiltonian.

When a system has such a symmetry group, the following two results can be shown to hold (Elliott & Dawber 1979*b*, p.90):

1. The eigenfunctions ψ and eigenvalues E of H may be labelled by the irreps T^λ of symmetry group G, so that we write ψ^λ and E^λ.

2. The energy E^λ will be at least $|T^\lambda|$–fold degenerate.

Returning to the labelling of states, we now find it useful to use the notion of ket spaces, introduced in section 2.2. For a Hamiltonian, one has a set of eigenvectors, which we write as kets,

$$|\lambda i\rangle, \tag{2.23}$$

where the $1 \leq i \leq |\lambda|$ enumerates the eigenvectors. The label λ is an irrep of a symmetry group G. Each ket is a partner of the irrep λ. (We may also include another label to indicate non–group theoretic information about the state). If the system has several symmetry groups, then λ may be a set of labels, as may i.

Consider the action of an operator R in an orthonormal ket basis, see equation (2.12). One defines the matrix element of the operator through the action

$$\begin{aligned} \langle i|R|j\rangle &= \langle i|k\rangle \sum_k M(R)_{kj}|k\rangle \\ &= \delta_{ik} \sum_k M(R)_{kj} \\ &= M(R)_{ij} \, . \end{aligned} \tag{2.24}$$

So for an operator O in a ket irrep space, one could for example write down matrix elements as,

$$M(O) = \langle \nu i|O|\mu k\rangle \, . \tag{2.25}$$

We shall see later that one can define linear operators labelled by irrep partners, just as the kets are.

Some of the most important physics arises in choosing what the i labels in the basis kets represent. Different choices of what i represents correspond to different choices of basis vectors for the irrep space of λ. In particular, when G contains a subgroup H, the i labels may represent irreps of H and the basis kets will be written

$$|\lambda m \nu i\rangle \, . \tag{2.26}$$

In this basis, i runs over the partners of the irrep space of ν of H, so $1 \leq i \leq |\nu|$. The label m is called a *branching multiplicity* label and is used to distinguish different copies of the same irrep ν contained in the irrep λ. For example, the G_2 irrep (40) contains two copies of each of the irreps 4, 6 and 8 of SO_3. This particular decomposition is relevant to our study, in chapter 6 and appendix A, of the delta function model of correlation crystal fields.

One of the most common types of states are simple angular momentum states, $|jm\rangle$. The j is an irrep label for the group SO_3, the angular momentum symmetry

group and the m is an irrep label for the group SO_2. SO_2 is the symmetry group of rotations in a plane. But there are infinitely many different planes in three–space and although it is standard to choose m to correspond to the z component, it is not necessary to do so. One cannot simultaneously choose more than one component, since rotations in different planes do not commute.

Physical systems generally contain more than one particle. Consider, for example, a system of two electrons. We can describe it as the product of kets for the single electrons, $|j_1 m_1\rangle|j_2 m_2\rangle$. Earlier we discussed direct products for matrices and irreps, equation (2.20), and here we introduce a direct product for kets or basis vectors (and vector spaces).

Consider a vector space V_1 spanned by the basis kets $|1i\rangle$ and another vector space V_2 spanned by the basis kets $|2j\rangle$. Taking the product of each basis ket in V_1, with each basis ket in V_2, generates a basis set, $|1i\rangle|2j\rangle = |1i, 2j\rangle$ for the direct or tensor product space, $V_1 \otimes V_2$. If V_1 and V_2 are irrep spaces, associated with a group G, we would label their basis vectors $|\lambda_1 i\rangle$ and $|\lambda_2 j\rangle$, respectively, for λ_1 and λ_2 irreps of G. The basis vectors of the space $V_1 \otimes V_2$, also a representation space for G, can then be labelled $|\lambda_1 i, \lambda_2 j\rangle$. But we could alternately label those product basis vectors by the direct product of the irreps λ_1 and λ_2. In section 2.3, we stated that this direct product will be a representation of the same group, and that it can be decomposed into irreps of G. Therefore we can write,

$$|\lambda_1 i, \lambda_2 j\rangle = \sum_{\lambda k} C^{\lambda k}_{\lambda_1 i, \lambda_2 j} |\lambda k\rangle \,, \tag{2.27}$$

where the C are coefficients which relate the two bases. We call the basis on the left hand side an uncoupled basis, that on the right hand side the coupled basis and the C coefficients, coupling coefficients. Coupling coefficients allow one to express many–particle states with known transformation properties in terms of products of fewer particle states.

We have described how states can be labelled by representations of groups. The Racah–Wigner calculus works on those labelling representations to interpret aspects of the system. It allows one to factor symmetry structures out of diverse problems, leaving a core specific to the states and operators. Before introducing the Racah–Wigner calculus formally, we give some background on the influence of atomic spectra in its development.

Atomic spectroscopy was very much at the centre of the applied group theory sphere during the 1920s and 1930s. But even in that field, most physicists were uncomfortable about the apparent need for abstract group theory. The famous paper of Slater (1929) dominated the calculations of atomic spectra in the latter half of that period. Slater (1929) provided a set of rules for calculating atomic spectra. Without using group theory, Slater was therefore able to calculate certain matrix elements (see section 2.4.1), vindicating in the eyes of some, the view that group theory could (or should) be avoided. This belief is best highlighted by a comment in Condon & Shortley (1935): 'We wish finally to make a few remarks concerning the place of the theory of groups in the study of the quantum mechanics of

atomic spectra. The reader will have heard that this mathematical discipline is of great importance for the subject. We manage to get along without it.' Throughout that text, algebraic techniques were applied extensively to the quantum theory of angular momentum.

Those algebraic techniques were simplified over the next one and a half decades. In 1940, Wigner (1940) made the first developments in what is now called the Racah–Wigner calculus. Wigner defined coupling coefficients (or $3jm$) which describe how one can couple states, and recoupling coefficients (or $6j$) which describe how to recouple states in different orders. Although Wigner's definitions were aimed at the angular momentum groups SO_3 and SO_2 (actually to any simply reducible group), it would later become clear that generalisations to other groups were possible.

But there was more than just a fundamental need to simplify the algebraic techniques. While the technique of Slater (1929) was satisfactory for s and p–shells and helpful for d–shells, the need to understand and interpret rare earth spectra (f–shell) demanded new techniques. Racah developed a technique, revolutionising the approach to spectral calculations of rare earth ions (Racah 1942*a*, Racah 1942*b*, Racah 1943). He demonstrated its use, by applying it in 1949 to find the energies of configurations of equivalent f–electrons (Racah 1949). Recognising the symmetries underlying many spectral calculations and noting that group theory and symmetry go hand in hand, Racah used the theory of continuous groups as the basis for his approach. Racah exploited the theory developed by mathematicians, such as Lie and Cartan and built on the group theoretical work of other physicists, particularly the work of Wigner. He showed that ideas introduced in his previous work, including tensor operators (see section 2.4.1) and coefficients of fractional parentage (see section 6.2), had group theoretical significance. Racah's methods have become a standard approach to understanding atomic and nuclear spectra. But at the time, they served to entrench group theory firmly in atomic spectroscopy.

Quantum mechanical many–body problems lead to the coupling coefficients being generalised to groups other than those considered by Wigner (1940). Derome & Sharp (1965) and Derome (1966) treated the symmetries of $6j$ and $3jm$ for non–simply reducible groups. A review by Butler (1975) discussed coupling and recoupling coefficients for group chains. The problem of calculating coupling and recoupling coefficients for *all* groups remains. We discuss the development of RACAH in section 7.1. RACAH is a program developed at Canterbury University for calculating coupling and recoupling coefficients. Recent work by Ross (1997) using category theory, provides a solid basis for the unification of those calculations (see section E.7).

Now let us return to look at transformations between bases constructed from states described earlier in this section. We introduced coupling coefficients in 2.27, but not in the common notation. The standard expression for coupling co-

efficients is,

$$|\lambda_1 i, \lambda_2 j\rangle = \sum_{\lambda k} \langle \lambda k | \lambda_1 i, \lambda_2 j \rangle | \lambda k \rangle \ . \tag{2.28}$$

Remembering that i may represent a set of labels, including subgroup labels, one writes the coupling coefficients for coupling angular momenta in the form,

$$|j_1 m_1, j_2 m_2\rangle = \sum_{jm} \langle jm | j_1 m_1, j_2 m_2 \rangle | j_1 j_2; jm \rangle \ . \tag{2.29}$$

Those particular coupling coefficients are known as Clebsch–Gordan coefficients (Cassels 1982, pp.126–127).

Although that notation is common, the coupling coefficients are often scaled to a more symmetrical form, $3jm$ factors or coefficients. The coupling coefficient and $3jm$ are related by a number of simpler coefficients, which we define first. Most of the results given can be found in Butler (1981) or Searle (1988), and as such may sometimes be for point groups rather than general groups. We draw attention to particular distinctions.

Every group has a one–dimensional irrep, called the *scalar* irrep, in which the representation matrix of every element is the number 1. The only product decomposition which the scalar irrep occurs in, is that of an irrep with its *complex conjugate* irrep. If one applies complex conjugation to the set of representation matrices $\lambda(g)$ associated with the matrix irrep $\lambda(G)$, one will obtain a new set of matrices, $\lambda(g)^*$. Those matrices also form an irrep of G, $\lambda(G)^*$, which will be similar to some other matrix irrep of G, $\lambda'(G)$. By being similar, we imply the irreps are related by a basis transformation,

$$\lambda'(g) = T\lambda(g)T^{-1} \ . \tag{2.30}$$

We say that $\lambda'(G)$ is the complex conjugate irrep of $\lambda(G)$ and write $\lambda^*(G) = \lambda'$ to indicate this.

Returning to our coefficients, we write,

$$|\lambda_1|^{\frac{1}{2}} \langle 0 | \lambda_1 l_1, \lambda_2 l_2 \rangle = \begin{pmatrix} \lambda_1 & \lambda_2 \\ l_1 & l_2 \end{pmatrix} , \tag{2.31}$$

to describe the coupling to the scalar by the renormalised coefficient appearing on the right hand side, a $2jm$ symbol. When the basis kets are labelled by groups and subgroups, as in equation (2.26), we call the equivalent coefficient a $2jm$ factor,

$$\begin{pmatrix} \lambda \\ a\sigma \end{pmatrix} = \frac{|\lambda|^{\frac{1}{2}}}{|\sigma|^{\frac{1}{2}}} \langle 0 | \lambda a_1 \sigma, \lambda^* a_2 \sigma^* \rangle \tag{2.32}$$

Although not necessary to do so, Butler (1975) and Butler & Wybourne (1976) proved that it is always possible to choose the $2jm$ factors diagonal in $a_1^* a_2$, and furthermore real. Since only complex conjugate pairs give non–zero values for $2jm$, a single column notation is often used.

We now consider $3jm$ symbols. Historically, various phases have been chosen (Wigner 1940, Condon & Shortley 1967, Fano & Racah 1959), but we use phase choices consistent with Butler (1981, p.45,equation 3.1.5),

$$\begin{pmatrix} \lambda_1 & \lambda_2 & \lambda \\ l_1 & l_2 & l \end{pmatrix}^r = |\lambda|^{-\frac{1}{2}} \binom{\lambda^*}{l^*} K(\lambda_1\lambda_2\lambda^*)\langle r\lambda^* l^* | \lambda_1 l_1, \lambda_2 l_2\rangle \,. \tag{2.33}$$

The $K(\lambda_1\lambda_2\lambda^*)$ is an historical phase factor, used to relate the definitions of Wigner (1940) and of Condon & Shortley (1935). As with the $2jm$, we call $3jm$ in which the partners of the irreps are labelled by irreps of subgroups, $3jm$ factors. An advantage with $3jm$ factors is that under an odd–permutation of the columns, one simply picks up a phase at each group level. For point groups those phases are independent of which odd–permutation, so the permutation need not be recorded. We then write the phase $\{\lambda_1\lambda_2\lambda_3 r\}$, and call it a $3j$.

Coupling coefficients describe the coupling of two partners of a group, but what if those partners are labelled by irrep labels for a whole sequence of subgroups, a group chain? Fortunately these complicated coefficients can be factorised into coupling coefficients pertaining to each group–subgroup pair in the chain. We state this Racah–Factorisation Lemma as it is given in Butler (1981, equation 2.3.13).

$$\langle j_1 a_1 \lambda_1 l_a, j_2 a_2 \lambda_2 l_2 | j a \lambda l\rangle = \sum_r \langle j_1 a_1 \lambda_1, j_2 a_2 \lambda_2 | j a \lambda\rangle_r \langle \lambda_1 l_1, \lambda_2 l_2 | r \lambda l\rangle \tag{2.34}$$

The index r records the multiplicity of λ in the product $\lambda_1 \times \lambda_2$.

The $3jm$ can be considered a generalisation of $2jm$ in the sense that $3jm$ couple three irreps to a scalar, just as $2jm$ couple 2 irreps to a scalar. One can generally consider n–jm which couple n irreps to a scalar. However, those higher order coefficients can be expressed in terms of $3jm$ and $2jm$, along with coefficients allowing for the ordering or recoupling of the couplings. These reordering coefficients are called recoupling coefficients, the symmetrised form being called nj. The $6j$, which describes the reordering of three irreps being coupled, is particularly of interest since the higher nj can be expressed in terms of it. When we refer to recoupling coefficients we imply the coefficients of Butler (1981, equation 3.2.16)

$$\langle (\lambda_1\lambda_2) r_{12}\lambda_{12}, \lambda_3; r\lambda | \lambda_1 (\lambda_2\lambda_3) r_{23}\lambda_{23}; s\lambda\rangle \tag{2.35}$$

which are related to the $6j$ by,

$$\begin{aligned} &\langle (\lambda_1\lambda_2) r_{12}\lambda_{12}, \lambda_3, r_2\lambda | \lambda_1 (\lambda_2\lambda_3) r_{23}\lambda_{23}, r_1\lambda\rangle \\ &\quad = |\lambda_{12}|^{\frac{1}{2}} |\lambda_{23}|^{\frac{1}{2}} K(\lambda_1\lambda_2\lambda_{12})_{r_{12}s_{12}} K(\lambda_{12}\lambda_3\lambda)_{r_2 s_2} K(\lambda_2 s \lambda_3 \lambda_{23})^*_{s_{23} r_{23}} \\ &\quad \times K(\lambda_1\lambda_{23}\lambda)^*_{s_1 r_1} \{\lambda_2\} M((12)\lambda_{12}\lambda_3\lambda^*)_{s_2 t_2} M((132)\lambda_2\lambda_3\lambda^*_{23})_{s_{23}t_{23}} \\ &\quad \times M((23)\lambda_1\lambda_2\lambda^*_{12})_{s_{12}t_{12}} \begin{Bmatrix} \lambda_1 & \lambda_{23} & \lambda^* \\ \lambda_3^* & \lambda_{12} & \lambda_2 \end{Bmatrix}_{t_{12}t_{23}t_2 s_1} , \end{aligned} \tag{2.36}$$

where the M factors are phases arising under the reordering of the coupling of the associated irreps. Earlier we mentioned that $3j$ arise from the ordering of columns in $3jm$. Those M phases are generalisations of the $3j$, in which different permutations on the same irreps result in different phases. Even–permutations may also then result in phase changes. When the odd–permutations do result in different signs we say the *triad* $\{\lambda_1\lambda_2\lambda_3\}$ is of *mixed symmetry*. The $6j$ themselves satisfy various symmetry relations under exchange of entries.

The names $2jm$ and $3jm$ arise because of the association with angular momentum, where the irreps are labelled by j and the partners by $|jm\rangle$. Each $2jm$ contains two j and two m labels. Each $3jm$ contains three j and three m labels. Similarly the $6j$ contains six j labels. This naming makes it clear that coupling or jm coefficients are associated with coupling group partners, and therefore generally involve group–subgroup type relations, whereas recoupling or $6j$ coefficients are at the group level only.

It is of great significance that coupling coefficients may be expressed in terms of recoupling coefficients (Butler 1981, equation 3.3.16).

$$\begin{Bmatrix} \lambda_1 & \lambda_2 & \lambda_3 \\ \mu_1 & \mu_2 & \mu_3 \end{Bmatrix}_{r_1r_2r_3r_4} = \sum_{m_1m_2m_3l_1l_2l_3} \begin{pmatrix} \mu_1 \\ m_1 \end{pmatrix}\begin{pmatrix} \mu_2 \\ m_2 \end{pmatrix}\begin{pmatrix} \mu_3 \\ m_3 \end{pmatrix} \times \begin{pmatrix} \lambda_1 & \mu_2^* & \mu_3 \\ l_1 & m_2^* & m_3 \end{pmatrix}^{r_1}\begin{pmatrix} \mu_1 & \lambda_2 & \mu_3^* \\ m_1 & l_2 & m_3^* \end{pmatrix}^{r_2} \times \begin{pmatrix} \mu_1^* & \mu_2 & \lambda_3 \\ m_1^* & m_2 & l_3 \end{pmatrix}^{r_3}\begin{pmatrix} \lambda_1 & \lambda_2 & \lambda_3 \\ l_1 & l_2 & l_3 \end{pmatrix}^{*r_4} \quad (2.37)$$

The calculation of coupling and recoupling coefficients may therefore be reduced to the calculation of $6j$ and $3jm$. We discuss RACAH, a computer package for the calculation of coefficients, and some details on the calculation of $6j$, in section 7.1. That later discussion mentions several results, which it is appropriate to state here. We give the $3jm, 6j$ forms, but refer also to the coupling, recoupling form of Butler (1981).

The Racah–Back–Coupling equation is (Searle 1988, equation (2.24), p.11),

$$\begin{Bmatrix} \lambda_1 & \lambda_2 & \lambda_3 \\ \mu_1 & \mu_2 & \mu_3 \end{Bmatrix}_{r_1r_2r_3r_4} = \sum_{\nu rr'} |\nu|\{\mu_2\}\{\mu_1\lambda_2\mu_3^* r_2\}\{\lambda_1\lambda_2\lambda_3 r_4\}\{\mu_1\lambda_1\nu^* r'\} \times \begin{Bmatrix} \lambda_2 & \lambda_1 & \lambda_3 \\ \mu_1 & \mu_2 & \nu \end{Bmatrix}_{rr'r_3r_4} \begin{Bmatrix} \lambda_1 & \mu_1 & \nu \\ \lambda_2 & \mu_2 & \mu_3 \end{Bmatrix}_{r_1r_2rr'} \quad (2.38)$$

The coupling, recoupling form is in Butler (1981, equation (3.3.24), p.61).

The Biedenharn–Elliott Sum is (Searle 1988, equation (2.25), p.11),

$$\sum_r \begin{Bmatrix} \lambda_1 & \lambda_2 & \lambda_3 \\ \mu_1 & \mu_2 & \mu_3 \end{Bmatrix}_{r_1r_2r_3r} \begin{Bmatrix} \lambda_1 & \lambda_2 & \lambda_3 \\ \nu_1 & \nu_2 & \nu_3 \end{Bmatrix}_{r_1r_2rr'} = \sum_{\nu t_1t_2t_3} |\nu|\{\lambda_1\}\{\mu_1\}\{(123)\lambda_1\nu_2^*\nu_3\}_{s_1s_1'}\{(132)\nu_1\lambda_2\nu_3^*\}_{s_2s_2'}$$

$$\times \{(13)\lambda_1\mu_2^*\mu_3\}_{r_1r_1'}\{(23)\mu_1\lambda_2\mu_3^*\}_{r_2r_2'}\{\mu_1^*\mu_2\lambda_3r_3\}\{\mu_1^*\nu_1\nu t_1\}$$
$$\times \{\mu_2^*\nu_2\nu t_2\}\{\mu_3^*\nu_3\nu t_3\}\left\{\begin{array}{ccc}\nu_2 & \mu_2^* & \nu\\ \mu_3 & \nu_3 & \lambda_1^*\end{array}\right\}_{s_1r_1t_3t_2}\left\{\begin{array}{ccc}\nu_3 & \mu_3^* & \nu\\ \mu_1 & \nu_1 & \lambda_2^*\end{array}\right\}_{s_2r_2t_1t_3}$$
$$\times \left\{\begin{array}{ccc}\nu_1 & \mu_1^* & \nu\\ \mu_2 & \nu_2 & \lambda_3^*\end{array}\right\}_{s_3r_3t_2t_1}. \qquad (2.39)$$

The form of the Biedenharn–Elliott Sum rule for coupling and recoupling coefficients is in Butler (1981, equations (3.3.25–3.3.26), pp.61–62).

The $3jm$ and $6j$ also satisfy orthonormality relations. The $3jm$ satisfy two different relations (Searle 1988, equation (2.26), p.11),

$$\sum_{\lambda_3 r a_3}\frac{|\lambda_3|}{|\sigma_3|}\left(\begin{array}{ccc}\lambda_1 & \lambda_2 & \lambda_3\\ a_1\sigma_1 & a_2\sigma_2 & a_3\sigma_3\end{array}\right)^{r*}_{s}\left(\begin{array}{ccc}\lambda_1 & \lambda_2 & \lambda_3\\ a_1'\sigma_1' & a_2'\sigma_2' & a_3\sigma_3\end{array}\right)^{r}_{s'}$$
$$= \delta_{ss'}\delta_{a_1a_1'}\delta_{a_2a_2'}\delta_{\sigma_1\sigma_1'}\delta_{\sigma_2\sigma_2'} \qquad (2.40)$$

and, (Searle 1988, equation (2.27), p.11)

$$\sum_{a_1a_2\sigma_1\sigma_2 s}\frac{|\lambda_3|}{|\sigma_3|}\left(\begin{array}{ccc}\lambda_1 & \lambda_2 & \lambda_3\\ a_1\sigma_1 & a_2\sigma_2 & a_3\sigma_3\end{array}\right)^{r*}_{s}\left(\begin{array}{ccc}\lambda_1 & \lambda_2 & \lambda_3'\\ a_1\sigma_1 & a_2\sigma_2 & a_3'\sigma_3\end{array}\right)^{r}_{s'}$$
$$= \delta_{rr'}\delta_{a_3a_3'}\delta_{\lambda_3\lambda_3'}. \qquad (2.41)$$

Butler (1981, equations (2.3.14–2.3.15),p.28) gives the coupling coefficient form of those orthonormality relations. The $6j$ satisfy just the one orthonormality relation (Searle 1988, equation (2.23), p.11),

$$\sum_{\nu r_1r_2}|\lambda_3||\nu|\left\{\begin{array}{ccc}\lambda_1 & \lambda_2 & \lambda_3\\ \mu_1 & \mu_2 & \nu\end{array}\right\}^{*}_{r_1r_2r_3r_4}\left\{\begin{array}{ccc}\lambda_1 & \lambda_2 & \lambda_3'\\ \mu_1 & \mu_2 & \nu\end{array}\right\}_{r_1r_2r_3'r_4'}$$
$$= \delta_{\lambda_3\lambda_3'}\delta_{r_3r_3'}\delta_{r_4r_4'} \qquad (2.42)$$

with the equivalent result for recoupling coefficients being in Butler (1981, equation (3.3.21), p.60).

With coupling and recoupling coefficients in hand, we now can address the problem of using those coefficients in solving problems.

2.4.1 Matrix elements and the Wigner–Eckart Theorem

We mentioned earlier that eigenfunctions span a function space induced by the coordinate transformations allowed by the symmetry group, and as such can be labelled by the group irreps. Similarly, we can introduce linear operators labelled by partners of irreps, as we shall sketch out here, following Butler (1981, pp.84–86).

Consider a vector space V, with basis vectors $\{|1\rangle, |2\rangle, \ldots, |n\rangle\}$. Equations (2.24) and (2.25) describe the matrix element of an operator within this basis. Consider also a mapping of the vector space into itself, by linear operators, described by $L : V \rightarrow V$. Those linear operators may be written in the form

$L_{l_1 l_2} = |l_1\rangle\langle l_2|$. If V can be decomposed under a group G into irrep spaces, with partners $|x\lambda i\rangle$, then we write,

$$O(g)L|x\lambda i\rangle = [O(g)LO(g^{-1})]O(g)|x\lambda i\rangle\ , \tag{2.43}$$

for $O(g)$ the operation performed by $g \in G$. This implies that since the basis kets transform under g as $O(g)|x\lambda i\rangle$, the linear operator L transforms under g as $O(g)LO(g^{-1})$.

One then considers the transformation of the basis operators L_{ij}, in braket form. Taking orthogonal linear combinations of the $L_{l_1 l_2}$ (Butler 1981, equation (4.1.5), p.85),

$$U_l^{r\lambda}(x_1\lambda_1 x_2\lambda_2) = \sum_{l_1 l_2} |x_1\lambda_1 l_1\rangle\langle x_2\lambda_2 l_2| \begin{pmatrix} \lambda_1 \\ l_1 \end{pmatrix} \begin{pmatrix} \lambda_1^* & \lambda & \lambda_2 \\ l_1^* & l & l_2 \end{pmatrix} \tag{2.44}$$

provides linear operators which transform exactly as the ket $|\lambda l\rangle$. Note however that the U operators specified above are dependent upon $x_1\lambda_1 x_2\lambda_2$, whereas the kets $|\lambda l\rangle$ obviously do_not. In order to transform in the same way as the ket $|\lambda l\rangle$, an operator must satisfy,

$$O(g)T_l^\lambda O(g^{-1}) = \sum_{l'} \lambda(g)_{l'l}, \tag{2.45}$$

implying that

$$T_l^\lambda = \sum_{x_1\lambda_1 x_2\lambda_2 r} U_l^{r\lambda}(x_1\lambda_1 x_2\lambda_2) c_{x_1\lambda_1 x_2\lambda_2 r} \tag{2.46}$$

where c is a function only of the subscripted variables.

One may collect together a set of such operators, one for each partner of an irrep, $\{T_1^\lambda, T_2^\lambda, \ldots, T_{|\lambda|}^\lambda\}$. Each operator in such an *irreducible tensorial set* is called a *tensor operator.* One standard set of such operators are the spherical harmonic tensor operators, which we use in our study of the delta function model of correlation crystal fields (see appendix A).

If one considers the matrix elements of a tensor operator, one finds, from equations (2.46) and (2.44),

$$\langle x_1\lambda_1 l_1|T_l^\lambda|x_2\lambda_2 l_2\rangle = \sum_r \begin{pmatrix} \lambda_1 \\ l_1 \end{pmatrix} \begin{pmatrix} \lambda_1^* & \lambda & \lambda_2 \\ l_1^* & l & l_2 \end{pmatrix} c_{x_1\lambda_1 x_2\lambda_2 r}\ . \tag{2.47}$$

The properties of the tensor operator T_l^λ are thus separated into the geometrical transformation properties, in the $2jm$ and $3jm$, and the remainder, in $c_{x_1\lambda_1 x_2\lambda_2 r}$. The $c_{x_1\lambda_1 x_2\lambda_2 r}$ are called reduced matrix elements and are usually written as,

$$\langle x_1\lambda_1 \| T^\lambda \| x_2\lambda_2\rangle_r\ . \tag{2.48}$$

The result relating the matrix elements and reduced matrix elements of tensor operators, is known as the Wigner–Eckart Theorem. We reproduce the result as it appears in Butler (1981, equation (4.2.3)),

$$\langle x_1\lambda_1 l_1|T^{\lambda l}|x_2\lambda_2 l_2\rangle = \sum_r \begin{pmatrix} \lambda_1 \\ l_1 \end{pmatrix} \begin{pmatrix} \lambda_1^* & \lambda & \lambda_2 \\ l_1^* & l & l_2 \end{pmatrix}^r \langle x_1\lambda_1 \| T^\lambda \| x_2\lambda_2\rangle_r\ . \tag{2.49}$$

The Wigner–Eckart theorem is particularly useful when using tensor operators labelled by a group–subgroup chain. The transformation properties of the operators, although labelled by a complete set of irreps, can be reduced to the reduced matrix elements at the top group level only. The link between each group–subgroup pair can be taken out using $2jm$ and $3jm$ combined with the Racah–Factorisation Lemma (equation (2.34)).

The reduced matrix elements of operators contain magnitude and scaling information free of the geometric transformation properties. The geometric transformation properties can be used by themselves to determine if an effect can even occur. Consider what happens when one acts upon an eigenfunction of a system, with an operator labelled by an irrep of the symmetry group of the system. The resulting function,

$$S_i^{\lambda}\psi^{\mu}, \tag{2.50}$$

will transform according to the direct product representation $\lambda \times \mu$. This representation can be expressed in terms of irreps of the same group (see section 2.3). This gives *selection rules*, since if an irrep labelling a wavefunction does not appear in the decomposition, then the wavefunction cannot be obtained from the original state by the action of the operator. Alternately, if one of the $3jm$ appearing in equation (2.49) vanishes, then the operator does not link those states.

The Wigner–Eckart theorem is one of the most useful results in applied group theory. We apply the result extensively in our calculation of spin–orbit matrix elements for a chromium trihalide system (see section 7.1 and appendix B). The spin–orbit effect is described by *coupled* tensor operators. Coupled operators are related to the product of uncoupled operators in the same manner that coupled and uncoupled states are related, that is by coupling coefficients (equation (2.28)). More details can be found in Butler (1981) and Piepho & Schatz (1983).

3. TRANSFORMATION COEFFICIENTS OF THE SYMMETRIC GROUPS

In this chapter we introduce the symmetric groups and begin our analysis of the transformation coefficients upon which a large proportion of our work has been concentrated. In section 3.1 we define and discuss some of the symmetric group concepts important for our analysis, after giving a brief historical note about the symmetric groups. This is followed, in section 3.2, by background on the representation theory of symmetric groups, including a discussion of the bases associated with chains of symmetric subgroups. Having defined the required bases we proceed in section 3.3 to discuss the transformations between those bases. We concentrate on the split–standard transformation coefficients, discussing previous techniques of calculation.

In section 3.4 we reproduce a paper on transformation coefficients between the standard Young–Yamanouchi basis and a dual basis. Initial stages of this investigation were largely carried out by Hamel and Butler, with Ross and myself providing significant input in the latter stages. Since publishing, we have gained a fuller appreciation of the result. In particular, we describe in section 3.5 a generalisation which makes the result more lucid. The record of research into symmetric groups is continued in chapters 4 and 5.

3.1 Introduction to the symmetric group

As we pointed out in section 2.1 the theory of equations was one of the predominate sources of group theory. General solutions for quadratics, cubics and quartics were known by the mid sixteenth century (Cardano 1545). The solutions to those 2^{nd}, 3^{rd} and 4^{th} order equations can all be built up from the polynomial coefficients by rational operations and roots (or radicals). Finding a "general solution by radicals" to higher order equations became a mathematical problem of major significance and difficulty. It was not until the last quarter of the eighteenth century that significant progress was made by Lagrange (1771) and to a lesser extent by Vandermonde (1771).

Lagrange made progress in understanding why the solutions to lower degree equations worked. A particular insight was to apply permutations to the roots of

polynomials. Permutations were not a new concept. Early in the fourteenth century ben Gershon (1321) demonstrated how to count the number of permutations, $n!$, of n objects. Prior to this, Chinese mathematicians were aware of the combinatorial structure underlying what became known as Pascal's triangle.

Making use of the still unproven *fundamental theorem of algebra* (Descartes 1637, p.159), Lagrange concluded that none of the known methods for equations of degree up to four would give solutions for higher degree equations, and furthermore speculated that solutions by radicals did not exist for such equations. Part of his argument lay in the realisation that the introduction of radicals reduces the symmetry of the solutions.

Ruffini (1799) confirmed for quintic equations that no solutions by radicals exist. Then Abel (1826) proved the impossibility of solving by radicals the general equation of degree greater than four. But this general theorem said nothing about the particular classes of equations which were known to be solvable using radicals, such as Gauss's $x^p = a$ for p a prime. Thus the tantalising question became: How was one to know if a particular equation was solvable by radicals (and if so what is the solution)? Abel made some progress on this classification, but Galois' introduction of group theory was the real breakthrough.

The work of Galois was mostly unpublished until some fourteen years after his death (Galois 1846). Galois introduced the name "group", and initialised the study of them. To Galois a group was understood only as a group of permutations on a finite set. The structural constraints (associativity, identity and invertability) were consequences of product closure in his "group", and thus not explicitly demanded. Thus the group of all permutations on n objects is known as the symmetric group, S_n. It arose in the context of the theory of equations, and was one of the first groups to be studied.

Cayley proved that every group of order n is isomorphic to a subgroup of S_n. In some cases the isomorphism is directly with a symmetric group, for example the six element group D_3 is isomorphic to S_3. This gave the symmetric group a significant place in the development of group theory.

Most texts on group theory in physics give discussions on symmetric groups, for example Hamermesh (1962), Elliott & Dawber (1979*a*) and Stancu (1996). We outline some details of significance for our work.

Because there are $n!$ distinct permutations of n objects, S_n has $n!$ elements. There are several different notations for a given permutation. Perhaps the simplest to understand initially is the two–row notation, generally expressed as,

$$\begin{pmatrix} 1 & 2 & \cdots & n-1 & n \\ P(1) & P(2) & P(...) & P(n-1) & P(n) \end{pmatrix} \tag{3.1}$$

where $P(x)$ is the number to which the permutation P carries x. But, for a given n, the top row will always be the same, and therefore is superfluous. Permutations, in general, mix up subsets of the elements 1 to n. For example the permuta-

tion,

$$\begin{pmatrix} 1 & 2 & 3 & 4 & 5 & 6 & 7 \\ 3 & 1 & 2 & 6 & 5 & 7 & 4 \end{pmatrix} \tag{3.2}$$

mixes up 1, 2 and 3 among themselves. Those subsets are called cycles and it is often convenient to express a permutation as a product of such cycles. Every permutation can be uniquely decomposed into cycles. We could write the previous example as $(132)(467)(5)$, or simply $(132)(467)$, where, for example, the cycle (132) represents the permutation taking 1 to 3, 3 to 2 and 2 to 1. Elements are normally omitted if they are invariant under the permutation.

The number of elements in a cycle is called the cycle length. If we order the cycles of a permutation in decreasing length order, and then list the lengths, we have a what is called partition of n. Thus in the example above the partition would be $[331]$. This partition is used to label the conjugacy classes of S_n. Permutations with the same partition are in the same class, since a relabelling will be enough to relate those permutations. We shall define partitions formally in section 3.2.

A permutation which changes only two elements, so those two elements are necessarily exchanged, can be written (i, j) and is called a two–cycle or a transposition. Every permutation can be written as a product of transpositions. Several processes are available to form such a decomposition, and the decomposition itself is not unique. Indeed it is always possible to express a permutation in terms of neighbouring (adjacent) transpositions, $\sigma_i = (i, i+1)$. Those adjacent transpositions may therefore be used to generate all other permutations. Similarly, representation matrices for arbitrary permutations can be obtained from the representation matrix of the adjacent transpositions. The defining relations for S_n, using the set of adjacent transpositions, $\{\sigma_1, \ldots, \sigma_{n-1}\}$ as the generators, are well known to be

$$\begin{array}{ll} \sigma_i^2 & i = 1, \ldots, n-1 \\ (\sigma_i \sigma_{i+1})^3 = 1 & i = 1, \ldots, n-2 \\ \sigma_i \sigma_j = \sigma_j \sigma_i & 1 \leq i < j-1 \leq n-2 \end{array} \tag{3.3}$$

Let us now move on to discuss the representation theory of the symmetric group. A brief background on representations of general groups was given in section 2.3.

3.2 Representation theory of the symmetric group

In section 2.3 we mentioned that the number of classes is equal to the number of inequivalent irreps. So in addition to using partitions of n to label the classes of S_n, we can use them to label irreps of S_n. A partition $[\lambda]$ of n into i parts may be written as $[\lambda_1, \lambda_2, \ldots, \lambda_i]$ such that $\sum_{j=1}^{i} \lambda_j = n$ and the λ_j are weakly decreasing ($\lambda_j \geq \lambda_{j+1}, \forall j$). We adopt an order on partitions such that,

$$\lambda < \rho \text{ if } \lambda_i = \rho_i \text{ for } 1 \leq i \leq k \text{ and}$$

$$\lambda_k > \rho_k. \tag{3.4}$$

Thus for S_4 the irreps are [4], [3 1], [2 2], [2 1 1] and [1 1 1 1].

A useful way to manipulate the irreps through the partition labels is to use tableaux. By forming a left-justified array with λ_j boxes on the j^{th} row and with the k^{th} row below the $(k-1)^{th}$ row, we obtain a Ferrers diagram (sometimes called a Young diagram). We give two examples in figure 3.1, for the partitions [5 2 2 1] and [3 2 1].

Fig. 3.1: Ferrers diagrams for [5 2 2 1] and [3 2 1]

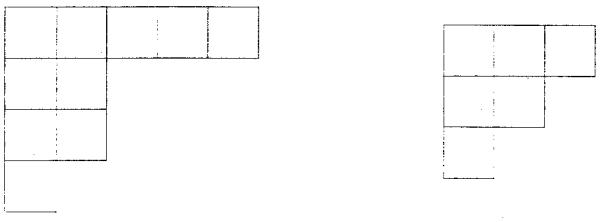

[5 2 2 1] [3 2 1]

Having identified the irreps of S_n we can discuss the basis vectors which span the irreps. One way of labelling the basis vectors is to look at their behaviour under the chain of subgroups,

$$S_n \supset S_{n-1} \supset S_{n-2} \ldots \supset S_2 \,. \tag{3.5}$$

In order to understand the resulting labelling let us first examine the reduction of irreps from S_n to S_{n-1}. The irreps of the group S_{n-1} may be labelled by partitions again. However the only allowed S_{n-1} partitions are those in which one part is 1 smaller than the same part in the S_n partition, and the other parts are equal in the two partitions. So for example

$$[4\ 2\ 1] \rightarrow [3\ 2\ 1] + [4\ 1\ 1] + [4\ 2] \tag{3.6}$$

Diagrammatically (see figure 3.2) this is equivalent to retaining Ferrers diagrams on $n-1$ boxes obtained by removing one outer box from the Ferrers diagram associated with the S_n irrep.

Recording both the S_n irrep (partition) and the S_{n-1} irrep (partition) we have a basis for the irreps in a $S_n \supset S_{n-1}$ group–subgroup chain. But this does not uniquely identify the basis vectors, since the S_{n-1} irreps will generally be of dimension greater than one. Only S_2 and S_1 have every irrep of dimension one. So if we extend the chain as in equation (3.5) we do obtain a set of irreps (partitions) which uniquely label each basis vector. We give an example in figure 3.3.

Fig. 3.2: The reduction of the irrep [4 2 1] from S_7 to S_6

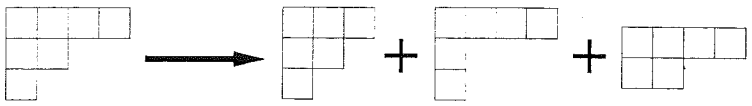

This diagram sequence is an awkward way to label the basis vectors. But the difference between each Ferrers diagram in a labelling sequence is that one box has been removed. So we can associate each sequence with a numbered Ferrers diagram. The box which is removed going from S_i to S_{i-1} is filled with i. Thus the procedure of generating the labelling of the basis vectors is equivalent to filling the Ferrers diagram with the numbers $1, \ldots, n$, such that each number appears exactly once and values strictly increase across rows and down columns. Those filled diagrams are called Young tableaux and for a given partition (Ferrers diagram) the number of Young tableaux corresponds to the irrep dimension. At the bottom of figure 3.3 we give Young tableaux for the basis vectors labelled by the sequences given.

Fig. 3.3: The set of irreps (partitions) associated with each of the basis vectors of the irrep [3 2]

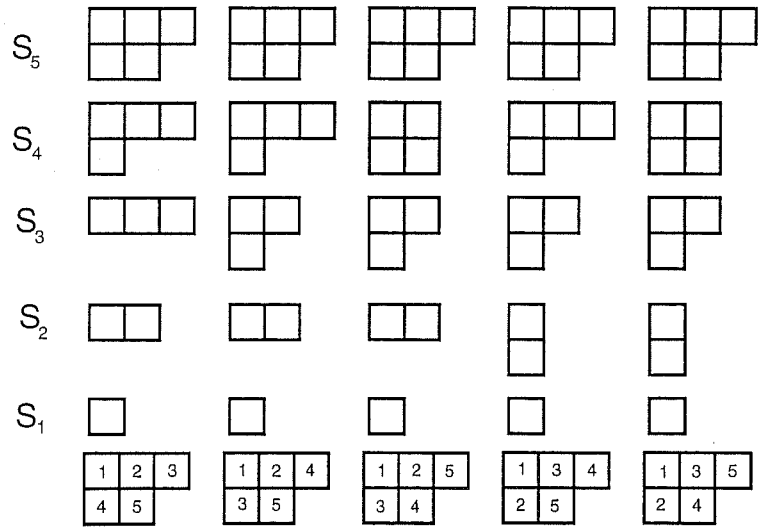

A more compact way of labelling the standard basis vectors uses the Young–Yamanouchi symbols. This symbol is written $Y = (r_n, r_{n-1}, \ldots r_i \ldots r_1)$, where r_i is the row in which the i^{th} number appears in the Young tableau. Therefore for the Young tableaux at the base of figure 3.3, the Young–Yamanouchi symbols are

respectively,

$$(22111), (21211), (12211), (21121), (12121) \tag{3.7}$$

The matrix representations in this standard basis, which we also call the S_n–basis, are well known (see, for example, Rutherford (1948), Hamermesh (1962), Young (1977)). We describe the procedure for calculating those matrix representations below.

Since any permutation can be generated as a product of adjacent transpositions, it suffices to consider just the representation matrices for such transpositions. These matrices can be calculated simply using the tableau parameter of *axial distance*. The axial distance between the box containing i, at (x_i, y_i), and the box containing j, at (x_j, y_j), is defined as $\tau_{ij} = (x_j - x_i) - (y_j - y_i)$. Define also ρ_{ij} to be the reciprocal of the axial distance τ_{ij}. We write the S_n–basis representation matrix for the adjacent transposition $(k-1, k)$ in the representation λ as $M^{\lambda}(k-1, k)$. For a more general permutation, σ, we write $M^{\lambda}(\sigma)$.

In a row of the matrix $M^{\lambda}((k-1, k))$ corresponding to a tableau, T, all elements are zero unless interchanging $k-1$ and k in T gives a valid tableau, S, or, unless $k-1$ and k are in the same row or column of T. When such an S exists the element in the positions (T, S) (and (S, T)) in $M^{\lambda}((k-1, k))$ is $\sqrt{1-\rho^2_{k-1,k}}$. The diagonal term (T, T) is $-\rho_{k-1,k}$, (and therefore (S, S) is $\rho_{k-1,k}$). If T has $k-1$ and k in the same row (respectively column) there clearly cannot exist an S, and the element is $+1$ (respectively -1), corresponding to the previous statement with $\rho = \mp 1$. (see Rutherford (1948, pp.41–49); also Young (1977, VI, pp.217–218) and Hamermesh (1962, section 7.7, pp. 214–231)).

But it is by choice that we chose a basis adapted to the chain of subgroups in equation (3.5). Other choices, with different adaptions, are possible. Some other bases are the natural (Rutherford 1948, Wu & Zhang 1994), semi–normal (Wu & Zhang 1994), Kazhdan–Lusztig (Garsia & McLarnan 1988) and tilted (Bergdolt 1995).

The particular non–standard representations we are interested in were first discussed by Elliott, Hope & Jahn (1954). They were interested, along with Jahn (1954), Kaplan (1961) and others, in constructing functions with a definite permutation symmetry, from functions for subsystems each of which has its own permutation symmetry. Elliott, Hope & Jahn (1954) therefore introduced a basis in which the S_n basis functions are adapted to S_n and to the direct product subgroup $S_a \times S_b$, where $a + b = n$. Each factor group, the S_a–basis and the S_b–basis, are standard basis adapted. Because, as we mentioned above, there are a number of different non–standard bases, we introduce a distinctive new term, *split–basis* to emphasise this. We denote such a split basis as a S_n–$S_{a,b}$–basis. In the trivial case, namely when $b = 1$, the S_n–$S_{n-1,1}$–basis is the S_n–basis. One can label the basis vectors of the split basis by a pair of tableaux, one with a boxes and the other with b boxes (or equivalently by two sets of Ferrers diagrams). These tableaux can be used to determine the representation matrices of the adjacent transpositions in the

split bases by using the method described above for the standard basis tableaux. The first tableau is used if the adjacent transposition is in S_a; the second tableau is used if the adjacent transposition is in S_b. It is of particular interest to us that multiplicities can arise in such bases. We leave our discussion of those multiplicities until chapter 5.

In defining different bases we make use of a combinatorial technique known as *jeu de taquin*. *Jeu de taquin*, or simply *jeu*, is due to Schützenbeger (1963) and is a procedure for removing a box from a Young tableau and then filling the hole created by this removal so that the ultimate result is itself a Young tableau of standard shape. *Jeu* can be described as follows:

> Remove a box from the Young tableau. Examine the number in the box to the right and the number in the box below the position of the removed box. Select the number that is smallest and move the box containing it into the empty space. While there are still boxes to the right in the same row as the hole, or lower in the same column as the hole, repeat this procedure.

Authors have made different order choices on the set of Young tableaux. One popular ordering is *last letter order*. This is the ordering used by Chen, Collinson & Gao (1983) for example, who call it decreasing page order. When we say that a is lower in a tableau than b, we mean a is either in a lower row, or in the same row and to the right of b. Given two tableaux, T and U, T precedes U in last letter order if the last letter of disagreement between the two is lower in T than in U. Last letter ordering is equivalent to ordering the vectors on the Young–Yamanouchi symbols of the Young tableaux. The complementary ordering is *first letter order*. Given two tableaux, T and U, T precedes U in first letter order if the first letter of disagreement between T and U is lower in U than it is in T (Young 1977, IV, p. 258). The Young tableaux we used as an example in figure 3.3 are listed in first letter order. Figure 3.4 gives the Young tableaux for the same example listed in first letter ordering.

Fig. 3.4: The Young tableaux associated with the irrep [3 2], ordered according to last letter

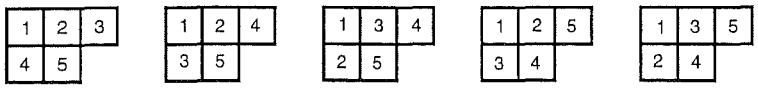

We will also make use of a third kind of ordering, one dependent on the form of the split–basis. To define this third ordering we first establish a correspondence between a tableau of shape λ in the S_n–basis and a pair of tableaux of shape (α, β) in the split S_n–$S_{a,b}$–basis. Given a tableau of shape λ in the S_n–basis, remove

the tableau α, consisting of the boxes containing the first a labels. This tableau is the first in the $S_a \times S_b$ pair. Then apply *jeu* to the remaining b boxes to make a tableau of standard shape, β. This tableau β is the second in the $S_a \times S_b$ pair. Note that this correspondence is many–to–one so that a single $\alpha\beta$ pair can have many tableaux of shape λ in the S_n–basis that map to it. Order the tableau pairs (α, β) in the S_n–$S_{a,b}$–basis in the following manner.

Order the (α, β) pairs by the α, using the partition order defined in (3.4) if the shapes in two pairs are different, and by first letter order if the shapes are the same. Then for pairs in which the first components are identical, order by the second components, again first using partition order, and then first letter order. When a pair occurs more than once, the situation known as product multiplicity, order those pairs according to the first letter ordered list of standard tableaux from which they came. This gives a unique ordering for any split basis.

We generally use first letter order, since it relates better to the usual split–basis ordering. We convert to the last letter order to compare results, particularly with those results given by Chen, Collinson & Gao (1983). We earlier used last letter order, and the published paper in section 3.4 uses last letter ordering.

3.3 Transformation coefficients of S_n

In the previous section we discussed some bases for the irreps of S_n. In this section we give background on the coefficients which transform from one basis to another. This includes a review of techniques developed by others for calculating the split–standard transformation coefficients.

We are specifically interested in matrix irreps, see section 2.3. We denote the matrix irrep of λ in the standard basis, for the permutation π, by $M^{\lambda}(\pi)$. The matrix irrep in the S_n–$S_{a,b}$–basis will be written $M^{\lambda}_{a,b}(\pi)$.

Transformation coefficients relate the basis vectors of one basis to the basis vectors of another basis. Thus the unprimed basis vectors , $|\lambda i\rangle$ are related to the primed basis vectors $|\lambda j\rangle'$ by

$$|\lambda i\rangle = \sum_j C^{\lambda}_{ij} |\lambda j\rangle', \tag{3.8}$$

where the C^{λ}_{ij} are the transformation coefficients. For matrix irreps we transform both the basis vectors labelling the rows and the basis vectors labelling the columns of the matrices. Thus the transformation from the M basis to the M' basis is given by the transformation matrix T, containing the transformation coefficients, in the expression

$$M' = TMT^t \,. \tag{3.9}$$

The transformation matrices are real and orthogonal, so that we have replaced T^{-1} with T^t.

3.3.1 *Split–standard transformation coefficients*

The split–basis was introduced by Elliott, Hope & Jahn (1954). Many attempts have since been made to calculate the transformation between split and standard bases. We obtain the expression for the relevant transformation coefficients from equation (3.9),

$$M^{\lambda}_{a,b}(\pi) = T^{\lambda}_{a,b} M^{\lambda}(\pi) (T^{\lambda}_{a,b})^{t} , \tag{3.10}$$

where we note that the irrep in the split basis is implied to be λ by the λ in the standard basis. We introduce the term split–standard transformation coefficients for the transformation coefficients $T^{\lambda}_{a,b}$.

Jahn (1954) and Kaplan (1961) introduced split–standard transformation coefficients in the construction of orbital wavefunctions for multishell configurations. These coefficients are significant in some calculations of nuclear, molecular and atomic structures. They are effectively coefficients of fractional parentage (see section 6.2), which relate physical coupled states of n particles to the physical states containing a particles and $n-a$ particles. We outline some of the techniques proposed for calculating the coefficients, concentrating particularly on the type and applicability of the results obtained.

Jahn (1954) used Young operators (Kaplan 1975, pp.41–43) to evaluate the split–standard transformation coefficients in a special case. In the words of Jahn (1954, p.989), the "special case where the state vectors are all different". A numerical procedure was obtained, and explicit results were given for the $S_4 \supset S_2 \times S_2$ cases.

Kaplan (1961) extended this result and obtained a technique for calculating any split–standard transformation coefficient, when there are no multiplicities in the split product. Kaplan (1961) and Kaplan (1975) gave explicit algebraic formulas for the transformation from the S_n–basis to the S_n–$S_{n-2,2}$–basis. We reproduce this result in equation 5.12. Kukulin, Smirnov & Majling (1967) point out how the Young operator technique becomes rapidly unwieldy as n increase. The main problem is with a large b, since the Young operator technique requires a summation over all permutations in the second subgroup.

The next intensive study was undertaken by Horie (1964). He also made use of Young operators but obtains a set of recursion relations which can be used to calculate the split–standard transformation coefficients for non–multiplicity cases. Horie (1964) shows the recursion relations reduce to the explicit formula of Kaplan (1961). Furthermore explicit formulas are given for the cases when the second irrep in the split basis pair is either the completely symmetric $[m]$ or the completely antisymmetric $[1^m]$ (a one column or one row partition).

In three papers, Kramer (1967), Kramer (1968), Kramer & Seligman (1969), progress was made linking the coefficients of the symmetric and unitary groups. The split–standard transformation coefficients were related to symmetric group $6j$, $6f$ and $9f$ symbols, which in turn were linked to double cosets. Those papers helped greatly to initiate the study of using double cosets to calculate transforma-

tion coefficients for symmetric and unitary groups (see section E.4).

Suryanarayana & Rao (1982) extended the explicit formulas obtained by Horie (1964), using essentially the same approach. Their result allows for irreps of S_b with dimension greater than one, but not for multiplicities in the product of the irreps of S_a and S_b. The formulas obtained are not completely general (even outside of the multiplicity issue). The formulas are for irreps of the form $[2^a 1^{n-2a}]$. Suryanarayana & Rao (1982) claim that Pauli's exclusion principle demands that one should not have any more than two cells in any row. This is true for their case, but the addition of isospin by nuclear physicists allows four cells per row. Furthermore, Schur–Weyl duality (Haase & Butler 1984*a*, Haase & Butler 1984*b*), which relates unitary group coefficients to those of the symmetric group, means the coefficients for all symmetric groups irreps can occur in other kinds of physical problems.

Sarma (1981) suggested a new algorithm for calculating the split–standard transformation coefficients. Chen, Collinson & Gao (1983) considered it inconvenient for implementation in computer calculations. It appears that the technique of Sarma (1981) is a more complicated version of the linear equation method used later by Pan & Chen (1993). We independently recovered this procedure during our investigation.

The method of Chen, Collinson & Gao (1983) *is* however numerically convenient. It is based upon the versatile eigenfunction method developed by Chen and co–workers. We shall discuss some details of this useful method in later sections (and chapters). Chen, Collinson & Gao (1983) give the coefficients up to and including $S_6 \supset S_3 \times S_3$, which contains the first multiplicity in the product of the split basis vectors. This is extremely useful for checking our results, although a few errors appear in the tables (see section 5.2.5). The solution of Chen, Collinson & Gao (1983) is strictly numerical, thus somewhat unsatisfying, although it is enough for any particular calculation.

Pan & Chen (1993) give a method for deriving algebraic results for Hecke algebras, the quantum extension of the symmetric group. They obtain algebraic results for the Hecke split–standard transformation coefficients, which can be reduced to give those of Chen, Collinson & Gao (1983). The solutions are algebraic in the sense of the dependence on the q–factor which is built into the solutions. Furthermore the technique can be used to derive algebraic formulas for coefficients. We do this in chapter 5, where we describe in detail the method of Pan & Chen (1993) (see section 5.2.3).

This discussion has not been exhaustive. Others, such as Mirman (1987*a*) and Mirman (1987*b*) and Haase & Butler (1985) have made contributions of clearly relevant material. We have however tried to steer a fairly direct path through the techniques for calculating the split–standard symmetric group transformation coefficients.

Those techniques allow one to calculate solutions numerically, and for some cases by explicit formula, but several problems are not addressed to any great sa-

tisfaction. In particular, how should the multiplicity separation be chosen? Chen, Collinson & Gao (1983) and Pan & Chen (1993) make different choices of separation, without alluding to any real need to make a choice at all. We leave this issue until chapter 5. For the rest of this chapter we discuss some initial probes at the structure of the transformation coefficients associated with the split–standard basis transformation. But let us first outline a general technique for calculating basis transformations.

3.3.2 Transformation by generator identification

Garsia & McLarnan (1988) outline a method which, given two different representations of S_n, will produce the matrix that transforms between them. The crucial element in this method is a formula deducible from a basic result in elementary representation theory. We briefly describe the method.

Let A and B be two representations of S_n. Then the great orthogonality theorem (Butler 1981, equation (2.4.11), p.32) shows that the transformation matrix, W, is

$$W_{sj} = \sum_{\sigma \in S_n} A_{ij}(\sigma) B_{sr}(\sigma^{-1}) \,, \tag{3.11}$$

where i and r are chosen such that $W_{ir}^{-1} \neq 0$. In practice it is not always possible to determine suitable i and r integers *a priori*. However, because W has a nonzero determinant the choice of $i = 1$ will always work. In practice, Garsia & McLarnan (1988) found $i = r = 1$ worked in all of the cases they considered.

In general often the difficulty is in obtaining the required matrices for each representation (see section E.9). Garsia & McLarnan (1988) were interested in transforming between the natural and the Kazhdan–Lusztig bases of S_n. The representation matrices can be simply calculated in both bases. For us the problem lies with the representation matrices in the S_n–$S_{a,b}$–basis, since the matrices for the S_n–basis are well–known.

As always, we need only be concerned with calculating the adjacent transpositions which generate the entire group. If an adjacent transposition is within the first factor group, S_a, the representation matrix is identified with the corresponding matrices in the representation for the standard basis. Similarly those contained within the second factor group, S_b, are identified with the corresponding matrices in the representation for the dual basis (Hamel et al. 1996). This follows from the pair of tableaux, or chain of partitions, used to label the basis vectors (see section 3.2).

The difficulty then is in calculating the representation matrix for what we call the "bridging transposition (permutation)", $(a, a+1)$. This bridges the two factor groups and the boxes are in different tableaux. At this stage we do not know how to calculate those matrices without first knowing the transformation matrix. Examples of two such bridging permutations are given near the start of section

4.1. It appears, from those and other examples, that the bridging permutation is in general simpler if b is small.

Even were it possible to calculate the bridging permutation, which is an interesting problem in its own right, this method is rather inefficient since in 3.11 we sum over all $n!$ permutations of S_n. The factorial rapidly becomes large, and realistically we cannot be satisfied with only calculating coefficients for n less than about 10.

3.4 Transformation between the Young–Yamanouchi basis and its dual

The following paper (from the next page to page 50 of this thesis, together with the cited references) appeared in the Journal of Physics A:Mathematical and General Physics, **29** (1996), 5935–5944. Although initial stages of the investigation leading to this paper were largely carried out by Hamel and Butler, Ross and myself provided significant input in the latter stages.

Transformation between the Young-Yamanouchi basis and its dual.

A.M. Hamel†, L.F. McAven‡, H.J. Ross‡, and P.H. Butler‡

† Dept. of Mathematics and Statistics, University of Canterbury, Christchurch, New Zealand.

‡ Dept. of Physics and Astronomy, University of Canterbury, Christchurch, New Zealand.

Motivated by the aim of finding generalised transformation coefficients for the symmetric group, we calculate the matrix which transforms the basis functions of the Young–Yamanouchi basis into the basis functions of its dual. Our approach is to derive the representation matrices for both bases and then determine the transformation matrix. The dual basis is associated with the subgroup chain $S_1 \times S_{n-1} \supset S_1 \times S_1 \times S_{n-2} \supset \ldots$, whereas the usual YY basis is associated with the subgroup chain $S_{n-1} \times S_1 \supset S_{n-2} \times S_1 \times S_1 \supset \ldots$. A combinatorial technique, *jeu de taquin*, is used to define the $\overline{YY}$ basis, via the Young–Yamanouchi symbols and Young tableaux with which the basis functions can be indexed.

Published: J.Phys.A:Math.Gen. **29** (1996) 5935-5944.

3.4.1 Introduction

Representations of the symmetric group, S_n, the associated matrices, characters, and basis functions, play an important role in the study of the many–electron problem in physics and quantum chemistry. A common choice among the wide range of bases is the Young–Yamanouchi, or YY basis (see Yamanouchi (1937), Rutherford (1948), Hamermesh (1962), or Kaplan (1975)), associated with the subgroup chain $S_{n-1} \times S_1 \supset S_{n-2} \times S_1 \times S_1 \supset \ldots \supset S_1 \times S_1 \times \ldots \times S_1$. The aim of finding generalised transformation coefficients for the symmetric group motivates us to calculate a special case. We calculate the matrix that transforms between the basis functions of the YY basis and what we shall call its dual, the $\overline{YY}$ basis. This basis is associated with the subgroup chain $S_1 \times S_{n-1} \supset S_1 \times S_1 \times S_{n-2} \supset \ldots \supset S_1 \times S_1 \times \ldots \times S_1$.

The YY basis is defined by a chain of maximal subgroups. Restrictions of generic basis functions of irreps of S_n will give a non-reduced basis for subgroups. The YY basis functions corresponding to the irreducible representations (irreps) of S_n are also basis functions of irreps of the subgroups $S_{n-1} \times S_1, S_{n-2} \times S_1 \times S_1, \ldots$. The irreps of such a direct product group can be expressed as the direct product of irreps of the factor groups. The only irrep of S_1 corresponds to the 1 dimensional unit matrix which is 1. Therefore the irreps of the subgroups in the YY basis can be simply labelled using the first factor of the subgroup. Each function can thus be identified with the irreps to which it will belong in $S_n, S_{n-1}, S_{n-2}, \ldots$, and this identification corresponds to the unique Young tableau with the property that the successive removal of the boxes labelled $n, n-1, \ldots$ yields Young tableaux that correspond to the irreps of S_{n-1}, etc.

A more general set of basis functions would correspond to the basis $S_{n_1} \times S_{n_2} \times \ldots \times S_{n_l}$, $n_1 + n_2 + \ldots + n_l = n$. In this subgroup basis the matrices of elements in the subgroup are direct sums of tensor products of matrix irreps of the factor groups (up to a permutation of the basis). The YY basis is the specific case of this where $n_i = 1, \ \forall i > 1$. We want to look at transformations between the YY basis and the more general basis where the n_i, $i > 1$ need not be equal to 1.

This problem is equivalent to looking for the matrix that transforms between $S_{m_1} \times S_{m_2} \times \ldots \times S_{m_k}$ and $S_{n_1} \times S_{n_2} \times \ldots \times S_{n_l}$ where $m_1 + m_2 + \ldots + m_k = n_1 + n_2 + \ldots n_l = n$. This general problem has been considered by Kaplan (1975), Horie (1964), and Suryanarayana & Rao (1982) among others. However, as Horie's method is recursive, and Suryanarayana and Kondala Rao have a closed formula only for representations of the form $\lambda = 2^a 1^{n-2a}$, there is still a need for other methods. The techniques we present here provide a straightforward and easily–explained approach to a specific sort of basis transformation, and we can avoid the Young operator techniques employed in other approaches.

In this paper we determine the transformation matrix for a specific case of the general transformation mentioned above. That is, for the transformation between

the YY basis and its dual. Our approach is to derive the representation matrices for both bases and then determine the transformation matrix. Since any permutation can be expressed as the product of adjacent transpositions, $(k, k+1)$, we can confine our discussion to the representation matrices for these. The representation matrices corresponding to the YY basis functions are well known (see, for example, Hamermesh (1962), Kaplan (1975) and also Wu & Zhang (1992), Wu & Zhang (1994)); those corresponding to the $\overline{YY}$ basis can be constructed using the same approach after defining the basis using the combinatorial technique of *jeu de taquin* due to Schützenbeger (1963) (see also Schützenbeger (1977)).

3.4.2 *Indexing the basis functions using jeu de taquin and the Young–Yamanouchi symbols*

The well–known Young–Yamanouchi, or YY, symbols (described below) are generated from tableaux by removing one box at a time from the Young tableaux, starting with the box labelled n. To derive the $\overline{YY}$ symbols for the $\overline{YY}$ basis functions we remove the boxes from the Young tableau one at a time starting with 1 instead of n and filling the holes with *jeu de taquin* at each stage. *Jeu de taquin* is a combinatorial technique that provides a means of indexing the $\overline{YY}$ basis functions with a sequence of integers. This technique is due to Schützenbeger (1963) (see also Schützenbeger (1977)) and is equivalent to the Robinson–Schensted algorithm (Thomas 1977). *Jeu de taquin* is a procedure for removing boxes from any part of a Young tableau (not just the perimeter) and filling the gap created so that the resulting object is a proper Young tableau. We describe it here first, later using it to define the representation matrices in the $\overline{YY}$ basis.

> Remove a box from the Young tableau. Examine the content of the box to the right of the removed box and that of the box below the removed box. Slide the box containing the smaller of these two numbers into the vacant position. Now repeat this procedure to fill the hole created by the slide. Repeat the entire process until no holes remain (i.e. the hole has worked itself to the perimeter of the tableau).

The tableaux of the YY basis are uniquely indexed by a sequence of integers, a so–called *Young–Yamanouchi symbol*, defined in the following manner:

> Locate the box containing n in the Young tableau. Remove that box and write down the index of the row that contained that box. Repeat the procedure for $n-1, n-2, \ldots, 2, 1$. The list of integers is the YY symbol.

The basis functions of the $\overline{YY}$ basis are also indexed by Young tableaux, and can similarly be indexed by a sequence of integers defined in the following manner:

Locate the box containing 1 in the Young tableau. Remove it and fill the hole it leaves using *jeu de taquin*. Write down the index of the row from which a box is ultimately removed after the *jeu de taquin*. Repeat this procedure for $2, 3, \ldots, n$. The list of integers is the $\overline{YY}$ symbol.

The set of $\overline{YY}$ symbols is, in fact, identical to the set of YY symbols. However, a given Young tableau will, in general, have different YY and $\overline{YY}$ symbols. We say a YY symbol and a $\overline{YY}$ symbol correspond if they are both generated by the same Young tableau.

Fig. 3.5: Example of *jeu de taquin* on $\lambda = 3, 2, 1$. The $\overline{YY}$ symbol is built up progressively underneath the tableau at each stage

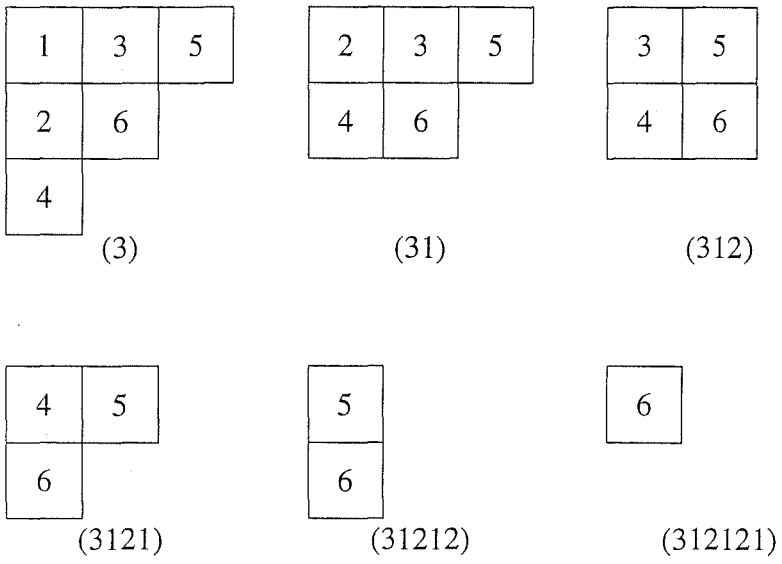

We define a companion tableaux, $\tilde{T}$, of T to be a tableaux such that the $\overline{YY}$ symbol of $\tilde{T}$ is equal to the YY symbol of T. The companion relation is a symmetric relation, i.e., the YY symbol of $\tilde{T}$ is equal to the $\overline{YY}$ symbol of T. We note that there is an object called the dual tableau (see Knuth (1973, pp. 58–59) for details) which is defined such that the YY symbols for it and for the original tableau are the same; however, the dual has the filling rules reversed (i.e. each entry in the dual tableau has to be greater than the entry to the left of or below it) and hence it would be necessary to use *jeu de taquin* to obtain the YY symbol. The dual tableau is, however, equivalent to our definition of companion tableau, and the correspondence can be simply seen by reversing the order of the labels and the order in which we remove the labels. The use of the companion rather

than the dual has the obvious advantage that the companion is within the original set of standard tableaux.

3.4.3 *Representation matrices*

The representation matrices indexed by the YY basis functions for adjacent transpositions are well known (Rutherford (1948), Hamermesh (1962)). Descriptions of the entries are in terms of a tableau parameter called *axial distance* and defined as follows. Let i be the box of the tableau in row r_i and column c_i, and let j be the box of the tableau in row r_j and columns c_j. Then the axial distance from i to j is $(c_j - r_j) - (c_i - r_i) \equiv \tau_{ij}$. We also define the reciprocal of this, $\rho := \frac{1}{\tau}$.

Since we will be indexing matrices by Young tableaux, we first impose a total order on the tableaux. Let λ be a partition. Take the set of all Young tableaux of shape λ, and order them using last–letter order, i.e. tableaux in which the largest letter occurs in a lower row are later in the ordering. For example, for $\lambda = 3, 2$, see Figure 3.6. The well–defined order of the tableaux imposes an ordering upon the associated YY symbols and their corresponding $\overline{YY}$ symbols. When we refer to the ordering of symbols it is this order to which we refer. The ordering of a set of tableaux, YY, and $\overline{YY}$ symbols are given in Figure 3.7.

Fig. 3.6: Example of tableaux of shape $\lambda = 3, 2$ ordered by last–letter order

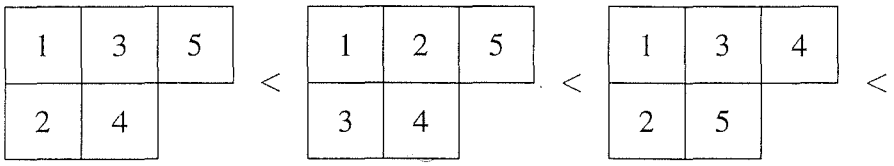

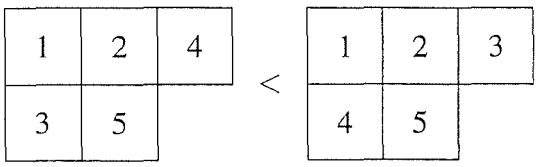

The YY representation matrix $M^{\lambda}_{(k-1,k)}$ for the transposition $(k-1, k)$ for the representation λ is defined as follows:

Fig. 3.7: Tableaux, YY symbols, and $\overline{YY}$ symbols for $\lambda = 3, 2, 1$

Tableau	YY symbol	$\overline{YY}$ symbol	Tableau	YY symbol	$\overline{YY}$ symbol
1 2 3 4 5 6	322111	123121	1 2 5 3 6 4	213211	132121
1 2 4 3 5 6	321211	121321	1 3 5 2 6 4	213121	312121
1 3 4 2 5 6	321121	211321	1 4 5 2 6 3	211321	321121
1 2 5 3 4 6	312211	231121	1 2 6 3 4 5	132211	231211
1 3 5 2 4 6	312121	213121	1 3 6 2 4 5	132121	213211
1 2 3 4 6 5	232111	123211	1 2 6 3 5 4	123211	232111
1 2 4 3 6 5	231211	132211	1 3 6 2 5 4	123121	322111
1 3 4 2 6 5	231121	312211	1 4 6 2 5 3	121321	321211

(1) $M^{\lambda}_{(k-1,k)}$ has $+1$ in position (r, r) if in the rth YY symbol, the $n-k+1$st and $n-k$th elements are identical (i.e. the rth tableau has $k-1$ and k in the same row).

(2) $M^{\lambda}_{(k-1,k)}$ has a -1 in position (r, r) if in the rth YY symbol the $n-k+1$st element, α, is one more than the $n-k$th element, β, and there does *not* exist another YY symbol that is identical to this YY symbol except that its $n-k+1$st element is β and its $n-k$th element is α (i.e. the rth tableau has $k-1$ and k in the same column).

(3) $M^{\lambda}_{(k-1,k)}$ has $-\rho$ in position (r, r), $\sqrt{1-\rho^2}$ in positions (r, s) and (s, r) and ρ in position (s, s), if $r < s$ and the rth and sth YY symbols are identical except that the $n-k+1$st element of the rth YY symbol is the $n-k$th element of the sth YY symbol and vice versa (i.e. the sth tableau is obtai-

ned from the rth tableau by interchanging $k-1$ and k). As noted above, ρ is the reciprocal of the axial distance from the box containing $k-1$ to the box containing k in the rth tableau.

(4) 0 in all other positions.

(see Rutherford (1948, pp. 41,49); also Young (1977, VI, pp. 217,218)). An example is given in section 3.4.6.

The $\overline{YY}$ representation matrix $\overline{M}^{\lambda}_{(k-1,k)}$ for the transposition $(k-1,k)$ for the representation λ is defined as follows:

(1) $\overline{M}^{\lambda}_{(k-1,k)}$ has $+1$ in position (r,r) if in the rth $\overline{YY}$ symbol the $k-1$st and kth elements are identical.

(2) $\overline{M}^{\lambda}_{(k-1,k)}$ has a -1 in position (r,r) if in the rth $\overline{YY}$ symbol the $k-1$st element, α, is one more than the kth element, β, and there does not exist another $\overline{YY}$ symbol that is identical to this $\overline{YY}$ symbol except that its $k-1$st element is β and its kth element is α.

(3) $\overline{M}^{\lambda}_{(k-1,k)}$ has $-\rho$ in position (r,r), $\sqrt{1-\rho^2}$ in positions (r,s) and (s,r) and ρ in position (s,s), if $r<s$ the rth and sth $\overline{YY}$ symbols are identical except that the $k-1$st element of the rth $\overline{YY}$ symbol is the kth element of the sth $\overline{YY}$ symbol and vice versa, where ρ is the reciprocal of the axial distance from $n-k+2$ to $n-k+1$ in the rth tableau.

(4) 0 in all other positions.

For an example, see the Appendix.

The $\overline{M}^{\lambda}_{(k-1,k)}$ matrix is not as well–known in the literature, although it has appeared in Kaplan (1975, p. 52) for a special case, and is easily derived by induction in a manner similar to Rutherford (1948, pp. 39–43) or Hamermesh (1962, pp. 215–223). In doing so we can choose the representation matrices of the $\overline{YY}$ basis to be related to the representation matrices of the YY basis by a permutation of the basis functions,

$$P\overline{M}^{\lambda}_{(k-1,k)}P^{-1} = M^{\lambda}_{(n-k+2,n-k+1)}. \tag{3.12}$$

At the end of the previous section we stated that the lists of $\overline{YY}$ and YY symbols, ordered by the last–letter order of the tableaux, contain the same elements, possibly in a different order. If we call those lists x and y, for the YY and $\overline{YY}$ symbols respectively, then

$$\begin{aligned} P_{i,j} &= \delta(x_i, y_j) \\ &= \delta(x_j, y_i) \end{aligned}$$

where δ is the Kronecker δ function: $\delta(a,b) = 1$ if $a = b$ and $\delta(a,b) = 0$ if $a \neq b$. Thus we say that the ordered list of $\overline{YY}$ symbols is carried to the ordered list of YY symbols by the permutation P, and that P takes each tableau to its companion tableau.

3.4.4 *Calculation of the transformation matrix*

The transformation matrix is the matrix T such that

$$\overline{M}^{\lambda}_{(k-1,k)} = T^{-1} M^{\lambda}_{(k-1,k)} T \qquad \forall\, k. \tag{3.13}$$

It can be calculated simply in two stages and expressed as the product of two matrices, P and Q. The first of these, the P matrix, is simply the permutation matrix that sends the set of $\overline{YY}$ symbols to the set of YY symbols. The application of P and P^{-1} to the right and left sides of $\overline{M}^{\lambda}_{(k-1,k)}$ brings it to the same form as $M^{\lambda}_{(n-k+2,n-k+1)}$.

$$\begin{aligned} P^{-1}Q^{-1}M^{\lambda}_{(k-1,k)}QP &= \overline{M}^{\lambda}_{(k-1,k)} \\ Q^{-1}M^{\lambda}_{(k-1,k)}Q &= P\overline{M}^{\lambda}_{(k-1,k)}P^{-1} \\ &= M^{\lambda}_{(n-k+2,n-k+1)} \end{aligned}$$

as in equation (3.13), so that

$$Q^{-1}M^{\lambda}_{(k-1,k)}Q = M^{\lambda}_{(n-k+2,n-k+1)} \tag{3.14}$$

The problem then reduces to finding a transformation matrix Q between representation matrices in the YY basis.

It is easily seen that the Q matrix is the representation matrix that sends $n, n-1, \ldots, 2, 1$ to $1, 2, \ldots, n-1, n$. Q can be calculated directly from the representation matrices in the YY basis for the adjacent transpositions, since it is well–known that any permutation σ can be expressed as a minimal length product of adjacent transpositions (Rutherford (1948, p. 6)). This minimal length is the number of inversions, i.e. the number of distinct pairs (i,j) with $i < j$ such that $\sigma(i) > \sigma(j)$. In particular, define $d_i = \text{card}\{j | j > k$ where $\sigma(k) = i$ and $\sigma(j) < i\}$. Then the permutation σ can be written as

$$\sigma = \ldots (\tau_{i-1}\tau_{i-2}\ldots\tau_{i-d_i})\ldots(\tau_{n-2}\tau_{n-3}\ldots\tau_{n-1-d_{n-1}})(\tau_{n-1}\tau_{n-2}\ldots\tau_{n-d_n})$$

where $\tau_i = (i, i+1)$ and the ith contribution is included only if $d_i \geq 1$.

In the case of Q, the length of the product will be $\binom{n}{2}$ and $d_i = i-1$, $1 \leq i \leq n$. Specifically, then,

$$Q = \prod_{i=2}^{n} \prod_{j=i-1}^{1} (j, j+1).$$

For our example of $\lambda = 3, 2, 1$,

$$\begin{aligned} Q &= (16)(25)(34) \\ &= (12)(23)(12)(34)(23)(12)(45)(34)(23)(12)(56)(45)(34)(23)(12), \end{aligned}$$

and the matrices P and Q are given in Figures 3.8 and 3.9 respectively.

3.4.5 Conclusion

We have presented a simple, straight–forward method for calculating the transformation matrix between the YY basis and its dual, the $\overline{YY}$ basis. The matrix itself is easy to describe, is intuitively pleasing, and is presented without the use of Young operator techniques. By using the well–known combinatorial technique of *jeu de taquin*, the method presented here further cements the link between combinatorics and mathematical physics. We anticipate that further links are possible, and that using variations on the methods presented here, we would be able to calculate transformation matrices between more general bases of symmetric groups, eg. between two bases of S_n of the form $S_{n_1} \times S_{n_2} \times \ldots \times S_{n_l}$, $n_1 + n_2 + \ldots + n_l = n$. This will be the subject of future work.

Fig. 3.8: The P matrix for $\lambda = 3, 2, 1$

$$P = \begin{bmatrix} 0 & 0 & 0 & 0 & 0 & 0 & 0 & 0 & 0 & 0 & 0 & 0 & 0 & 0 & 1 & 0 \\ 0 & 0 & 0 & 0 & 0 & 0 & 0 & 0 & 0 & 0 & 0 & 0 & 0 & 0 & 0 & 1 \\ 0 & 0 & 0 & 0 & 0 & 0 & 0 & 0 & 0 & 0 & 1 & 0 & 0 & 0 & 0 & 0 \\ 0 & 0 & 0 & 0 & 0 & 0 & 0 & 1 & 0 & 0 & 0 & 0 & 0 & 0 & 0 & 0 \\ 0 & 0 & 0 & 0 & 0 & 0 & 0 & 0 & 0 & 1 & 0 & 0 & 0 & 0 & 0 & 0 \\ 0 & 0 & 0 & 0 & 0 & 0 & 0 & 0 & 0 & 0 & 0 & 0 & 0 & 1 & 0 & 0 \\ 0 & 0 & 0 & 0 & 0 & 0 & 0 & 0 & 0 & 0 & 0 & 1 & 0 & 0 & 0 & 0 \\ 0 & 0 & 0 & 1 & 0 & 0 & 0 & 0 & 0 & 0 & 0 & 0 & 0 & 0 & 0 & 0 \\ 0 & 0 & 0 & 0 & 0 & 0 & 0 & 0 & 0 & 0 & 0 & 0 & 1 & 0 & 0 & 0 \\ 0 & 0 & 0 & 0 & 1 & 0 & 0 & 0 & 0 & 0 & 0 & 0 & 0 & 0 & 0 & 0 \\ 0 & 0 & 1 & 0 & 0 & 0 & 0 & 0 & 0 & 0 & 0 & 0 & 0 & 0 & 0 & 0 \\ 0 & 0 & 0 & 0 & 0 & 0 & 1 & 0 & 0 & 0 & 0 & 0 & 0 & 0 & 0 & 0 \\ 0 & 0 & 0 & 0 & 0 & 0 & 0 & 0 & 1 & 0 & 0 & 0 & 0 & 0 & 0 & 0 \\ 0 & 0 & 0 & 0 & 0 & 1 & 0 & 0 & 0 & 0 & 0 & 0 & 0 & 0 & 0 & 0 \\ 1 & 0 & 0 & 0 & 0 & 0 & 0 & 0 & 0 & 0 & 0 & 0 & 0 & 0 & 0 & 0 \\ 0 & 1 & 0 & 0 & 0 & 0 & 0 & 0 & 0 & 0 & 0 & 0 & 0 & 0 & 0 & 0 \end{bmatrix}$$

Acknowledgements

The first author wishes to acknowledge the support of this research initially by the Natural Sciences and Engineering Research Council (NSERC) of Canada, and

Fig. 3.9: The Q matrix for $\lambda = 3, 2, 1$ calculated using MATLAB

$$
\begin{bmatrix}
0 & \frac{1}{8\sqrt{2}} & \frac{\sqrt{3}}{8\sqrt{2}} & \frac{\sqrt{3}}{8\sqrt{2}} & \frac{3}{8\sqrt{2}} & 0 & \frac{\sqrt{3}}{8\sqrt{2}} & \frac{3}{8\sqrt{2}} & \frac{\sqrt{10}}{16} & \frac{\sqrt{15}}{8\sqrt{2}} & 0 & \frac{\sqrt{10}}{16} & \frac{\sqrt{15}}{8\sqrt{2}} & \frac{\sqrt{15}}{8\sqrt{2}} & \frac{3\sqrt{10}}{16} & 0 \\
\frac{1}{8\sqrt{2}} & \frac{1}{16} & \frac{\sqrt{3}}{8} & \frac{\sqrt{3}}{8} & -\frac{3}{16} & \frac{\sqrt{3}}{8\sqrt{2}} & \frac{\sqrt{3}}{16} & \frac{3}{8} & -\frac{\sqrt{5}}{16} & 0 & \frac{\sqrt{15}}{8\sqrt{2}} & \frac{\sqrt{5}}{8} & -\frac{\sqrt{15}}{16} & -\frac{\sqrt{15}}{16} & 0 & \frac{3\sqrt{10}}{16} \\
\frac{\sqrt{3}}{8\sqrt{2}} & \frac{\sqrt{3}}{8} & -\frac{3}{16} & \frac{5}{16} & 0 & -\frac{1}{8\sqrt{2}} & -\frac{1}{8} & \frac{\sqrt{3}}{16} & 0 & \frac{3\sqrt{5}}{16} & \frac{3\sqrt{10}}{16} & -\frac{\sqrt{15}}{16} & 0 & 0 & -\frac{\sqrt{15}}{16} & -\frac{\sqrt{15}}{8\sqrt{2}} \\
\frac{\sqrt{3}}{8\sqrt{2}} & \frac{\sqrt{3}}{8} & \frac{5}{16} & -\frac{3}{16} & 0 & \frac{3}{8\sqrt{2}} & \frac{3}{8} & \frac{5\sqrt{3}}{16} & 0 & \frac{\sqrt{5}}{16} & -\frac{\sqrt{10}}{16} & -\frac{\sqrt{15}}{16} & 0 & 0 & -\frac{\sqrt{15}}{16} & -\frac{\sqrt{15}}{8\sqrt{2}} \\
\frac{3}{8\sqrt{2}} & -\frac{3}{16} & 0 & 0 & \frac{5}{16} & -\frac{\sqrt{3}}{8\sqrt{2}} & \frac{\sqrt{3}}{16} & 0 & \frac{3\sqrt{5}}{16} & \frac{\sqrt{15}}{8} & -\frac{\sqrt{15}}{8\sqrt{2}} & 0 & -\frac{\sqrt{15}}{16} & -\frac{\sqrt{15}}{16} & -\frac{\sqrt{5}}{8} & \frac{\sqrt{10}}{16} \\
0 & \frac{\sqrt{3}}{8\sqrt{2}} & -\frac{1}{8\sqrt{2}} & \frac{3}{8\sqrt{2}} & -\frac{\sqrt{3}}{8\sqrt{2}} & 0 & \frac{3}{8\sqrt{2}} & -\frac{\sqrt{3}}{8\sqrt{2}} & \frac{\sqrt{15}}{8\sqrt{2}} & -\frac{\sqrt{10}}{16} & 0 & \frac{\sqrt{15}}{8\sqrt{2}} & -\frac{\sqrt{10}}{16} & \frac{3\sqrt{10}}{16} & -\frac{\sqrt{15}}{8\sqrt{2}} & 0 \\
\frac{\sqrt{3}}{8\sqrt{2}} & \frac{\sqrt{3}}{16} & -\frac{1}{8} & \frac{3}{8} & \frac{\sqrt{3}}{16} & \frac{3}{8\sqrt{2}} & \frac{3}{16} & -\frac{\sqrt{3}}{8} & -\frac{\sqrt{15}}{16} & 0 & -\frac{\sqrt{10}}{16} & \frac{\sqrt{15}}{8} & \frac{\sqrt{5}}{16} & -\frac{3\sqrt{5}}{16} & 0 & -\frac{\sqrt{15}}{8\sqrt{2}} \\
\frac{3}{8\sqrt{2}} & \frac{3}{8} & \frac{\sqrt{3}}{16} & \frac{5\sqrt{3}}{16} & 0 & -\frac{\sqrt{3}}{8\sqrt{2}} & -\frac{\sqrt{3}}{8} & -\frac{1}{16} & 0 & -\frac{\sqrt{15}}{16} & -\frac{\sqrt{15}}{8\sqrt{2}} & -\frac{3\sqrt{5}}{16} & 0 & 0 & \frac{\sqrt{5}}{16} & \frac{\sqrt{10}}{16} \\
\frac{\sqrt{10}}{16} & -\frac{\sqrt{5}}{16} & 0 & 0 & \frac{3\sqrt{5}}{16} & \frac{\sqrt{15}}{8\sqrt{2}} & -\frac{\sqrt{15}}{16} & 0 & \frac{1}{16} & -\frac{\sqrt{3}}{8} & \frac{\sqrt{3}}{8\sqrt{2}} & 0 & \frac{5\sqrt{3}}{16} & \frac{\sqrt{3}}{16} & -\frac{3}{8} & \frac{3}{8\sqrt{2}} \\
\frac{\sqrt{15}}{8\sqrt{2}} & 0 & \frac{3\sqrt{5}}{16} & -\frac{\sqrt{5}}{16} & \frac{\sqrt{15}}{8} & -\frac{\sqrt{10}}{16} & 0 & -\frac{\sqrt{15}}{16} & -\frac{\sqrt{3}}{8} & -\frac{3}{16} & \frac{3}{8\sqrt{2}} & \frac{\sqrt{3}}{16} & -\frac{3}{8} & \frac{1}{8} & \frac{\sqrt{3}}{16} & -\frac{\sqrt{3}}{8\sqrt{2}} \\
0 & \frac{\sqrt{15}}{8\sqrt{2}} & \frac{3\sqrt{10}}{16} & -\frac{\sqrt{10}}{16} & -\frac{\sqrt{15}}{8\sqrt{2}} & 0 & -\frac{\sqrt{10}}{16} & -\frac{\sqrt{15}}{8\sqrt{2}} & \frac{\sqrt{3}}{8\sqrt{2}} & \frac{3}{8\sqrt{2}} & 0 & \frac{\sqrt{3}}{8\sqrt{2}} & \frac{3}{8\sqrt{2}} & -\frac{1}{8\sqrt{2}} & -\frac{\sqrt{3}}{8\sqrt{2}} & 0 \\
\frac{\sqrt{10}}{16} & \frac{\sqrt{5}}{8} & -\frac{\sqrt{15}}{16} & -\frac{\sqrt{15}}{16} & 0 & \frac{\sqrt{15}}{8\sqrt{2}} & \frac{\sqrt{15}}{8} & -\frac{3\sqrt{5}}{16} & 0 & \frac{\sqrt{3}}{16} & \frac{\sqrt{3}}{8\sqrt{2}} & -\frac{5}{16} & 0 & 0 & \frac{3}{16} & \frac{3}{8\sqrt{2}} \\
\frac{\sqrt{15}}{8\sqrt{2}} & -\frac{\sqrt{15}}{16} & 0 & 0 & -\frac{\sqrt{15}}{16} & -\frac{\sqrt{10}}{16} & \frac{\sqrt{5}}{16} & 0 & \frac{5\sqrt{3}}{16} & -\frac{3}{8} & \frac{3}{8\sqrt{2}} & 0 & \frac{3}{16} & -\frac{5}{16} & \frac{\sqrt{3}}{8} & -\frac{\sqrt{3}}{8\sqrt{2}} \\
\frac{\sqrt{15}}{8\sqrt{2}} & -\frac{\sqrt{15}}{16} & 0 & 0 & -\frac{\sqrt{15}}{16} & \frac{3\sqrt{10}}{16} & -\frac{3\sqrt{5}}{16} & 0 & \frac{\sqrt{3}}{16} & \frac{1}{8} & -\frac{1}{8\sqrt{2}} & 0 & -\frac{5}{16} & \frac{3}{16} & \frac{\sqrt{3}}{8} & -\frac{\sqrt{3}}{8\sqrt{2}} \\
\frac{3\sqrt{10}}{16} & 0 & -\frac{\sqrt{15}}{16} & -\frac{\sqrt{15}}{16} & -\frac{\sqrt{5}}{8} & -\frac{\sqrt{15}}{8\sqrt{2}} & 0 & \frac{\sqrt{5}}{16} & -\frac{3}{8} & \frac{\sqrt{3}}{16} & -\frac{\sqrt{3}}{8\sqrt{2}} & \frac{3}{16} & \frac{\sqrt{3}}{8} & \frac{\sqrt{3}}{8} & -\frac{1}{16} & \frac{1}{8\sqrt{2}} \\
0 & \frac{3\sqrt{10}}{16} & -\frac{\sqrt{15}}{8\sqrt{2}} & -\frac{\sqrt{15}}{8\sqrt{2}} & \frac{\sqrt{10}}{16} & 0 & -\frac{\sqrt{15}}{8\sqrt{2}} & \frac{\sqrt{10}}{16} & \frac{3}{8\sqrt{2}} & -\frac{\sqrt{3}}{8\sqrt{2}} & 0 & \frac{3}{8\sqrt{2}} & -\frac{\sqrt{3}}{8\sqrt{2}} & -\frac{\sqrt{3}}{8\sqrt{2}} & \frac{1}{8\sqrt{2}} & 0
\end{bmatrix}
$$

subsequently by the Foundation for Research, Science, and Technology (FRST) of New Zealand.

3.4.6 *Appendix*

Representation matrices for $\lambda = 3, 2, 1$ in the YY basis. The basis functions are ordered according to the last–letter order of the tableaux, as given in Figure 3.7.

$$(12) = \begin{vmatrix} 1 & & & & & & & & & & & \\ & 1 & & & & & & & & & & \\ & & -1 & & & & & & & & & \\ & & & 1 & & & & & & & & \\ & & & & -1 & & & & & & & \\ & & & & & 1 & & & & & & \\ & & & & & & 1 & & & & & \\ & & & & & & & -1 & & & & \\ & & & & & & & & 1 & & & \\ & & & & & & & & & -1 & & \\ & & & & & & & & & & -1 & \\ & & & & & & & & & & & 1 \\ & & & & & & & & & & & & -1 \\ & & & & & & & & & & & & & -1 \end{vmatrix}$$

$$(23) = \begin{vmatrix} 1 & & & & & & & & & & & & & & \\ & -\frac{1}{2} & \frac{\sqrt{3}}{2} & & & & & & & & & & & & \\ & \frac{\sqrt{3}}{2} & \frac{1}{2} & & & & & & & & & & & & \\ & & & -\frac{1}{2} & \frac{\sqrt{3}}{2} & & & & & & & & & & \\ & & & \frac{\sqrt{3}}{2} & \frac{1}{2} & & & & & & & & & & \\ & & & & & 1 & & & & & & & & & \\ & & & & & & -\frac{1}{2} & \frac{\sqrt{3}}{2} & & & & & & & \\ & & & & & & \frac{\sqrt{3}}{2} & \frac{1}{2} & & & & & & & \\ & & & & & & & & -\frac{1}{2} & \frac{\sqrt{3}}{2} & & & & & \\ & & & & & & & & \frac{\sqrt{3}}{2} & \frac{1}{2} & & & & & \\ & & & & & & & & & & -1 & & & & \\ & & & & & & & & & & & -\frac{1}{2} & \frac{\sqrt{3}}{2} & & \\ & & & & & & & & & & & \frac{\sqrt{3}}{2} & \frac{1}{2} & & \\ & & & & & & & & & & & & & -\frac{1}{2} & \frac{\sqrt{3}}{2} \\ & & & & & & & & & & & & & \frac{\sqrt{3}}{2} & \frac{1}{2} \\ & & & & & & & & & & & & & & -1 \end{vmatrix}$$

$$(34) = \begin{vmatrix} -\frac{1}{3} & \frac{\sqrt{8}}{3} & & & & & & & & & & & & & \\ \frac{\sqrt{8}}{3} & \frac{1}{3} & & & & & & & & & & & & & \\ & & 1 & & & & & & & & & & & & \\ & & & 1 & & & & & & & & & & & \\ & & & & -1 & & & & & & & & & & \\ & & & & & -\frac{1}{3} & \frac{\sqrt{8}}{3} & & & & & & & & \\ & & & & & \frac{\sqrt{8}}{3} & \frac{1}{3} & & & & & & & & \\ & & & & & & & 1 & & & & & & & \\ & & & & & & & & -1 & & & & & & \\ & & & & & & & & & -\frac{1}{3} & \frac{\sqrt{8}}{3} & & & & \\ & & & & & & & & & \frac{\sqrt{8}}{3} & \frac{1}{3} & & & & \\ & & & & & & & & & & & 1 & & & \\ & & & & & & & & & & & & -1 & & \\ & & & & & & & & & & & & & -1 & \\ & & & & & & & & & & & & & & -\frac{1}{3} & \frac{\sqrt{8}}{3} \\ & & & & & & & & & & & & & & \frac{\sqrt{8}}{3} & \frac{1}{3} \end{vmatrix}$$

$(45) =$

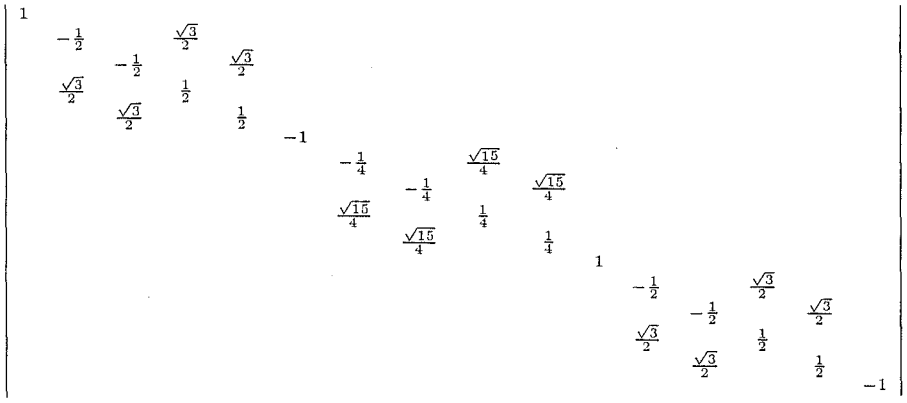

$(56) =$

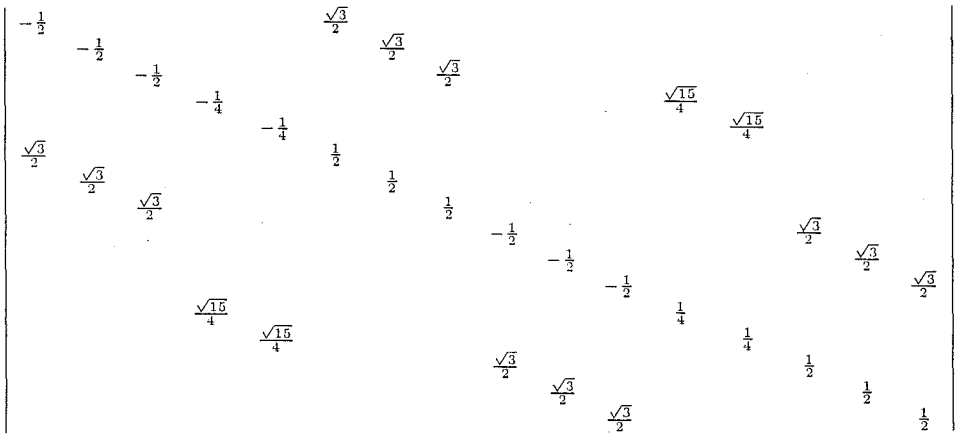

Representation matrices for $\lambda = 3, 2, 1$ in the $\overline{YY}$ basis. The basis functions are ordered according to the last–letter order of the tableaux, as given in Figure 3.7.

$(12) =$

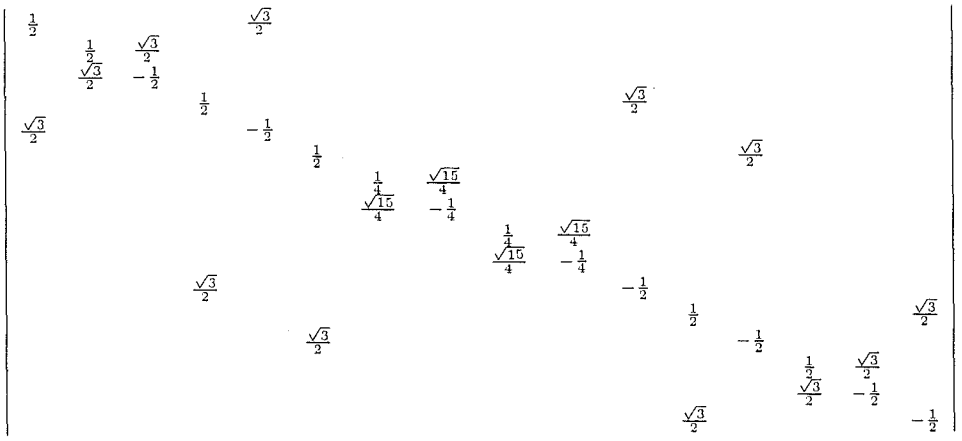

$$(23) = \begin{vmatrix}
\frac{1}{2} & & & & & & & & \frac{\sqrt{3}}{2} & & & & & & \\
 & -1 & & & & & & & & & & & & & \\
 & & 1 & & & & & & & & & & & & \\
 & & & -\frac{1}{4} & \frac{\sqrt{15}}{4} & & & & & & & & & & \\
 & & & \frac{\sqrt{15}}{4} & \frac{1}{4} & & & & & & & & & & \\
 & & & & & \frac{1}{2} & \frac{\sqrt{3}}{2} & & & & & & & & \\
 & & & & & \frac{\sqrt{3}}{2} & -\frac{1}{2} & & & & & & & & \\
\frac{\sqrt{3}}{2} & & & & & & & -\frac{1}{2} & & & & & & & \frac{\sqrt{3}}{2} \\
 & & & & & & & & -\frac{1}{2} & & & & & & \\
 & & & & & & & & & \frac{1}{2} & \frac{\sqrt{3}}{2} & & & & \\
 & & & & & & & & & \frac{\sqrt{3}}{2} & -\frac{1}{2} & & & & \\
 & & & & & & & & & & & -\frac{1}{4} & \frac{\sqrt{15}}{4} & & \\
 & & & & & & & & & & & \frac{\sqrt{15}}{4} & \frac{1}{4} & & \\
 & & & & & & & & & & & & & -1 & \\
 & & & & & & & & & & & & & & 1 \\
 & & & & & & & \frac{\sqrt{3}}{2} & & & & & & & -\frac{1}{2}
\end{vmatrix}$$

$$(34) = \begin{vmatrix}
-\frac{1}{3} & \frac{\sqrt{8}}{3} & & & & & & & & & & & & & \\
\frac{\sqrt{8}}{3} & \frac{1}{3} & & & & & & & & & & & & & \\
 & & \frac{1}{3} & & \frac{\sqrt{8}}{3} & & & & & & & & & & \\
 & & & 1 & & & & & & & & & & & \\
 & & \frac{\sqrt{8}}{3} & & -\frac{1}{3} & & & & & & & & & & \\
 & & & & & -1 & & & & & & & & & \\
 & & & & & & 1 & & & & & & & & \\
 & & & & & & & 1 & & & & & & & \\
 & & & & & & & & -1 & & & & & & \\
 & & & & & & & & & -1 & & & & & \\
 & & & & & & & & & & 1 & & & & \\
 & & & & & & & & & & & \frac{1}{3} & \frac{\sqrt{8}}{3} & & \\
 & & & & & & & & & & & -1 & & & \\
 & & & & & & & & & & & \frac{\sqrt{8}}{3} & -\frac{1}{3} & & \\
 & & & & & & & & & & & & & -\frac{1}{3} & \frac{\sqrt{8}}{3} \\
 & & & & & & & & & & & & & \frac{\sqrt{8}}{3} & \frac{1}{3}
\end{vmatrix}$$

$$(45) = \begin{vmatrix}
\frac{1}{2} & & & & & \frac{\sqrt{3}}{2} & & & & & & & & & \\
 & -1 & & & & & & & & & & & & & \\
 & & -1 & & & & & & & & & & & & \\
 & & & \frac{1}{2} & & & & & & & & & & & \\
 & & & & \frac{1}{2} & & & & & & & \frac{\sqrt{3}}{2} & & & \\
\frac{\sqrt{3}}{2} & & & & & -\frac{1}{2} & & & & & & & \frac{\sqrt{3}}{2} & & \\
 & & & & & & -\frac{1}{2} & & \frac{\sqrt{3}}{2} & & & & & & \\
 & & & & & & & -\frac{1}{2} & & \frac{\sqrt{3}}{2} & & & & & \\
 & & & & & \frac{\sqrt{3}}{2} & & & -\frac{1}{2} & & & & & & \\
 & & & & & & \frac{\sqrt{3}}{2} & & \frac{1}{2} & & & & & & \\
 & & & & & & & & & \frac{1}{2} & & & & & \frac{\sqrt{3}}{2} \\
 & & \frac{\sqrt{3}}{2} & & & & & & & & -\frac{1}{2} & & & & \\
 & & & \frac{\sqrt{3}}{2} & & & & & & & & -\frac{1}{2} & & & \\
 & & & & & & & & & & & & 1 & & \\
 & & & & & & & & & & & & & 1 & \\
 & & & & & & & & & \frac{\sqrt{3}}{2} & & & & & \frac{1}{2}
\end{vmatrix}$$

$$(56) = \begin{vmatrix}
-1 & & & & & & & & & & & & & & \\
 & -1 & & & & & & & & & & & & & \\
 & & -1 & & & & & & & & & & & & \\
 & & & -1 & & & & & & & & & & & \\
 & & & & -1 & & & & & & & & & & \\
 & & & & & 1 & & & & & & & & & \\
 & & & & & & 1 & & & & & & & & \\
 & & & & & & & 1 & & & & & & & \\
 & & & & & & & & -1 & & & & & & \\
 & & & & & & & & & -1 & & & & & \\
 & & & & & & & & & & -1 & & & & \\
 & & & & & & & & & & & 1 & & & \\
 & & & & & & & & & & & & 1 & & \\
 & & & & & & & & & & & & & 1 & \\
 & & & & & & & & & & & & & & 1 \\
 & & & & & & & & & & & & & & 1
\end{vmatrix}$$

3.5 *Permuting bases*

The dual basis in the last section corresponded to removing the lowest S_1 factor at each level, as opposed to the standard basis in which the highest S_1 factor is removed at each level. In this section we generalise that result to bases described in terms of the removal of any S_1 factor at each level. We interpret this as dealing with a standard basis on a rearranged list of labels. We show that the transformation matrix we require is a representation matrix for S_n in the standard basis.

The procedure closely follows Hamermesh's (Hamermesh 1962) derivation of the representation matrices in the standard basis. In his derivation, Hamermesh works recursively, assuming the representation matrices for the first $n-1$ elements are known and deriving the matrix for the transposition $(n-1, n)$. Here we consider choosing the set of $n-1$ elements to differ from the set of n elements by a different element than the last. We label the element excluded by p. (Thus "removing the box labelled p first".) Then given $\sigma \in S_n$ that leaves p invariant, there exists some permutation $\pi \in S_n$ such that for all such σ, the permutation $\pi\sigma\pi^{-1}$ leaves the object labelled n invariant. We can then proceed as Hamermesh did for the S_n–basis but with the permutation $\pi^{-1}\sigma\pi$ in our modified basis occupying the same role σ did in the S_n–basis.

It remains now to describe π. Clearly π needs to carry n to p, p to $p+1$, $p+1$ to $p+2$, and so on until $n-1$ to n, while at the same time leaving the other elements fixed. Hence,

$$\pi = \begin{pmatrix} 1 & 2 & \dots & p-1 & p & p+1 & \dots & n-1 & n \\ 1 & 2 & \dots & p-1 & p+1 & p+2 & \dots & n & p \end{pmatrix} \tag{3.15}$$

This is similar to the procedure carried out in the previous section and is perhaps best understood in the context of an example, which we shall give at the end of this section.

Having removed any factor at the S_n level, we can just as easily consider also removing any box at the S_{n-1}, and the S_{n-2} level, and so on. In particular, we can consider a variation on the split S_n–$S_{1,n-1}$–basis, where the S_{n-1}–basis is adapted, not to the standard basis, but to the group-subgroup chain $S_1 \times S_{b-1} \supset S_1 \times S_1 \times S_{b-2} \supset \dots \supset S_1 \times S_1 \times \dots \times S_1$, such that each factor is removed from the left. This describes the dual basis of the last section. Denoting a subgroup adapted to the dual basis $S_{\tilde{a}}$ we can write the dual basis of the previous section as S_n–$S_{1,\overline{n-1}}$, or simply as the $S_{\tilde{n}}$–basis. Clearly, setting p equal to one at each level in the basis chain produces the π of the previous section.

$$\pi = \begin{pmatrix} 1 & 2 & \dots & n-1 & n \\ n & n-1 & \dots & 2 & 1 \end{pmatrix}. \tag{3.16}$$

Note that in Hamel et al. (1996) $M^{\lambda}(\pi)$ was denoted by Q.

Another way of understanding this result is to look back to the discussion in section 3.2 and examine how the basis vectors are labelled. If we remove the boxes in the Young tableaux in a different order we will in general obtain a different

partition chain relating to a different Young tableaux for the same irrep. So we have the same irrep, just with all the labels mixed up. We still have a Ferrers diagram for each integer $i \leq n$.

Although those transformations are somewhat limited in value we can use them to calculate some of the transformation matrices of Chen, Collinson & Gao (1983). We illustrate our technique with a particular example, corresponding to the transformation between the S_5–basis and the S_5–$S_{1,4}$–basis for the irrep [3 2] (Chen, Collinson & Gao 1983, Table II.5).

According to the prescription in equation (3.16) the relevant permutation is $\begin{pmatrix} 1 & 2 & 3 & 4 & 5 \\ 5 & 1 & 2 & 3 & 4 \end{pmatrix}$, since $p = 1$ and the S_4 factor is Young–Yamanouchi adapted. The representation matrix, calculated using the MATLAB programs described in appendix D, is

$$M^{[3\ 2]}\left(\begin{pmatrix} 1 & 2 & 3 & 4 & 5 \\ 5 & 1 & 2 & 3 & 4 \end{pmatrix}\right) = \begin{pmatrix} \frac{-1}{3} & \frac{-\sqrt{2}}{3} & 0 & \frac{-\sqrt{2}}{\sqrt{3}} & 0 \\ \frac{-\sqrt{2}}{3} & \frac{1}{12} & \frac{-\sqrt{3}}{4} & \frac{1}{4\sqrt{3}} & \frac{-3}{4} \\ \frac{\sqrt{2}}{\sqrt{3}} & \frac{-1}{4\sqrt{3}} & \frac{-1}{4} & \frac{-1}{4} & \frac{-\sqrt{3}}{4} \\ 0 & \frac{-\sqrt{3}}{4} & \frac{-3}{4} & \frac{1}{4} & \frac{\sqrt{3}}{4} \\ 0 & \frac{3}{4} & \frac{-\sqrt{3}}{4} & \frac{-\sqrt{3}}{4} & \frac{1}{4} \end{pmatrix} . \quad (3.17)$$

In figures 3.3 and 3.4 we see that the first letter ordering, used by us above, and the last letter ordering, used by Chen, Collinson & Gao (1983), differ only in the order of the third and fourth basis vectors. So we exchange the third and fourth rows, and the third and fourth columns of (3.17). The basis vectors in the basis with the "non–standard" order correspond directly to the basis vectors in the standard basis. This gives the transformation matrix of Chen, Collinson & Gao (1983), although the first three rows differ in sign.

This approach, while general, still considers removing one box at a time. In the next chapter we move on to consideration of bases which are adapted to product subgroups with two factors greater than one.

4. TRANSFORMATIONS AMONG SPLIT BASES AND THE BLOCK SELECTIVE CONJECTURE

The hidden harmony is better than the obvious one [1]

In chapter 3 we concluded with a discussion of bases differing from the standard basis only in that the labels were relabelled. In section 4.1 we extend this permutation of labels to consider permuting split bases, thus considering the transformation from the S_n–$S_{a,b}$–basis to the S_n–$S_{b,a}$–basis.

In section 4.2 we discuss our block selective conjecture, a new technique for calculating the transformation matrices between split and standard bases. This technique builds upon the permutation structures discussed in considering transformations which reorder bases.

4.1 Split basis transformations

In this section we address the problem of transforming among split–bases, as defined in section 3.2, where the two factors in the direct product subgroup are simply swapped. That is, we are transforming from the S_n–$S_{a,b}$–basis to the S_n–$S_{b,a}$–basis.

Consider the matrix $M^{\lambda}_{a,b}(\pi^{a,b})$, where

$$\pi^{a,b} = \begin{pmatrix} 1 & 2 & \dots & b & b+1 & \dots & n-1 & n \\ a+1 & a+2 & \dots & n & 1 & 2\dots & a-1 & a \end{pmatrix}. \tag{4.1}$$

This matrix carries the representation matrices in the S_n–$S_{a,b}$–basis to the representation matrices in the S_n–$S_{b,a}$–basis by the relation

$$PM^{\lambda}_{a,b}(\pi^{a,b})M^{\lambda}_{a,b}(\sigma)(PM^{\lambda}_{a,b}(\pi^{a,b}))^{-1} = M^{\lambda}_{b,a}(\sigma), \tag{4.2}$$

where the P is a permutation matrix used to reorder the basis vectors so that the representation matrices are all ordered according to our standard prescription. We will give the procedure for obtaining P later in this section.

Before discussing this result in more detail, we consider an example. Consider the S_5–$S_{3,2}$–basis and the S_5–$S_{2,3}$–basis. The tableaux pairs used to label those bases are given in figures 4.1 and 4.2 respectively, each ordered according to our prescription in section 3.2.

As pointed out in section 3.3.2, we cannot calculate the representation matrices for the bridging permutations directly. We have instead calculated them using

[1] *Heraclitus, 6th–5th century B.C. Taken from Pickover (1997, p. 29)*

Fig. 4.1: The pair tableaux used to label the basis vectors, for the irrep [32], in the S_5–$S_{3,2}$–basis. They are ordered according to our prescription in section 3.2.

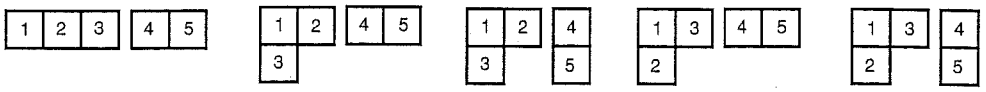

the split–standard transformation matrices of Chen, Collinson & Gao (1983). We give the matrix representations in figure 4.3. Having obtained the representation matrices one could use the technique of generator identification, described in section 3.3.2, to calculate the transformation matrix. However, our permutation technique is much more efficient. The appropriate permutation π for transforming from the S_5–$S_{2,3}$–basis to the S_5–$S_{3,2}$–basis is $\pi^{2,3} = \begin{pmatrix} 1 & 2 & 3 & 4 & 5 \\ 3 & 4 & 5 & 1 & 2 \end{pmatrix}$. To transform back the other way, the permutation is $\pi^{3,2} = \begin{pmatrix} 1 & 2 & 3 & 4 & 5 \\ 4 & 5 & 1 & 2 & 3 \end{pmatrix}$. The two representation matrices used in the transformations are then calculated, using a product of adjacent transpositions, to give,

$$M^{[3\ 2]}(\pi^{2,3}) = \begin{pmatrix} \frac{1}{3} & \frac{\sqrt{2}}{3} & \frac{\sqrt{2}}{\sqrt{3}} & 0 & 0 \\ \frac{-2\sqrt{2}}{3} & \frac{1}{6} & \frac{1}{2\sqrt{3}} & 0 & 0 \\ 0 & 0 & 0 & \frac{-1}{2} & \frac{-1\sqrt{3}}{2} \\ 0 & \frac{\sqrt{3}}{2} & \frac{-1}{2} & 0 & 0 \\ 0 & 0 & 0 & \frac{\sqrt{3}}{2} & \frac{-1}{2} \end{pmatrix}, \tag{4.3}$$

and

$$M^{[3\ 2]}(\pi^{3,2}) = \begin{pmatrix} \frac{1}{3} & \frac{2\sqrt{2}}{3} & 0 & 0 & 0 \\ \frac{-1\sqrt{2}}{3} & \frac{1}{6} & \frac{\sqrt{3}}{2} & 0 & 0 \\ 0 & 0 & 0 & \frac{-1}{2} & \frac{\sqrt{3}}{2} \\ \frac{-1\sqrt{2}}{\sqrt{3}} & \frac{1}{2\sqrt{3}} & \frac{-1}{2} & 0 & 0 \\ 0 & 0 & 0 & \frac{-1\sqrt{3}}{2} & \frac{-1}{2} \end{pmatrix}. \tag{4.4}$$

Fig. 4.2: The pair tableaux used to label the basis vectors, for the irrep [32], in the S_5–$S_{2,3}$–basis. They are ordered according to our prescription in section 3.2.

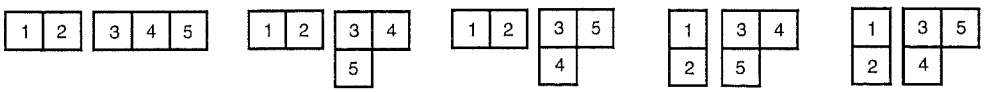

Fig. 4.3: The matrix representations of the generators of S_5, for the irrep [3 2]. In the S_5–$S_{3,2}$–basis (left column) and the S_5–$S_{2,3}$–basis (right column).

$$(12) = \begin{pmatrix} 1 & 0 & 0 & 0 & 0 \\ 0 & 1 & 0 & 0 & 0 \\ 0 & 0 & 1 & 0 & 0 \\ 0 & 0 & 0 & -1 & 0 \\ 0 & 0 & 0 & 0 & -1 \end{pmatrix} \qquad (12) = \begin{pmatrix} 1 & 0 & 0 & 0 & 0 \\ 0 & 1 & 0 & 0 & 0 \\ 0 & 0 & 1 & 0 & 0 \\ 0 & 0 & 0 & -1 & 0 \\ 0 & 0 & 0 & 0 & -1 \end{pmatrix}$$

$$(23) = \begin{pmatrix} 1 & 0 & 0 & 0 & 0 \\ 0 & -\frac{1}{2} & 0 & \frac{\sqrt{3}}{2} & 0 \\ 0 & 0 & -\frac{1}{2} & 0 & \frac{\sqrt{3}}{2} \\ 0 & \frac{\sqrt{3}}{2} & 0 & \frac{1}{2} & 0 \\ 0 & 0 & \frac{\sqrt{3}}{2} & 0 & \frac{1}{2} \end{pmatrix} \qquad (23) = \begin{pmatrix} -\frac{1}{3} & \frac{1}{3\sqrt{2}} & \frac{1}{\sqrt{6}} & \frac{1}{\sqrt{6}} & \frac{1}{\sqrt{2}} \\ \frac{1}{3\sqrt{2}} & -\frac{1}{6} & \frac{1}{\sqrt{3}} & \frac{1}{\sqrt{3}} & -\frac{1}{2} \\ \frac{1}{\sqrt{6}} & \frac{1}{\sqrt{3}} & \frac{1}{2} & -\frac{1}{2} & 0 \\ \frac{1}{\sqrt{6}} & \frac{1}{\sqrt{3}} & -\frac{1}{2} & \frac{1}{2} & 0 \\ \frac{1}{\sqrt{2}} & -\frac{1}{2} & 0 & 0 & \frac{1}{2} \end{pmatrix}$$

$$(34) = \begin{pmatrix} \frac{-1}{3} & \frac{\sqrt{2}}{3} & \frac{-1\sqrt{2}}{\sqrt{3}} & 0 & 0 \\ \frac{\sqrt{2}}{3} & \frac{5}{6} & \frac{1}{2\sqrt{3}} & 0 & 0 \\ \frac{-1\sqrt{2}}{\sqrt{3}} & \frac{1}{2\sqrt{3}} & \frac{1}{2} & 0 & 0 \\ 0 & 0 & 0 & \frac{-1}{2} & \frac{-1\sqrt{3}}{2} \\ 0 & 0 & 0 & \frac{-1\sqrt{3}}{2} & \frac{1}{2} \end{pmatrix} \qquad (34) = \begin{pmatrix} 1 & 0 & 0 & 0 & 0 \\ 0 & 1 & 0 & 0 & 0 \\ 0 & 0 & -1 & 0 & 0 \\ 0 & 0 & 0 & 1 & 0 \\ 0 & 0 & 0 & 0 & -1 \end{pmatrix}$$

$$(45) = \begin{pmatrix} 1 & 0 & 0 & 0 & 0 \\ 0 & 1 & 0 & 0 & 0 \\ 0 & 0 & -1 & 0 & 0 \\ 0 & 0 & 0 & 1 & 0 \\ 0 & 0 & 0 & 0 & -1 \end{pmatrix} \qquad (45) = \begin{pmatrix} 1 & 0 & 0 & 0 & 0 \\ 0 & -\frac{1}{2} & \frac{\sqrt{3}}{2} & 0 & 0 \\ 0 & \frac{\sqrt{3}}{2} & \frac{1}{2} & 0 & 0 \\ 0 & 0 & 0 & -\frac{1}{2} & \frac{\sqrt{3}}{2} \\ 0 & 0 & 0 & \frac{\sqrt{3}}{2} & \frac{1}{2} \end{pmatrix}$$

The appropriate permutation matrix for the transformations is

$$P = \begin{pmatrix} 1 & 0 & 0 & 0 & 0 \\ 0 & 1 & 0 & 0 & 0 \\ 0 & 0 & 0 & 1 & 0 \\ 0 & 0 & 1 & 0 & 0 \\ 0 & 0 & 0 & 0 & 1 \end{pmatrix} . \tag{4.5}$$

Having completed the example, we return to the general method.

In order to gain an appreciation of this method, we use some developments of Chen & Gao (1982), also used in Chen, Collinson & Gao (1983) to calculate the split–standard transformation coefficients. Chen, Collinson & Gao (1983) followed Chen & Gao (1982) in introducing complete sets of commuting operators (CSCOs). We give some details about the CSCOs here, more can be found in Chen & Gao (1982).

Let us define an operator, which Chen, Collinson & Gao (1983) call a two–cycle class operator, as

$$C(l) = \sum_{i>j=1}^{l} (i,j) . \tag{4.6}$$

For example, $C(4) = (12)+(13)+(14)+(23)+(24)+(34)$. Chen & Gao (1982) showed that the set of these two–cycle class operators $C(n), C(n-1), \ldots, C(2)$, of the permutation groups $S_n, S_{n-1}, \ldots, S_2$, constitute a complete set of commuting operators. We denote the set $\{C_n(i)\}$, noting that i runs from 2 to n.

Chen, Collinson & Gao (1983) refer to this complete set of commuting operators as the second kind of CSCO, or CSCO–II. The simultaneous eigenvectors of those operators constitute the Young–Yamanouchi basis of S_n. The correspondence with operators in the groups S_i, $2 \leq i \leq n$, is in accordance with the sequence of Ferrers diagrams used to label basis vectors of symmetric group irreps, or alternately the Young tableaux themselves (see section 3.2). Similarly, CSCO–IIs can be defined for the S_a and S_b groups appearing in the direct product subgroup in the split basis. Explicitly, the CSCO–II of S_a is,

$$\{C_a(i)\} = \{C(a), C(a-1), C(a-2), \ldots, C(2)\} , \tag{4.7}$$

where each $C(l)$ is as in equation 4.6. The CSCO–II of S_b is,

$$\{C'_b(i)\} = \{C'(b), C'(b-1), C'(b-2), \ldots, C'(2)\} , \tag{4.8}$$

where we add a prime to the two–cycle class operators, since the operators differ slightly to those in (4.7),

$$C'(l) = \sum_{i>j=a+1}^{a+l} (i,j) . \tag{4.9}$$

Since the S_a part of the split basis is already adapted to the standard basis, the transformation depends on transforming the S_b. The matrix elements in a particular basis are then restricted by the requirement that the appropriate CSCOs be diagonal. Thus the problem of transforming from standard to split basis requires the CSCO–II associated with the second factor group, S_b, to be diagonalised. We will return to that problem in section 4.2. For now we continue to consider transforming from the S_n–$S_{a,b}$–basis to the S_n–$S_{b,a}$–basis.

Chen & Gao (1982) point out that it is more convenient for computer computation to collect all the set of operators in a CSCO into one operator. Thus instead of $(C(a))$ we consider

$$M_1^{a,b} = \sum_{l=2}^{b} k_l C(l) \,, \tag{4.10}$$

and instead of $(C'(b))$ we consider

$$M_2^{a,b} = \sum_{l=2}^{b} k_l C'(l) \,. \tag{4.11}$$

The coefficients k_l and k'_l can be freely chosen (as long as the eigenvalues are non–degenerate), so that the CSCOs span classes of operators. Chen, Collinson & Gao (1983) choose $k_i = i + 7$. We have similar CSCO-IIs for the S_n–$S_{b,a}$–basis, obtained from (4.10) and (4.11) by swapping the symbols a and b.

In a basis the CSCO–IIs associated with that basis are diagonal. Thus, if we could map the CSCO–IIs of the S_n–$S_{a,b}$–basis into the CSCO–IIs of the S_n–$S_{b,a}$–basis, we would have a mapping between the two bases. But simply relabelling the elements is enough to do this. Consider first then our example from earlier in this section. For the S_5–$S_{2,3}$–basis and the S_5–$S_{3,2}$–basis,

$$M_1^{2,3} = k_2(1\ 2) \,, \tag{4.12}$$
$$M_2^{2,3} = k'_2(3\ 4) + k'_3\left[(3\ 4) + (3\ 5) + (4\ 5)\right] \,, \tag{4.13}$$
$$M_1^{3,2} = k_2(1\ 2) + k_3\left[(1\ 2) + (1\ 3) + (2\ 3)\right] \,, \tag{4.14}$$
$$M_2^{3,2} = k'_2(4\ 5) \,. \tag{4.15}$$

If we relabel the elements in the CSCOs of the S_5–$S_{2,3}$–basis, according to the permutation $\pi^{2,3} = \begin{pmatrix} 1 & 2 & 3 & 4 & 5 \\ 3 & 4 & 5 & 1 & 2 \end{pmatrix}$, for example, we will obtain the same form for the CSCOs as in the S_n–$S_{3,2}$–basis. The variation of k_l or k'_l generates the same class of operators, so that the permutation carries one class of operators to the other. Hence the operator that performs the transformation from the S_5–$S_{2,3}$–basis to the S_5–$S_{3,2}$–basis is the matrix $Q^{2,3} = M^{\lambda}(\pi^{2,3})P$, where

$$\pi^{2,3} = \begin{pmatrix} 1\,2\,3\,4\,5 \\ 3\,4\,5\,1\,2 \end{pmatrix} \,,$$

and P is again a matrix used to reorder the basis vectors. The permutation π obviously depends on the bases we are transforming between, but is independent of the representation.

Since adjacent transpositions are self invertible, it is clear that the permutation π is not unique. For this example, we need only insure that one of the $S_{2,3}$ labels 1 and 2 becomes one of the $S_{3,2}$ labels 4 and 5, and the other of those two $S_{2,3}$ labels becomes the other $S_{3,2}$ label. Thus, 1 to 5 and 2 to 4 is a valid alternative. Similarly the label 3 of $S_{2,3}$ could go to 2 of $S_{3,2}$, 4 of $S_{2,3}$ to 1 of $S_{3,2}$, leaving the label 5 of $S_{2,3}$ to go to 3 of $S_{3,2}$. So how can this freedom be explained? In the S_5–$S_{2,3}$–basis the adjacent transpositions (1 2) and (3 4) must be diagonal, since they are elements in the CSCO–II of that basis. Being orthogonal, they must also have ± 1 in each diagonal position. Thus, they can at most change the signs of rows of the matrix representation of π in the S_5–$S_{2,3}$–basis. (See for this example the representation matrices of (1 2) and (3 4) in the S_5–$S_{2,3}$–basis in figure (4.3).)

Returning to the general forms of the CSCO–IIs, from (4.10) and (4.11),

$$\begin{aligned} M_1^{a,b} &= k_2(1\,2) + k_3\left[(1\,2) + (1\,3) + (2\,3)\right] + \ldots \\ &\quad + k_a\left[(1\,2) + (1\,3) + (2\,3)\ldots(a-2,a) + (a-1,a)\right] \end{aligned} \tag{4.16}$$

$$\begin{aligned} M_2^{a,b} &= k_2'(a+1,a+2) + k_3'\left[(a+1,a+2) + (a+1,a+3) + (a+2,a+3)\right] \\ &\quad + \ldots + k_b[(a+1,a+2) + (a+1,a+3) + \ldots \\ &\quad + (n-2,n) + (n-1,n)] \end{aligned} \tag{4.17}$$

$$\begin{aligned} M_1^{b,a} &= k_2(1\,2) + k_3\left[(1\,2) + (1\,3) + (2\,3)\right] + \ldots \\ &\quad + k_b\left[(1\,2) + (1\,3) + (2\,3)\ldots(b-2,b) + (b-1,b)\right] \end{aligned} \tag{4.18}$$

$$\begin{aligned} M_2^{b,a} &= k_2'(b+1,b+2) + k_3'\left[(b+1,b+2) + (b+1,b+3) + (b+2,b+3)\right] \\ &\quad + \ldots + k_a[(b+1,b+2) + (b+1,b+3) \\ &\quad + \ldots(n-2,n) + (n-1,n)]\,, \end{aligned} \tag{4.19}$$

we see that the permutation given in equation (4.1) performs the transformation.

The permutation P which acts to reorder the basis vectors is simply calculated from the basis vectors. The effect of π on the basis vectors is to renumber the boxes in the pair of tableaux. The lower numbered boxes are then in the second tableau of the pair. But it is standard to have the lower numbered boxes in the first tableau of the pair. So we swap the first and second parts of all the basis tableaux. But now the new basis ordering will, in general, not be standard. The permutation P is required to standardise the ordering in the new basis. For the example considered, the permutation is simply swapping the third and fourth basis vectors.

One can also apply this CSCO analysis to derive the result in section 3.5, which is a special case. The bases referred to in that section relate to always removing one box at each level. In this section, we have considered bases where we remove more than one box, but only at one level. Bases can be defined with respect to product subgroups of S_n with three or more factors, for example S_n–$S_a \times S_b \times S_c$. Another alternative adaption for a basis is to have split–bases at

several levels. For example, a basis could be adapted to S_n, $S_a \times S_b, n = a + b$, and $S_c \times S_d, a = c + d$. All those bases can be rearranged using permutations derived from this CSCO analysis.

Before investigating the calculation of the split–standard transformation coefficients, we make one final point. Since one can transform between split–bases via the standard basis, a relationship between the split–standard transformation matrices and the reordering matrices can be obtained. This relationship can be written

$$T^{\lambda}_{a,b}(T^{\lambda}_{b,a})^t = M^{\lambda}_{b,a}(\pi^{b,a}) \,. \tag{4.20}$$

4.2 The block selective conjecture

The block selective conjecture is a method I have discovered for calculating the split–standard transformation coefficients. Although unproven, it builds on our results presented in the current and previous chapters.

The problem we want to solve is to find the matrix, $T^{\lambda}_{a,b}$, which satisfies equation (3.10), that is

$$M^{\lambda}_{a,b}(\sigma) = T^{\lambda}_{a,b} M^{\lambda}(\sigma)(T^{\lambda}_{a,b})^t \tag{4.21}$$

for all permutations σ of $n = a + b$ elements. We continue to use $M^{\lambda}(\sigma)$ as the matrix irrep of σ in the irrep λ.

Let us first describe this method in a formal step by step manner.

1. List in first letter order the tableaux representing the basis vectors of the standard basis. Store this list in L.

2. Using standard methods (Hamermesh 1962) and the basis vectors above, construct the representation matrix $Q = M^{\lambda}(\pi^{a,b})$, where the permutation

$$\pi^{a,b} = \begin{pmatrix} 1 & 2 & \dots & b & b+1 & \dots & n-1 & n \\ a+1 & a+2 & \dots & n & 1 & \dots & a-1 & a \end{pmatrix} . \tag{4.22}$$

3. Generate L', the list of pair tableaux for labelling the basis vectors of the split basis. The following procedure is used for each standard basis vector.

   a. Remove the boxes containing the last a labels, leaving a standard tableau T_1 of b boxes.

   b. Remove the boxes containing the first b labels, and use *jeu* (section 3.2) to obtain a standard tableau T_2 of a boxes.

   c. Apply the permutation $\pi^{a,b}$ in equation (4.22) to the labels in the pair of tableaux T_1, T_2.

   d. Since the lower labels are now in T_2 we reorder the pair tableaux so that the basis vectors are labelled by T_2, then T_1. This is the same action as we took in section 4.1.

4. Order the basis vectors in L' according to the standard prescription for split bases, in section 3.2. Record the permutation required to reorder the basis vectors. in P. Call the ordered list of split–basis vectors $\tilde{L}$.

5. Construct a block–selective matrix, $B = \{B_{ij}\}$. If the first tableau in the ith split–basis is equal to the sub–tableau of the first a boxes in the jth standard basis tableau, then $B_{ij} = 1$. Otherwise $B_{ij} = 0$.

6. Form $T_{ij} = B_{ij}(PQ)_{ij}$.

7. Normalise the rows of $T = \{T_{ij}\}$ and call the result T^N.

8. The matrix T^N is the transformation $T^{\lambda}_{a,b}$.

We have used this procedure to generate all the transformation coefficients of Chen, Collinson & Gao (1983), except for that corresponding to $T^{[3\ 2\ 1]}_{3,3}$. In that case, we do not obtain the rows relating to the product multiplicity correctly, although the other rows in the matrix are correct. We return to discuss product multiplicities in chapter 5.

There are a number of points to be made about this method, but let us first present an example which we use to illustrate some of those points. We do not give all the results we obtained, since they are the same (to within phases) as those given by Chen, Collinson & Gao (1983).

The case we shall consider is for the irrep [3 2], with the transformation from the standard to the S_5–$S_{2,3}$–basis. The basis vectors for the standard and split bases are given in figures 3.3 and 4.2, respectively. The permutation associated with our algorithm is

$$\pi^{2,3} = \begin{pmatrix} 1 & 2 & 3 & 4 & 5 \\ 3 & 4 & 5 & 1 & 2 \end{pmatrix} . \tag{4.23}$$

The representation matrix of this permutation in the standard basis is

$$Q = M^{2,3}(\pi^{2,3}) = \begin{pmatrix} \frac{1}{3} & \frac{\sqrt{2}}{3} & \frac{\sqrt{2}}{\sqrt{3}} & 0 & 0 \\ \frac{-1}{3\sqrt{2}} & \frac{-1}{3} & \frac{1}{2\sqrt{3}} & \frac{\sqrt{3}}{2} & 0 \\ \frac{-1}{\sqrt{6}} & \frac{-1}{\sqrt{3}} & \frac{1}{2} & \frac{-1}{2} & 0 \\ \frac{-1}{\sqrt{6}} & \frac{1}{2\sqrt{3}} & 0 & 0 & \frac{\sqrt{3}}{2} \\ \frac{-1}{\sqrt{2}} & \frac{1}{2} & 0 & 0 & \frac{-1}{2} \end{pmatrix} . \tag{4.24}$$

The results of step 3 are described in figure 4.4. Comparing the order of the pair tableaux in figure 4.4, with the standard ordering in figure 4.2, we see that the permutation matrix in step 4 of the algorithm is

$$P = \begin{pmatrix} 1 & 0 & 0 & 0 & 0 \\ 0 & 0 & 1 & 0 & 0 \\ 0 & 0 & 0 & 0 & 1 \\ 0 & 1 & 0 & 0 & 0 \\ 0 & 0 & 0 & 1 & 0 \end{pmatrix} . \tag{4.25}$$

Fig. 4.4: The relationship between split and standard tableaux for the [3 2] example, prescribed by the block–selective conjecture

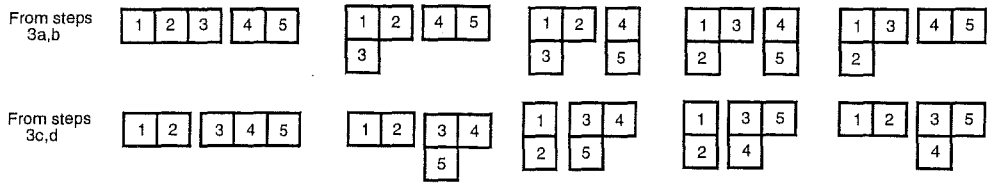

We see from figures 3.3 and 4.2 that the B matrix for this case is

$$B = \begin{pmatrix} 1 & 1 & 1 & 0 & 0 \\ 1 & 1 & 1 & 0 & 0 \\ 1 & 1 & 1 & 0 & 0 \\ 0 & 0 & 0 & 1 & 1 \\ 0 & 0 & 0 & 1 & 1 \end{pmatrix} . \tag{4.26}$$

As mentioned in section 3.5, where we also used the irrep [3 2] for an example, to compare our result with Chen, Collinson & Gao (1983) the third and fourth columns must be exchanged. The third and fourth rows have already been reordered by our algorithm to the split–basis order. The split–basis order we use is consistent with that used by Chen, Collinson & Gao (1983), so that no reordering on the split–basis vector need be used for the comparison.

Having presented an example, let us return to a general discussion of the block selective conjecture.

The critical feature in the technique is identifying the permutation matrix in the standard basis with the transformation matrix. This is clearly motivated by the CSCO material considered in section 4.1. The permutation $\pi^{a,b}$ is the same as that given in equation (4.1). The matrix representation of $\pi^{a,b}$ in the S_n–$S_{a,b}$–basis was used to transform from the S_n–$S_{a,b}$–basis to the S_n–$S_{b,a}$–basis. In the block selective conjecture however, the permutation is represented in the standard basis.

We mentioned in section 4.1 that the problem of transforming from the standard to the split–basis requires the diagonalisation of the CSCO–II associated with the second factor group, S_b. The CSCO–II associated with the first factor group S_a is already diagonal in the standard basis and we want it to remain diagonal after applying the transformation matrix. The matrix representation of the permutation $\pi^{a,b}$ in equation (4.22) will clearly diagonalise the CSCO–II of the second factor group, S_b. But it is also apparent that the CSCO–II of the first factor group, S_a, will, in general, no longer be diagonal. This problem is overcome by the block selection (steps 5 and 6), but we do not understand why. The block selection does not upset the diagonalisation of the CSCO–II associated with S_b either.

The permutation structure of this method emphasises the strong link between the matrix elements of permutations and the ratios of split–standard transformation coefficients. Effectively, each row of the transformation matrix is a row from the representation matrix of $\pi^{a,b}$ in the standard basis. The block selection, steps 5 and 6, ensures that the product of the split basis pair tableaux contains the standard basis tableaux.

This technique obviously needs further investigation. We need to confirm for irreps of larger symmetric groups that the correct results are obtained. Since the multiplicity solution is not correctly obtained, we can compare the numbers that appear with possible multiplicity separated coefficients. In spite of lacking rigour, this is an exciting method, particularly because of its directness. Whereas Chen, Collinson & Gao (1983) for example, require diagonalising a CSCO–II matrix in the standard basis, we have a formula for changing the representation matrix into the transformation matrix required.

5. MULTIPLICITY SEPARATION IN SYMMETRIC GROUP TRANSFORMATION COEFFICIENTS

> *In the past few years, the combinatorial substructure, based on the* jeu de taquin, *which underlies the formalism of S–functions and in particular the Littlewood–Richardson rule, has become much better understood*[1].

In this chapter we examine the problem of multiplicity separation in symmetric group transformation coefficients. We firstly introduce, in section 5.1, the Littlewood–Richardson rule and the multiplicities associated with it. We then consider the general case of the simplest *type* of multiplicity, which appears in the decomposition of S_n to the product subgroup $S_{n-3,3}$. A complete solution for this "removal of three boxes" has been obtained and the work has been submitted for publication. We include the submitted paper in section 5.2.

We give some selection rules for the product of a general irrep with basis tableaux of the irrep [2 1], in section 5.3. Those rules are implied by the non–multiplicity solutions given in section 5.2.

In section 5.4 we discuss progress in the investigation of more difficult multiplicities.

5.1 Product multiplicities and the Littlewood–Richardson rule

Consider a collection of n_1 particles, with symmetry described by the irrep $[\lambda_1]$ of S_{n_1}. Consider also a similar collection of n_2 particles, with symmetry described by the irrep $[\lambda_2]$ of S_{n_2}. The states of the combined system are going to have symmetries described by a representation of S_n, where $n = n_1 + n_2$. The representation of S_n is the outer product ($\otimes$) of the irreps of S_{n_1} and S_{n_2}. That representation can be decomposed into a sum of irreps of S_n. Thus one writes,

$$[\lambda_1] \otimes [\lambda_2] = [\lambda_2] \otimes [\lambda_1] = \sum_{[\lambda]} m^{\lambda}_{\lambda_1 \lambda_2} [\lambda] \,, \tag{5.1}$$

to indicate that the irrep $[\lambda]$ appears $m^{\lambda}_{\lambda_1 \lambda_2}$ times in the decomposition of the product of $[\lambda_1]$ and $[\lambda_2]$. The $m^{\lambda}_{\lambda_1 \lambda_2}$ are called multiplicities.

[1] Macdonald (1979, p.vi)

The Littlewood–Richardson rule is a combinatorial technique used to determine the $m^{[\lambda]}_{[\lambda_1][\lambda_2]}$, that is, which $[\lambda]$ occur in the product and how often. The Littlewood–Richardson rule was first stated, without proof, by Littlewood & Richardson (1934, p.119). The subsequent proof by Robinson (1938) was incomplete and remained so until it was completed by Macdonald (1979). According to Macdonald (1979), the first published proofs were due to Thomas (1974) and to Lascoux and Schützenbeger (1977). A more recent proof can be found in Sternberg (1994)

We present, without proof, the Littlewood–Richardson rule as a step by step operation acting on the partitions associated with the irreps $[\lambda_1]$ and $[\lambda_2]$ (Elliott & Dawber 1979*a*, Sternberg 1994, Stancu 1996). Since the outer product is commutative, see equation (5.1), it is common to order the irreps being multiplied, so that the second partition is of a number no higher than that of the first partition. Although it makes no difference to the rule we describe, we will assume this has been done, since it makes most calculations simpler. We denote the Ferrers diagrams associated with the partitions $[\lambda_1]$ and $[\lambda_2]$, F_1 and F_2 respectively.

(1) For each row i of F_2, place a number i in each box.

(2) Add the filled boxes of F_2 to F_1, using the following rules:

  (i) The i boxes are added before the $i+1$ boxes, for all i.

  (ii) With the addition of each box, a valid Ferrers diagram must be obtained.

  (iii) No identical numbers may appear in the same column.

  (iv) For each resulting diagram list the entries in the numbered boxes. The list is formed from right to left starting, with the top row and moving down. This list is the *word* of the added diagram. This word must be a *lattice permutation* for the diagram to be valid. This means that there must be at least as many is as $i+1$s, at any position in the word.

(3) The value of $m^{\lambda}_{\lambda_1\lambda_2}$ is then the number of tableaux of shape $[\lambda]$.

The problem we address in section 5.2 relates to the interesting problem of when $m^{\lambda}_{\lambda_1\lambda_2} > 1$. We say in that case, that a multiplicity exists. More specifically, we sometimes say that we have a multiplicity $m^{\lambda}_{\lambda_1\lambda_2}$ case. The significance is that the Littlewood–Richardson rule then no longer gives a one–to–one correspondence between the shapes $[\lambda_1]$ and $[\lambda_2]$, and the shape $[\lambda]$. This leaves a freedom in choosing how the pair shapes are related to the two or more $[\lambda]$ shapes.

Let us illustrate the Littlewood–Richardson rule with an example relevant to our analysis of the split–standard transformation coefficients. We look at the first occurrence of a multiplicity, in the product of the irreps [2 1] and [2 1]. In figure 5.1, we give the valid diagrams generated by the Littlewood–Richardson rule.

Fig. 5.1: The diagrammatic representation of the Littlewood–Richardson rule for the example given in equation (5.2). We have included the lattice permutations associated with each diagram

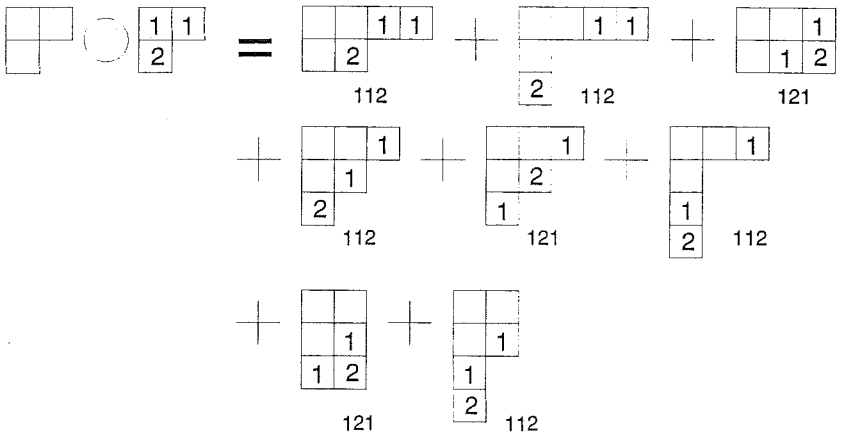

We see therefore, that the outer product of the irrep [2 1] with the irrep [2 1] is,

$$[2\,1]\otimes[2\,1] = [4\,2]+[4\,1\,1]+[3\,3]+2[3\,2\,1]+[3\,1\,1\,1]+[2\,2\,2]+[2\,2\,1\,1]\,. \quad (5.2)$$

Of particular interest are the two copies of the irrep [3 2 1], a multiplicity two case. The split–standard transformation coefficients for the irrep [3 2 1], in the S_6–basis, and the [2 1], [2 1] pair, in the S_6–$S_{3,3}$–basis, have been considered on two previous occasions (Chen, Collinson & Gao 1983, Pan & Chen 1993). However, different solutions were given. The very nature of the multiplicity implies an ambiguity in the relationship between the pair of [2 1] irreps and the copies of the irrep [3 2 1]. We will prove in section 5.2 that the Littlewood–Richardson rule does not fix a particular choice of the relationship. There are not enough equations to specify the split–standard transformation coefficients.

5.2 Multiplicity separation in symmetric group transformation coefficients

This section contains a slightly modified version of a paper submitted for publication to the Journal of Physics A:Mathematical and General Physics (December 1997).

Multiplicity separation in symmetric group transformation coefficients.

L F McAven, A M Hamel and P H Butler

Department of Physics and Astronomy, University of Canterbury, Christchurch, New Zealand.

We consider matrices transforming between the standard Young–Yamanouchi basis of the symmetric group S_n and the basis where three boxes are removed together. We derive closed formulas for all such transformation coefficients. A choice of multiplicity separation is required when the three removed boxes are all non-adjacent. The multiplicity separation links the S_n–$S_{n-3,3}$–basis functions with the basis functions of the standard basis. We discuss considerations which can be applied to obtain simple forms for the transformation coefficients and for the multiplicity separation. Some simple, natural separations are obtained. However, we show that the combinatorial and algebraic structure of the Littlewood–Richardson rule, also known as the pattern calculus, does not fix the separation.

Classification number: 02.20

5.2.1 Introduction

The coupling $(3jm)$ and recoupling $(6j)$ coefficients of unitary groups are often useful for simplifying many–body calculations in physics and chemistry. Schur–Weyl duality relates the unitary group coefficients to different types of symmetric group coefficients (Elliott, Hope & Jahn 1954, Kramer 1968, Vanagas 1971, Haase & Butler 1984*a*, Haase & Butler 1984*b*). In particular, the unitary group $6j$ are related to subduction coefficients of S_n. The S_n subduction coefficients transform between one basis adapted to S_n, to $S_a \times S_b$, and then to $S_a \times S_e \times S_d$; and a second basis, adapted to S_n, to $S_c \times S_d$, and to $S_a \times S_e \times S_d$, where $a+b = a+e+d = c+d = n$.

The subduction coefficients can be expressed in terms of transformation coefficients between the standard Young–Yamanouchi basis and a second basis adapted to a direct product subgroup of the form $S_a \times S_b$. Elliott, Hope & Jahn (1954) introduced this particular type of non–standard basis. We call it a *split–basis*, and denote it as the S_n–$S_{a,b}$–basis.

Studies of the split–standard transformation coefficients have yielded general numerical techniques for calculating the transformation, coefficients (Horie 1964,

Kaplan 1961, Kaplan 1975, Chen, Collinson & Gao 1983, Pan & Chen 1993) as well as closed formulas for particular cases (Kaplan 1975, Suryanarayana & Rao 1982). The method of Pan & Chen (1993) is particularly useful since it provides q–dependent algebraic solutions for the Hecke algebra, $H_n(q)$. Suryanarayana & Rao (1982) extend a formula obtained by Horie (1964) to give a closed formula for irreps of S_b with at most two columns. These results include multi–dimensional irreps of S_b but no multiplicities in the product of the irreps of S_a and S_b. We are particularly interested in this product multiplicity (Butler 1981, p.25)). Both Chen, Collinson & Gao (1983) and Pan & Chen (1993) present calculations for at least one case with such a multiplicity. However, they choose different multiplicity separations.

The first symmetric group in which a product multiplicity occurs is S_6, where the decomposition into the direct product subgroup $S_3 \times S_3$ contains multiplicity two terms. We derive the general solution for S_n–$S_{n-b,b}$–bases for $b = 3$ in analogy with Kaplan's solution for removing two boxes from the right (where $b = 2$). We use the linear equation method of Pan & Chen (1993) to derive the formulas for the coefficients associated with shapes remaining after removing the S_a irrep from the S_n irrep.

For the case where product multiplicities occur, we give the general solution before a choice of multiplicity separation is made. We discuss considerations which can be applied to obtain simple forms for the separation and thus for the transformation coefficients. We find a class of particularly simple separations.

The paper is structured as follows.

In section 5.2.2 we define the standard basis and the split–bases. We provide the background for constructing the representation matrices in the standard basis. Various orderings of the basis tableaux are given.

In section 5.2.3 we outline and discuss the linear equation method of Pan & Chen (1993). We describe a general method for building up the matrix containing the entire set of linear equations which must be satisfied. This allows us to reduce the problem of finding the transformation coefficients, to one of solving a homogeneous system of linear equations.

In section 5.2.4 we derive algebraic formulas. We first re–derive the formula of Kaplan (1975) for removing two boxes from the right. We then consider the cases relating to the removal of three boxes from the right, that is, the cases defined by the relative positions of the last three boxes in the basis tableaux. For small hook lengths these cases are related. For example, cases $\mathcal{C}_1$ and $\mathcal{C}_2$ with a hook length of 1 reduce to the solutions associated with cases $\mathcal{A}$ and $\mathcal{B}$. We give the coefficients for the case in which a multiplicity two term occurs in the decomposition of the tableaux.

In section 5.2.5 we present six considerations which can be used to identify which sets of transformation coefficients are to be considered simple. We demonstrate that one set of separations is particularly simple. We also relate the phases of the various cases by restrictions of the type mentioned above.

We summarise and discuss our results in section 5.2.6.

5.2.2 *Symmetric group bases: Description and ordering*

In this section we outline the necessary background on symmetric group bases and on the ordering of basis tableaux. We will work with the standard orthogonal basis for symmetric group representations (see, for example, Rutherford (1948), Hamermesh (1962), Young (1977)) and will also call it the S_n–basis.

The irreducible representations of S_n may be labelled by partitions $[\lambda]$ of n. A partition of n into i parts may be written as $[\lambda_1, \lambda_2, \ldots, \lambda_i]$ such that $\sum_{j=1}^{i} \lambda_j = n$ and the λ_j are weakly decreasing. By forming a left-justified array with λ_j boxes on the j^{th} row and with the k^{th} row below the $(k-1)^{th}$ row, we obtain a Ferrers diagram. Filling the Ferrers diagram with the numbers $1, \ldots, n$ such that each number appears exactly once and values strictly increase across rows and down columns, generates Young tableaux. The number of Young tableaux for a given irrep is equal to the dimension of the irrep, so that each basis vector can be associated with a unique tableau.

Since any permutation can be generated as a product of adjacent transpositions, it suffices to consider just the representation matrices for such transpositions. These matrices can be calculated simply using the tableau parameter of *axial distance*. The axial distance between the box containing i, at (x_i, y_i), and the box containing j, at (x_j, y_j), is defined as $\tau_{ij} = (x_j - x_i) - (y_j - y_i)$. Define also ρ_{ij} to be the reciprocal of the axial distance τ_{ij}. We write the S_n–basis representation matrix for the adjacent transposition $(k-1, k)$ in the representation λ as $M^{\lambda}(k-1, k)$. For a more general permutation, σ, we write $M^{\lambda}(\sigma)$.

In a row of the matrix $M^{\lambda}((k-1, k))$ corresponding to a tableau, T, all elements are zero unless interchanging $k-1$ and k in T gives a valid tableau, S, or, unless $k-1$ and k are in the same row or column of T. When such an S exists the element in the positions (T, S) (and (S, T)) in $M^{\lambda}((k-1, k))$ is $\sqrt{1 - \rho_{k-1,k}^2}$. The diagonal term (T, T) is $-\rho_{k-1,k}$, (and therefore (S, S) is $\rho_{k-1,k}$). If T has $k-1$ and k in the same row (respectively column) there clearly cannot exist an S, and the element is $+1$ (respectively -1), corresponding to the previous statement with $\rho = \mp 1$. (see Rutherford (1948, pp.41–49); also Young (1977, VI, pp.217–218) and Hamermesh (1962, section 7.7, pp. 214–231)).

An alternative basis for S_n has basis functions adapted to S_n and to the direct product subgroup $S_a \times S_b$, where $a + b = n$. Each factor group, the S_a–basis and the S_b–basis, are standard basis adapted. We shall call this alternative basis a *split–basis* and denote it as the S_n–$S_{a,b}$–basis. In the trivial case, namely when $b = 1$, the S_n–$S_{n-1,1}$–basis is the S_n–basis. One can label the basis vectors of the split basis by a pair of tableaux, one with a boxes and the other with b boxes. These tableaux can be used to determine the representation matrices of the adjacent transpositions in the split bases, by using the method described above for the standard basis tableaux. The first tableau is used if the adjacent transposition is

in S_a; the second tableau is used if the adjacent transposition is in S_b.

In defining different bases we make use of a combinatorial technique known as *jeu de taquin*. *Jeu de taquin*, or simply *jeu*, is due to Schützenbeger (1963) and is a procedure for removing a box from a Young tableau and then filling the hole created by this removal, so that the ultimate result is itself a Young tableau of standard shape. *Jeu* can be described as follows:

> Remove a box from the Young tableau. Examine the number in the box to the right and the number in the box below the position of the removed box. Select the number that is smallest and move the box containing it into the empty space. While there are still boxes to the right in the same row as the hole, or lower in the same column as the hole, repeat this procedure.

Authors have made different order choices on the set of Young tableaux. One popular ordering is *last letter order*. This is the ordering used by Chen, Collinson & Gao (1983), who call it decreasing page order. When we say that a is lower in a tableau than b, we mean a is either in a lower row, or in the same row and to the right of b. Given two tableaux, T and U, T precedes U in last letter order if the last letter of disagreement between the two is lower in T than in U. The complementary ordering is *first letter order*. Given two tableaux, T and U, T precedes U in first letter order if the first letter of disagreement between T and U is lower in U than it is in T (Young 1977, IV, p. 258). We will also make use of a third kind of ordering, one dependent on the form of the split–basis. Chen, Collinson & Gao (1983) use this ordering for the split–basis without describing it in the manner we do now. Pan & Chen (1993) use a similar ordering, but are not completely consistent in their tables.

To define this third ordering, we first establish a correspondence between a tableau of shape λ in the S_n–basis and a pair of tableaux of shape (α, β) in the split S_n–$S_{a,b}$–basis. Given a tableau of shape λ in the S_n–basis, remove the tableau, α, consisting of the boxes containing the first a labels. This tableau is the first in the $S_a \times S_b$ pair. Then apply *jeu* to the remaining b boxes to make a tableau of standard shape, β. This tableau β is the second in the $S_a \times S_b$ pair. Note that this correspondence is many–to–one, so that a single $\alpha\beta$ pair can have many tableaux of shape λ in the S_n–basis that map to it. Order the tableau pairs (α, β) in the S_n–$S_{a,b}$–basis in the following manner. First adopt an order on partitions such that $\lambda < \rho$ if $\lambda_i = \rho_i$ for $1 \leq i \leq k$ and $\lambda_k > \rho_k$. Now order the (α, β) pairs by the α, using the partition order defined above if the shapes in two pairs are different, and by first letter order if the shapes are the same. Then for pairs in which the first components are identical, order by the second components, again first using partition order, and then first letter order. When a pair occurs more than once, the situation known as product multiplicity, order those pairs according to the first letter ordered list of standard tableaux from which they came. This gives a unique ordering for any split basis.

5.2.3 *A linear equation method*

For particular cases, Pan & Chen (1993) tabulate matrices that transform from the standard to the split–bases of the Hecke algebras. The Hecke algebra, $H_n(q)$, is a generalisation of the symmetric group algebra. However, rather than the adjacent transpositions squaring to one as for the symmetric group, an additional factor is obtained. Specifically $g_i^2 = g_i(q - q^{-1}) + 1$. It is clear that setting $q = 1$ will reduce to the symmetric group relation.

To obtain symmetric group results from the tables in Pan & Chen (1993) one simply sets $q = 1$, so that their $[x]$ and $[x]'$ both reduce to x by L'Hôpital's rule. A few sign errors in the tables are to be noted (Table 5, row 7, column 4; Table 6, row 4, column 2; and Table 6, row 11, column 6).

We devote this section to formalising the method Pan & Chen (1993) applied to the calculation of transformations between the $H_n(q)$–basis and a split $H_n(q)$–$H_{n_1,n_2}(q)$–basis, briefly generalising the basis notation introduced in section 5.2.2 to suit the Hecke algebra.

Assume that $\{g_1, g_2, \ldots, g_{n-1}\}$ is a set of adjacent transpositions which generate $H_n(q)$. Assume also that $\{g_1, g_2, \ldots, g_{n_1-1}\}$ generates $H_{n_1}(q)$ and that $\{g_{n_1+1}, \ldots, g_{n-1}\}$ generates $H_{n_2}(q)$.

The expansion of the $H_n(q)$–$H_{n_1,n_2}(q)$–basis in terms of the $H_n(q)$–basis is given by Pan & Chen (1993, equation (2.9)) as

$$\left|[\lambda], \tau \begin{matrix} \alpha & \beta \\ m_1 & m_2 \end{matrix} \right\rangle_q = \sum_m \left| \begin{matrix} [\lambda] \\ m \end{matrix} \right\rangle_q \left\langle \begin{matrix} [\lambda] \\ m \end{matrix} \right| [\lambda], \tau \begin{matrix} \alpha & \beta \\ m_1 & m_2 \end{matrix} \Big\rangle_q . \tag{5.3}$$

Pan & Chen (1993) derive two sets of linear equations (Pan & Chen 1993, equations (3.1a) and (3.1b)) using the g_i and the g_j generators. An equivalent means of deriving the sets is to consider the left and right actions of an operator between a state labelled by a standard basis vector and a state labelled by a split basis vector.

$$\begin{aligned} \left\langle [\lambda], \tau \begin{matrix} \alpha & \beta \\ m_1 & m_2 \end{matrix} \middle| \mathrm{g}_{i,j} \middle| \begin{matrix} [\lambda] \\ m \end{matrix} \right\rangle_q &= \left\langle [\lambda], \begin{matrix} \tau & \alpha & \beta \\ & m_1 & m_2 \end{matrix} \middle| \left(\mathrm{g}_{i,j} \middle| \begin{matrix} [\lambda] \\ m \end{matrix} \right\rangle_q \right) \\ &= \left(\left\langle [\lambda], \tau \begin{matrix} \alpha & \beta \\ m_1 & m_2 \end{matrix} \middle| \mathrm{g}_{i,j} \right) \middle| \begin{matrix} [\lambda] \\ m \end{matrix} \right\rangle_q \end{aligned} \tag{5.4}$$

The action of the generators are known and depend upon various axial distances: from i to $i+1$ in the first tableau of the split basis (d_{1i}), from j to $j+1$ in the second tableau of the split basis (d_{2j}), and from i to $i+1$ and j to $j+1$ in the standard tableau (d_i and d_j). However, the first set of equations obtained by Pan & Chen have not been suitably reduced since the axial distance from i to $i+1$ in the standard basis (d_i) is the same as the axial distance from i to $i+1$ in the split–basis (d_{1i}). Thus in equation (3.1a) of Pan & Chen (1993) the left hand side

vanishes, the coefficients on the right hand side are equal to within a sign, and we obtain

$$\left\langle \begin{matrix}[\lambda]\\ m'\end{matrix} \middle| [\lambda],\tau \begin{matrix}\alpha & \beta\\ m_1 & m_2\end{matrix} \right\rangle_q = \pm \left\langle \begin{matrix}[\lambda]\\ m\end{matrix} \middle| [\lambda],\tau \begin{matrix}\alpha & \beta\\ m_1' & m_2\end{matrix} \right\rangle_q . \tag{5.5}$$

This is simply a representation of Schur's lemma. As Chen, Collinson & Gao (1983) point out, the transformation coefficients are independent of m_1 because of Schur's lemma.

The other set of equations is,

$$\begin{aligned}\left(\frac{q^{d_j}}{[d_j]} - \frac{q^{d_j^b}}{[d_j^b]}\right) \left| \begin{matrix}[\lambda]\\ m\end{matrix} \right\rangle_q \left\langle \begin{matrix}[\lambda]\\ m\end{matrix} \middle| [\lambda],\tau \begin{matrix}\alpha & \beta\\ m_1 & m_2\end{matrix} \right\rangle_q \\ = \left(\frac{[d_j^b+1][d_j^b-1]}{[d_j^b]^2}\right)^{\frac{1}{2}} \left| \begin{matrix}[\lambda]\\ m\end{matrix} \right\rangle_q \left\langle \begin{matrix}[\lambda]\\ m\end{matrix} \middle| [\lambda],\tau \begin{matrix}\alpha & \beta\\ m_1 & m_2'\end{matrix} \right\rangle_q \\ - \left(\frac{[d_j+1][d_j-1]}{[d_j]^2}\right)^{\frac{1}{2}} \left| \begin{matrix}[\lambda]\\ m\end{matrix} \right\rangle_q \left\langle \begin{matrix}[\lambda]\\ m'\end{matrix} \middle| [\lambda],\tau \begin{matrix}\alpha & \beta\\ m_1 & m_2\end{matrix} \right\rangle_q .\end{aligned} \tag{5.6}$$

In addition to those relationships there are orthonormality conditions on the transformation coefficients,

$$\sum_m \left\langle \begin{matrix}[\lambda]\\ m\end{matrix} \middle| [\lambda],\tau \begin{matrix}\alpha & \beta\\ m_1 & m_2\end{matrix} \right\rangle_q^2 = 1 . \tag{5.7}$$

The equations given by Schur's lemma allow us to solve our system in blocks, where the blocks are labelled by αm_1. The different m_1 are not mixed, orthogonality is satisfied, and the blocks can be solved separately. This is implicit in the very nature of the two bases since the internal behaviour of the subgroup S_a on the first a labels is the same. Within each block there are sub–blocks of rows which are related by the generators of the second subgroup. However, because of orthonormality, we calculate the complete block.

Having described the equations generated, we will now construct a computational method of formally constructing the general system of linear equations. Because blocks can be treated independently, the matrix is constructed for a particular block. We will construct a matrix X for the transformation coefficients appearing in the block which contains all the equations from equation (5.4) obtained using the generators of the second factor group in the direct product subgroup.

All the pair tableaux labelling this block will have the same first tableau. They may differ in the second tableau. When we remove the shape associated with the irrep α from the upper left hand corner of the shape associated with the irrep λ, we obtain a skew shape. We call the number of ways of filling this skew shape N. N can be calculated according to Young tableaux rules and is equal to the

dimension of our block. This skew shape is used in section 5.2.4 to distinguish among different cases for removing α shapes made of $n-3$ boxes.

We order the list of transformation coefficients first on the split tableaux, then on the standard tableaux, and then store in the list L. Thus, if we have a list of four standard tableaux, $U = \{A, B, C, D\}$ and an associated list of four pair tableaux, $V = \{A', B', C', D'\}$, we would have

$$\begin{aligned} L = \{&\langle A'|A\rangle, \langle A'|B\rangle, \langle A'|C\rangle, \langle A'|D\rangle, \\ &\langle B'|A\rangle, \langle B'|B\rangle, \langle B'|C\rangle, \langle A'|D\rangle, \\ &\langle C'|A\rangle, \langle C'|B\rangle, \langle C'|C\rangle, \langle A'|D\rangle, \\ &\langle D'|A\rangle, \langle D'|B\rangle, \langle D'|C\rangle, \langle D'|D\rangle\} \, . \end{aligned}$$

The basis tableaux in both bases are ordered in U and V according to the conventions described in section 5.2.2. We define m =dim(U)=dim(V).

The first row of X corresponds to the two–way expansion of $\langle A'|g_a|A\rangle$, as in equation (5.4). The next m^2-1 rows relate to expansion associated with the generator g_a of the other transformation coefficients in L . We then move to the next generator, g_{a+1}, and return to the start of L. We know from (5.6) that at most three entries in each row of X will be non–zero, so that X is sparse.

The algorithm for calculating X using the representation matrices of the generators g_j, $a+1 \leq j \leq n-1$ in each basis, is

$X = \text{zeros}[(n-b)m^2, m^2]$	initialise X to zeros
for i from 1 to b	loop over generators
for j from 1 to m	loop over split basis
for k from 1 to m	loop over standard basis
$r = (i-1)m^2 + (j-1)m + k$	which row to fill
for p from 1 to m	operator action
$s = (p-1)m + k$	column for left action
$t = (j-1)m + p$	column for right action
$X[r,s] = X[r,s] + N[j,p]$	insert value
$X[r,t] = X[r,t] - M[k,p]$	insert negative value
end p loop	
end k loop	
end j loop	
end i loop	

where we denote the matrix representations for the generator g_j in the representation λ, by $M^{\lambda}(g_j) \equiv M$ in the standard basis and by $M^{\lambda}_{a,b}(g_j) \equiv N$ in the split–basis.

This algorithm can be modified to allow one to consider the calculation of non–square blocks of transformation coefficients, as we require in section 5.2.4 for the 4×6 block with the multiplicity separation. Not all the equations in X are required, but this algorithm ensures that no information is overlooked. The redundant equations in X are removed by applying Gauss–Jordan elimination to obtain reduced row echelon form. Because the algebraic conditions are the same for

transformation coefficients differing only in the product multiplicity, one needs only calculate a sub–block associated with one multiplicity. The solutions for the other multiplicities can be obtained simply by a relabelling of variables, but orthonormality conditions between those sub–blocks must also be considered.

The procedure in the algorithm is equivalent to listing all the equations described by

$$T^{a,b}M(g_i) = M^{a,b}(g_i)T^{a,b} \,, \tag{5.8}$$

where the generators g_i are those for the second subgroup in the split basis.

With X constructed, we solve the homogeneous system of equations

$$XL = 0, \tag{5.9}$$

together with the orthonormality conditions, equation (5.7). For cases without product multiplicities, as described earlier, we need only make phase choices.

5.2.4 Formulas for removing three boxes

Consider a general transformation from the S_n–basis to the S_n–$S_{n-b,b}$–basis. We can split the transformation matrix into cases associated with the shape of the tableau obtained by removing $n-b$ blocks from the basis tableau of the S_n–basis. This produces two shapes, α and λ/α. The first is standard and associated with irreps of the S_{n-b} subgroup; the second shape is skew and associated with (non–standard) irreps of the S_b subgroup. Standardising the second shape gives the second irrep of the pair labelling the split basis, β. Permutations cannot change the shape of the first irrep of the pair. Indeed as Chen, Collinson & Gao (1983) point out Schur's lemma furthermore implies that the transformation coefficient is the same for each basis vector of this first irrep. Thus we can split the transformation coefficient matrix into blocks. The blocks are of the dimension, $|\lambda/\alpha|$, of the skew shape remaining after removing the first $n-b$ boxes. The basis vectors of the split basis associated with the basis vectors of the S_n–basis are given by the process described in section 5.2.2.

Each of the dimension one irreps, $[b]$ and $[1^b]$, will always give rise to a single 1×1 block with a simple phase freedom.

Let us first consider the two–box example of Kaplan (1975). There are three cases. See figure 5.2. The transformation coefficients of the first and last are phases ± 1. The interesting case is $\mathcal{B}$.

We begin by ordering the basis tableaux according to the prescription of section 5.2.2. Label them alphabetically according to this order. Consider then the two–way expansions, equation (5.4), of the entries on the diagonal of the 2×2 transformation matrix,

$$\begin{aligned} \langle A'|(n-1,n)|A\rangle &= \langle A'|A\rangle \\ &= -\frac{1}{d}\langle A'|A\rangle + \frac{\sqrt{d^2-1}}{d}\langle A'|B\rangle \,, \end{aligned} \tag{5.10}$$

Fig. 5.2: The skew shapes remaining after the removal of $(n-2)$ boxes from the left

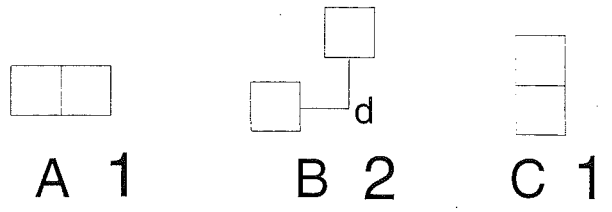

where d is the absolute value of the axial distance from the box containing $n-1$ to the box containing n, in the tableau labelled A. With the same d,

$$\begin{aligned}\langle B'|(n-1,n)|B\rangle &= -\langle B'|B\rangle \\ &= \frac{1}{d}\langle B'|A\rangle + \frac{\sqrt{d^2-1}}{d}\langle B'|B\rangle \end{aligned} \tag{5.11}$$

Applying normality gives, with θ a phase ± 1,

$$\begin{pmatrix} \theta\sqrt{\frac{d-1}{2d}} & \theta\sqrt{\frac{d+1}{2d}} \\ -\theta\sqrt{\frac{d+1}{2d}} & \theta\sqrt{\frac{d-1}{2d}} \end{pmatrix}. \tag{5.12}$$

Notice that the ordering differs from that of Kaplan (1975, equation (2.65), p.51)

Now let us proceed to removing three boxes. The cases are listed in figure 5.3, which gives the skew shape and the relevant dimension for the associated transformation matrix.

Fig. 5.3: The skew shapes remaining after the removal of $(n-3)$ boxes from the left.

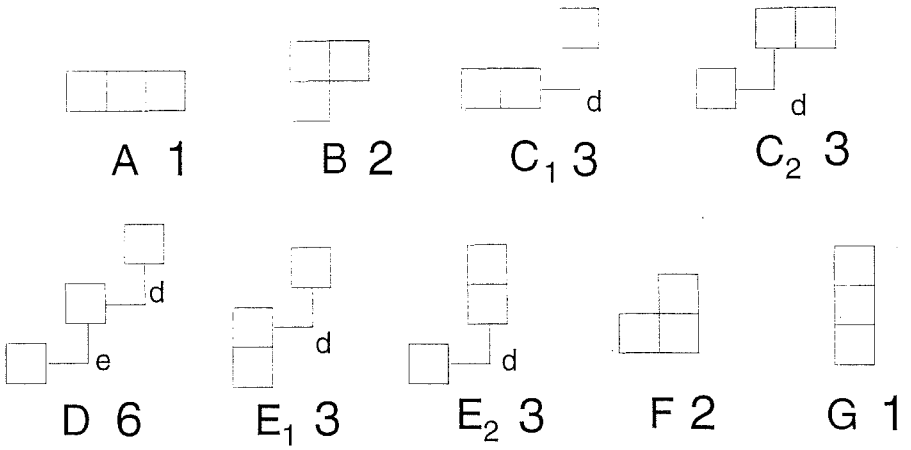

We used the package MAPLE to implement our algorithm of section 5.2.3. This gives the general formulas which follow. The formulas depend on the va-

rious hook lengths, $d, e, f = d+e, d_+ = d+1$ as well as augmented hook lengths $h_\pm = h \pm 1$. Two phases, θ and ϕ, occur in the multiplicity free cases.

Case $\mathcal{A}$ Completely symmetric, θ.

Case $\mathcal{B}$

$$\begin{pmatrix} \theta & 0 \\ 0 & \theta \end{pmatrix}. \tag{5.13}$$

Case $\mathcal{C}_1$

$$\begin{pmatrix} \theta\sqrt{\frac{d_-}{3d_+}} & \theta\sqrt{\frac{d_-d_{++}}{3dd_+}} & \theta\sqrt{\frac{d_{++}}{3d}} \\ -\phi\sqrt{\frac{d_{++}}{6d_+}} & -\phi\frac{d_{++}}{\sqrt{6dd_+}} & \phi\sqrt{\frac{2d_-}{3d}} \\ -\phi\sqrt{\frac{d_{++}}{2d_+}} & \phi\sqrt{\frac{d}{2d_+}} & 0 \end{pmatrix}. \tag{5.14}$$

Case $\mathcal{C}_2$

$$\begin{pmatrix} \theta\sqrt{\frac{d_-}{3d_+}} & \theta\sqrt{\frac{d_-d_{++}}{3dd_+}} & \theta\sqrt{\frac{d_{++}}{3d}} \\ -\phi\sqrt{\frac{2d_{++}}{3d_+}} & \phi\frac{d_-}{\sqrt{6d_+d}} & \phi\sqrt{\frac{d_-}{6d}} \\ 0 & -\phi\sqrt{\frac{d_+}{2d}} & \phi\sqrt{\frac{d_-}{2d}} \end{pmatrix}. \tag{5.15}$$

Case $\mathcal{D}$ The multiplicity part of this case corresponds to the four central rows, and is given in the equations in (4.9) below. The first and last rows do not have multiplicity freedom, and are

$$\begin{pmatrix} \theta\sqrt{\frac{d_-e_-f_-}{6def}} & \theta\sqrt{\frac{d_-e_+f_-}{6def}} & \theta\sqrt{\frac{d_+e_-f_-}{6def}} & \theta\sqrt{\frac{d_-e_+f_+}{6def}} & \theta\sqrt{\frac{d_+e_-f_+}{6def}} & \theta\sqrt{\frac{d_+e_+f_+}{6def}} \\ \phi\sqrt{\frac{d_+e_+f_+}{6def}} & -\phi\sqrt{\frac{d_+e_-f_+}{6def}} & -\phi\sqrt{\frac{d_-e_+f_+}{6def}} & \phi\sqrt{\frac{d_+e_-f_-}{6def}} & \phi\sqrt{\frac{d_-e_+f_-}{6def}} & -\phi\sqrt{\frac{d_-e_-f_-}{6def}} \end{pmatrix} \tag{5.16}$$

Case $\mathcal{E}_1$

$$\begin{pmatrix} \theta\sqrt{\frac{d_-}{2d}} & \theta\sqrt{\frac{d_+}{2d}} & 0 \\ -\theta\sqrt{\frac{d_-}{6d}} & \theta\frac{d_-}{\sqrt{6d_+d}} & \theta\sqrt{\frac{2d_{++}}{3d_+}} \\ \phi\sqrt{\frac{d_{++}}{3d}} & -\phi\sqrt{\frac{d_-d_{++}}{3d_+d}} & \phi\sqrt{\frac{d_-}{3d_+}} \end{pmatrix}. \tag{5.17}$$

Case $\mathcal{E}_2$

$$\begin{pmatrix} 0 & -\theta\sqrt{\frac{d}{2d_+}} & -\theta\sqrt{\frac{d_{++}}{2d_+}} \\ -\theta\sqrt{\frac{2d_-}{3d}} & -\theta\frac{d_{++}}{\sqrt{6d_+d}} & \theta\sqrt{\frac{d_{++}}{6d_+}} \\ \phi\sqrt{\frac{d_{++}}{3d}} & -\phi\sqrt{\frac{d_-d_{++}}{3d_+}} & \phi\sqrt{\frac{d_-}{3d_+}} \end{pmatrix}. \tag{5.18}$$

Case $\mathcal{F}$

$$\begin{pmatrix} \frac{\theta}{2} & \frac{\sqrt{3}\theta}{2} \\ \frac{\sqrt{3}\theta}{2} & -\frac{\theta}{2} \end{pmatrix}. \tag{5.19}$$

Case $\mathcal{G}$ Completely anti-symmetric, θ.

We now return to consideration of the four central rows of case $\mathcal{D}$, the multiplicity case. The system of equations includes three orthonormality equations, thus three independent phase choices exist, θ, ϕ, ψ. There is one free factor governing multiplicity separation. We express all coefficients in terms of two judiciously chosen variables, x and y and their ratio, $r = y/x$. We let

$$x = 1/\sqrt{6def(2de + d - e + 1)(1 + 3d_+d_-e_+e_-f_+f_-r^2)} \tag{5.20}$$

The solutions, where a_{ij} denotes the element in the ith row and jth column of the four central rows of $\mathcal{D}$, are

$$a_{11} = \sqrt{d_-/d_+}\, a_{13} \qquad a_{12} = \sqrt{f_-/f_+}\, a_{14} \qquad a_{15} = \sqrt{e_-/e_+}\, a_{16}$$

$$\begin{aligned} a_{13} &= -d_+\sqrt{f_-}\,[\theta e_{++}x + 3\psi d_-e_+e_-f_+y] \\ a_{14} &= \sqrt{d_+d_-e_+e_-f_+}\,[2\theta x - 3\psi f_+f_-y] \\ a_{16} &= \sqrt{e_+e_-f_+}\,[-\theta d_{--}x + 3\psi d_+d_-e_+f_-y] \end{aligned}$$

$$a_{21} = \sqrt{d_-/d_+}\, a_{23} \qquad a_{22} = \sqrt{f_-/f_+}\, a_{24} \qquad a_{25} = \sqrt{e_-/e_+}\, a_{26}$$

$$\begin{aligned} a_{23} &= -\sqrt{3d_+d_-e_+e_-f_+}\,[x + \phi d_+e_{++}f_-y] \\ a_{24} &= f_+\sqrt{3f_-}\,[-x + 2\phi d_+d_-e_+e_-y] \\ a_{26} &= e_+\sqrt{3d_+d_-f_-}\,[x - \phi d_{--}e_-f_+y] \end{aligned}$$

$$a_{31} = -\sqrt{d_+/d_-}\, a_{33} \qquad a_{32} = -\sqrt{f_+/f_-}\, a_{34} \qquad a_{35} = -\sqrt{e_+/e_-}\, a_{36}$$

$$a_{33} = d_-\sqrt{3f_-}\,[-\theta ex + \psi d_+e_+e_-f_+y]$$
$$a_{34} = \psi(2de + d - e + 1)f_-\sqrt{3d_+d_-e_+e_-f_+}\,y$$
$$a_{36} = \sqrt{3e_+e_-f_+}\,[\theta dx + \psi d_+d_-e_-f_-y]$$

$$a_{41} = -\sqrt{d_+/d_-}\,a_{43} \qquad a_{42} = -\sqrt{f_+/f_-}\,a_{44} \qquad a_{45} = -\sqrt{e_+/e_-}\,a_{46}$$

$$a_{43} = \sqrt{d_+d_-e_+e_-f_+}\,[x - 3\phi d_-ef_-y] \tag{5.21}$$
$$a_{44} = (2de + d - e + 1)\sqrt{f_-}\,x$$
$$a_{46} = e_-\sqrt{d_+d_-f_-}\,[x + 3\phi de_+f_+y]$$

5.2.5 Choices of phase and multiplicity separation

We want to find the simplest and most natural form for these symmetric group transformation coefficients. There are a number of important considerations in this regard.

I The transformation coefficients should be chosen to be real if possible. (In sections 5.2.3 and 5.2.4 the expressions assume this reality choice.)

II The general formulas obtained depend only upon the hook lengths, and are independent of n. Thus phases and the multiplicity separation should be chosen independent of n.

III When either of the hook lengths d or e is unity, the multiplicity is lifted. The expression for the multiplicity two coefficients must reduce to the multiplicity free solutions.

IV The multiplicity separation is to be chosen so that a maximal number of zero coefficients is obtained.

V It is desirable to have the coefficients expressible as a single surd of the form $a\sqrt{b}/c$, with a, b, c integers.

VI We ask that the prime factors which occur in the surds are as small as possible (relative to d and e).

Butler (1981, p.241) has raised some of these considerations before. Butler (1981) proved that some transformation coefficients, in particular the set of T–D_2 $3jm$, satisfy neither I nor V. Butler & Ford (1979) also proved that IV and VI were equivalent for octahedral $6j$ and derived a table of $6j$ which had both smaller prime numbers and more zeros than Griffith (1962).

In section 5.2.4 we expressed the coefficients in a form so that the above considerations may be easily taken into account.

Particular choices of x (and y) will cause various pairs of coefficients to vanish. There are twelve such zero conditions, which are distinct, so that consideration IV gives a maximum of two zeros. All zero conditions satisfy V. Indeed, only if $r = y/x$ is a rational function of d and e do all the coefficients satisfy V. Pan & Chen (1993) choose a separation that satisfies V, but not IV.

Zero conditions on coefficients which differ only in the labelling of the multiplicity, for example (a_{11}, a_{13}) and (a_{21}, a_{23}), give sets of coefficients differing only in the multiplicity label. This symmetry allows us to retain just the six zero conditions associated with first and third row coefficients.

Of the six distinct zero conditions we now ask which satisfy VI. We see that the largest potentially prime factors in the transformation coefficients appear in x, $\sqrt{2de + d - e + 1}$ and $\sqrt{1 + 3d_+d_-e_+e_-f_+f_-r^2}$. The former is of order two in hook lengths, but the latter, which can be written

$$\sqrt{1 + 3(d^2 - 1)(e^2 - 1)(f^2 - 1)r^2}\,, \tag{5.22}$$

is potentially troublesome. However, for all of the zero conditions, we can factorise this expression into terms of no greater than order two in d and e. For example, setting $a_{35} = a_{36} = 0$ gives $r = -\theta d/(\psi d_+d_-e_-f_-)$, so that (5.22) reduces to

$$\sqrt{(2d^2 + 2de + 2d + e - 1)(2de + d - e + 1)/(d_+d_-e_-f_-)}\,. \tag{5.23}$$

To distinguish between the six zero conditions let us use III to look at the restriction of hook lengths so that the multiplicity is lifted. This occurs when either d or e is unity. However, because of the d_-e_- term in (5.20), the dependence of x on r is lost. Putting this degeneracy aside and setting $d = e = 1$ in (5.21) we obtain the submatrix

$$\begin{pmatrix} 0 & 0 & -\theta & 0 & 0 & 0 \\ 0 & -\frac{1}{2} & 0 & -\frac{\sqrt{3}}{2} & 0 & 0 \\ 0 & 0 & 0 & 0 & -\theta & 0 \\ 0 & -\frac{\sqrt{3}}{2} & 0 & \frac{1}{2} & 0 & 0 \end{pmatrix}. \tag{5.24}$$

From figure 5.3 we see that those coefficients reduce to those for cases $\mathcal{B}$ and $\mathcal{F}$, given in (5.13) and (5.19) respectively. The second and fourth columns relate to $\mathcal{F}$ and the third and fifth to $\mathcal{B}$. The first and last columns correspond to the irreps $[1^3]$ and $[3]$, not $[2\,1]$, and so must be zero. Four of the six zero conditions have zeros in positions that either conflict directly with (5.24), or with the corresponding matrices when only one of d or e is unity.

The six considerations for simplicity do not strongly distinguish between the two remaining solutions: (a_{12}, a_{14}) and (a_{32}, a_{34}). The magnitudes of coefficients

for the former condition are dependent upon phase choices. Choosing $\psi\phi\theta = 1$ gives the simplest magnitudes, and the resulting coefficients are related to coefficients of the (a_{32}, a_{34}) solution. Thus we conclude that the solution associated with this (a_{32}, a_{34}) zero condition is the simplest and thus best choice of multiplicity separation. Defining $\alpha = \sqrt{6def(2de + e - d + 1)}$ we have our solution as

$$\begin{array}{ll} a_{13} = -\theta d_+ e_{++}\sqrt{f_-}/\alpha & a_{23} = -\sqrt{3d_+d_-e_+e_-f_+}/\alpha \\ a_{14} = 2\theta\sqrt{d_+d_-e_+e_-f_+}/\alpha & a_{24} = -f_+\sqrt{3f_-}/\alpha \\ a_{16} = -\theta d_{--}\sqrt{e_+e_-f_+}/\alpha & a_{26} = e_+\sqrt{3d_+d_-f_-}/\alpha \\ a_{33} = -\theta e d_-\sqrt{3f_-}/\alpha & a_{43} = \sqrt{d_+d_-e_+e_-f_+}/\alpha \\ a_{34} = 0 & a_{44} = (2de + d - e + 1)\sqrt{f_-}/\alpha \\ a_{36} = \theta d\sqrt{3e_+e_-f_+}/\alpha & a_{46} = e_-\sqrt{d_+d_-f_-}/\alpha \end{array} \tag{5.25}$$

This is the choice of multiplicity separation made by Chen, Collinson & Gao (1983) for the $d = e = 2$ case. The choice of Pan & Chen (1993), for the Hecke algebras (see section 5.2.3) is different. They introduce a symmetry requirement on their S_6 separation which is inconsistent with our consideration IV. Both published solutions for S_6 satisfy VI, having the largest prime in a surd as 5. (Note that there are a few errors in the tables of Chen *et al* : Table I.1 of phase factors Λ^{μ}_{m}, the 6th factor for [3 1 1] has the wrong sign; Table II.16 $\{1122\}$ with 1 has the wrong sign; Table II.17 $\{2111\}$ with 8 should be 5 rather than 0; Table II.22 $\{2132\}$ with 16 should be 2 rather than 0).

Let us now use the considerations II, III and IV to examine phase choices for all solutions.

For $d = 1$, cases $\mathcal{C}_1, \mathcal{C}_2$ and $\mathcal{E}_1, \mathcal{E}_2$ collapse to cases $\mathcal{A}, \mathcal{B}, \mathcal{F}$ and $\mathcal{G}$. This gives the following relations between the phases.

$$\begin{array}{llll} \theta_{C_1} = \theta_A & \phi_{C_1} = -\theta_F & \theta_{C_2} = \theta_A & \phi_{C_2} = -\theta_B \\ \theta_{E_1} = \theta_B & \phi_{E_1} = \theta_G & \theta_{E_2} = -\theta_F & \phi_{E_2} = \theta_G \end{array} \tag{5.26}$$

Setting $d = e = 1$ in the first and last rows of case $\mathcal{D}$, as given in section 5.2.4, we find that

$$\theta_D = \theta_A \quad \phi_D = \theta_G \,. \tag{5.27}$$

We thus need to choose four phases. We choose,

$$\theta_A = \theta_B = -\theta_F = \theta_G = 1, \tag{5.28}$$

where we use the negative θ_F so that $\theta_G = \phi_{C_2}$ in (5.26).

5.2.6 Summary

The investigation in this paper was motivated by three factors. First, a general formula for the split–standard transformation coefficients is not available and we

wished to extend the two box formulas of Kaplan (1975) to the case of three boxes. Second, we observe that Pan & Chen (1993) and Chen, Collinson & Gao (1983) differ in their choices of multiplicity for the first situation where such a choice is necessary. The third, and main motivation, was the desire to find out if the Littlewood–Richardson rule was enough to give a canonical multiplicity separation.

We have presented the explicit formula for the transformation coefficients between the standard (Young–Yamanouchi) basis and the split–basis corresponding to the removal of three boxes. The results are presented in terms of the nine cases distinguished by the skew shape remaining after removing $n-3$ boxes from the left. We have obtained the general multiplicity two solutions for the S_n–$S_{n-3,3}$–basis. We have discussed six considerations so as to compare transformation coefficients for simplicity. The simpler separations were found to correspond to one of twelve zero conditions. These occurred in pairs linked by relabelling the multiplicity. Two of these six pairs matched the solutions of degenerate cases. We finally fixed upon a solution where phases and magnitudes had their simplest numerical form.

In our complete solution to this multiplicity problem we have proved that the Littlewood–Richardson rule (the pattern calculus of (Biedenharn & Louck 1981)) does not provide a specific separation. When no multiplicities exist, the Littlewood Richardson rule gives the pattern relations between the split and standard bases. But the pattern relations implicit in the combinatorial structure of the Littlewood Richardson rule do not determine a canonical set of basis functions for the bases labelled by multiplicity labels. Rather, a choice must be made using criteria beyond the Littlewood Richardson rule.

We reviewed and extended considerations for making the choice of the multiplicity separation. We showed that in this $S_n \rightarrow S_n$–$S_{n,n-3}$–basis transformation, these six considerations could be simultaneously satisfied. A next step for a combinatorial recipe for a multiplicity separation could be to look at the first multiplicity three case. Note that this case first occurs in the decomposition of $[4\ 3\ 2\ 1]$ of S_{10} into $[3\ 2\ 1] \times [3\ 1]$ of $S_6 \times S_4$.

5.3 *Zero coefficients and selection rules on three boxes*

Section 5.2 contains solutions for the three box removal case, S_n–$S_{n-3,3}$–basis transformation. We here explore one aspect of note.

For some of the cases without multiplicity, the transformation matrix contains some zero coefficients. In case $\mathcal{B}$, equation (5.13), the off–diagonal entries are zero. In each of the cases $\mathcal{C}_1, \mathcal{C}_2, \mathcal{D}_1$ and $\mathcal{D}_2$, equations (5.14)–(5.18), a different "corner" entry of the matrix is zero.

Each of those zeros arise in our results because the relations generated by the algorithm imply each of those zero coefficients are equal to the negative of themselves. Those zeros are selection rules for the product of a general irrep with a basis vector of the irrep [2 1]. We give those selection rules in figures 5.4 and 5.5.

Fig. 5.4: Three of the selection rules obtained for the multiplication of an arbitrary irrep with the basis vectors of the irrep [2 1]. The case letters correspond to the case, in section 5.2, from which the rule to the left has been obtained

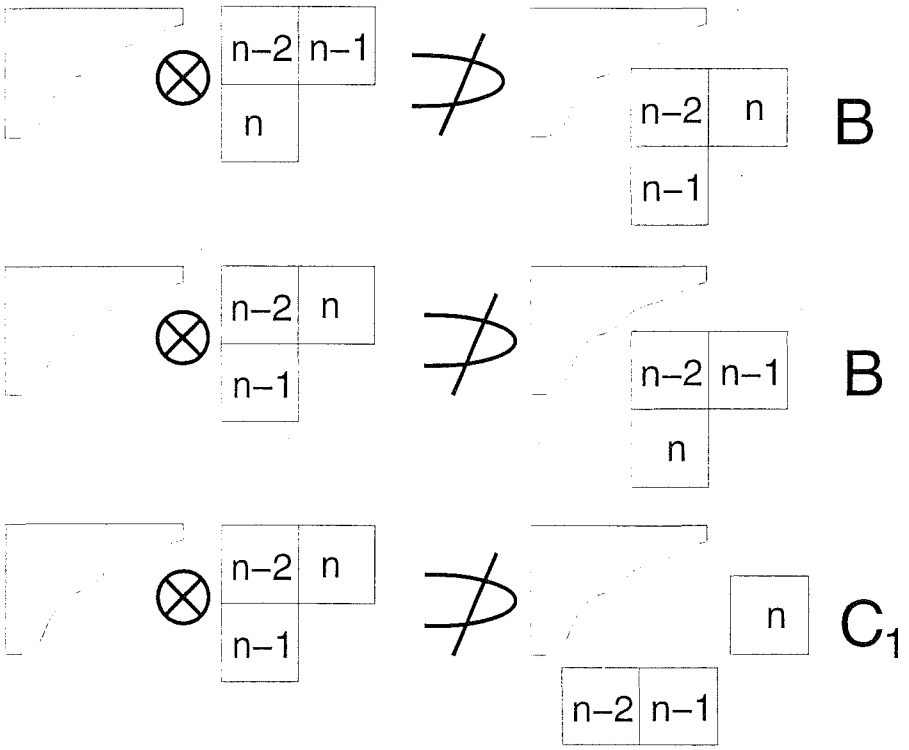

It is of interest and signifance to note that the selection rules are not provided by the Littlewood–Richardson rule for the product of irreps (see section 5.1). The Littlewood–Richardson rule considers the product of irreps or shapes, rather than basis vectors or tableaux. The rules we have given can, however, be simply proven using *Jeu de taquin*. For all the zero coefficients, the symmetry of the at-

Fig. 5.5: Three of the selection rules obtained for the multiplication of an arbitrary irrep with the basis vectors of the irrep [2 1]. The case letters correspond to the case, in section 5.2, from which the rule to the left has been obtained

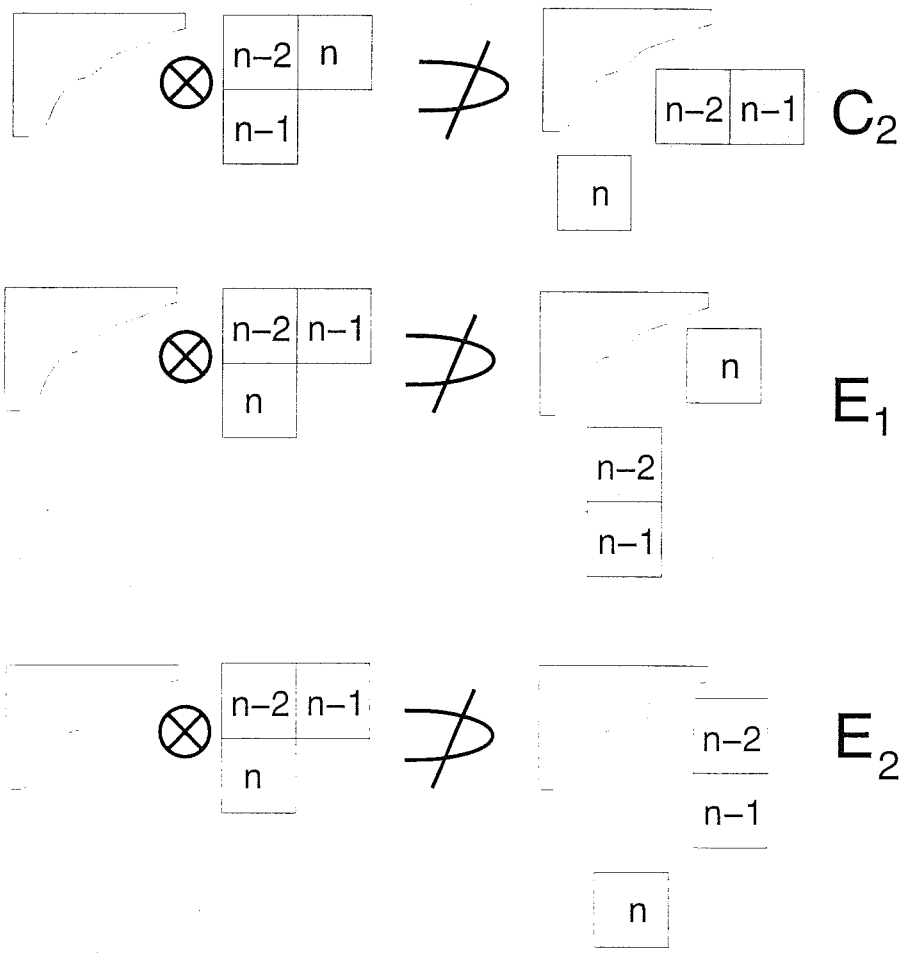

tachment of the $n-2, n-1$ pair of boxes differs between the two bases. When the boxes containing the labels from 1 to $n-3$ are removed from the standard basis tableau, *jeu* demonstrates that this pair symmetry cannot be changed. In general, *jeu* gives the tableaux which are obtained. We do not expand on the *jeu* based proof, since the selection rules are already proven by equations (5.13)–(5.18).

5.4 More on multiplicities: The harder problems

In section 5.2, we presented our detailed analysis of the general multiplicity two case, contained in the three box removal case. That is the simplest general multiplicity case in terms of the number of equations which must be solved (see equa-

tion (5.9)). In order to confirm our ideas about multiplicity separation, and the simplicity of the resulting coefficients, we need to calculate other general results.

The next general multiplicities which arise are in the four box removal case. As with section 5.2, we can express the interesting coefficients in terms of the skew diagram remaining after the removal of the lower $n-4$ boxes, and in terms of the second of the pair tableau labelling the split basis. There are twenty four tableaux with the four disjoint boxes skew shape. The split tableaux are associated with the irreps [4], [3 1], [2 2], [2 1 1] and [1^4]. [3 1] and [211] are three dimensional irreps, [2 2] is a two dimensional irrep and [4] and [1^4] are one dimensional irreps. The reduction, using *jeu*, of the skew tableaux gives: one copy of the basis tableau of the irreps [4] and [1^4], two copies of each basis tableau of the irrep [2 2], and three copies of each basis tableau of the irreps of [3 1] and [2 1 1]. The total number of split basis tableaux is then $1\times 1+3\times 3+2\times 2+3\times 3+1\times 1=24$, equalling the number of standard basis tableaux as as it must.

Thus we have another general multiplicity two case, [2 2], and two related multiplicity three problems, [3 1] and [2 1 1]. Although in section 5.2.6 we suggested that the next step might be to consider the first multiplicity three case, we will here consider some details of the multiplicity two problem, which is simpler.

The algorithm described in section 5.2.3 gives X as a set of 288 equations for 96 variables. The ninety six variables are written $a_{i,j}$, where $1\leq i\leq 4$ and $1\leq j\leq 24$. MAPLE has trouble finding which equations to eliminate in reducing the system to reduced row echelon form. Although it was able to deal with parts of the system, the whole was too large. However, by breaking the system into parts, we obtained the reduced set of the ninety two equations (5.29) to (5.72).

The system itself contains three independent hook lengths, d, e and f. We also make use of the hook lengths, $g=d+e, h=e+f$ and $i=d+e+f$. The subscripting of plus and minus signs for addition or subtraction of unity is again used to simplify the expressions.

The following forty eight relations are from the ninety six equations arising from the action of the generator $(n-3,n-2)$, as described in equation (5.4).

$$a_{1,1}=\sqrt{d_-/d_+}\,a_{1,7}\qquad a_{1,2}=\sqrt{d_-/d_+}\,a_{1,8}\qquad a_{1,3}=\sqrt{g_-/g_+}\,a_{1,9}\tag{5.29}$$

$$a_{1,4}=\sqrt{i_-/i_+}\,a_{1,10}\qquad a_{1,5}=\sqrt{g_-/g_+}\,a_{1,11}\qquad a_{1,6}=\sqrt{i_-/i_+}\,a_{1,12}\tag{5.30}$$

$$a_{1,13}=\sqrt{e_-/e_+}\,a_{1,15}\qquad a_{1,14}=\sqrt{h_-/h_+}\,a_{1,16}\qquad a_{1,17}=\sqrt{f_-/f_+}\,a_{1,18}\tag{5.31}$$

$$a_{1,19}=\sqrt{e_-/e_+}\,a_{1,21}\qquad a_{1,20}=\sqrt{h_-/h_+}\,a_{1,22}\qquad a_{1,23}=\sqrt{f_-/f_+}\,a_{1,24}\tag{5.32}$$

$$a_{2,1}=\sqrt{d_-/d_+}\,a_{2,7}\qquad a_{2,2}=\sqrt{d_-/d_+}\,a_{2,8}\qquad a_{2,3}=\sqrt{g_-/g_+}\,a_{2,9}\tag{5.33}$$

$$a_{2,4}=\sqrt{i_-/i_+}\,a_{2,10}\qquad a_{2,5}=\sqrt{g_-/g_+}\,a_{2,11}\qquad a_{2,6}=\sqrt{i_-/i_+}\,a_{2,12}\tag{5.34}$$

$$a_{2,13} = \sqrt{e_-/e_+}\, a_{2,15} \qquad a_{2,14} = \sqrt{h_-/h_+}\, a_{2,16} \qquad a_{2,17} = \sqrt{f_-/f_+}\, a_{2,18} \tag{5.35}$$

$$a_{2,19} = \sqrt{e_-/e_+}\, a_{2,21} \qquad a_{2,20} = \sqrt{h_-/h_+}\, a_{2,22} \qquad a_{2,23} = \sqrt{f_-/f_+}\, a_{2,24} \tag{5.36}$$

$$a_{3,1} = -\sqrt{d_+/d_-}\, a_{3,7} \qquad a_{3,2} = -\sqrt{d_+/d_-}\, a_{3,8} \qquad a_{3,3} = -\sqrt{g_+/g_-}\, a_{3,9} \tag{5.37}$$

$$a_{3,4} = -\sqrt{i_+/i_-}\, a_{3,10} \qquad a_{3,5} = -\sqrt{g_+/g_-}\, a_{3,11} \qquad a_{3,6} = -\sqrt{i_+/i_-}\, a_{3,12} \tag{5.38}$$

$$a_{3,13} = -\sqrt{e_+/e_-}\, a_{3,15} \qquad a_{3,14} = -\sqrt{h_+/h_-}\, a_{3,16} \qquad a_{3,17} = -\sqrt{f_+/f_-}\, a_{3,18} \tag{5.39}$$

$$a_{3,19} = -\sqrt{e_+/e_-}\, a_{3,21} \qquad a_{3,20} = -\sqrt{h_+/h_-}\, a_{3,22} \qquad a_{3,23} = -\sqrt{f_+/f_-}\, a_{3,24} \tag{5.40}$$

$$a_{4,1} = -\sqrt{d_+/d_-}\, a_{4,7} \qquad a_{4,2} = -\sqrt{d_+/d_-}\, a_{4,8} \qquad a_{4,3} = -\sqrt{g_+/g_-}\, a_{4,9} \tag{5.41}$$

$$a_{4,4} = -\sqrt{i_+/i_-}\, a_{4,10} \qquad a_{4,5} = -\sqrt{g_+/g_-}\, a_{4,11} \qquad a_{4,6} = -\sqrt{i_+/i_-}\, a_{4,12} \tag{5.42}$$

$$a_{4,13} = -\sqrt{e_+/e_-}\, a_{4,15} \qquad a_{4,14} = -\sqrt{h_+/h_-}\, a_{4,16} \qquad a_{4,17} = -\sqrt{f_+/f_-}\, a_{4,18} \tag{5.43}$$

$$a_{4,19} = -\sqrt{e_+/e_-}\, a_{4,21} \qquad a_{4,20} = -\sqrt{h_+/h_-}\, a_{4,22} \qquad a_{4,23} = -\sqrt{f_+/f_-}\, a_{4,24} \tag{5.44}$$

The next twenty relations are obtained from the ninety six equations arising from the action of the generator $(n-1, n)$, as described in equation (5.4).

$$a_7 = \sqrt{f_-/f_+}\, a_8 \qquad a_9 = \sqrt{h_-/h_+}\, a_{11} \qquad a_{10} = \sqrt{e_-/e_+}\, a_{12} \tag{5.45}$$

$$a_{15} = \sqrt{i_-/i_+}\, a_{21} \qquad a_{16} = \sqrt{g_-/g_+}\, a_{22} \qquad a_{18} = \sqrt{d_-/d_+}\, a_{24} \tag{5.46}$$

$$a_{2,7} = \sqrt{f_-/f_+}\, a_{2,8} \qquad a_{2,9} = \sqrt{h_-/h_+}\, a_{2,11} \qquad a_{2,10} = \sqrt{e_-/e_+}\, a_{2,12} \tag{5.47}$$

$$a_{2,15} = \sqrt{i_-/i_+}\, a_{2,21} \qquad a_{2,16} = \sqrt{g_-/g_+}\, a_{2,22} \qquad a_{2,18} = \sqrt{d_-/d_+}\, a_{2,24} \tag{5.48}$$

$$a_{3,7} = -\sqrt{f_+/f_-}\, a_{3,8} \qquad a_{3,9} = -\sqrt{h_+/h_-}\, a_{3,11} \qquad a_{3,10} = -\sqrt{e_+/e_-}\, a_{3,12} \tag{5.49}$$

$$a_{3,15} = -\sqrt{i_+/i_-}\, a_{3,21} \qquad a_{3,16} = -\sqrt{g_+/g_-}\, a_{3,22} \qquad a_{3,18} = -\sqrt{d_+/d_-}\, a_{3,24} \tag{5.50}$$

$$a_{4,7} = -\sqrt{f_+/f_-}\, a_{4,8} \qquad a_{4,9} = -\sqrt{h_+/h_-}\, a_{4,11} \qquad a_{4,10} = -\sqrt{e_+/e_-}\, a_{4,12} \tag{5.51}$$

$$a_{4,15} = -\sqrt{i_+/i_-}\, a_{4,21} \qquad a_{4,16} = -\sqrt{g_+/g_-}\, a_{4,22} \qquad a_{4,18} = -\sqrt{d_+/d_-}\, a_{4,24} \tag{5.52}$$

The final twenty relations are obtaining from the set of ninety six equations arising from the action of the generator $(n-2, n-1)$. Those relations are more complicated than the previous two sets.

$$a_{1,1} = \frac{-2\sqrt{e^2-1}\,a_3 + \sqrt{3}\,e a_{3,1}}{e_{--}} \tag{5.53}$$

$$a_{1,3} = -\frac{-2\sqrt{e^2-1}\,a_{3,1} + e_{--}a_{3,3}}{\sqrt{3}\,e} \tag{5.54}$$

$$a_{1,5} = \frac{-2\sqrt{f^2-1}\,a_6 + \sqrt{3}\,f a_{3,5}}{f_{--}} \tag{5.55}$$

$$a_{1,6} = -\frac{-2\sqrt{f^2-1}\,a_{3,5} + f_{--}a_{3,6}}{\sqrt{3}\,f} \tag{5.56}$$

$$a_{1,9} = \frac{-2\sqrt{d^2-1}\,a_{15} + \sqrt{3}\,d a_{3,9}}{d_{--}} \tag{5.57}$$

$$a_{1,11} = \frac{-2\sqrt{i^2-1}\,a_{17} + \sqrt{3}\,i a_{3,11}}{i_{--}} \tag{5.58}$$

$$a_{1,15} = -\frac{-2\sqrt{d^2-1}\,a_{3,9} + d_{--}a_{3,15}}{\sqrt{3}\,d} \tag{5.59}$$

$$a_{1,17} = -\frac{-2\sqrt{i^2-1}\,a_{3,11} + i_{--}a_{3,17}}{\sqrt{3}\,i} \tag{5.60}$$

$$a_{1,22} = \frac{-2\sqrt{e^2-1}\,a_{24} + \sqrt{3}\,e a_{3,22}}{e_{--}} \tag{5.61}$$

$$a_{1,24} = -\frac{-2\sqrt{e^2-1}\,a_{3,22} + e_{--}a_{3,24}}{\sqrt{3}\,e} \tag{5.62}$$

$$a_{2,1} = \frac{-2\sqrt{e^2-1}\,a_{2,3} + \sqrt{3}\,e a_{4,1}}{e_{--}} \tag{5.63}$$

$$a_3 = -\frac{-2\sqrt{e^2-1}\,a_{4,1} + e_{--}a_{4,3}}{\sqrt{3}\,e} \tag{5.64}$$

$$a_{2,5} = \frac{-2\sqrt{f^2-1}\,a_{2,6} + \sqrt{3}\,f a_{4,5}}{f_{--}} \tag{5.65}$$

$$a_{2,6} = -\frac{-2\sqrt{f^2-1}\,a_{4,5} + f_{--}a_{4,6}}{\sqrt{3}\,f} \tag{5.66}$$

$$a_{2,9} = \frac{-2\sqrt{d^2-1}\,a_{2,15} + \sqrt{3}\,d a_{4,9}}{d_{--}} \tag{5.67}$$

$$a_{2,11} = \frac{-2\sqrt{i^2-1}\,a_{2,17} + \sqrt{3}\,i a_{4,11}}{i_{--}} \tag{5.68}$$

$$a_{2,15} = -\frac{-2\sqrt{d^2-1}\,a_{4,9} + d_{--}a_{4,15}}{\sqrt{3}\,d} \tag{5.69}$$

$$a_{2,17} = -\frac{-2\sqrt{i^2-1}\,a_{4,11} + i\_\_a_{4,17}}{\sqrt{3}\,i} \tag{5.70}$$

$$a_{2,22} = \frac{-2\sqrt{e^2-1}\,a_{2,24} + \sqrt{3}\,e a_{4,22}}{e\_\_} \tag{5.71}$$

$$a_{2,24} = -\frac{-2\sqrt{e^2-1}\,a_{4,22} + e\_\_a_{4,24}}{\sqrt{3}\,e} \tag{5.72}$$

The last set of twenty equations is divided into pairs differing only in the multiplicity label, $a_{1,i}$ and $a_{3,i}$ being given the multiplicity 1 label, and $a_{2,i}$ and $a_{4,i}$ the second label.

Those 92 relations (48 + 24 + 20) are fairly simple, but they are not enough to solve for the 96 variables (the coefficients). We need to consider the orthonormality equations. This is where we run into real trouble. For the three box removal case considered in section 5.2 we only had six coefficients in each row. In this case we have twenty four coefficients in each row. This makes the orthonormality equations very large. Maple could not solve them. I have made some progress on simplifying those equations, but it is not a simple exercise.

6. INVESTIGATIONS INTO THE DELTA FUNCTION MODEL

The δ–function must have had a very sad childhood ...[1]

In this chapter, we discuss an analysis of the delta function model of a correlation crystal field. My honours project (1994) involved the investigation of this interaction using the theory of continuous groups. We originally concentrated on the interaction for electrons in the f–shell. Extensions of the results to d–shell electrons were subsequently completed. We also clarified some of the unresolved issues that arose in the project. This research has been published (McAven, Reid & Butler 1996) and the paper is reproduced in appendix A.

Section 6.1 contains a brief description of correlation crystal fields and the delta function model. The necessary continuous groups are introduced in section 6.2. We also discuss coefficients of fractional parentage in that section. An outline of the research project is given in 6.3.

6.1 Correlation crystal fields

Calculating spectra requires the identification of states and the appropriate Hamiltonian for the significant interactions. The set of eigenvalues of the Hamiltonian is the spectrum. For a free ion we have the Hamiltonian,

$$\mathcal{H} = -\frac{\hbar^2}{2m}\sum_{i=1}^{N}\nabla_i^2 - \sum_{i=1}^{N}\frac{Ze^2}{r_i} + \sum_{i>j}^{N}\frac{e^2}{r_{ij}} + \mathcal{H}_{\text{relativistic}} \tag{6.1}$$

where the last term includes various relativistic interactions, such as spin–spin and spin–orbit.

If these ions are in crystals, we must also include the effect of the crystal environment on the spectra, which implies the need to add more interaction terms to the Hamiltonian in order to build up a complete picture. Those additional terms can be thought of as perturbing the free ion energies. Bethe (1929) provided the initial development and the initial group theoretical interpretation of the so–called crystal field theory. This theory requires the use of only one–body operators and

[1] *since neither mathematicians nor physicists recognised it as belonging to their domain. If mathematicians used it, it was an intuitive physical notion with no mathematical reality .... On the other hand, physicists usually considered the δ-function, ..., as a pure mathematical idealisation which did not exist in nature (Lützen 1982, p.110).*

is adequate for explaining most, but not all, features of the spectra of lanthanide ions in crystals.

Conventional crystal field theory considers each $4f$ electron in an environment independent of each other and we have one–body operators to describe this. In reality, the electrons interact with each other via the Coulomb interaction and we need to use many–body operators. This Coulomb interaction is often modelled by correlation crystal fields and requires two–body operators.

The $1/r$ terms which appear in the interaction can be expanded in terms of spherical harmonics, but the radial dependence of the interaction makes exact solutions difficult to obtain. If one instead treats the electrons as interacting at a point (a limiting case), the radial component of the interaction is lost, and the treatment of the interaction is greatly simplified. Judd (1978) proposed a simple model based on such an interaction,

$$I_{\text{ligand}} = -A\delta(\mathbf{r}_1 - \mathbf{R})\delta(\mathbf{r}_2 - \mathbf{R}) \,. \tag{6.2}$$

This is the (double) delta function model of correlation crystal fields.

We shall briefly discuss our approach to the analysis of this system, but first let us introduce the continuous groups.

6.2 *Continuous groups*

In this section, we briefly discuss the continuous groups used to label the states and operators of the delta function model(Butler 1981).

Late in the nineteenth century, Lie investigated the structure of continuous matrix groups. He showed that they can be classified into four series and five exceptional groups. Those classes of classical Lie groups are unitary (U_n), symplectic (Sp_{2n}), and odd (SO_{2n+1}) and even (SO_{2n}) orthogonal. In his complete classification of the classical Lie groups, Cartan (1894) labelled Lie's classes as $A_n = SU_{n+1}, B_n = SO_{2n+1}, C_n = Sp_{2n}$ and $D_n = SO_{2n}$. Cartan further extended this labelling when he demonstrated that the five exceptional groups, E_6, E_7, E_8, F_4 and G_2, are the only other classical Lie groups.

The classification of the series of groups can be discussed by firstly considering the group of all $n \times n$ matrices with complex entries. Subgroups of this general linear group are then considered to obtain the series given above.

Quantum mechanics expresses symmetries using unitary (or anti–unitary operators), so within GL_n we only want those matrices which correspond to unitary transformations, thus unitary matrices. Matrix unitarity implies the matrix U has $|\det(U)| = +1$. The set of all $n \times n$ unitary matrices form the unitary group U_n under matrix multiplication. We label the irreps by a pair of partitions, $\{\lambda;\mu\}$, although usually one partition is enough for SU_n. Partitions were discussed in section 3.2 in the context of symmetric groups. This use of partitions to label the irreps of both is more than a coincidence, unitary and symmetric groups are related by Schur–Weyl duality (Haase & Butler 1984*a*, Haase & Butler 1984*b*).

The subset of unitary matrices with $\det(U) = +1$ form a subgroup of U_n under matrix multiplication. This subgroup is denoted SU_n and called the special unitary group.

For odd n, each SU_n contains the group, SO_n. For even n, each SU_n contains both SO_n and Sp_n. The group SO_n, the special orthogonal matrices are a restriction (with $\det(O) = +1$) of the orthogonal group, O_n, of all $n \times n$ orthogonal matrices. We label the irreps of the special orthogonal group SO_{2n+1} or SO_{2n} by $[W]$, where W is a partition of n parts.

As we pointed out above, the symplectic group, Sp_n, occurs only for even n. The matrices X in Sp_n satisfy $XJX^t = J$, where

$$J = \begin{pmatrix} 0_{\frac{n}{2}} & I_{\frac{n}{2}} \\ -I_{\frac{n}{2}} & 0_{\frac{n}{2}} \end{pmatrix} . \tag{6.3}$$

One particular use of the continuous groups is in the calculation of coefficients of fractional parentage for identical electrons. Coupling coefficients tell one how to construct coupled states. Because physical states are generally believed to be either symmetrised (bosons) or anti-symmetrised (fermions), not all of those coupled states need to be physical. The physical states can be constructed using coefficients of fractional parentage (cfps) (Silver 1976, Butler 1981).

Cfps relate the symmetrised states containing N electrons to the symmetrised states containing $N-1$ electrons. They were first introduced by Goudsmit & Bacher (1934). It was the systematic investigation by Racah (1949) though which showed that this building up could be done without loss of phase information, and in a manner vastly superior to simple determinantal methods. Expanding the N–electron state, $|\Omega\rangle$, as a linear combination of products of $N-1$ electron states, which we denote $|\bar{\Omega}\rangle$, and single electron states, $|\omega\rangle$ we obtain

$$|\Omega\rangle = \sum_{\bar{\Omega}\omega} |\bar{\Omega}\rangle|\omega\rangle\langle\bar{\Omega},\omega|\Omega\rangle . \tag{6.4}$$

The number $\langle\bar{\Omega},\omega|\Omega\rangle$ is a cfp. While the above equation gives the cfp the form of a coupling coefficient, it should not be identified as such until Ω, $\bar{\Omega}$ and ω are shown to be labels of partners of irreps of some group.

For example, states of N f–shell electrons can be written in the spin–orbit or SL coupling scheme as, $|f^N \alpha S M_S L M_L\rangle$, where the α distinguishes between the states with the same S, M_S, L and M_L quantum numbers. We can use the SL coupling scheme ($\mathrm{SU_2}^S \times \mathrm{SO_3}^L$) to write the cfp as the product of a coupling coefficient for $\mathrm{SU_2}^S$, another for $\mathrm{SO_3}^L$ and a third coefficient independent of both M_S and M_L. Thus the general expansion for those states is

$$\begin{aligned} |f^N \alpha S M_S L M_L\rangle \quad = \sum_{\substack{\alpha' S' M'_S L' \\ M'_L m_s m_l}} & |f^{N-1} \alpha' S' M'_S L' M'_L\rangle |s m_s l m_l\rangle \\ & \times \langle f^{N-1} \alpha' S' L', sl | f^N \alpha S L\rangle \langle S' M'_S, s m_s | S M_S\rangle \\ & \times \langle L' M'_L, l m_l | L M_L\rangle . \end{aligned} \tag{6.5}$$

One can demonstrate that the label f^N is an irrep label of U_{14} (Butler 1981). The antisymmetric N–fold irrep of U_{14} is written $\{1^N\}$, or sometimes $\{111\ldots1\}$. We can identify the third coefficient as a coupling coefficient for the chain $U_{14} \supset \mathrm{SU_2}^S \times \mathrm{SO_3}^L$, that is

$$\langle f^{N-1}\alpha' S'L', sl|f^N \alpha SL\rangle = \langle\{1^{N-1}\}\alpha' S'L', \{1\}sl|\{1^N\}\alpha SL\rangle^{U_{14}}_{\mathrm{SU_2}\times\mathrm{SO_3}^L}. \tag{6.6}$$

The labels α and α' are branching multiplicities, which Racah (1949) recognised as being labels of the various subgroups of U_{14} containing $\mathrm{SU_2}^S \times \mathrm{SO_3}^L$. The full group chain associated with the f shell is,

$$U_{14} \supset Sp_{14} \supset SU_2^S \times \{SO_7 \supset G_2 \supset SO_3^L\}\,. \tag{6.7}$$

Having made the observation that G_2 is a group intermediate to SO_7 and SO_3, Racah (1949) realised that G_2 is useful in f–shell calculations. The other exceptional groups are not considered to be as useful, although some have found use in proposed fundamental particle schemes. In our paper, which appears in appendix A, the presence of G_2 is critical to understanding the vanishing of some terms which would generally be expected to contribute the interaction.

6.3 *The delta function model*

When fitting parameters, and in theoretical investigations of the properties of correlation crystal field models, it has proved useful to have operators that have well–defined transformation properties under the groups of Racah's parentage group chain. Judd (1977) introduced a set of two–body crystal–field operators, the g_i^k, with such properties. A modification by Reid (1987) made each operator orthogonal to all others.

We would like to describe our model in terms of the g_i^k operators. But how can we get to the g_i^k operators from the interaction described by equation (6.2)? Firstly, one expands the delta functions in terms of spherical harmonic tensor operators, operators such as those mentioned in section 2.4.1. Those operators are recoupled and scaled to a set of v operators. As with the spherical harmonic operators, those v operators have well–defined transformation properties with respect to SO_3 and SO_2.

The delta function model has been analysed previously (Judd 1978, Judd & Lister 1984, Lo 1993, Lo & Reid 1993) at the angular momentum (SO_3) coupled level. However, since the v and g operators have different transformation properties the transformation between the operators was calculated using brute force. Essentially they calculated and compared the matrix elements in each basis.

We take a different approach, with the aim of obtaining explicit expressions for the transformation coefficients. In order to do this, we relate the C operators at the SO_3–SO_2 level, and thus the v operators also, to different C operators

with well–defined transformation properties under the groups of Racah's parentage group chain. Having related those operators, we can then relate the v and g and thus obtain an explicit expression for the transformation coefficients.

Early studies (Judd 1978, Judd & Lister 1984, Lo 1993, Lo & Reid 1993) found that g_{11} vanishes, as it does in the expansion of the point charge model. But they showed the operators $g_4 \ldots g_9$ vanish also. The matrix element comparison gives little insight into this, although it was recognised that the irrep [22] of SO_7 (for the f–shell) is always absent. Our direct approach allows us to explain the absence of this irrep in terms of certain zero G_2–SO_3–$3jm$. We also provide an interesting explanation in terms of "overlapping" irrep products of two different forms of the delta function interaction.

We leave the presentation of the complete analysis of the coefficients till appendix A, where we reproduce the paper published on this research.

7. CHROMIUM TRIHALIDES AND THE KERR ROTATION: A CASE FOR RACAH

There are no such things as orbitals [1]

In this chapter, we discuss a specific application arising from the use of RACAH, a computer package developed in the Department of Physics and Astronomy at the University of Canterbury.

7.1 RACAH *and the Racah–Wigner calculus*

The Racah–Wigner calculus is applicable to *all* groups, but the calculations and results obtained are by no means standardised across the wide spectrum of the various classes of groups. The RACAH project at Canterbury is centred around a broad vision. We would like to see the Racah–Wigner calculus and other techniques of group representation theory applied to all appropriate problems. But the Racah–Wigner calculus is not something one learns in a week. Many solid state physicists and molecular chemists will not take advantage of the algebra because they do not understand it, nor do they want to spend the time learning the subtle details.

Therefore, to realise our vision, we need to translate the Racah–Wigner calculus into a more accessible format. The RACAH computer package is our means of doing this. In 1968 Butler needed to calculate particular $3jm$. The $3jm$ wanted, fractional parentage coefficients for the $(s+p+d)^n$ mixed atomic configuration, were inaccessible through the approaches of Racah (1949) and the extensions by Judd (1963). Faced with a choice between extending the unsymmetrised coefficients of the Racah/Judd approach, or following work by Hamermesh (1962) and Derome & Sharp (1965) on symmetrised coefficients, Butler chose the latter.

Hamermesh (1962) used a recursive technique to calculate coupling coefficients for symmetric groups. Recursion on SO_3 $6j$ had previously been (briefly) considered by Fano & Racah (1959) and Edmonds (1965). A review of the symmetrised Racah–Wigner calculus by Butler (1975), was followed by papers describing a systematic 'building up' principle (Butler & Wybourne 1976, Butler

[1] *Orbitals, we emphasise continually, lack physical evidence; they are merely mathematical functions in one particular approach .... In other words there are no such things as orbitals, not things tangible, material objects, as chemists generally consider nuclei and electrons (Ogilvie 1994, p.182)*

1976). This recursive technique allowed the calculation of angular momentum $3jm$ and $6j$ without use of the special properties of angular momentum operators. During this time, the development of RACAH began.

Although the versions to date have been difficult for the uninitiated to apply, they are useful. RACAH was used to calculate all the point group $3jm$ and $6j$ given in Butler (1981). Since 1981, RACAH has been re–worked, new algorithms have been developed by Searle (1988) and others, and the program has undergone several language changes. Prior to Butler's book, Algol was used, then the Pascal version developed during the 1980s, before the initial conversions to C began in 1990.

Butler & Ross (1990) reviewed progress, at an early stage of RACAH v3.0 (C) development. Butler & Ross (1990) outlined how a building–up process, beginning only with a knowledge of selection rules, appears to allow $6j$ and other coefficients to be calculated for a group (Butler & Wybourne 1976, Searle & Butler 1988*b*, Searle & Butler 1988*a*). This building–up procedure potentially requires extensive recursion.

As early as Butler & Wybourne (1976), recursion was known to reduce the set of all $6j$ to a small class of $6j$, known as *primitive* $6j$. The primitive $6j$ each contain a (usually small) irrep chosen to be the primitive representation. This reduction uses the Biedenharn–Elliott Sum rule, equation (2.39). The problem then becomes how to calculate the primitive $6j$, for which the recursion no longer seems useful. The early prescription was to construct a set of equations in the $6j$, using the Biedenharn–Elliott Sum rule (2.39), the Racah Back Coupling equation (2.38), unitarity constraints (2.42) and symmetry relations between the $6j$. While this procedure was successful (Butler 1976, Butler 1981, Bickerstaff et al. 1982), there are numerous equations of which most are redundant. The procedure for eliminating the redundant equations was essentially by brute force.

Searle (see Searle & Butler (1988*b*), Searle & Butler (1988*a*) and also Searle (1988) made a significant advance by demonstrating a recursion within the primitive set, reducing the unknown coefficients to a *core* set. But the problem of calculating the core set remains. Improvements have been made by Ross (1997), but further work is needed to understand the implications of the results contained therein.

The other side of the RACAH project relates to applying the coefficients to physical systems. Although RACAH v2, as discussed by Butler & Ross (1990), was more user–friendly, versatile and capable of dealing with larger problems than the Algol version, it still lacked the direct applicability to problems necessary to realise our vision. A visit from Professor Kiminari Shinagawa, Toho University (Japan) in 1992 made this short–coming clear. Shinagawa wanted RACAH to check his hand calculations of spin–orbit coupling coefficients for a $CrBr_3$ cluster, which he had methodically and tediously calculated. Such a calculation, not an untypical one, requires extensive use of the Wigner–Eckart Theorem. It was therefore necessary to extend the structure in RACAH until the Wigner–Eckart Theo-

rem could be applied to states containing several shells. The need to implement the new algorithms of Searle, required enough of an overall that a rewrite to C was undertaken. Group structures such as

$$\{(SU_2\times O_h,\ SU_2\times O_h)\downarrow SU_2\times O_h,\ SU_2\times O_h\}\downarrow SU_2\times O_h\downarrow O\times O\downarrow O\downarrow D_3\downarrow C_3, \qquad (7.1)$$

can now be recognised and calculations within such schemes can be carried out. Much of the programming necessary for the structural implementation of such calculations was performed by Ross.

We have published work (Ross et al. 1996) on using RACAH to calculate spin–orbit coupling coefficients for a chromium tribromide system. The paper is reproduced in appendix B. We present in figure 7.1 a diagrammatic representation, with some explanation, of the coupling undertaken in that project. Such coupling of shells is common in the analysis of multi–shell systems.

Although RACAH cannot do everything in calculating the spin–orbit coupling coefficients, it does do a great deal. Marsden funding [2] has been obtained by the RACAH group at Canterbury to further develop the Racah–Wigner calculus, with particular emphasis on making it more accessible to application in spectroscopy.

The development of RACAH is an ongoing project. Improvements to the core of the program will continue as new algorithms are developed (see section E.7). But we are at the stage where much of this core development should be driven by feedback from applied users. While we have said that libraries will need to be added for specific applications, we would like RACAH to be as versatile, robust and general as possible. Calculations of matrix elements from different fields of physics differ only in the groups and operators used. The technique of calculating those matrix elements should be (mostly) universal. We have distributed RACAH to a number of people, who are finding it useful and we would like input from others. I have been responsible for interacting with and distributing copies to interested persons.

Currently Searle is leading the team that is rewriting RACAH into C++. Some aspects of the C version are retained, but the rewrite is centred around new algorithms based on aspects of Ross (1997). In particular the separate recursion on $3jm$ and $6j$ is replaced by a single recursion on any sort of transformation braket. The Biedenharn–Elliott Sum rule (Butler 1981, equation 3.3.28) and the Wigner equation (Butler 1981, equation 3.3.29) are replaced by a single equation derived as a pentagon equation in category theory. $3jm$ and $6j$ take a back seat to the generalised transformation coefficients which unify and simplify recursion, without the need for the specific symmetries of the $3jm$ and $6j$.

My role has included assisting in designing the algorithm (see section E.7) and testing RACAH as various parts of the program are completed.

While the rewrite by Searle is focused around the new algorithms, the goal of making RACAH applicable is never far away. Knowledge about what applications and capabilities users would like RACAH to have will allow us to build the

[2] Contract Number UOC704: *The Racah–Wigner Calculus for Spectroscopy*

appropriate calculations relevant to other applications into the core program, and perhaps to develop libraries for special one–off calculations.

Once the C++ version is completed, the calculation of spin–orbit coupling coefficients, or indeed any other matrix element based coefficient, should be possible with RACAH. And possible in a manner such that specific knowledge about the Racah–Wigner calculus is not required by the user.

7.2 *The point groups*

In section 6.2, we briefly discussed the orthogonal groups, O_n. One member of that class of groups is of particular significance in the analysis of atomic and molecular systems. The orthogonal group in three dimensions, O_3, is the group of real, orthogonal transformations in 3–space, having determinant ± 1. Alternately, it is the group of all symmetries of a sphere. O_3 is the direct product of the group of rotations in 3–space, SO_3 and the inversion group, C_i.

In crystal field theory (see section 6.1) one treats an atomic site of interest as if it is in a potential described by the surrounding electric charges. The symmetry of this potential has the symmetry of the site of the atom. This atom necessarily has some of the symmetries of a sphere and therefore it has a symmetry described by a subgroup of O_3. Each subgroup of O_3 is called a point group, since every operation of the group leaves the origin invariant. Point groups occur as symmetry groups of molecules or isolated atoms. Once an atom is embedded in a crystal, the possible point symmetries are restricted, but translations must now be included. A symmetry group must now also transform a lattice into itself. Elements of this more exclusive set of symmetry groups of atoms in a crystal, are known as crystallographic point groups or crystal classes. A natural way to introduce those groups is to briefly discuss some points in the historical analysis of the structure of matter (especially crystals).

Early philosophers argued about the fundamental nature of matter. The atomistic philosophy probably originated with Leucippus, in the fifth century B.C. One of his students, Democritus, was the most famous of those atomists. His atomistic philosophy was characterised by the belief in the reality of both empty space and the indivisible units, atoms, which filled it. Plato went further and identified geometric structures with the four elements of his cosmos: cube for earth, tetrahedron for fire, octahedron for air and icosahedron for water. Plato also identified the universe as a whole with the dodecahedron (Beck, Bleicher & Crowe 1969).

However, Aristotle proposed that since not all of those objects fill space, the model allows for the existence of vacua which Aristotle considered unphysical. If on the other hand they could fill space in some combination, how could one then explain motion, argued Aristotle (Senechal 1990). The arguments of Aristotle and others were convincing and this atomic–type theory did not resurface until the seventeenth century. Of course this was not purely the result of such arguments. The infrastructure of religious, scientific and political societies and the

interactions between them led to environments which could perhaps be described as rampantly conservative.

Crystals in particular were recognised, but the classification and description tended to be based upon imagined properties. It wasn't until Kepler, Hooke and Steno all proposed that crystals were conglomerates of spheres or of polyhedral building blocks, that a more consistent approach developed. Investigations into the structure and properties of crystals intensified in the eighteenth century, culminating in the research of Haüe in the late eighteenth and early nineteenth centuries. Incidentally, the early nineteenth century also saw the revival of atomic theory.

Haüe proposed that crystals were built from blocks, with shapes specific to the type of crystal. One particular problem had been that the same substance often had differing external forms. Haüe demonstrated that those building blocks could be put together in different ways, so that although the substance is the 'same', the appearance may differ. But then, which building blocks are possible? Haüe proposed that, somewhat like Plato's theory for fundamental building blocks, the blocks needed to be able to fill space. In a plane, only triangles, squares and hexagons can fill space. In particular the five–fold symmetry of the pentagon is excluded.

This insight into the anatomy of crystals allowed the crystal classes to be enumerated by Frankenheim in 1826. Hessel proved in 1830 that the thirty two geometric crystal classes proposed by Frankenheim, were the only such classes in 3–space. The work of Hessel lay hidden for some sixty years though. We shall return to this point in the development of crystal analysis later.

In order to outline how one would enumerate those groups, consider the transformations which leave a sphere and the centre of the sphere, the origin, invariant (Janssen 1973, Senechal 1990, Nowick 1995). There are three different types of such transformations:

1. *Rotation* by any angle, in any plane passing through the origin.

2. *Reflection* about any mirror plane passing through the origin.

3. *Inversion* about the origin. Inversion is the operation which takes

$$(x, y, z) \rightarrow (-x, -y, -z). \tag{7.2}$$

The restriction that space must be filled by an object with a crystallographic point group symmetry, allows only rotations with two–fold, three–fold, four–fold or six–fold axes.

The simplest groups are the cyclic groups $C_n, n = 1, 2, 3, 4$ and 6 , which are invariant only under rotations about a particular n–fold axis. Combining the cyclic groups with reflections and inversions, we can build up other crystallographic

point groups. Symmetry under reflections in different planes, defined relative to the axes of rotation, is indicated by different subscripts: h for horizontal (perpendicular), v for vertical and d for diagonal. Thus C_{2h} contains both a two–fold rotation axis and a reflection plane perpendicular to that axis.

Another class of groups of pure rotations is the dihedral D_n class, $n = 2, 3, 4$ and 6. Those contain the n–fold axis as C_n, but in addition, n two–fold axes in the plane perpendicular to that axis. The group D_n, transforms a regular n–gon into itself. Again, combination with reflections and inversions generates some new groups.

Another two pure rotation groups exist. The tetrahedral group T, is the group of rotations transforming a regular tetrahedron into itself. The octahedral group O, is the group of rotations which transforms an octagon and a cube into themselves. One can also apply reflections and inversions to those groups.

Although we shall not discuss the details, we should point out that not all reflections and inversions added will necessarily generate new groups. It is of particular significance in this context to mention the distinction between different symmetries with isomorphic abstract groups. For example $T_d \sim O$ and $C_{4v} \sim D_4$. Sternberg (1994, Figure 1.19, pp.42–44) gives a list of all the crystallographic point groups, along with examples of crystals known to have that symmetry.

It is clear that many of those crystallographic point groups contain other crystallographic point groups. Figure 12.2 of Butler (1981) contains all of those group–subgroup relations. In our analysis of $CrBr_3$, we are particularly interested in the chain $O \supset D_3 \supset C_3$. We add in spin and parity (through inversion) groups at each level. The labelling of the symmetry structure is discussed in section B.2. The reader is also referred to figure 7.1.

Butler (1981) points out that O_3 and all subgroups of O_3, have true and spin representations. Spin representations are such that there are two transformations for each group element, rather than a unique transformation, as true representation have (see section 2.3). We do not discuss details here, but note that it is of significance for our RACAH analysis of $CrBr_3$.

Let us return to the historical development of crystal analysis. After the work of Haüe (1822), it became evident that regularity of the crystal form suggests regularity of crystal structure. Theoretical investigations into lattices of points and their symmetries, the discrete repetitive patterns, were underway. Frankenheim and Bravais studied and made significant progress in the classification of those discrete repetitive patterns. Those patterns effectively correspond to looking at how one may take a unit and perform symmetry operations to relate it to every other unit in a structure. Translations and screws (twists) are allowed and the number of groups is clearly greater than the number of crystallographic point groups. Indeed Fedorov (1890), Schoenflies(1891) and Barlow(1894) independently showed that there are two hundred and thirty crystallographic groups, or space groups, in three dimensions.

So those space groups are the symmetry groups of regular systems of points. The point group of a crystal is combined with a lattice structure (represented in a translation group) to give an overall symmetry to a system (Senechal 1990). In Kittel (1986, p.4) the structure of a crystal is summed up in the relation,

$$\text{lattice} + \text{basis} = \text{crystal structure} . \tag{7.3}$$

Kittel (1986) follows this up with a brief discussion of the fourteen allowed Bravais lattices.

The success of space group theory in predicting results obtained using the X–ray analysis, developed in 1912 by von Laue, solidified the place of symmetry in the study of crystals. But, as discussed in section 2.4, the attitude of physicists to group theory was less than friendly at this time. The use in crystallography of symmetry was therefore very much in an applied sense, with the possible abstraction of group theory avoided where possible. Crystallography did however provide a useful testing ground for the mathematics of group theory. It was Klein for example who suggested to Schoenflies the problem of enumerating space groups.

The first release of the computer program RACAH, discussed in section 7.1, was primarily developed for point groups, as the title of Butler (1981) suggests. We would like it to be useful for the space groups also. Point groups are useful for studying localised properties, where one can treat a system effectively as an extended molecule. In our study of the $CrBr_3$ system, which is an insulator, the transitions are localised and the use of points groups is appropriate. Space groups are needed to study some properties though.

Intermediate to those two general types of groups are what we shall call the cluster groups. Studies using clusters to model an entire system are not unusual, indeed we consider the $CrBr_3$ system as a cluster. But what symmetry, if any, is then appropriate? Perkins & Stewart (1980) suggested using groups on the finite lattices of clusters. It is likely that some of that work has been presented previously, perhaps in a more mathematical context. Recent work by Stewart (1998) has improved the direct applicability to two–dimensional cluster structures. With the new algorithms to be implemented into RACAH, calculations with such groups should be possible.

We now move onto our investigation into aspects of the chromium trihalide systems.

7.3 Chromium trihalides and Kerr rotation

Later in this section we shall discuss some details of the theoretical analyses performed on the chromium trihalide systems. But in the first two subsections we briefly introduce the chromium trihalide systems and Kerr rotation.

Some characteristics of the chromium trihalides are presented in table 7.1. Those characteristics are mostly taken from Dillon, Kamimura & Remeika (1966,

Table 1), and most are of little significance for our study. More information can be found in that paper, in references in that paper, and in other references given in this thesis. For example, the space groups C_{2h}^3 and C_{3i}^2 are discussed in Carricaburu et al. (1986, p. 4986).

It is of significance that the low temperature structures of $CrCl_3$, $CrBr_3$ and CrI_3 are extremely similar. A hexagonal net of chromium ions lies between two close packed layers of halogen ions. Within this sandwich structure the bonding is predominantly covalent (electron sharing), with successive layers held together by comparatively weak van der Waals bonds. Figure 7.2 contains a diagrammatic representation of the relative positions (with respect to a chromium plane) of the ions in a chromium trihalide system.

Tab. 7.1: Some characteristics of the trihalide systems $CrCl_3$, $CrBr_3$ and CrI_3.

Compound	$CrCl_3$	$CrBr_3$	CrI_3
Lower temp. space group	C_{3i}^2	C_{3i}^2	C_{3i}^2
Transition temp.(K)	≈ 238	≈ 400	???
Higher temp. space group	C_{2h}^3	C_{2h}^3	C_{2h}^3
Halogen packing (low temp.)	h.c.p[a]	h.c.p	h.c.p
Cr site point symmetry	C_3	C_3	C_3
Hexagonal cell a_0 (Å)	5.942	6.26	6.86
c_0 (Å)	17.333	18.20	19.88
X–ray density (g/cm^3)	2.95	4.75	5.36
T_C (K)	16.8	32.56	68
4π M_0	3880	3390	2690
2K/M at 0K (Oe)	≈ 0	6500	28,600
Cr^{3+} ions/cm^3	1.12×10^{22}	1.0×10^{22}	0.75×10^{22}

[a] Hexagonal close–packed structure

Kerr rotation, also known as the Kerr *magneto–optic effect*, was discovered in 1888 (by Kerr). This is not to be confused with the Kerr effect discovered thirteen years earlier, which is an electro–optic effect.

When linearly polarised light is reflected at about normal incidence from the surface of an ferromagnet, the light becomes, in general, elliptically polarised with the major axis of the ellipse rotated with respect to the incident light. The change in the state of polarisation depends on the orientation of the ferromagnet's magnetisation, relative to the surface and plane of incidence. Because of this, Kerr rotation can be used to probe the domain structure of ferromagnets.

A similar effect for transmitted light, is known as the Faraday effect, or Faraday rotation, and was discovered in 1845 by Faraday.

Ferromagnetic materials have non–zero magnetic moments even in zero applied magnetic field. This non–zero moment implies electron spins and magnetic moments are arranged in a regular, but not necessarily simple, manner. The value

of $2K/M$ in table 7.1 demonstrates that chromium chloride is not ferromagnetic, and thus should not exhibit Kerr rotation, whereas the other two systems are ferromagnetic so may exhibit Kerr rotation.

We now turn our attention to the spectroscopic investigations resulting from collaboration with Shinagawa.

7.4 *Charge–transfer transitions in chromium trihalides*

The unrestricted self–consistent field (USCF)–Xα–scattering wave (SW) method is a non–empirical molecular orbital method. This method was developed by Johnson & Smith (1972). One–particle Schrödinger equations are solved numerically with the following approximations. Firstly, the potential is approximated by a muffin–tin potential. This approximation is particularly reasonable for the octahedral cluster treated in this study. Secondly, the exchange interaction is approximated by a local statistically averaged exchange, multiplied by a factor α (Slater 1951), deduced from the atomic calculations (Schwartz 1972).

In the muffin–tin approximation to the potential, the atomic sites are surrounded by non–overlapping spheres and the potential is spherically averaged within these spheres. All the spheres are surrounded by the outer sphere, which touches all the ligand spheres. In the interstitial region, that is between the atomic spheres, a constant average potential is used. In this study, the sphere radii of M^- (M=Cl, Br or I) are assumed to be the ionic radii. In addition, to account approximately for the neighbours of the cluster, we used Watson spheres with the same positive charges as the negative charges of the cluster. The radius of the Watson sphere was assumed to be the same as that of the outer sphere. The parameters used in this study are listed in table 7.2. Here it should be noted that our Cr^{3+} radius differs from that adopted by Larsson & Connolly (1974) (1.80 au). Furthermore, for simplicity, we assumed that all the orbitals, except 3s, 3p and 4d of Cr^{3+} and the highest ns and np of the ligands, were the core orbitals in the calculations. The transition energies are calculated using the Slater transition states, where half an electron is removed from the initial level and added to the final level.

Tab. 7.2: Parameters for the USCF–Xα–SW calculations

Cluster	$(CrCl_6)^{3-}$ Radius (au)	α	$(CrCl_6)^{3-}$ Radius (au)	α	$(CrCl_6)^{3-}$ Radius (au)	α
Chromium	1.180	0.7135	1.180	0.7135	1.180	0.7135
Ligand	3.320	0.7233	3.620	0.7061	4.090	0.6987
Outer	7.820	0.7214	8.420	0.7075	9.360	0.7015

A more detailed discussion on the techniques used in this paper can be found,

for example, in Slater (1979). The abstract of the paper on this research is given in appendix C. The remainder of this chapter relates to the third paper in our series, the body of the paper itself is left until chapter 8.

7.5 *The LCAO program*

In order to calculate energy levels for our cluster systems I wrote a C program, with some assistance from Ross (A Ph.D. student at that time). We used the interatomic matrix elements given in Harrison (1980, p.481), and originally given by Slater & Koster (1954). Those matrix elements are calculated using a linear combination of atomic orbitals (LCAO) approach.

We called the program TB, since it was initially developed for tribromide. The format for using the program is,

Format:: `TB input.file output.file`

The program is structured to work through the following steps:

- ◇ `Reads in data file`: The number of sites, the site coordinates and non–core shells on each site are taken from the input file and stored.

- ◇ `Calculates distance matrix`: The interatomic distances and the breakdown of the distance in x, y and z coordinates are calculated and stored in a distance matrix.

- ◇ `Sets up orbitals`: Each s shell has one orbital, s. Each p shell has three orbitals, labelled x, y and z. Each d shell has five orbitals, xy, yz, xz, $x^2 - y^2$, and $3z^2 - r^2$.

- ◇ `Calculates interatomic matrix elements`: Each row of the interaction matrix is associated with a different orbital on a major site. The orbitals are ordered by site order in the input file and by orbital as above.

- ◇ `Output`: The distance matrix and interatomic interaction matrix are outputted in a format readable by MATLAB. The default output file is named `output.LCAO`.

Once TB has completed its job, we will be left with an output file readable by MATLAB. We have developed some MATLAB scripts used to process the interaction matrix. Let us very briefly describe what the scripts do.

We put our interaction matrix in a standard order. We split the d–orbitals into T_{2g} and E_g parts, by changing the diagonal elements in the Hamiltonian matrix. We obtain the projection operators for the irreps of the groups O, D_3 and C_3, and use them to label the rows and columns of our matrix by irreps of $O \supset D_3 \supset C_3$. Finally we change the phases of the vectors labelling the rows and columns to obtain a real Hamiltonian matrix.

7.6 *Analysis of the reflectance data*

The second part of the work on the chromium trihalides has involved taking experimental data and fitting Gaussians, to give qualitative information about the transitions. This is useful in identifying the transitions in relation to our energy level calculations. We describe in this section the procedure undertaken to fit Gaussians to the different imaginary parts of the dielectric constant.

For $CrBr_3$ the data available on the imaginary part of the dielectric constant was not in enough detail for electronic scanning. For this reason, we began by scanning the reflectance spectra from Pollini et al. (1989). The reflectance spectra can be used to calculate the components of the dielectric constant. Data for the $CrCl_3$ system was of much better resolution (Carricaburu et al. 1986) and we were able to scan the imaginary part of the dielectric constant directly. However we did still perform the analysis of the reflectance data. The description which follows generally relates to $CrBr_3$, although we shall make some points about $CrCl_3$.

We took 365 data points off the scanned curve between the energies 2.59eV and 10.49eV, taking particular care in the detailed regions of the spectra. Having recorded that data and scaled the x and y axes to fit the actual data, we augmented this data with extra points in the range 12 to 30eV, to improve the applicability of the Kramers–Kronig analysis (which we describe later). Those data points were also taken from Pollini et al. (1989).

Although the curve the $CrBr_3$ reflectance data is scanned from is in arbitrary units, we were able to use another curve in the same paper to rescale and express the reflectance as a percentage.

Guizetti et al. (1976) used interference fringes to calculate the reflectance of $CrBr_3$ in the region close to zero. They found that the reflectance is close to zero, which we take into account in our analysis. They also used a tail on the reflectance data above 10eV, up to some value and of a form which gave continuity of ϵ_2 and a good fit with the reflectance data in the lower energy range. We didn't need such an approximate tail since data points are available up to 30eV ((Pollini et al. 1989)).

Similarly for $CrCl_3$, the reflectance spectra is close to zero near zero, and we can use a curve which is zero up to about a value not much lower than 3eV, at which point it rises to meet the experimental data (with boundary conditions on continuity). Furthermore we can add on a tail up to 30eV using data taken from Carricaburu et al. (1986).

A interesting point is that in Carricaburu et al. (1986, figure 6), the low temperature reflectance spectra includes a shoulder to the left of the first main peak. Although such a shoulder is not visible in the reflectance data for $CrBr_3$, we found that the fitting program naturally tended to put a transition in that position.

The MATLAB command for running the entire fitting setup is `Kerrinit`. This contains two separate instructions. The first,

```
[E,P,K,n,R,r,E1,E2]=fittingCrBr3(steps,start,end) ,   (7.4)
```

takes the scanned reflectance data (already in the fittingCrBr3 file) and calculates the imaginary part of the dielectric constant. The second,

```
[AAA,Intensity,E,F,K,n,R,r,E1,E2,hw,H,J]      (7.5)
    = Kerrdat(steps,E,F,K,n,R,r,E1,E2),
```

takes the imaginary part of the dielectric constant, fits the Gaussians to it, and calculates the resulting Kerr rotation curve. We describe most of the various input and output parameters as we describe the analysis procedure. Note though that E is the vector of energies at which the various other output vectors have values.

In the two subsections which follow we describe what the two commands in the equations above do, and how.

7.6.1 From reflectance to elements of the dielectric constants

We want to fit Gaussians to the imaginary part of the dielectric constant. For $CrBr_3$ we begin only with the reflectance data, but fortunately this is enough to obtain everything we want to know.

The scanned data is set up in `fittingCrBr3`, and the first step is to replace this data with a cubic spline interpolation with "steps" points. This is done to smooth out small fluctuations in the data points due to resolution imperfections in the experimental graphs and the identification of points. We use 1500 points. The reflectance data is processed to calculate the imaginary part of the dielectric constants. We discuss in this subsection how the dielectric constant is related to the reflectance data.

The reflectance R is defined as the ratio of the reflected intensity to the incident intensity. We write $E_{incident}$ and $E_{reflected}$ as the incident and reflected electric fields respectively. At the sample surface, for a given frequency ω we call the ratio of those fields the reflectivity coefficient $r(\omega)$. But intensity is simply related to the field, and we therefore have a relation between R and r,

$$\begin{aligned} R &= \frac{E^*_{reflected} E_{reflected}}{E^*_{incident} E_{incident}} \\ &= r^* r \, . \end{aligned}$$

Since the reflectivity will be complex in general one can express it as an amplitude times a phase[3].

$$r(\omega) = \rho(\theta) \exp\left(i\theta(\omega)\right) \tag{7.6}$$

At the surface of the sample the components of the electric and magnetic fields parallel to the surface must be continuous. This constraint relates the reflectivity to the refractive index, $n(\omega)$, and the extinction coefficient, $K(\omega)$, in the crystal.

$$r(\omega) = \frac{n + iK - 1}{n + iK + 1} \tag{7.7}$$

[3] We use P as the output parameter for the phase

The definitions of the refractive index and extinction coefficient introduce the dielectric function $\epsilon(\omega)$,

$$n(\omega) + iK(\omega) = \sqrt{\epsilon(\omega)} .$$

If we now distinguish between the complex and imaginary parts of the dielectric function, thus $\epsilon = \epsilon_1 + i\epsilon_2$, inverting the last equation gives,

$$\begin{aligned} \epsilon_1 &= n^2 - K^2, \text{ and} \\ \epsilon_2 &= 2nK . \end{aligned} \tag{7.8}$$

Earlier we stated that from the reflectance data all the other coefficients can be calculated. Equations 7.6 and 7.7 can be used to express the refractive index and extinction coefficients in terms of the real and imaginary parts of the reflectivity coefficient. Having obtained n and K one then uses equation 7.8 to calculate the real and imaginary parts of the dielectric function. Thus everything is related back to the real and imaginary parts of the reflectivity coefficient. We know that $R = r^*r = \rho^2$ gives us the amplitude of the reflectivity coefficient, but how does one obtain the phase?

One can express the relation between reflectivity, reflectance and phase as

$$\ln r(\omega) = \ln R^{\frac{1}{2}}(\omega) + i\theta(\omega)$$

Kramers–Kronig analysis (Kittel 1986, pp.292–294) applied to this gives the phase in terms of the reflectance as,

$$\theta(\omega) = -\frac{1}{2\pi}\int_0^\infty \ln\left|\frac{s+\theta}{s-\theta}\right| \frac{d\ln R(s)}{ds} ds . \tag{7.9}$$

This integral is over all energies, and thus we cannot hope to gain exact phase information. We do however have good reasons to have a high level of confidence in the phase information calculated from our limited range reflectance data. Our aim is to calculate the imaginary part of the dielectric constant in the target range 2.85–6.7eV. Since the dielectric constant can be obtained from *local* information about the phase and amplitude of the reflectivity, we need only have accurate phase information in this range. The function $\ln\left|\frac{s+\theta}{s-\theta}\right|$ is small when $s \ll w$ or when $s \gg w$, and therefore the contribution far from the target range will make only small contributions. At the edge of our reflectance data (30eV) this ln term is 0.45, which does not seem all that small. However the reflectance spectra is fairly constant here, and the term $\frac{d\ln R(s)}{ds}$ close to zero, so that the contribution is still minimal.

This process is set up in the fitting programme so that upon entering the MATLAB command in 7.4 the various output parameters are calculated. We present in figures 7.3, 7.4, 7.5, and 7.6 graphs of those parameters in the region of interest.

Having obtained the important imaginary part of the dielectric constant we discuss the fitting of Gaussians in the next section.

7.6.2 *Fitting the Gaussians*

One of the important aspects in fitting the Gaussians to our curve is to choose an energy range which covers the region where the charge transfer effects are dominant. By charge transfer effects we mean both charge transfer transitions, and charge transfer excitons. The Kramers–Kronig analysis gives us the imaginary part of the dielectric constant up to about 30eV, allowing us some freedom in this choice. According to Pollini et al. (1989) the first inter–band transitions begin at 8eV in $CrBr_3$, and above 9.5eV in $CrCl_3$. Prior to this, between about 7eV and 8eV in $CrBr_3$, there are inter–band excitons. Avoiding those we choose to fit Gaussians to the $CrBr_3$ region between 2.85eV and 6.7eV, and to the $CrCl_3$ region between 3eV and 8eV. The lower bound is partially based on the lack of specific information about the link between the lower energy reflectance data and the data which we have scanned.

To fit Gaussians to the data we used a general fitting package built into MATLAB. This package implements a Nelder–Mead type simplex search method. The method attempts to find a local minimum of some function in the region of a starting point. Although we do not have specific details about the Nelder–Mead type simplex search method, the generic simplex method has been around for close to half a century and details can be found in various texts on data analysis (Osborne 1985).

As we implied above, we need to have a fairly good starting point to obtain a reasonable solution. We compared the solutions obtained using a range of starting positions and found that the technique was stable enough for our purposes. The actual fitting itself uses Gaussians, of the form,

$$G_i = c_i \exp\left(-\frac{(E - E_i)^2}{a_i}\right) . \tag{7.10}$$

We used the transition energies E_i and the half–widths a_i, as fitting parameters. For any given values of those parameters the c_i giving the lowest error could be exactly calculated.

We shall leave a detailed discussion on the number of transitions fitted until section 8.6. However we should point out that we fitted varying numbers of Gaussians as a further means of testing the stability of solutions and for highlighting the dominant transitions in the region.

Fig. 7.1: The chromium trihalide cluster symmetry structure expressed as a coupled group chain

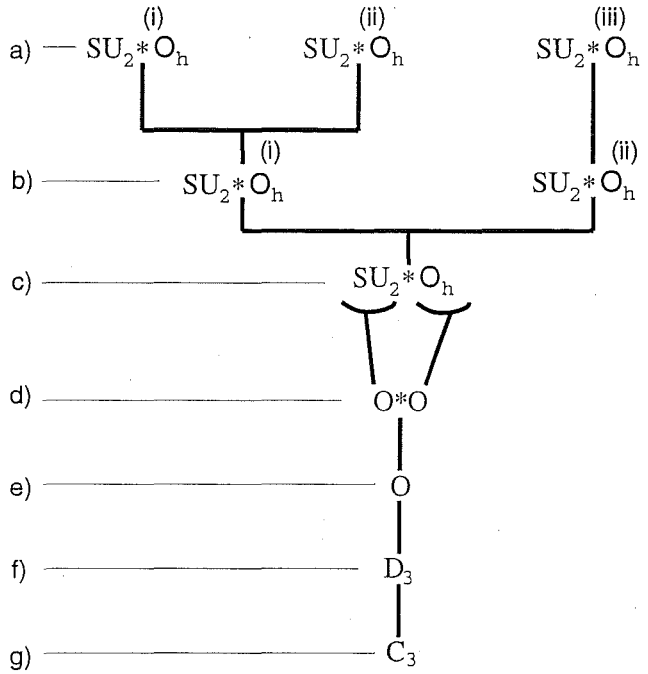

Level (a) contains the three open shells in the charge transfer states.
(i) and (ii) are the two open shells on the chromium center.
(iii) is the open shell on the six coupled bromine ions.
Level (b) considers separate labelling for the coupled chromium and coupled bromine states.
Level (c) considers one spin–orbital labelling for the cluster.
At level (d) the spin and orbital parts are both branched to the octahedral symmetry of the cluster.
At level (e) the separate octahedral parts are coupled to give an overall octahedral label.
This label is then branched to the dihedral and cyclic groups appropriate for the trigonally distorted cluster.

One can choose to carry through the appropriate parity labels, but we have not done so here.

Fig. 7.2: The chromium trihalide lattice

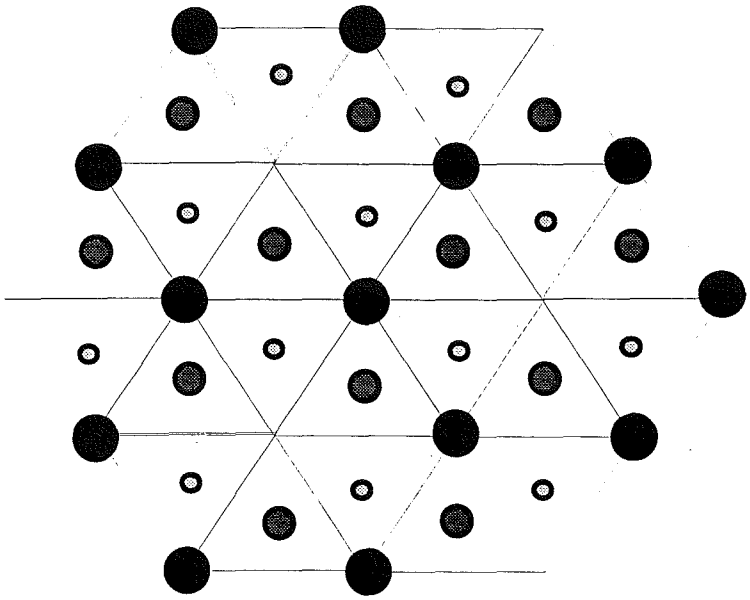

A chromium ion in the ''plane''.

A halogen ion above the ''plane''.

A halogen ion below the ''plane''.

Fig. 7.3: Extinction coefficient $K(\theta)$ in the charge transfer active region of $CrBr_3$

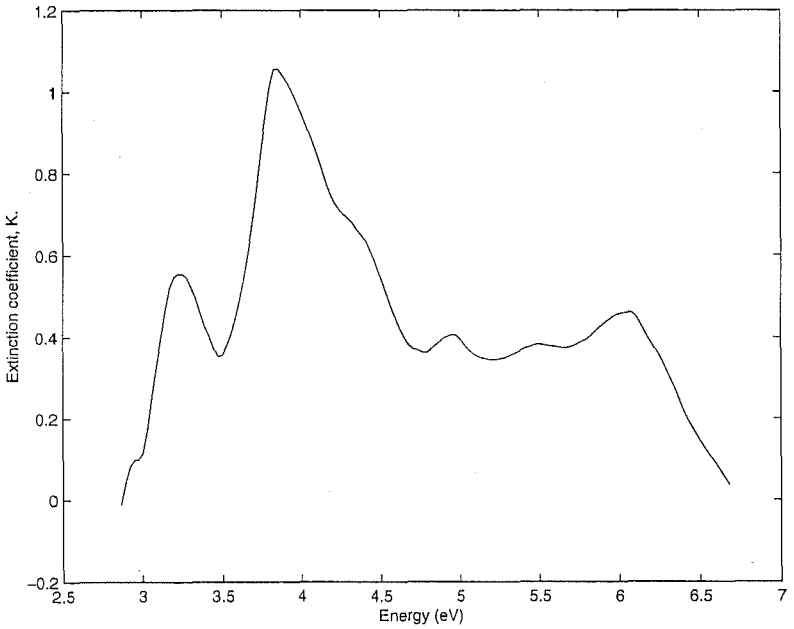

Fig. 7.4: The refractive index $n(\theta)$ for the charge transfer active region of $CrBr_3$

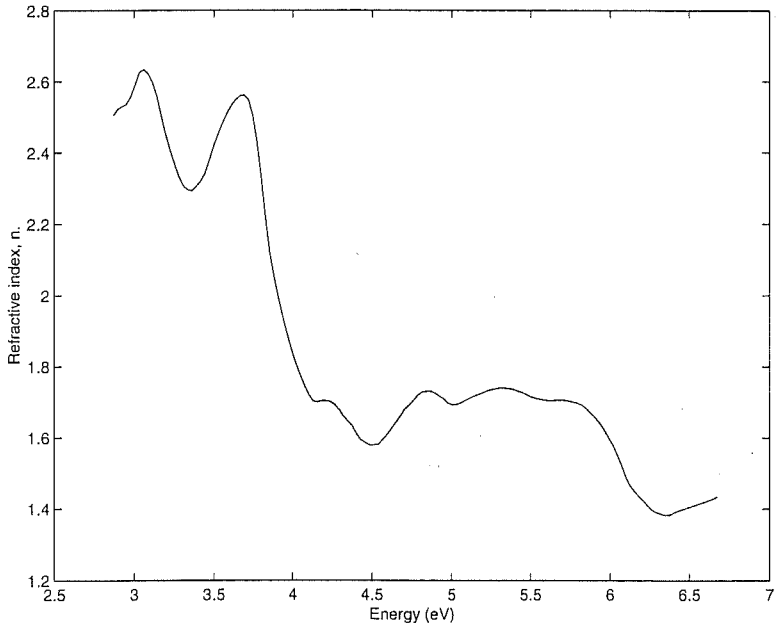

Fig. 7.5: Real part of the dielectric constant in the charge transfer active region of $CrBr_3$

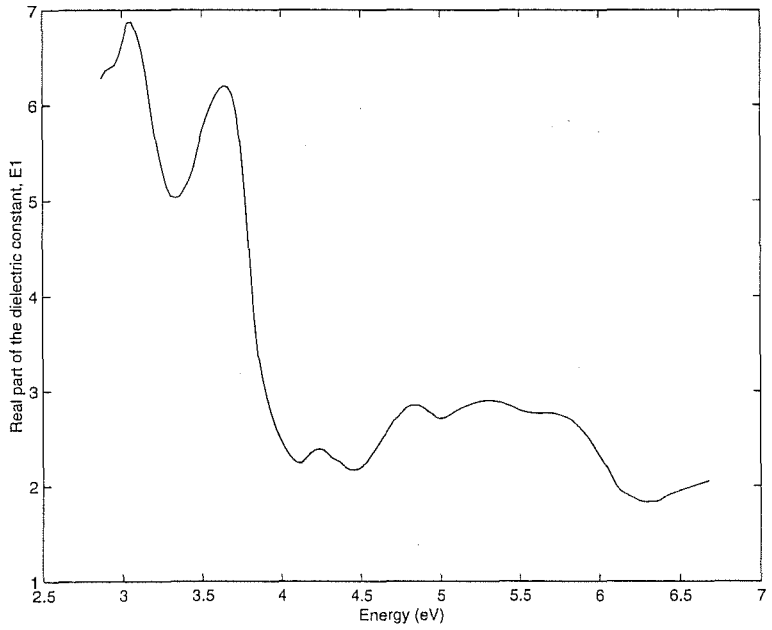

Fig. 7.6: Imaginary part of the dielectric constant in the charge transfer active region of $CrBr_3$

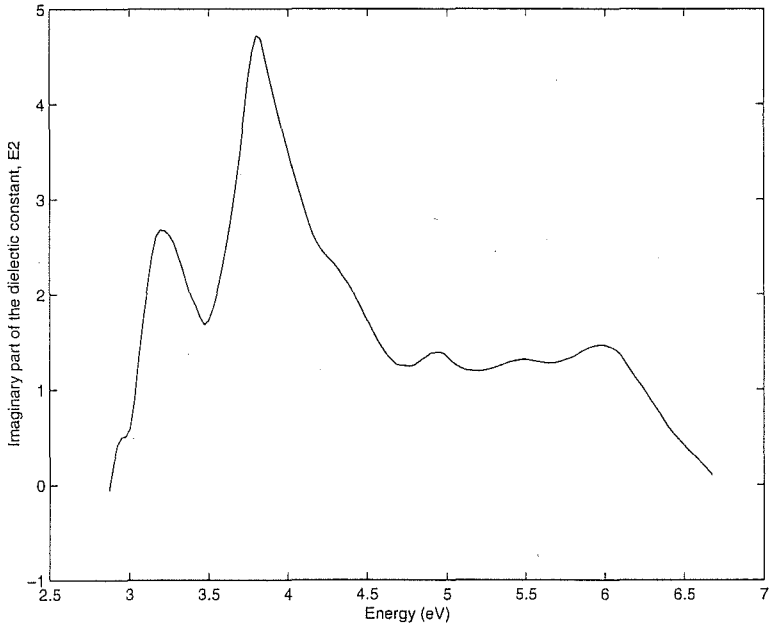

8. KERR ROTATION IN CHROMIUM TRIHALIDES

In this chapter we present the body of a paper to be submitted to Journal of Physics B:Atomic, Molecular and Optical Physics.

The Kerr magneto–optic effect in ferromagnetic $CrBr_3$.

Luke F McAven, Hughan J Ross, Kiminari Shinagawa† and Philip H Butler

Department of Physics and Astronomy, University of Canterbury, Private Bag 4800, Christchurch, New Zealand
† Department of Physics, Toho University, Funabashi–City, Chiba, 274 Japan

In ferromagnetic $CrBr_3$ the Kerr rotation is a significant effect which is not fully understood. Early investigations suggested that $t_{1u}(\pi) \rightarrow t_{2g}^*$ and $t_{2u}(\pi) \rightarrow t_{2g}^*$ and $t_{1u}(\sigma) \rightarrow e_g^*$ and/or $t_{2g}^* \rightarrow t_{1u}^*$ were the contributing transitions. Recent investigations have overturned those assignments. Instead, a pair of transitions, $t_{1u}(\pi) \rightarrow e_g^*$ and $t_{2u}(\pi) \rightarrow e_g^*$, with negative and positive spin–orbit coupling coefficients respectively, were shown to explain the Kerr rotation. A simplistic LCAO calculation on a small cluster, combined with Gaussian fits to data, supports those reassignments. We present results of a similar LCAO calculation and Gaussian fit for $CrCl_3$.

Classification Numbers: 31.20.E, 78.20.L

8.1 Introduction

Ferromagnetic materials with high magneto–optical effects have been applied to devices such as optical isolators, magnetic sensors and rewritable optical memories (Abe & Gomi 1990, Dillon 1990). In recent years there has been an increasing demand for materials with higher magneto–optical effects, such as Kerr rotation. Although magnetic circular dichroism gives similar information on the states, the Kerr rotation is more important than magnetic circular dichroism from an applied viewpoint.

The magneto–optical effects in ferromagnetic materials originate mainly from the spin–orbit effect in the excited state (Argyres 1955). Therefore it is important to know the magnitude of the spin–orbit coupling constants in each ferromagnetic material. This often involves the calculation of the matrix elements between electron configurations with many open shells. For these matrix elements, the Racah–Wigner mathematical formalism is helpful (Butler 1981, Piepho & Schatz 1983). However, this formalism is not familiar to experimentalists and can be tiresome in long calculations. A software package called RACAH has been developed at Canterbury which is a smarter and much more general version of the program which produced the tables of Butler (1981).

In an earlier paper (Ross et al. 1996) we adopted, as an example, the Kerr effect in ferromagnetic $CrBr_3$ and showed how to calculate the spin–orbit matrix elements using RACAH. Having knowledge about the spin–orbit coupling coefficients is vital in understanding the Kerr rotation, the effect investigated in this paper. We concentrate on this effect because of its importance from the applied point of view.

The Kerr effect in ferromagnetic $CrBr_3$ was measured by Jung (1965) and showed a positive Kerr rotation peak at 23500cm^{-1} and a negative Kerr rotation peak at 26700cm^{-1}, both of a few degrees. Dillon, Kamimura & Remeika (1966) were the first to suggest a mechanism for this effect. These Kerr rotations were assigned to the charge transfer (CT) transitions of electrons from the bromine orbitals to the chromium orbital, that is $t_{1u}(\pi) \rightarrow t_{2g}^*$ and $t_{2u}(\pi) \rightarrow t_{2g}^*$, and the CT transition $t_{1u}(\sigma) \rightarrow t_{2g}^*$ or the internal transition in the chromium $t_{2g}^* \rightarrow t_{1u}^*$, respectively.

One of the authors performed calculations (Shinagawa et al. 1995, Shinagawa 1996) for an octahedral cluster of 6 bromine ions surrounding a single chromium ion, and concluded that the Kerr rotations have been assigned to the wrong transitions by Dillon, Kamimura & Remeika (1966). In section 8.2 we outline the approach taken by Shinagawa et al. (1995), and state the proposed reassignments.

In section 8.3 we discuss the problem of labelling and classifying the states of the cluster, in a manner useful for adding the spin–orbit term to our LCAO calculated energy levels. In section 8.4 we briefly discuss some of the pertinent allowed transitions. We calculate energy levels using a simplistic LCAO calculation, presenting details of this in section 8.5. Our calculation give us strong indications

about the levels of mixing between different states, section 8.5.1, as well as the actual energies of the states.

One of the main objectives of this paper is to make correct assignments to the transitions in the CT region of the spectra. In section 8.6 we fit Gaussians to data, providing valuable information about the positioning and relative strengths of the transitions. This is itself is useful information. Assignments are then made, using our calculated energy levels and the information obtained by Gaussian fitting. The assignments for $CrBr_3$, given in section 8.7, are then checked by calculating the Kerr rotation spectrum for our theoretical transitions. This spectrum is evaluated and presented in section 8.8, after the energy shifts are calculated using the previously spin–orbit coupling coefficients (Ross et al. 1996).

We summarise our results in section 8.9.

Although Kerr rotation is known to be less significant in $CrCl_3$ we also apply the LCAO analysis to that structures. We again fit Gaussians to data and discuss briefly the transitions. We were unable to extend the fitting results to the next chromium trihalide, CrI_3, since we could not find reflectance data. Much of the discussion in this paper is related specifically to $CrBr_3$, although the general techniques used are similar for $CrCl_3$.

8.2 Electronic Transition Reassignments

Using an unrestricted self–consistent field (USCF)–X α scattering wave(SW) method (Slater 1979), Shinagawa et al. (1995) calculated one electron energy levels of the $(CrBr_6)^{3-}$ cluster in the ground state. Each level is labelled by irreps of O_h, and a "$*$" is used to indicate that an orbital is of mostly chromium character. In the ground state the thirty–six 4p electrons of the six Br^- ions completely occupy up to the t_{1g} bromine 4p–like orbitals, and three 3d electrons of the Cr^{3+} ion occupy the t^*_{2g} upspin level.

Three CT transitions are allowed from the bromine 4p–like t_{1u} or t_{2u} upspin level to the empty 3d–like e^*_g level. The internal transition from the 3d–like t^*_{2g} level to the 4p–like t^*_{1u} level in the chromium is also allowed, but is of a much higher energy. From Slater transition calculations, the transition energies were found to be 22800cm^{-1}, 27100cm^{-1}, and 34300cm^{-1}. The energy of the internal transition was found to be much higher, 56500cm^{-1}.

Shinagawa et al. (1995) noted that the Kerr rotation peaks observed by Jung (1965) therefore seem to correspond to the CT transition $t_{1u} \rightarrow e^*_g$, for the positive rotation peak, and the CT transition $t_{2u} \rightarrow e^*_g$, for the negative rotation peak. These assignments are different from those given in Jung (1965). We will investigate these assignments by an alternative approach.

8.3 *Electronic States of the Cluster*

In this section we discuss the electronic states of $CrBr_3$ and $CrCl_3$. For simplicity we refer to the $CrBr_3$ system, although the discussion applies similarly to $CrCl_3$ (or CrI_3 say).

Being an insulator, the electronic states of $CrBr_3$ may be approximated by the states of a $(CrBr_6)^{3-}$ octahedral cluster (Dillon, Kamimura & Remeika 1966). We can build the molecular orbitals from the linear combinations of 3d+3p+4s orbitals of the Cr^{3+} ion, and 4s+4p orbitals of the six Br^- ions (Ballhausen & Gray 1964, Shinagawa et al. 1995).

We would like to be able to calculate the spectrum of the $(CrBr_6)^{3-}$ cluster accurately and compare the results with the known experimental spectrum. *Ab initio* calculations have been done for $(CrF_6)^{3-}$, and energies for the bands agree to within $2000cm^{-1}$ (Pierloot & Vanquickenbourne 1990). The calculations using a USCF–X α SW method (Shinagawa et al. 1995, Shinagawa 1996) cannot provide this level of accuracy, and therefore we seek to examine the assignments discussed in section 8.2 with a different sort of calculation.

We use a modified LCAO method, making the assumption that all orbitals, except 3d in chromium and 4s+4p in bromine, are core orbitals. The crystal symmetry is hexagonally close packed, with a space group symmetry of C_{3i}. The octahedral arrangement of bromide ions in the cluster is distorted by the three neighbouring chromium ions to give the cluster D_3 symmetry about the central chromium ion. This calculation allows us to include the consequent trigonal distortion as part of the fundamental interaction scheme, rather than as a perturbation to the basic Hamiltonian. We give details in section 8.5. We find it useful to extend the cluster in a manner consistent with the labelling of this section.

We consider the CT transitions where an electron from one of the bromide ions jumps to the chromium $3d$ orbital. Dillon, Kamimura & Remeika (1966) includes the intra–atomic transitions of an electron from a chromium 3d to a 4s orbital, we do not, having excluded the chromium 4s orbitals from our LCAO calculation. Since the states of the six bromide ions are an integral part of the CT transitions we need to classify these states, as well as those of the chromium. This makes the problem significantly harder than that of a chromium ion in an octahedral ligand field, since it introduces many more parameters than we are likely to obtain from an experiment. The effects of electron correlation, and of the electrostatic field from the surrounding atomic centres, would have some influence on the bromide orbitals that are combined to produce cluster states. However we choose to ignore these contributions and assume that we are dealing with the orbitals of an isolated bromide ion.

We therefore divide the cluster into two packages;

- ◇ the central chromium ion, which we assume is in a trigonally distorted octahedral crystal field,

◇ and the six bromide ions, whose orbitals we take to be linear combinations of the atomic bromine orbitals.

Given that the octahedral field is "strong", we classify the orbital parts of the chromium orbitals using O_h. With the addition of spin our classifying group becomes $SU_2 \times O_h$. Similarly the orbitals on the individual bromine atoms are classified using $SU_2 \times O_h$. The bromine atomic orbitals are then combined into Br_6 molecular orbitals. The Br_6 orbitals are not only characterised by the symmetry properties under the O_h group but also by the extent to which they partake in the bonding of the bromides to the chromium. We have σ type bonding orbitals, π type anti–bonding orbitals and non–bonding orbitals which we choose to label as ρ orbitals. This differs from Dillon, Kamimura & Remeika (1966), who label the non–bonding orbitals with a superscript n, as in ${t_{1g}}^n(\pi)$ which becomes $t_{1g}(\rho)$ in our notation.

We now briefly examine our labelling scheme for the excited states of the cluster. In the CT states there are three open shells, two on the Cr centre and one on the Br_6 "molecule". The overall symmetry of the state of the cluster, without considering the trigonal distortion, must be $SU_2 \times O_h$ and so we couple these three orbitals at the $SU_2 \times O_h$ level. Although we can couple them in any order it is natural to couple the two Cr orbitals together first and then add the Br_6 orbital. Thus our group chain is

$$\left\{\left((SU_2 \times O_h)_{t_{2g}},\ (SU_2 \times O_h)_{e_g}\right) \downarrow (SU_2 \times O_h)_{\mathrm{Cr}},\ (SU_2 \times O_h)_{\mathrm{Br_6}}\right\} \downarrow (SU_2 \times O_h)_{\mathrm{Cluster}}, \tag{8.1}$$

where $\downarrow$ represents a branching. This completes the classification of states imposed by the terms in the Hamiltonian that have O_h symmetry. The remaining terms are the spin–orbit contribution, the trigonal term and the magnetic exchange interaction. The spin–orbit and trigonal terms do not have simultaneous eigenstates and since they are of comparable size we would have to solve a secular perturbation problem. The exchange interaction was taken to be $3.8\mathrm{cm}^{-1}$ by Dillon, Kamimura & Remeika (1966). Nosenzo, Samoggia & Pollini (1984) proposed using $200\mathrm{cm}^{-1}$ in an attempt to explain the Kerr rotation dispersion as arising from the two bands split by the exchange interaction. In this work we do not treat the exchange interaction as a major contributor to the Kerr rotation, preferring to use the value of $5.7\mathrm{cm}^{-1}$ given by Davis & Narath (1964), which was later adopted by Cobb et al. (1971).

We can write the ground state with respect to our group chain as (Ross et al. 1996),

$$|t_{2g}^3\left({}^4A_{2g}\right) U'.A_2\ U'E''\tfrac{3}{2}\rangle\ . \tag{8.2}$$

Similarly the excited states allowed by the electric–dipole mechanism can be expressed as

$$\left|\mathcal{P}\left\{\left(t_{2g}^3\left({}^4A_{2g}\right),\ e_g\left({}^2E_g\right)\right){}^5E_g,\ t_{1u}^5\left({}^2T_{1u}\right)\right\}{}^4T_{2u}\ U'.T_{2u}\ r\ \lambda\ \mu\ l\right\rangle \tag{8.3}$$

and

$$\left|\mathcal{P}\left\{\left(t_{2g}^{3}\left({}^{4}A_{2g}\right),\ e_g\left({}^{2}E_g\right)\right){}^{5}E_g,\ t_{2u}^{5}\left({}^{2}T_{2u}\right)\right\}{}^{4}T_{2u}\ U'.T_{2u}\ r\ \lambda\ \mu\ l\right\rangle \tag{8.4}$$

being excitations from the t_{1u} and t_{2u} open shells respectively.

8.4 Allowed Transitions

Figure 8.1 shows the energy levels and the transitions for $(CrBr_6)^{3-}$ in a ferromagnetic state. The arrows show the transitions allowed by the light of left or right circular polarisation, and the numbers attached to the arrows are the calculated relative transition strengths (Shinagawa et al. 1988). The excited state ${}^{4}T_{2u}$ is equivalent to the atomic ${}^{4}P(L=1)$ state, so the spin–orbit interaction splits it into three levels specified by the total angular momentum $J = \frac{5}{2}$, $\frac{3}{2}$ and $\frac{1}{2}$. Similarly the excited state ${}^{4}T_{1u}$ is equivalent to the atomic ${}^{4}P(L=1)$ state. In the ferromagnetic state the molecular field further splits each level into $2J+1$ levels labelled by J_z.

At low temperature the transitions possible are from the lowest $J_z = \frac{3}{2}$ ground level only. The measurements of Kerr rotation at 1.5K make this a valid assumption. Thus, the differences in the selection rules for the two circular polarisations induces the Kerr effect in $CrBr_3$, and its sign and magnitude depends upon the sign and magnitude of the spin–orbit constant λ in the excited state. In order to make assignments to the Kerr rotation peaks we therefore must calculate the spin–orbit constant. Although this calculation is tiresome, the effort can be greatly reduced using our software package RACAH (Ross et al. 1996). The values of the spin–orbit constants are shown in table 8.8.

It should be noted that the signs of the spin–orbit constant λ differ in the two CT states, contrary to a previous study by Dillon, Kamimura & Remeika (1966). This means that Kerr rotations originating from the two transitions have an opposite sign, consistent with observations by Jung (1965).

The spin–orbit constant is defined, in the same manner by all authors, as

$$\lambda = -\frac{\langle {}^{4}T_2 \| \mathcal{H}_{so} \| {}^{4}T_2 \rangle}{\langle L \| L \| L \rangle \langle S \| S \| S \rangle} \tag{8.5}$$

where $\langle S \| S \| S \rangle = \sqrt{S(S+1)(2S+1)}$ and for this case $\langle L \| L \| L \rangle = -\sqrt{6}$.

8.5 LCAO approach

We need to provide a calculation which would, among other things, demonstrate that the levels of a $CrBr_3$ cluster, without the trigonal distortion of the chromium ions, are not just moved by the trigonal distortion but mixed together by it. This demonstrates that a standard perturbation type calculation, which merely shifts

Fig. 8.1: Energy level diagram including the allowed CT transitions in a $(CrBr_6)^{3-}$ octahedral cluster. Reproduced from Shinagawa *et al* (1995). Note in particular the spin–orbit splitting, of the $^4T_2$ state into three levels with differing values of J. The shifts in energy are $3/2\lambda$, $-\lambda$ and $-5/2\lambda$ for those levels.

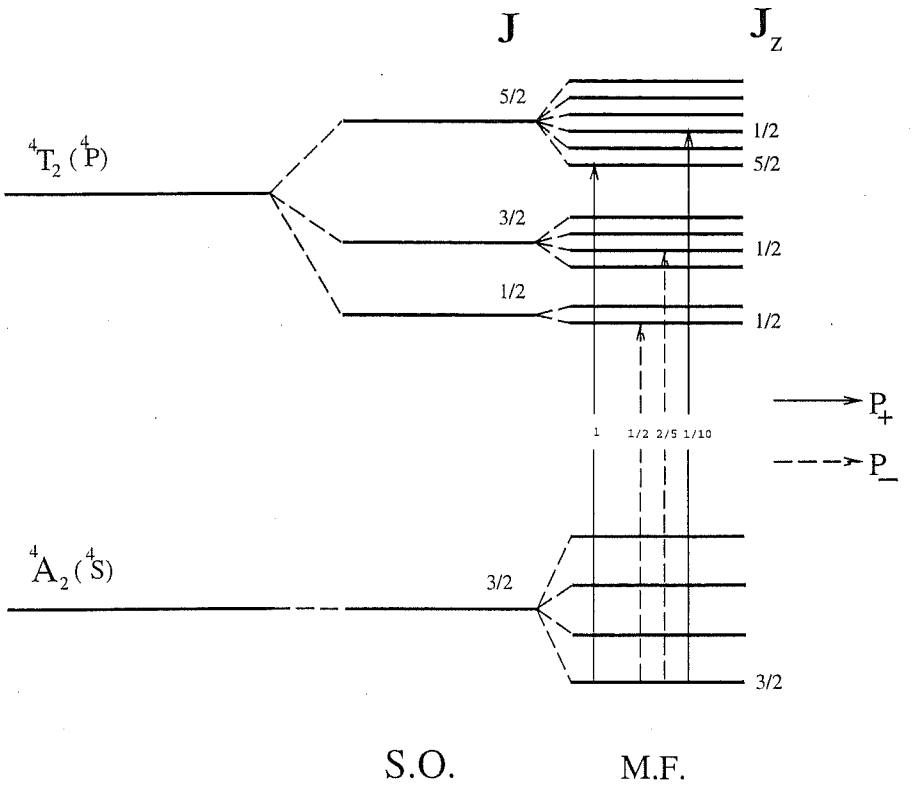

the level, does not provide the full picture. An LCAO calculation, including orbitals from bromine and chromium ions, provides the information in which we are interested, in a non–perturbative manner.

Our calculation is similar that of Mattheiss (1969) for ReO_3. Our computer program calculates the energy matrix at K=0, taking the potentials for the individual interactions between orbitals from Harrison (1980, table 20–1). For each bromine ion we include an "s" and a "p" orbital set, and for each chromium ion a "d" orbital set. In order to produce an $CrBr_3$ energy level structure similar to that of Antoci & Mihich (1978, figure 3) we choose the s orbitals to have a base of -15.5 eV, and the p orbitals a base of -3.6 eV. The d orbitals are assigned the energies -0.66 eV and 0.99 eV for the T_{2g} and E_g parts respectively, giving a $-4Dq$ and $+6Dq$ split about the zero of energy. For $CrCl_3$ we choose the s orbitals with a base of -16.8 eV, the p orbitals a base of -4.75 eV, and the d orbitals -0.70 eV and 1.05 eV for the T_{2g} and E_g parts respectively. In both cases we chose the axis of D_3 symmetry to be the [111] axis.

Our program is versatile enough to examine the effect of turning the trigonal distortion on and off, we simply remove the chromium sites from the input data file. In addition it allows for sites to be identified with other sites, in the sense that the interaction for a site is given by the average over the sites with which each site is identified. We therefore can reduce the number of included energy levels, while maintaining the D_3 symmetry of the extended cluster. This allows us to explicitly enter only six bromine and two chromium ions, but model twenty–four bromine and four chromium ions in an extended cluster.

Our program produces the energy matrix, in a MATLAB format, in an orbital basis. We would much prefer however to be able to parameterise it in a basis more pertinent to this particular problem. The basis $SO_3 \supset O_h \supset D_3 \supset C_3$ is the ideal choice since our spin–orbit calculations have been done with respect to this basis. Using projection operator methods we can perform a transformation to the new basis. However, Butler, Ford & Reid (1983) have shown that projection operator methods do not contain all phase information, and therefore do not give symmetry–adapted basis functions consistent with a given set of $3jm$ symbols. This phase problem means that standard transformation tables in Butler (1981) must be modified. By multiplying each basis vector by a phase, see table 8.1, we obtain a real Hamiltonian matrix in a $SO_3 \supset O_h \supset D_3 \supset C_3$ basis. In the table we see that the phase is either a simple unit, $\{1, -1, i, -i\}$, or expressible in terms of $\{a, a^*\}$ multiplied by a simple unit, where $a = \frac{\sqrt{3}}{2} + \frac{i}{2} = \exp\frac{i\pi}{6}$.

We attempted to parameterise this Hamiltonian in that basis, following Butler (1981, chapter 9), but were not surprised to find that such a parameterisation was not possible. This failure is due to the symmetry of the system being only $O_h \supset D_3 \supset C_3$, as the SO_3 label is "artificial".

Tab. 8.1: The phases applied to each basis vector to give a real Hamiltonian in a $SO_3 \supset O_h \supset D_3 \supset C_3$ basis. See section 8.5. We use $\bar{1}$ to represent the irrep label -1. $a = \frac{\sqrt{3}}{2} + \frac{i}{2} = \exp(\pi/6)$

Vector	Phase	Vector	Phase	Vector	Phase
$\|22^+1\bar{1}\rangle$	$-a^*$	$\|11^-1\bar{1}\rangle$	i	$\|11^-1\bar{1}\rangle$	$-a^*$
$\|22^+11\rangle$	$-a$	$\|11^-\tilde{0}0\rangle$	1	$\|11^-\tilde{0}0\rangle$	1
$\|2\tilde{1}^+11\rangle$	ia	$\|22^+11\rangle$	1	$\|22^+11\rangle$	1
$\|2\tilde{1}^+1\bar{1}\rangle$	$-ia^*$	$\|22^+1\bar{1}\rangle$	1	$\|22^+1\bar{1}\rangle$	1
$\|2\tilde{1}^+10\rangle$	1	$\|00^+00\rangle$	1	$\|2\tilde{1}^+11\rangle$	$-ia^*$
$\|22^-1\bar{1}\rangle$	$-a^*$	$\|11^+11\rangle$	1	$\|2\tilde{1}^+1\bar{1}\rangle$	ia
$\|22^-11\rangle$	$-a$	$\|11^+1\bar{1}\rangle$	1	$\|2\tilde{1}^+00\rangle$	1
$\|2\tilde{1}^-11\rangle$	ia	$\|11^+\tilde{0}0\rangle$	1	$\|2\tilde{1}^-11\rangle$	ia
$\|2\tilde{1}^-1\bar{1}\rangle$	$-ia^*$	$\|11^-11\rangle$	1	$\|2\tilde{1}^-1\bar{1}\rangle$	$-ia^*$
$\|2\tilde{1}^-10\rangle$	1	$\|11^-1\bar{1}\rangle$	a^*	$\|2\tilde{1}^-00\rangle$	1
$\|00^+00\rangle$	1	$\|11^-\tilde{0}0\rangle$	a		
$\|11^-11\rangle$	$-i$	$\|11^-11\rangle$	1		

8.5.1 Energy level mixing

The Hamiltonian calculated in section 8.5, $\mathcal{H}'$, can be diagonalised to find the energies of the states. The eigenvectors provide information about which $SO_3 \supset O_h \supset D_3 \supset C_3$ basis vectors are used to build up those states, and in what proportions they contribute. Tables 8.2 and 8.3 gives those proportions for $CrBr_3$ and $CrCl_3$ respectively. It is interesting that many halogen centred states are spread over several basis vectors. This makes the calculation of spin–orbit constants required for transitions involving those states slightly more difficult. Just as interesting is that the mixing between the molecular orbitals on the halide and chromium sites is very small, less than 0.5% in all cases. This would suggest that applying perturbation theory to a system with *ab initio* chromium cluster levels embedded in *ab initio* halogen cluster levels is a reasonable thing to do. Some states, formed from orbitals on the halogen sites, are observed to have significant components with different parities.

8.5.2 Bonding Strengths

A particular feature of our LCAO program is helpful in identifying the ground states. We can perform the energy calculation including our choice of interactions. We can, for example, turn off p–p σ or p–d σ interactions and see the effects on the energy levels of our system. This shows, for example, that the 16^{th} state in table 8.2 is not affected by p–d bonding. In several cases this provides useful information which we keep in mind in making assignments to the transitions.

8.6 Fitting Gaussians to the spectrum

In order to discuss the assignments of Shinagawa et al. (1995) and others, we need to classify the transitions appearing in the reflectance spectra. Although the methods of the previous sections provide a great deal of information, another approach is useful in assists our assignments. By fitting Gaussians to the imaginary part of the dielectric constant we gain some idea of the comparative magnitudes and spreads of the main transitions. We provide fittings for both the p–d CT excitons, and the p–d CT transitions in one calculation across the range 2.85 eV to 6.7 eV. It is in this region that those CT effects are dominant.

We took the data for the reflectance spectra of $CrBr_3$ from Pollini et al. (1989, figure 6), by electronically scanning the graph and then reading data points off the magnified image. The data was entered into a MATLAB script, and accurately reproduced the reflectance spectra. A Kramers–Kronig type analysis gave us graphs of the reflectivity coefficient, the refractive index, extinction coefficient, and finally the real and imaginary parts of the dielectric constant. The graphs obtained were consistent with those basic graphs produced in Pollini et al. (1989). For the $CrCl_3$ system, data for the imaginary part of the dielectric constant was taken

directly from (Carricaburu et al. 1986). This simplified the analysis of the $CrCl_3$ somewhat.

From Pollini et al. (1989) it is clear that there are at least three peaks in the reflectance spectra within the exciton region of $CrBr_3$. Those peaks are at approximately 2.90 eV, 3.10 eV, and 3.80 eV. The other possible peak at 4.25 eV is not given by Pollini et al. (1989) as either a p–d exciton or a p–d CT transition. It is also clear that in the transition region of $CrBr_3$ there are at least three peaks at about 4.90, 5.40 and 5.95 eV.

The most significant difference in the spectra of $CrCl_3$ is the exciton region. The CT transition regions are similar, but rather than the two main distinct peaks in the exciton region of $CrBr_3$, $CrCl_3$ contains a single broader peak with bumps on each side. It is apparent in Carricaburu et al. (1986, figure 6) that close to the left of top of the main peak in $CrCl_3$, there is another transition. We naturally expect the four transitions in the charge transfer exciton regions of $CrCl_3$ and $CrBr_3$ to be related. Figures 8.2 and 8.3 contain the fitted transitions, emphasising the presence of seven transitions in total. The eighth transition in the $CrCl_3$ spectra is used to take into account the influence of higher transitions, and in itself should not be considered to result from a charge transfer effect.

We give the Gaussians in table 8.4, in the form,

$$G_i = c_i \exp\left(-\frac{(E - E_i)^2}{a_i}\right) . \tag{8.6}$$

The Gaussians in table 8.4 are modified from the raw ones obtained by the fitting procedure. The procedure produced a Gaussian between the first and second in the table. While the reflectance spectra of $CrBr_3$ clearly show the other four peaks up to 4.5 eV, this additional Gaussian implied that the transition at 3.10 eV is in fact slightly split and the result of two very nearly superimposed bands with similar characteristics. Since we could not physically justify such superimposed bands we removed one of them, modifying the first and second Gaussians to take this into account. The seven $CrBr_3$ Gaussians and their resultant, can be seen in figure 8.2, in comparison with the experimentally based measurement of the dielectric constant. We see that it is possible to obtain a good fit by this method. It is important to recognise that we constrain our Gaussians to centre at places where transitions are known to occur. Without this restriction other (probably less physical) fits are obtained. A similar procedure gives a good fit to the $CrCl_3$ spectra.

The first four peaks of $CrBr_3$ are of the most interest to us. The first and second correspond to those used by Shinagawa et al. (1995) to explain the Kerr rotation. It is also interesting to note that the second and third transitions have very similar Gaussian parameters. The fourth is a very broad band, at an energy on the reflectance spectra of a small bump on the large 3.80 eV peak. The intensities of the first two bands, expressed relative to the broad fourth band, are significantly different.

8.7 Assignments to the transitions

The results of the previous two sections can be used to make assignments to the transitions. The first thing to look at is the energy separation between excited states, and thus between transitions.

The Coulomb and octahedral terms should contribute to the difference between the transition to e_g^* and the transition to t_{2g}^* in a manner determined by the values of the Racah parameters B, C and the octahedral parameter Dq. Using the tables given in McClure (1959) (taken from Tanabe & Sugano (1954a,b)), and the values determined by Bermudez & McClure (1979a,b): $B = 430\text{cm}^{-1}$, $C = 3500\text{cm}^{-1}$, and $Dq = 1330\text{cm}^{-1}$ we have

$$\begin{aligned} t^4(^3T_1) - t^3e(^5E) &= (-16Dq - 15B + 5C) - (-6Dq - 21B) \\ &= 6B + 5C - 10Dq \\ &= 6 \times 430 + 5 \times 3500 - 10 \times 1330 \qquad (8.7) \\ &= 6780 \end{aligned}$$

(8.8)

Several of our fitted Gaussians are separated by approximately 6780cm^{-1} or 0.84 eV, and thus we suggest they probably correspond to a pair of transitions like $t_{2u}(\pi) \rightarrow e_g^*$ and $t_{2u}(\pi) \rightarrow t_{2g}^*$.

We can repeat this calculation for $CrCl_3$. For $CrCl_3$ Bermudez & McClure (1979a,b) give $B = 525\text{cm}^{-1}$, $C = 3275\text{cm}^{-1}$, and $Dq = 1410\text{cm}^{-1}$ so that the difference above becomes 5425cm^{-1}.

In tables 8.2 and 8.3 we have the energy levels obtained from our LCAO calculations. In order to calculate the transition energies we find the difference between those levels, and then add in the change due to the change in octahedral terms. We have explicitly entered the $10Dq$ split between the two levels due just to the Coulomb effect (see section 8.5), and thus do not need to include Coulomb terms in our current calculation. The changes in octahedral terms have the following effects:

$$\begin{aligned} t^4(^3T_1) - t^3(^4A_2) &= 5C \\ &= 17500 \qquad (8.9) \end{aligned}$$

$$\begin{aligned} t^3e(^5E) - t^3(^4A_2) &= -6B \\ &= -2580 \qquad (8.10) \end{aligned}$$

For $CrCl_3$ the effects of those two are 16375cm^{-1} and -3150cm^{-1}.

Having calculated the transition energies between our states we may write down our assignments to the experimental transitions in terms of the labels associated with our states. The first step in identifying those Gaussian transitions

involves matching up the positions of the Gaussians with transition energies, given by the difference between cluster state energies. As mentioned above, we include Coulomb and octahedral contributions in this calculation. In particular we are interested in the transitions to the chromium sites from the bromine sites, that is, CT transitions. Table 8.6 summarises our assignments for $CrBr_3$, with the assignments for $CrCl_3$ given in table 8.7.

As yet we have not justified the irrep and bonding labels associated with the states given in tables 8.2 and 8.3. That table however makes the composition of states, in terms of irreps, clear. Electric dipole transitions are forbidden between states of the same parity. Thus when states are significantly mixed, as with $CrBr_3$ state 10/11, parity can be used to identify the most significant contributors to the transition. The state to which the transition is made is built into the transition calculated, and is an integral part of the parity argument used above.

Having all that information, how then have we distinguished between π, σ, and ρ bonding? In section 8.5.2 we mentioned that by turning off certain interactions we can see how states are effected, in a non–perturbative way. Those variations make the assignments natural to our approach.

Our energy level calculations suggest that the second $CrBr_3$ Gaussian is a superposition of two transitions, (see table 8.6). Generally, the pi transition should be weak compared with the sigma one, since the overlap of the wavefunction between the ligands and the central ion (Cr^{3+}) is small. Shinagawa et al. (1995) assumed that two transitions contributing to the Kerr rotation, $t_{1u}(\pi) \rightarrow e_g$ and $t_{2u}(\pi) \rightarrow e_g$, were of the same transition strength. This is consistent with the Gaussians we have obtained and we therefore adopt the same assumption in the next section. The second Gaussian is predominantly the result of the $t_{1u+2u}(\pi) \rightarrow e_g$ transition. That transition has a spin–orbit coupling constant dependent upon the small overlap, $|S|$, between $p(\sigma)$ and $p(\pi)$ orbitals on neighbouring bromine ions and therefore cannot be expected to significantly contribute to the Kerr rotation.

8.8 Calculation of Kerr Rotation Spectrum

To check the results of our LCAO based assignments, we calculate the Kerr rotation spectrum using the optical data measured by Pollini et al. (1989). The measurements of the Kerr rotation were measured using the normal reflection from the x–y plane, since the z–axis was taken along the c–axis in the experiments. The Kerr rotation Θ_K is given by Jung (1965) as

$$\Theta_K = \frac{n(3k^2 - n^2 + 1)\epsilon'_{xy} - k(3n^2 - k^2 - 1)\epsilon''_{xy}}{(n^2 + k^2)[(n^2 - k^2 - 1)^2 + (2nk)^2]} \tag{8.11}$$

where n and k are the real and imaginary parts of the index of refraction respectively, $N = n - ik$. Those can be related to the dielectric tensor, $\epsilon_{xx} = \epsilon'_{xx} - i\epsilon''_{xx}$,

by

$$n^2 - k^2 = \epsilon'_{xx} \tag{8.12}$$

$$2nk = \epsilon''_{xx} \tag{8.13}$$

The ϵ'_{xy} and ϵ''_{xy} are the real and imaginary parts of the xy–component of the dielectric tensor, $\epsilon_{xy} = \epsilon'_{xy} - i\epsilon''_{xy}$, which is given at absolute zero by,

$$\epsilon_{xy} = iC \sum_j \theta_j^2 \frac{(p_+^j)^2 - (p_-^j)^2}{[\theta(\theta_j^2 - (\theta - i\gamma_j)^2)]} \tag{8.14}$$

where C is a constant dependent on the concentration of Cr^{3+} ions, θ is the frequency of the incident light, θ_j is the transition energy of the j^{th} transition, $(p_+^j)^2$ and $(p_-^j)^2$ are the transition strengths of the j^{th}–transition for the right and left circularly polarised light (Shinagawa et al. 1995), and γ_j is the half width of the j_{th} transition.

We take the transition energies for the Gaussians straight from our fit. We do not however use the half–width, or intensity, information from our Gaussian fit in calculating the Kerr rotation. The two significant transitions, $t_{1u}(\pi) \rightarrow e_g$ and $t_{2u}(\pi) \rightarrow e_g$, split into three levels each, at $E + \frac{3\lambda}{2}$, $E - \lambda$, and $E - \frac{5\lambda}{2}$. The half–widths for those, taken from Shinagawa et al. (1995), are 2000, 1800 and 1350cm^{-1} in energy order. Since the first transition has a negative spin–orbit coupling constant, and the second has a positive spin–orbit coupling constant, the half–widths for the two transitions of importance are in a different order.

The broad shape of the Kerr rotation curve for a given transition is essentially independent of the half–widths. The half–widths act as fitting parameters in the calculation of the Kerr rotation spectrum.

The spin–orbit coupling constant, ζ_{4p}^{Br}, was taken to be 2460cm^{-1} (Dillon, Kamimura & Remeika 1966). C is used as a scaling factor and is obtained by scaling the calculated Kerr rotation curve to fit the experimental data. C was found to be $\frac{1}{43}$.

The Kerr rotation spectrum, calculated using equation (8.11), is shown in figure 8.4. in comparison with the observed one. We see that the observed Kerr rotation spectrum is reproduced quite well. The divergence between our theory and the experimental results at energies higher than that of the negative Kerr rotation peak may be due to the Kerr rotation of other peaks being excluded in our work.

8.9 Summary

In this work we have investigated the energy band structure of $CrBr_3$ and $CrCl_3$, with the aim of making assignments to the Kerr rotation peaks present in the ferromagnetic $CrBr_3$. By fitting Gaussians to the imaginary component of the dielectric constant we can locate the position of the transitions contributing significantly

to the Kerr effect, as well as other transitions in the region of CT dominance. We have placed the two peaks of significance at 23800cm^{-1} and 25900cm^{-1} in the imaginary part of the dielectric curve. The observed peaks of Kerr rotation are given by Jung (1965) at 23500cm^{-1} and 26500cm^{-1}. Jung (1965) states that "Except for the crystal–field transition region, the room temperature dielectric constant data could be fitted within the experimental error by assuming two absorption bands having Gaussian dispersion located at 24310cm^{-1} and 29580cm^{-1}." In line with this we could identify our first and second Gaussians together as the first band of Jung (1965), and the third and fourth Gaussians as the second band of Jung (1965).

Part of this paper involves the calculation of energy levels of $CrBr_3$ and $CrCl_3$ clusters. We modelled a cluster of twenty–four halogen and four chromium ions using a modified LCAO approach where only eight ions are explicitly entered. Rather than simply moving the energy levels, as in perturbation theory type calculations, information pertaining to the mixing of states is inherent in our calculation. We have shown that there is significant mixing between the various halogen orbitals (see tables 8.2 and 8.3), and that levels are not simply being moved. Mixing is small between other orbitals. This supports making *ab initio* cluster calculations for the chromium and halogen clusters independently, and then using perturbation theory to study the overall interacting $CrBr_3$ cluster.

Having discussed the positioning and assignments of the energy levels, and thus the transitions, we proceeded to predict the Kerr rotation from this information. We have adopted the half widths given by Shinagawa et al. (1995) for our corresponding levels. The first transition is clearly identifiable as $t_{1u}(\pi) \rightarrow e_g$, and has a negative spin–orbit coupling constant. The second transition however is more interesting, and our energy level calculations suggest it is composed of $t_{1u+2u}(\sigma) \rightarrow e_g$ and $t_{2u}(\pi) \rightarrow e_g$. The first of these is of much greater intensity but the second, with a positive spin–orbit coupling constant, contributes much more significantly to the Kerr rotation. Although the Gaussian fit did not resolve a large and small level at this position, the freedom in the fit allows consistency with our energy level calculations. Those two π transitions are assumed to be of similar magnitude.

The calculated Kerr rotation curve fits the experimental data, using just those two π transitions, see figure 8.4. This agreement supports the reassignments made by Shinagawa et al. (1995). While agreement at the peaks is particularly good, our curve is significantly flatter to the right of the negative Kerr rotation peak. Indeed the experimental results indicate a small positive Kerr rotation is obtained. However the inclusion of Kerr rotation due to the other charge transfer transitions, such as $t_{1u+2u}(\sigma) \rightarrow e_g$, is expected to improve the agreement between the observed and theoretical Kerr rotation curves.

Further investigations should consider the assignments made to the third to seventh transitions in table 8.6, since those are very tentative. In particular, the transitions to t_{2g} (such as $t_{1u} \rightarrow t_{2g}$) are spin–forbidden and should be weak,

contrary to the assignments we have made.

Tab. 8.2: The $CrBr_3$ orbitals with which we end up are seen to be a mix of different octahedral–parity labelled orbitals, as is shown in this table. Also given is the energies of the level and the orbital number, in the first column.

No.	Energy	a_{1g}^{Br}	e_g^{Br}	e_g^{Cr}	t_{1u}^{Br}	t_{1g}^{Br}	t_{2u}^{Br}	t_{2g}^{Br}	t_{2g}^{Cr}
1	-17.8873	99.66	0	0	0	0	0	0.34	0
2	-16.2567	0	0	0	99.53	0.47	0	0	0
3	-14.6683	0	74.88	0.02	24.97	0	0.02	0.10	0
4	-14.6683	0	74.88	0.02	24.97	0	0.02	0.10	0
5	-14.6659	0	24.97	0.01	74.93	0	0.06	0.03	0
6	-14.6659	0	24.97	0.01	74.93	0	0.06	0.03	0
7	-5.7128	33.62	0	0	0	0	0	66.33	0.05
8	-4.7215	0	5.25	0.01	29.75	0	2.57	62.35	0.07
9	-4.7215	0	5.25	0.01	29.75	0	2.57	62.35	0.07
10	-4.7191	0	1.75	0	69.76	0	7.68	20.79	0.02
11	-4.7191	0	1.75	0	69.76	0	7.68	20.79	0.02
12	-4.7037	49.99	0	0	0	0	24.99	24.99	0.03
13	-4.7029	16.72	0	0	0	0	74.99	8.28	0.01
14	-3.9150	0	0	0	100.00	0	0	0	0
15	-3.9150	0	0	0	100.00	0	0	0	0
16	-3.5024	0	0	0	0.47	99.53	0	0	0
17	-2.7449	0	44.77	0.22	32.63	0	22.38	0	0
18	-2.7449	0	44.77	0.22	32.63	0	22.38	0	0
19	-2.7396	0	15.24	0.08	17.41	0	67.26	0	0
20	-2.7396	0	15.24	0.08	17.41	0	67.26	0	0
21	-2.2612	0	0	0	0	100.00	0	0	0
22	-2.2612	0	0	0	0	100.00	0	0	0
23	-2.1130	0	32.88	0.23	50.15	0	0	16.59	0.15
24	-2.1130	0	32.88	0.23	50.15	0	0	16.59	0.15
25	-0.6641	0.01	0	0	0	0	0.01	0.04	99.94
26	-0.6577	0	0	0	0.02	0	0	0.04	99.93
27	-0.6577	0	0	0	0.02	0	0	0.04	99.93
28	-0.6563	0	0.04	0	0.08	0	0	0.05	99.83
29	-0.6563	0	0.04	0	0.08	0	0	0.05	99.83
30	-0.6518	0.01	0	0	0	0	0.01	0.01	99.97
31	0.9981	0	0.12	99.76	0.06	0	0.05	0.01	0
32	0.9981	0	0.12	99.76	0.06	0	0.05	0.01	0
33	1.0053	0	0.15	99.69	0.08	0	0.05	0.03	0
34	1.0053	0	0.15	99.69	0.08	0	0.05	0.03	0

Tab. 8.3: The $CrCl_3$ orbitals with which we end up are seen to be a mix of different octahedral–parity labelled orbitals, as is shown in this table. Also given is the energies of the level and the orbital number, in the first column.

No.	Energy	a_{1g}^{Cl}	e_g^{Cl}	e_g^{Cr}	t_{1u}^{Cl}	t_{1g}^{Cl}	t_{2u}^{Cl}	t_{2g}^{Cl}	t_{2g}^{Cr}
1	-19.4733	99.60	0	0	0	0	0	0.40	0
2	-17.6642	0	0	0	99.45	0.55	0	0	0
3	-15.9055	0	74.86	0.03	24.97	0	0.02	0.12	0
4	-15.9055	0	74.86	0.03	24.97	0	0.02	0.12	0
5	-15.9022	0	24.96	0.01	74.92	0	0.07	0.04	0
6	-15.9022	0	24.96	0.01	74.92	0	0.07	0.04	0
7	-7.1014	33.68	0	0	0	0	0	66.27	0.04
8	-5.9967	0	5.29	0.01	29.73	0	2.57	62.33	0.06
9	-5.9967	0	5.29	0.01	29.73	0	2.57	62.33	0.06
10	-5.9941	0	1.76	0	69.74	0	7.70	20.78	0.02
11	-5.9941	0	1.76	0	69.74	0	7.70	20.78	0.02
12	-5.9750	49.99	0	0	0	0	24.99	24.99	0.02
13	-5.9741	16.72	0	0	0	0	74.99	8.28	0.01
14	-5.0996	0	0	0	100.00	0	0	0	0
15	-5.0996	0	0	0	100.00	0	0	0	0
16	-4.6475	0	0	0	0.55	99.45	0	0	0
17	-3.8012	0	44.78	0.19	32.65	0	22.38	0	0
18	-3.8012	0	44.78	0.19	32.65	0	22.38	0	0
19	-3.7954	0	15.24	0.06	17.44	0	67.25	0	0
20	-3.7954	0	15.24	0.06	17.44	0	67.25	0	0
21	-3.2641	0	0	0	0	100.00	0	0	0
22	-3.2641	0	0	0	0	100.00	0	0	0
23	-3.0988	0	32.93	0.18	50.20	0	0	16.61	0.08
24	-3.0988	0	32.93	0.18	50.20	0	0	16.61	0.08
25	-0.7058	0.01	0	0	0	0	0.01	0.04	99.95
26	-0.6975	0	0	0	0.02	0	0	0.04	99.94
27	-0.6975	0	0	0	0.02	0	0	0.04	99.94
28	-0.6963	0	0.02	0	0.04	0	0	0.03	99.90
29	-0.6963	0	0.02	0	0.04	0	0	0.03	99.90
30	-0.6896	0.01	0	0	0	0	0.01	0.01	99.98
31	1.0591	0	0.11	99.78	0.05	0	0.05	0	0
32	1.0591	0	0.11	99.78	0.05	0	0.05	0	0
33	1.0677	0	0.12	99.74	0.06	0	0.05	0.02	0
34	1.0677	0	0.12	99.74	0.06	0	0.05	0.02	0

Tab. 8.4: The parameters for the Gaussians found to fit the CT exciton and transition region, 2.85–6.7 eV of the spectrum of $CrBr_3$. By intensity in the last column we imply area under the Gaussian, relative to the 4^{th} Gaussian which has the greatest area underneath it. Those are the modified Gaussians (see section 8.6).

i	E_i (cm^{-1})	E_i (eV)	c_i	a_i (eV)	Relative Intensity
1	23800	2.95	0.10	0.001	0.002
2	25900	3.21	2.02	0.034	0.212
3	30600	3.80	2.05	0.032	0.210
4	32300	4.00	2.84	0.384	1.000
5	40600	5.04	1.07	0.161	0.246
6	44000	5.46	0.44	0.040	0.050
7	48000	5.95	1.44	0.227	0.386

Tab. 8.5: The parameters for the Gaussians found to fit for the CT exciton and transition region, 3–8 eV eV of the spectrum of $CrCl_3$. By intensity in the last column we imply area under the Gaussian, relative to the 2^{nd} Gaussian which has the greatest area underneath it.

i	E_i (cm^{-1})	E_i (eV)	c_i	a_i (eV)	Relative Intensity
1	30500	3.78	0.92	0.159	0.214
2	36300	4.50	3.91	0.192	1.000
3	38100	4.73	1.58	0.030	0.160
4	42200	5.23	2.51	0.133	0.534
5	48400	6.00	1.93	0.205	0.510
6	52300	6.48	0.34	0.031	0.035
7	55600	6.89	2.35	0.362	0.822
8	64000	7.94	0.48	0.260	0.081

Tab. 8.6: The $CrBr_3$ assignments to the transitions at energies found in our Gaussian fit. We specify the levels assignment in relation to the energy levels given in table 8.2. The transition assignments are tentatively based upon information in that table and bond type analysis.

Transition	Gaussian Energy (cm^{-1})	Levels Assignment	Transition Assignment	Calculated Energy	Spin-Orbit
1	23800	23/24	$t_{1u}(\pi) \rightarrow e_g$	22570	-62
2	25900	19/20	$t_{2u}(\pi) \rightarrow e_g$	27570	+62
		17/18	$t_{1u+2u}(\sigma) \rightarrow e_g$	27620	+123||S||
3	30600	23/24	$t_{1u}(\pi) \rightarrow t_{2g}$	29250	-62
4	32300	19/20	$t_{2u}(\pi) \rightarrow t_{2g}$	34250	+62
		17/18	$t_{1u+2u}(\sigma) \rightarrow t_{2g}$	34300	+123||S||
5	40600	14/15	$t_{1u}(\rho) \rightarrow e_g$	37100	
6	44000	12/13	$t_{1u}(\pi + \sigma) \rightarrow e_g$	43350	
		10/11	$t_{2u}(\pi) \rightarrow e_g$	43370	
7	48000	12/13	$t_{1u}(\pi + \sigma) \rightarrow t_{2g}$	50030	
		10/11	$t_{2u}(\pi) \rightarrow t_{2g}$	50140	

Tab. 8.7: The $CrCl_3$ assignments to the transitions at energies found in our Gaussian fit. We specify the levels assignment in relation to the energy levels given in table 8.3. The transition assignments are tentatively based upon information in that table and bond type analysis. We exclude the last Gaussian peak, at 64000cm^{-1} since it included for the purpose of taking into account higher energy transitions, and is probably not the result of a charge transfer effect

Transition	Gaussian Energy (cm^{-1})	Levels Assignment	Transition Assignment	Calculated Energy
1	30500	23/24	$t_{1u}(\pi) \rightarrow e_g$	30460
2	36300	19/20	$t_{2u}(\pi) \rightarrow e_g$	36080
		17/18	$t_{1u+2u}(\sigma) \rightarrow e_g$	36120
3	38100	23/24	$t_{1u}(\pi) \rightarrow t_{2g}$	35750
		20/21	$t_{1g}(\pi) \rightarrow t_{2g}$	37080
4	42200	19/20	$t_{2u}(\pi) \rightarrow t_{2g}$	41370
		17/18	$t_{1u+2u}(\sigma) \rightarrow t_{2g}$	41410
5	48400	14/15	$t_{1u}(\rho) \rightarrow e_g$	46590
6	52300	12/13	$t_{1u}(\pi+\sigma) \rightarrow e_g$	53650
		10/11	$t_{2u}(\pi) \rightarrow e_g$	53810
7	55600	12/13	$t_{1u}(\pi+\sigma) \rightarrow t_{2g}$	58940
		10/11	$t_{2u}(\pi) \rightarrow t_{2g}$	59100

Tab. 8.8: The calculated spin-orbit constants in $CrBr_3$ (Ross *et al* 1996)

Transition	Spin-orbit constant	Value
$\lambda_{1u}(\pi)$	$-\frac{1}{20}\zeta_{4p}^{\mathrm{Br}}$	-123
$\lambda_{2u}(\pi)$	$\frac{1}{20}\zeta_{4p}^{\mathrm{Br}}$	123
$\lambda_{1u}(\sigma)$	$\frac{1}{10}\lvert S\rvert\zeta_{4p}^{\mathrm{Br}}$	$\lvert S\rvert$246
λ_{2g^*}	$\frac{1}{6}\left(\zeta_{4p}^{\mathrm{Cr}}-\zeta_{3d}^{\mathrm{Cr}}\right)$	-40

Fig. 8.2: The spectrum of the imaginary part of the dielectric constant over the 2.85–6.7 eV region of $CrBr_3$ in which CT effects are dominant

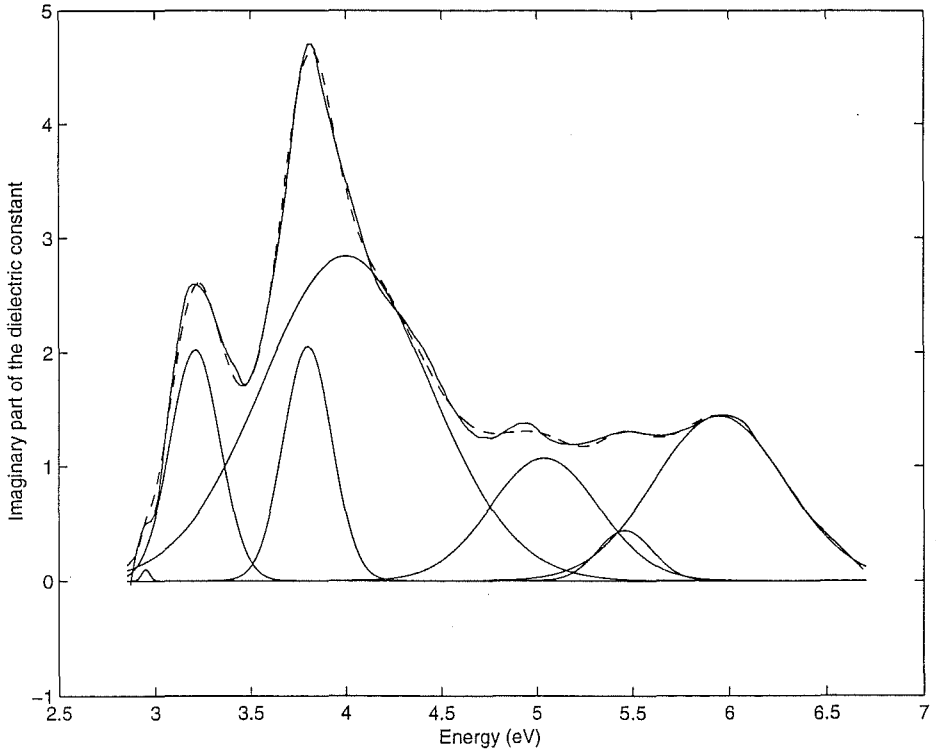

Fig. 8.3: The spectrum of the imaginary part of the dielectric constant over the 3.00–8.00 eV region of $CrCl_3$ in which CT effects are dominant

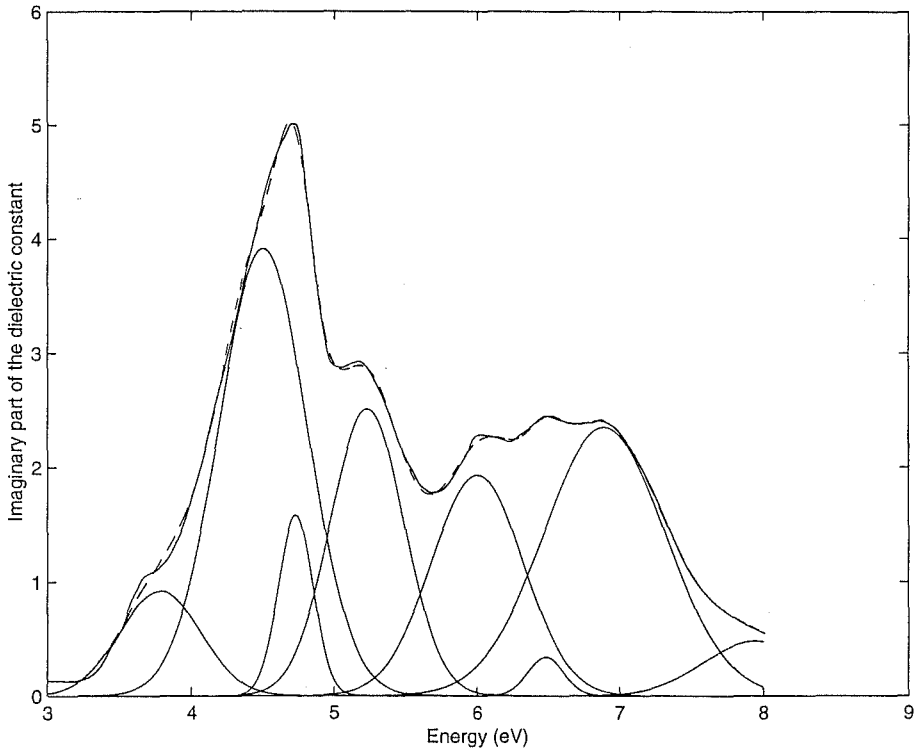

Fig. 8.4: Kerr rotation for $CrBr_3$. The solid line experimental Kerr rotation compared with the calculated Kerr rotation given in the dashed line

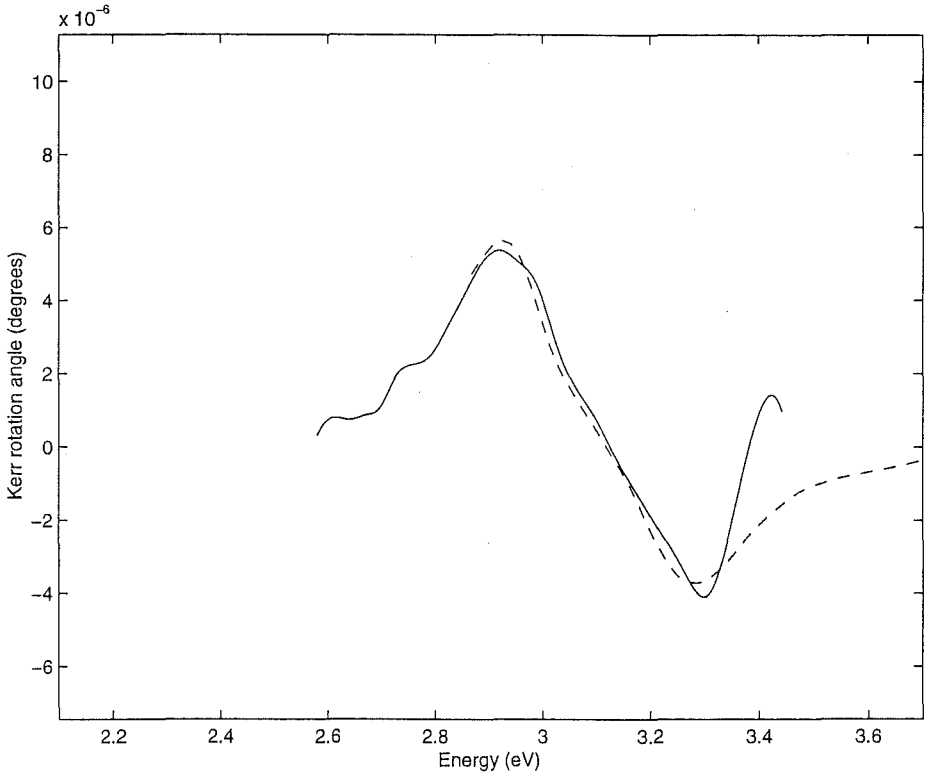

9. SUMMARY

Confused people say weird things, but nature does not[1]

This thesis contains various developments in the application of group theory. Calculations of coefficients in the Racah–Wigner calculus have been presented, as have several applications of such coefficients to physical systems. In this section we will briefly summarise our work.

In chapters 3, 4 and 5 we discussed transformation coefficients for symmetric groups.

In chapters 3 and 4 we have calculated transformations between permuted bases. The same set of tableaux and basis functions label the representations in each basis. Therefore the same set of representation matrices can be used also. We have described the permutation which will carry out this transformation.

We have proposed in chapter 4 the block–selective conjecture for calculating split–standard transformation coefficients. The basis functions differ in general between the split and standard bases, but this conjecture uses the representation of a permutation to obtain a more direct link between the bases than has previously been suggested. In some sense the block selective conjecture offers hope of finding a combinatorial recipe for resolving the decomposition of the product of basis functions.

We have calculated in section 5.2 the general algebraic solution for transforming from the S_n–basis to the S_n–$S_{n-3,3}$–basis (McAven, Hamel & Butler 1998). This extends the work of Kaplan (1975), in which explicit formulas for the transformations between the S_n–basis and S_n–$S_{n-2,2}$–basis were given.

This general case includes the first multiplicity case. We present solutions *before* any choice of separation is made. We have proved that the Littlewood–Richardson rule does not fix the choice of multiplicity separation. We have discussed the choice of separation and given criteria for simplicity of the solutions obtained.

In chapter 5 we have also considered some selection rules for the product of basis functions, not irreps as in the Littlewood–Richardson rule. Those selection rules arise naturally in the general algebraic solution for transforming from the S_n–basis to the S_n–$S_{n-3,3}$–basis.

The last two results reflect interesting aspects of the block selective conjecture. The selection of blocks is based on the Littlewood–Richardson rule, but the

[1] Mirman (1995*a*)

solution appears to give results consistent with the specific selection rules obtained. This suggests a rich substructure which may unlock many of the problems in calculating the symmetric group coefficients, including giving insight into the awkward multiplicities. However the conjecture as it stands does not select a valid multiplicity separation.

Chapter 6 concerns the delta function model of correlation crystal fields. One significant feature of the model is the vanishing of some terms, effectively due to the vanishing of coefficients relating two bases. Previously those transformation coefficients had been calculated by brute force, essentially by comparing the matrix elements in each basis. We took a different approach which involved coupling chains of continuous groups. We obtained an explicit expression for those transformation coefficients. This was used to gain insight into the vanishing of terms (McAven, Reid & Butler 1996).

In chapters 7 and 8, we discussed several projects broadly related to the energy structure of the chromium trihalides. In particular, we collaborated with Shinagawa and others in considering the proposed reassignment of transitions significant to Kerr rotation in chromium tribromide. The reassignments were made based on spin–orbit calculations by RACAH, a computer program developed at the University of Canterbury (Ross et al. 1996). The aim of RACAH is to facilitate the use of the Racah–Wigner algebra in physical calculations.

Two independent calculations of energy structure have been made, using an USCW–Xα–SW method (Shinagawa et al. 1996) and an LCAO method (McAven et al. 1998). Transitions were fitted to the spectra of $CrBr_3$ and $CrCl_3$, using the LCAO calculated energy structure.

APPENDIX

A. DELTA FUNCTION MODEL

The following paper appeared in the Journal of Physics B:Atomic, Molecular and Optical Physics, **29** (1996), 1421–1431. A correction to table A.4, corrected in this version, appeared in the same journal, **29** (1996), 4319–4321. This error was pointed out by Dr Gary Burdick.

Transformation properties of the delta function model of correlation crystal fields.

Luke F McAven, Michael F Reid and Philip H Butler

Department of Physics and Astronomy
University of Canterbury
Christchurch
New Zealand.

Classification Numbers:71.70.C, 31.20.Tz, 02.20
Short Title: Crystal field delta function correlation

Judd proposed a delta function model for f–shell correlation crystal field effects that uses an operator that is a product of two delta functions. This operator contains no parts that transform according to the irreducible representations [220] and [111] of the group SO_7. We explain these absences in terms of the ratios of certain G_2–SO_3–$3jm$ factors. The corresponding operator for the d–shell is discussed also.

A.1 Introduction

Ordinary crystal field theory, which uses only one–body operators, is adequate to explain most features of the spectra of lanthanide ions in crystals. However, there is considerable experimental evidence that two–body operators, which can take into account electron correlation, are necessary for a complete description. Recently it has been found that a simple model proposed by Judd (1978) can account for a large proportion of the correlation crystal field effect, particularly for Nd^{3+} systems (Li & Reid (1990), Burdick et al. (1994)).

Judd's operator is a simple product of delta functions:

$$I_{\text{ligand}} = -A\delta(\mathbf{r}_1 - \mathbf{R})\delta(\mathbf{r}_2 - \mathbf{R}), \tag{A.1}$$

where A is positive, and $\mathbf{r}_1$ and $\mathbf{r}_2$ are the coordinates of two $4f$ electrons. $\mathbf{R}$ is taken to be a point on the lanthanide–ligand axis where the interaction is assumed to be localised. This model may be rationalised by the observation that covalency and charge overlap are thought to give rise to rather short–range crystal–field effects, which tend to dominate over the longer–range point–charge electrostatic effects.

When fitting parameters and in theoretical investigations of the properties of correlation crystal field models, it has proved useful to have operators that have well defined transformation properties under Racah's parentage group chain

$$U_{14} \supset Sp_{14} \supset SU_2^S \times \{SO_7 \supset G_2 \supset SO_3^L\}. \tag{A.2}$$

Judd (1977) introduced a set of two–body crystal–field operators, denoted g_i^k. Reid (1987) introduced a slight modification of the g_2^k operators, in order to render them orthogonal to all g_1^k. We adopt Reid's conventions (see table A.1). Observe that three pairs of operators, g_4 & g_5, g_6 & g_7 and g_8 & g_9, differ within each pair only in the $(-1)^S$ appearing in the definitions of g_5, g_7 and g_9. The irreps for each operator within a pair are the same apart from the symplectic group label of Sp_{14}. Table A.2 gives the transformation properties of the g–operators pertinent to the d–shell.

Lo & Reid (1993) used the g operators to investigate the delta–function and point–charge models. The expansions in terms of the g operators were found to differ greatly between the two models, despite the initial expressions for their respective operators being similar in a basis of spherical tensor operators. The point–charge model eliminates only g_{11} of the g operators, while the delta model also eliminates g_4–g_9.

The Pauli Exclusion Principle rules out electrons with parallel spins at the same position. We know therefore that the operator for the delta–function model cannot connect triplet states. The matrix elements of g_{11} are zero for singlet states, so g_{11} cannot contribute. Why the g_4–g_9 operators should not contribute is not so obvious. Judd stated, "Their absence corresponds to the vanishing of all matrix

elements of I_{ligand} for the triplets of f^2..." (Judd 1978). (Actually Judd was referring to the SO_7 irrep (220) being excluded but we see later that this is equivalent to the absence of g_4 to g_9). However, investigations by Lo and Reid(Lo 1993) led them to suggest that not all the zeros were related to spin–triplets, that the vanishing was a special property of the delta–function model.

Previous work, (Judd 1978, Reid 1987, Kooy & Reid 1993, Lo & Reid 1993) has concentrated on recoupling the correlation operator at the SO_3 level. In section A.3 we recouple the operator I_{ligand} at each of the group levels in the chain of groups used by Racah (equation (A.2)), to give more insight into the vanishing of various matrix elements.

Necessary relationships between some $3jm$ factors for the parentage groups are found when this approach is compared with the matrix methods. We give examples of those relationships for both the d–shell and the f–shell.

Judd & Lister (1984) used a different double delta function operator to discuss Laporte–Platt degeneracies. We use an alternative form for the I_{ligand} operator, $\delta(\mathbf{r}_1 - \mathbf{R})\delta(\mathbf{r}_1 - \mathbf{r}_2)$, and their work to gain further insight into the nature of the delta interaction.

A.2 Coupling at the SO_3 level.

Our starting point is the I_{ligand} operator defined in equation (A.1). As discussed by Lo & Reid (1993) the delta function may be expressed as sums of products of spherical tensors C^k, yielding

$$I_{\text{ligand}} = \frac{-A\delta(r_1 - R)\delta(r_2 - R)}{16\pi^2 R^4} \sum_{k_1,k_2} [k_1, k_2](\mathrm{C}_1^{k_1} \cdot \mathrm{C}_L^{k_1})(\mathrm{C}_2^{k_2} \cdot \mathrm{C}_L^{k_2}). \quad \text{(A.3)}$$

Recoupling the products of the tensor operators at the SO_3 level gives

$$I_{\text{ligand}} = B \sum_{k_1,k_2} \sum_{K,q} (-1)^q [k_1, k_2][K]^{\frac{1}{2}} \begin{pmatrix} k_1 & K & k_2 \\ 0 & 0 & 0 \end{pmatrix} (C_1^{k_1} C_2^{k_2})^{Kq} C_L^{K-q}, \quad \text{(A.4)}$$

where we define

$$B = \frac{-A\delta(r_1 - R)\delta(r_2 - R)}{16\pi^2 R^4}.$$

We adopt the convention of writing all irrep labels as superscripts so C_L^{K-q} denotes a spherical tensor acting on the ligand L, and transforming as K of SO_3 and $-q$ of SO_2. This will be useful later when we use Racah's group chain.

Spherical tensors connect states within and between shells. Since I_{ligand} will be used solely with a single shell (l) we can recast our expressions in terms of the classical v operators (Judd 1963) to obtain

$$I_{\text{ligand}} = B \sum_{k_1,k_2} \sum_{K,q} (-1)^q J_{k_1,k_2,K} (v_1^{k_1} v_2^{k_2})^{Kq} C_L^{K-q}, \quad \text{(A.5)}$$

where

$$J_{k_1,k_2,K} = [k_1,k_2,K]^{\frac{1}{2}}[l]^2 \begin{pmatrix} k_1 & K & k_2 \\ 0 & 0 & 0 \end{pmatrix} \begin{pmatrix} l & k_1 & l \\ 0 & 0 & 0 \end{pmatrix} \begin{pmatrix} l & k_2 & l \\ 0 & 0 & 0 \end{pmatrix} \quad \text{(A.6)}$$

We thus have I_{ligand} in the form of a sum over the coupled product of two v operators. Note that the last two $3jm$ of the previous equation imply k_1 and k_2 are even.

We now introduce Judd's two–body operators, the g_i^{0K}. We use the notation g_i^{0K}, with the 0 to indicate the operators are reduced to a scalar with respect to the spin space. Because of the restriction to the l–shell I_{ligand} can be written as a sum of g_i^{0K}.

$$I_{\text{ligand}} = \sum_{\alpha,K,q} \sum_{L} G_i^{Kq} g_i^{0Kq} \quad \text{(A.7)}$$

If we consider only one ligand on the z axis only the $q = 0$ operators need be considered. We denote the G_i^{K0} as $\bar{G}_i^K$, which are commonly referred to as intrinsic parameters.

$$I_{\text{ligand}} = \sum_{\alpha,K} \bar{G}_i^K g_i^{0K0} \quad \text{(A.8)}$$

Previously (Lo & Reid 1993), comparisons of matrix elements of the g_i^{0K} and $(v^{k_1}v^{k_2})^{K0}$ operators were used to determine expressions for the intrinsic parameters. We give the intrinsic parameters in tables A.3 and A.4 for the d– and f–shells respectively. The table for the d–shell corrects for some errors in Kooy (1994).

In the next section we will calculate the transformation more directly by considering the properties of the v operators with respect to groups higher in Racah's group chain of continuous groups and coupling them at the parentage group U_{14}. This will allow us to investigate the zeroes in tables A.3 and A.4 more directly.

A.3 Coupling in the parentage groups, for the f–shell

We use $\lambda\beta$ to represent the $U_{14} \cdots G_2$ irrep labels, for the group chain in equation (A.2). The U_{14} irreps are labelled by λ, and the β labels are shorthand for the other parentage labels and can be thought of as branching multiplicity between U_{14} and SO_3. We also drop the now unnecessary subscripts 1 and 2 on the operators, which we have used to indicate which electron we are dealing with. We begin with the expression for the coupled product of operators (Butler 1981, equation (4.3.1))

$$(C^{\lambda_1}C^{\lambda_2})^{\lambda\beta Kq} = \sum_{\beta_1,\beta_2} \sum_{k_1,k_2} \sum_{q_1,q_2} C^{\lambda_1\beta_1k_1q_1} C^{\lambda_2\beta_2k_2q_2} \langle \lambda_1\beta_1k_1q_1, \lambda_2\beta_2k_2q_2 | \lambda\beta Kq \rangle. \quad \text{(A.9)}$$

We apply the Racah factorisation lemma to the coupling coefficient, expressing it as a product of group–subgroup factors along the shell chain. The same

SO_3 to SO_2 factor occurs in both this expansion and in the ordinary SO_3 coupling. Since λ and β are uniquely determined by k for a one–body operator we can simply add the various λ and β labels to the one–body operators in the SO_3 recoupling expression. A direct comparison between the coupling at the two levels gives

$$(C^{\lambda_1}C^{\lambda_2})^{\lambda\beta Kq} = \sum_{\beta_1,\beta_2}\sum_{k_1,k_2}(C^{k_1}C^{k_2})^{Kq}\langle\lambda_1\beta_1 k_1, \lambda_2\beta_2 k_2|\lambda\beta K\rangle. \qquad \text{(A.10)}$$

where the vector coupling coefficient in this equation is one of factors appearing in the factorisation of the vector coupling coefficient in (A.9). We can use the orthonormality (Butler 1981, equation (2.3.4)) of the coupling coefficients to rewrite this as

$$(C^{k_1'}C^{k_2'})^{Kq} = \sum_{\lambda,\beta}\langle\lambda\beta K|\lambda_1\beta_1' k_1', \lambda_2\beta_2' k_2'\rangle(C^{\lambda_1}C^{\lambda_2})^{\lambda\beta Kq}. \qquad \text{(A.11)}$$

A.4 Expansion coefficients of the g–operators

Having coupled the operators at the U_{14} level we proceed to find the $\bar{G}_i^K$ in the expansion of I_{ligand}, equation (A.8). Comparison of equations (A.8) and (A.5) gives us a means of finding those coefficients directly, rather than by the indirect matrix manipulations (Lo & Reid 1993). Each i, such as those on the g–operators, is equivalent to a set of labels $\{\lambda\beta\}$, so that the relationship between these equations is simply

$$\bar{G}_i^K g_i^{0K} = B\sum_{k_1,k_2} J_{k_1,k_2,K}\langle\lambda\beta K|\lambda_1\beta_1 k_1, \lambda_2\beta_2 k_2\rangle(v^{\lambda_1}v^{\lambda_2})^{\lambda\beta K0}. \qquad \text{(A.12)}$$

The coupling coefficient can be rewritten in terms of a general $3jm$ (Butler 1981, equation (3.3.6)), and then factorised into $3jm$ factors (Butler 1981, equation (3.1.9)). It then is a sum over product multiplicities of products of $3jm$ between neighbouring groups in the chain.

In order make our transformation complete we need to find the normalisations of both sets. For the relevant $\{iK\}$ the g operators are conveniently normalised. The normalisation $N(iK)$ of the U_{14} coupled v operators is

$$N(iK) = \sum_{\lambda'\beta'S'L'}\sum_{\lambda''\beta''S''L''}\langle\lambda'\beta'S'L'|(v^{\lambda_1}v^{\lambda_2})^{\lambda\beta K0}|\lambda''\beta''S''L''\rangle \qquad \text{(A.13)}$$
$$\times\langle\lambda''\beta''S''L''|(v^{\lambda_1}v^{\lambda_2})^{\lambda\beta K0}|\lambda'\beta'S'L'\rangle$$

We use equation (A.11), in combination with a generalisation of the Wigner–Eckart theorem (Butler 1981, equation (4.3.7)), to re–express the normalisation as a many layered sum of products of $3jm$ and $9j$. Application of $9j$ (Condon &

Odabaşi 1980, pp 182) and $3jm$ (Butler 1981, equation (3.3.15)) orthonormality allow us to reduce this to

$$N(iK) = \sum_{\alpha',\alpha''} \sum_{k_1,k_2} [K,S]. \tag{A.14}$$

We are now able to write down an explicit expression for the $\bar{G}_i^K$. The index r indicates the product multiplicity which is present for some products of G_2.

$$\bar{G}_i^K = H(iK) \sum_{k_1,k_2} \sum_r [k_1,k_2,K]^{\frac{1}{2}} \begin{pmatrix} k_1 & K & k_2 \\ 0 & 0 & 0 \end{pmatrix} \begin{pmatrix} 3 & k_1 & 3 \\ 0 & 0 & 0 \end{pmatrix} \tag{A.15}$$
$$\times \begin{pmatrix} 3 & k_2 & 3 \\ 0 & 0 & 0 \end{pmatrix} \begin{pmatrix} \omega_1 & \omega_2 & \omega \\ U_1 & U_2 & U \end{pmatrix}_{\substack{SO_7 \\ \mathrm{r}G_2}} \begin{pmatrix} U_1 & U_2 & U \\ 0 & 0 & \tau \\ K_1 & K_2 & K \end{pmatrix}_{\substack{\mathrm{r}G_2 \\ SO_3}}$$

Factors above the SO_7 level are included in $H(iK)$, which we define as,

$$H(iK) = \frac{49B[\lambda]^{\frac{1}{2}}}{\sqrt{N(iK)}} \begin{pmatrix} \lambda \\ \sigma \\ \omega \\ {}^0U \\ {}^0K \end{pmatrix} \begin{pmatrix} \lambda_1 & \lambda_2 & \lambda^* \\ \sigma_1 & \sigma_2 & \sigma \end{pmatrix}_{\substack{U_{14} \\ Sp_{14}}} \tag{A.16}$$
$$\times \begin{pmatrix} \sigma_1 & \sigma_2 & \sigma \\ {}^0\omega_1 & {}^0\omega_2 & {}^0\omega \end{pmatrix}_{\substack{Sp_{14} \\ SU_2 \times SO_7}}$$

The SO_3–SO_2–$3jm$ were calculated using an explicit formula of Edmonds (1965, equation (3.7.17)). The values of the G_2–SO_3–$3jm$ were provided by Ross (1994), who calculated them using RACAH (Butler & Associates 1995), with the G_2–$6j$ chosen to be those given by Searle (1988), see table A.5.

In each the case the vanishing of the $\bar{G}_i^K$ can be related to ratios between certain SO_7–SO_3–$3jm$. In most cases this reduces to simple ratios between G_2–SO_3–$3jm$. As an example we consider the pair $\bar{G}_8^{10}$ and $\bar{G}_9^{10}$. For this case there is no sum over product multiplicity r, so we need not consider the SO_7–G_2–$3jm$. Since the various G_2–SO_3–$3jm$ are symmetric with respect to exchange of the first two columns the contributions from $k_1 = 4, k_2 = 6$ and $k_1 = 6, k_2 = 4$ are equal.

$$\bar{G}_8^{10} = 2\times[4,6]^{\frac{1}{2}} \begin{pmatrix} 4 & 10 & 6 \\ 0 & 0 & 0 \end{pmatrix} \begin{pmatrix} 3 & 4 & 3 \\ 0 & 0 & 0 \end{pmatrix} \begin{pmatrix} 3 & 6 & 3 \\ 0 & 0 & 0 \end{pmatrix} \begin{pmatrix} 20 & 20 & 22 \\ 4 & 6 & 10 \end{pmatrix}_{\substack{G_2 \\ SO_3}}$$
$$+[6,6]^{\frac{1}{2}} \begin{pmatrix} 6 & 10 & 6 \\ 0 & 0 & 0 \end{pmatrix} \begin{pmatrix} 3 & 6 & 3 \\ 0 & 0 & 0 \end{pmatrix} \begin{pmatrix} 3 & 6 & 3 \\ 0 & 0 & 0 \end{pmatrix} \begin{pmatrix} 20 & 20 & 22 \\ 6 & 6 & 10 \end{pmatrix}_{\substack{G_2 \\ SO_3}}$$

Working this out we find that $\bar{G}_8^{10} = \bar{G}_9^{10} = 0$, with the two G_2–SO_3–$3jm$ being in the ratio

$$\begin{pmatrix} 20 & 20 & 22 \\ 4 & 6 & 10 \end{pmatrix} \begin{matrix} G_2 \\ SO_3 \end{matrix} = -\sqrt{\frac{5}{23}} \begin{pmatrix} 20 & 20 & 22 \\ 6 & 6 & 10 \end{pmatrix} \begin{matrix} G_2 \\ SO_3 \end{matrix} \tag{A.17}$$

A.5 Vanishing of $3jm$ factors

The vanishing of the $\bar{G}_i^K$ depends the values of the SO_7–G_2–$3jm$. In turn those $3jm$ are dependent upon the choice of G_2–$6j$ made, a choice being necessary because of the product multiplicity at the G_2 level, $(20) \times (20) \supset 2(20)$. We provide table A.5 from Searle (1988, Table 7.1) with some of the G_2–$6j$.

Following the $6j$ choices of Searle (1988) in calculating the G_2–SO_3–$3jm$ (Ross 1994) we find that for $\bar{G}_4^6$ to vanish so too must the $3jm$

$$\begin{pmatrix} [200] & [200] & [220] \\ (20) & (20) & (20) \end{pmatrix} \begin{matrix} SO_7 \\ 0\ G_2 \end{matrix} , \tag{A.18}$$

where the 0 next to the G_2 represents the product multiplicity label. We see that the $3jm$ above must vanish by inspection of equation (A.15) for $\bar{G}_4^6$,

$$\bar{G}_4^6 = -\frac{7260\sqrt{(65)}}{251559} \begin{pmatrix} [200] & [200] & [220] \\ (20) & (20) & (20) \end{pmatrix}_0 + 0 \begin{pmatrix} [200] & [200] & [220] \\ (20) & (20) & (20) \end{pmatrix}_1 \tag{A.19}$$

The coefficients $-\frac{7260\sqrt{(65)}}{251559}$ and 0 are dependent not only upon the G_2–$6j$ choices, through the G_2–SO_3–$3jm$ which appear in equation (A.15), but also the delta function model itself. The second $3jm$ above cannot be zero, since $\bar{G}_4^6$ is not zero in other models. It is only the particular ratio of terms, as specified by the delta function model in (A.15), which gives the 0 coefficient of the non–zero $3jm$, and therefore gives the $\bar{G}_4^6$ zero.

We can express the $3jm$ in (A.18) in terms of G_2–$6j$. This allows us to demonstrate that it follows from our choices of the G_2–$6j$ that the $3jm$ is zero. This will also demonstrate that the second $3jm$ in equation (A.21) must be non–zero.

The scaled orthonormality of the $3jm$, (Butler 1981, equation (3.3.15)), is written in this case as,

$$\sum_r \frac{|\lambda|}{|(20)|} \begin{pmatrix} [200] & [200] & \lambda \\ (20) & (20) & (20) \end{pmatrix}_{\mathrm{r}} \begin{pmatrix} [200] & [200] & \lambda' \\ (20) & (20) & (20) \end{pmatrix}^*_{\mathrm{r}} = \delta_{\lambda\lambda'} \tag{A.20}$$

allowing one to write the $3jm$ in equation (A.18) as one entry of a 2×2 unitary matrix,

$$\begin{pmatrix} \begin{pmatrix} [200] & [200] & [200] \\ (20) & (20) & (20) \end{pmatrix} \begin{matrix} SO_7 \\ 0G_2 \end{matrix} & \begin{pmatrix} [200] & [200] & [200] \\ (20) & (20) & (20) \end{pmatrix} \begin{matrix} SO_7 \\ 1G_2 \end{matrix} \\ \frac{56}{9} \begin{pmatrix} [200] & [200] & [220] \\ (20) & (20) & (20) \end{pmatrix} \begin{matrix} SO_7 \\ 0G_2 \end{matrix} & \frac{56}{9} \begin{pmatrix} [200] & [200] & [220] \\ (20) & (20) & (20) \end{pmatrix} \begin{matrix} SO_7 \\ 1G_2 \end{matrix} \end{pmatrix} \tag{A.21}$$

A property of 2×2 unitary matrices is that if an entry is zero, so too is the diagonally opposite entry. To find the top right entry, we apply the Wigner relation, (Butler 1981, equation (3.3.29)). The requirement that the triads in the $6j$ be valid reduces the sum to just one term,

$$\begin{pmatrix} [200] & [200] & [200] \\ (20) & (20) & (20) \end{pmatrix}_1 \begin{Bmatrix} [200] & [200] & [200] \\ [100] & [100] & [100] \end{Bmatrix} = \begin{pmatrix} [100] & [100] & [100] \\ (10) & (10) & (10) \end{pmatrix}$$
$$\times \begin{pmatrix} [200] & [100] & [100] \\ (20) & (10) & (10) \end{pmatrix} \begin{pmatrix} [100] & [200] & [100] \\ (10) & (20) & (10) \end{pmatrix} \begin{pmatrix} [100] & [100] & [200] \\ (10) & (10) & (20) \end{pmatrix}$$
$$\times \begin{Bmatrix} (20) & (20) & (20) \\ (10) & (10) & (10) \end{Bmatrix}_1$$

We see that the top right $3jm$ in (A.21) can be written as a multiple of the G_2–$6j$,

$$\begin{Bmatrix} (20) & (20) & (20) \\ (10) & (10) & (10) \end{Bmatrix}_1$$

In table A.5 we see that this has been chosen to be zero. Thus the $3jm$ in equation (A.18) is also zero. In addition, the unitary nature of the matrix in equation (A.21) ensures that the other $3jm$ appearing in (A.20) is non–zero, as earlier stated.

The $3jm$ was verified as being zero, with the same choice of G_2–$6j$, by Ross (1994) using RACAH (Butler & Associates 1995).

A.6 Discussion of the U_{14} coupled results

Completing the calculations above produces all the zeroes in table A.4. This is, of course, in agreement with the previous work of Judd (1978), Lo (1993) and Lo & Reid (1993). The explicit form that we have calculated for the $\bar{G}_i^K$ emphasises the importance of the SO_7–SO_3 part of the chain. In particular it is this part which is zero for the vanishing coefficients of g_4 to g_9.

The operators could not contribute if either $\langle 1^4 \rangle$ of Sp_{14}, or $[220]$ of SO_7, were excluded. (The irrep $\langle 1^4 \rangle$ of Sp_{14} because of the pairing mentioned in section A.1). The SO_7–SO_3 part of the chain is shown by our calculations to provide the key constraint.

The absence of operators labelled by $[220]$ of SO_7 is related to the ratios between certain G_2–SO_3–$3jm$. While this "selection rule" is not the result of branching or product rules, it may be the result of an "accidental" vanishing of a coupling coefficient, as studied by Judd and his co–workers(Judd & Wadzinski 1967, Judd & Lister 1990). The physical meaning of the ratios goes beyond the understanding which can be extracted by group theory alone.

A.7 SO_3 and parentage group coupling in the d–shell

For the d–shell, calculations analogous to those in sections A.2 and A.3 give

$$\bar{G}_i^K = H(iK) \sum_{k_1,k_2} \sum_r [k_1,k_2,K]^{\frac{1}{2}} \begin{pmatrix} k_1 & K & k_2 \\ 0 & 0 & 0 \end{pmatrix} \begin{pmatrix} 2 & k_1 & 2 \\ 0 & 0 & 0 \end{pmatrix} \begin{pmatrix} 2 & k_2 & 2 \\ 0 & 0 & 0 \end{pmatrix} \times \begin{pmatrix} \omega_1 & \omega_2 & \omega \\ K_1 & K_2 & K \end{pmatrix}^{SO_5}_{SO_3} \tag{A.22}$$

where SO_5, rather than SO_7 is the "cut–off" group. Table A.2 gives the transformation properties of the g–operators pertinent to the d–shell.

Factors above SO_5 are included in $H(iK)$, which we define as,

$$H(iK) = \frac{25B[\lambda]^{\frac{1}{2}}}{\sqrt{N(iK)}} \begin{pmatrix} \lambda \\ \sigma \\ {}^0\omega \end{pmatrix} \begin{pmatrix} \lambda_1 & \lambda_2 & \lambda^* \\ \sigma_1 & \sigma_2 & \sigma \end{pmatrix}^{U_{10}}_{Sp_{10}} \times \begin{pmatrix} \sigma_1 & \sigma_2 & \sigma \\ {}^0\omega_1 & {}^0\omega_2 & {}^0\omega \end{pmatrix}^{Sp_{10}}_{SU_2 \times SO_5} \tag{A.23}$$

Table A.3 gives the d–shell the expansion of the I_{ligand} operator into g operators. The zeroes in the table occur because of the following ratios between SO_5–SO_3–$3jm$.

$$\begin{pmatrix} (20) & (20) & (22) \\ 2 & 2 & 0 \end{pmatrix}^{SO_5}_{SO_3} = -\frac{3}{\sqrt{5}} \begin{pmatrix} (20) & (20) & (22) \\ 4 & 4 & 0 \end{pmatrix}^{SO_5}_{SO_3}$$

$$\begin{pmatrix} (20) & (20) & (22) \\ 2 & 2 & 2 \end{pmatrix}^{SO_5}_{SO_3} + \frac{3}{\sqrt{5}} \left[\begin{pmatrix} (20) & (20) & (22) \\ 2 & 4 & 2 \end{pmatrix}^{SO_5}_{SO_3} + \begin{pmatrix} (20) & (20) & (22) \\ 4 & 2 & 2 \end{pmatrix}^{SO_5}_{SO_3} \right] = -\frac{3\sqrt{2}}{\sqrt{11}} \begin{pmatrix} (20) & (20) & (22) \\ 4 & 4 & 2 \end{pmatrix}^{SO_5}_{SO_3}$$

$$\begin{pmatrix} (20) & (20) & (22) \\ 2 & 2 & 4 \end{pmatrix}^{SO_5}_{SO_3} + \sqrt{10} \left[\begin{pmatrix} (20) & (20) & (22) \\ 2 & 4 & 4 \end{pmatrix}^{SO_5}_{SO_3} + \begin{pmatrix} (20) & (20) & (22) \\ 4 & 2 & 4 \end{pmatrix}^{SO_5}_{SO_3} \right] = -\frac{27}{\sqrt{715}} \begin{pmatrix} (20) & (20) & (22) \\ 4 & 4 & 4 \end{pmatrix}^{SO_5}_{SO_3}$$

$$\begin{pmatrix} (20) & (20) & (22) \\ 2 & 4 & 6 \end{pmatrix}^{SO_5}_{SO_3} + \begin{pmatrix} (20) & (20) & (22) \\ 4 & 2 & 6 \end{pmatrix}^{SO_5}_{SO_3} = -\frac{1}{\sqrt{5}} \begin{pmatrix} (20) & (20) & (22) \\ 4 & 4 & 6 \end{pmatrix}^{SO_5}_{SO_3}$$

A.8 An alternative form for the delta function operator

Judd & Lister (1984) used the product of delta function to discuss Laporte–Platt degeneracies. In doing so they expressed delta functions in terms of Racah's e operators (Racah 1949). Their expressions can be used to express the double delta

operator in terms of SO_{2l+1} irreps, to which the e operators relate. To consider the whole operator in this way, we consider each delta term in the operator in terms of SO_{2l+1} irreps, and then examine the direct product.

The double delta operator can be expressed in the following two forms

$$\begin{aligned} I_{\text{ligand}} &= -A\delta(\mathbf{r}_1 - \mathbf{R})\delta(\mathbf{r}_2 - \mathbf{R}), \\ &= -A\delta(\mathbf{r}_1 - \mathbf{R})\delta(\mathbf{r}_1 - \mathbf{r}_2). \end{aligned} \tag{A.24}$$

Those forms relate to, respectively, electron with ligand, electron with ligand and electron with ligand, electron with electron interactions. The second form is more easily recognised as a correlation operator, as a product of physical factors and energy denominators, and the origin of the $-A$ is more apparent.

Since spherical tensor operators connect states within and between shells, and since the delta function is simply a weighted sum over spherical tensors the double delta function should allow for intermediate states outside of the f–shell. That is

$$\langle f^2|\delta\delta|f^2\rangle = \sum_a \langle f^2|\delta|a\rangle\langle a|\delta|f^2\rangle, \tag{A.25}$$

where a is not restricted to f^2.

On the other hand SO_7 irreps are specified within the f–shell. Therefore taking the direct product of the parts of the double delta operator, expressed in terms of SO_7 irreps, should give only the "internal part" of the operator.

Judd & Lister (1984) show that, for the f–shell in terms of irreps of SO_7,

$$\delta(\mathbf{r}_1 - \mathbf{r}_2) \sim [400] + [000]. \tag{A.26}$$

$\delta(\mathbf{r}_i - \mathbf{R})$ transforms as an even k one–body operator, that is it transforms as

$$\delta(\mathbf{r}_i - \mathbf{R}) \sim [200] + [000]. \tag{A.27}$$

We form direct products of equation (A.26) with equation (A.27) and of equation (A.27) with itself, in accordance with the two equivalent forms of the double delta operator.

$$\begin{aligned} ([000] + [400]) \times ([000] + [200]) = {} & [600] + [510] + [420] \\ & + 2[400] + [310] + 2[200] + [000] \end{aligned} \tag{A.28}$$

$$\begin{aligned} ([000] + [200]) \times ([000] + [200]) = {} & [400] + [310] + [220] \\ & + 3[200] + [110] + 2[000] \end{aligned} \tag{A.29}$$

But if those forms are equivalent then it could only transform according to irreps of SO_7 which appear in both products, those are

$$[400] + 2[200] + [000]. \tag{A.30}$$

But those are just the SO_7 irreps which occur in the expansion of I_{ligand} in terms of the g_i^k. That is, all possible operators arise even when a is restricted to f^2, in (A.25).

This argument is trivially satisfied in the s and p–shells, no irreps are excluded and no [400] exists for the appropriate group. Thus the s–, p– and f–shells all shells have the property of the double delta operator effectively acting internally.

Judd & Lister (1984) show the single d–shell delta function decomposes into a scalar irrep only. Since the double delta function includes [40] of SO_5 we can conclude that calculations must include the intermediate states outside of the d–shell.

A.9 Conclusions

We have given expressions for the expansion of the double delta function operator, in terms of g operators, for both the f– and d–shells. This has been achieved through use of Racah's parentage groups and various intermediate operators, especially the $(v^{k_1}v^{k_2})^{\lambda\beta 0K}$.

Using an alternate form for the double delta function we have shown that for the s–, p– and f–shells, the delta function model transforms as if external intermediate states are excluded. This is not the case for the d–shell.

For f– and d–shells the expansion of I_{ligand} contains only the irreps $[4], 2[2]$ and $[0]$. We have shown that the irrep $[22]$ is absent in the f–shell delta function expansions because of ratios between G_2–SO_3–$3jm$. The restriction is also found in the d–shell because of ratios between SO_5–SO_3–$3jm$. This "selection rule" is not the result of branching or product rules. However it may be the result of an "accidental" vanishing of particular coupling coefficients, as studied by Judd & Wadzinski (1967) and Judd & Lister (1990).

Tab. A.1: The transformation properties of the g operators with respect to Sp_{14}, SO_7, G_2 and SO_3 for f^2.

g_i^{0K}	$\langle\sigma\rangle WUK$	$\langle SL\|\|g_i^{0K}\|\|SL'\rangle$	Condition
g_1^K	$\langle 1^2\rangle[200](20)K$	$[S]^{\frac{1}{2}}\langle SL\|\|U^{(K)}\|\|SL'\rangle$	
g_2^k	$\langle 1^2\rangle[200](20)K$	$1/4(f^2SL+f^2SL'\|\}f^4[200](20)K)$	if $L,L'\neq S$
		$\langle {}^1S\|\|g_2^{(0K)}\|\|{}^1K\rangle=\sqrt{10/21}$	
g_3^K	$\langle 2^2\rangle[200](20)K$	$21/\sqrt{176}(f^{21}L+f^{21}L'\|\}f^4[200](20)K)$	if $S=0$
		$-\sqrt{11}/4(f^{23}L+f^{23}L'\|\}f^4[200](20)K)$	if $S=1$
g_4^K	$\langle 1^4\rangle[220](20)K$	$(f^2SL+f^2SL'\|\}f^4[220](20)K)$	
g_5^K	$\langle 2^2\rangle[220](20)K$	$(-1)^S(f^2SL+f^2SL'\|\}f^4[220](20)K)$	
g_6^K	$\langle 1^4\rangle[220](21)K$	$(f^2SL+f^2SL'\|\}f^4[220](21)K)$	
g_7^K	$\langle 2^2\rangle[220](21)K$	$(-1)^S(f^2SL+f^2SL'\|\}f^4[220](21)K)$	
g_8^K	$\langle 1^4\rangle[220](22)K$	$(f^2SL+f^2SL'\|\}f^4[220](22)K)$	
g_9^K	$\langle 2^2\rangle[220](22)K$	$(-1)^S(f^2SL+f^2SL'\|\}f^4[220](22)K)$	
g_{10}^K	$\langle 2^2\rangle[400](40)\tau K$	$\sqrt{28}(f^4[220](20)L+f^{21}L'\|\}f^6[222](40)K)$	
g_{11}^K	$\langle 2^2\rangle[111]UK$	$\delta(S,1)(f^{23}L+f^{23}L'\|\}f^4[111]UK)$	

Tab. A.2: The transformation properties of the g operators with respect to Sp_{10}, SO_5 and SO_3 for d^2.

g_i^{0K}	$\langle\sigma\rangle WK$	$\langle SL\|\|g_i^{0K}\|\|SL'\rangle$	Condition
g_1^K	$\langle 11\rangle(2)K$	$[S]^{\frac{1}{2}}\langle SL\|\|\mathbf{U}^K\|\|S'L'\rangle$	
g_2^K	$\langle 11\rangle(2)K$	$(d^2SL + d^2S'L'\|\}d^4(2)K)$	if $L, L' \neq S$
		$\langle {}^1S\|\|g_2^K\|\|{}^1K\rangle = \frac{3}{5}\sqrt{10}$	
g_3^K	$\langle 22\rangle(2)K$	$\frac{5}{6}\sqrt{3}(d^{21}L + d^{21}L'\|\}d^4(2)K)$	if $S = 0$
		$-\frac{1}{2}\sqrt{3}(d^{23}L + d^{23}L'\|\}d^4(2)K)$	if $S = 1$
		$\langle {}^1S\|\|g_3^K\|\|{}^1K\rangle = 0$	
g_4^K	$\langle 1^4\rangle(22)K$	$(d^2SL + d^2S'L'\|\}d^4(22)K)$	
g_5^K	$\langle 22\rangle(22)K$	$(-1)^S(d^2SL + d^2S'L'\|\}d^4(22)K)$	
g_6^K	$\langle 22\rangle(4)K$	Orthonormalised	
		$\langle {}^3L\|\|g_6^K\|\|{}^3L'\rangle = 0$	
		$\langle {}^1S\|\|g_6^K\|\|{}^1K\rangle = 0$	
g_7^K	$\langle 22\rangle(1)K$	$(d^{23}L + d^{23}L'\|\}d^4(1)K)$	

Tab. A.3: The coefficients, $\bar{G}_i^K$, of the g operators in the expansion of I_{ligand} in the d–shell. $-$ represents a zero by selection rule and 0 represents a calculated zero. This table gives the coefficients to within a proportionality constant, $A\frac{[R_d(R_L)]^4}{16\pi^2 R_L^4}$, where $R_d(r)$ is the radial wavefunction of the d electron. This table is taken from Kooy (1994) with G_1^4, G_3^4 and G_6^4 corrected.

$\bar{G}_i^K/K$	0	2	4	6	8
i					
1	-	$\frac{5^2\sqrt{5}}{2^2\sqrt{2.7}}$	$\frac{-3^2.5\sqrt{5}}{2^2\sqrt{2.7}}$	-	-
2	-	$\frac{5^2\sqrt{5}}{2^2\sqrt{7}}$	$\frac{-3^3.5\sqrt{5}}{2^2\sqrt{7}}$	-	-
3	-	$\frac{-5^2\sqrt{5}}{\sqrt{3.7}}$	$\frac{3.5\sqrt{3.5}}{\sqrt{7}}$	-	-
4	0	0	0	0	-
5	0	0	0	0	-
6	-	$\frac{2^2.5^2\sqrt{5}}{\sqrt{3.7.11}}$	$\frac{-2.3.5^2\sqrt{2.3}}{\sqrt{7.11.13}}$	$\frac{2.3.5\sqrt{2.5.13}}{\sqrt{7.11}}$	$\frac{-2.3.5\sqrt{2.5.17}}{\sqrt{11.13}}$
7	-	0	-	-	-

Tab. A.4: The coefficients, $\bar{G}_i^K$, of the g operators in the expansion of I_{ligand} in the f–shell. $-$ represents a zero by selection rule, and 0 represents a calculated zero. This table gives the coefficients to within a proportionality constant, $A\frac{[R_{4f}(R_L)]^4}{16\pi^2 R_L^4}$, where $R_{4f}(r)$ is the radial wavefunction of the $4f$ electron. This table is taken from Kooy (1994)

$\bar{G}_i^K/K$	0	2	4	6	8	10	12
i							
1	$\frac{-7\sqrt{7}}{2.13}$	$\frac{7\sqrt{5.7}}{2.3\sqrt{3}}$	$\frac{-3.7\sqrt{7}}{2\sqrt{2.11}}$	$\frac{5.7\sqrt{7.13}}{2.3\sqrt{3.11}}$	-	-	-
2	-	$\frac{5.7\sqrt{7}}{3\sqrt{2}}$	$\frac{-3.7\sqrt{3.5.7}}{2\sqrt{11}}$	$\frac{5.7\sqrt{5.7.13}}{3\sqrt{2.11}}$	-	-	-
3	-	$\frac{-5.7\sqrt{7}}{\sqrt{2.11}}$	$\frac{3^2.7\sqrt{3.5.7}}{2.11}$	$\frac{-5.7\sqrt{5.7.13}}{11\sqrt{2}}$	-	-	-
4	-	0	0	0	-	-	-
5	-	0	0	0	-	-	-
6	-	0	0	-	0	-	-
7	-	0	0	-	0	-	-
8	0	0	0	0	0	0	-
9	0	0	0	0	0	0	-
10a	$\frac{-2.7\sqrt{2.7}}{\sqrt{3.5.11.13}}$	$\frac{-2^2.7\sqrt{3.5.7}}{\sqrt{11.13}}$	$\frac{2^2.3.7\sqrt{2.3.7}}{\sqrt{5.11.13}}$	$\frac{2^3.7\sqrt{3.5.7.13}}{\sqrt{11.19.31}}$	$\frac{2^3.7^2\sqrt{2.5.17}}{\sqrt{11.13.31}}$	$\frac{-2^2.3^2.5.7^2\sqrt{2.5.7}}{\sqrt{11.13.17.19.23}}$	$\frac{2^3.5^3.7\sqrt{7}}{\sqrt{13.17.19.23}}$
10b	$\frac{-2.7\sqrt{2.7}}{\sqrt{3.5.11.13}}$	$\frac{-2^2.7\sqrt{3.5.7}}{\sqrt{11.13}}$	$\frac{2^3.3.7^3\sqrt{3}}{11\sqrt{5.13.17}}$	$\frac{2^2.3.7^2\sqrt{5.13}}{11\sqrt{17.31}}$	$\frac{-2.3.5.7\sqrt{2.3.7.17}}{\sqrt{11.13.19.31}}$	$\frac{-2^2.3^2.5.7^2\sqrt{2.5.7}}{\sqrt{11.13.17.19.23}}$	$\frac{2^3.5^3.7\sqrt{7}}{\sqrt{13.17.19.23}}$
11	0	0	0	0	-	-	-

Tab. A.5: Some $6j$ of G_2. The values are a select number taken from Searle (1988, Table 7.1). The four numbers in the second column are the product multiplicities of the respective triads in the order given by Butler (1981, equation (3.3.17)). The $6j$ of particular relevance in section A.5 is third from the bottom, with a value of 0.

1	1	1		
1	1	1	0000	$-\frac{1}{2.7}$
2	1	1		
1	1	1	0000	$\frac{1}{2.3.7}$
2	1	1	0000	$\frac{5}{2.3^3.7}$
2	2	1		
1	1	1	0000	$\frac{1}{2.3^2}$
1	1	2	0000	$\frac{1}{2.3.7}$
2	1	1	0000	$-\frac{1}{2.3^3}$
2	2	2		
1	1	1	0000	$\frac{\sqrt{5.11}}{2.3^3\sqrt{7}}$
1	1	1	0001	0
2	1	1	0000	$\frac{\sqrt{11}}{2.3^3\sqrt{5.7}}$
2	1	1	0001	$\frac{2^2}{3^3\sqrt{5.7}}$

B. CALCULATING SPIN–ORBIT MATRIX ELEMENTS WITH RACAH

Calculating Spin–Orbit Matrix Elements with RACAH

Hughan J Ross, Luke F McAven, Kiminari Shinagawa†, Philip H Butler

Department of Physics and Astronomy, University of Canterbury, Private Bag 4800, Christchurch, New Zealand
† Department of Physics, Toho University, Funabashi–City, Chiba, 274 Japan

RACAH is a computer program developed to simplify calculations involving generalised coupling coefficients. As a demonstration of its usefulness in doing this, we apply it to calculating the spin–orbit matrix elements of $CrBr_3$. From those matrix elements we can derive the spin–orbit coupling coefficients, vital to discussing Kerr Rotation. We base our calculations on a cluster consisting of a Cr^{3+} ion, surrounded by six Br^- ions in an octahedral configuration. The Racah–Wigner calculus, useful for doing such calculations, is built into RACAH in such a way as to provide a natural approach to choosing between possible group chains.

Published: J.Comp.Phys. **128**(2) (1996) 331–340.
Classification Numbers: 65–01, 65K05, 81–08, 81V55

B.1 Introduction

Many spectroscopic problems require the evaluation of matrix elements. To calculate these matrix elements a sophisticated mathematical formalism, the Racah–Wigner calculus, is extremely useful (Butler 1981, Piepho & Schatz 1983). However, this formalism is not familiar to experimentalists and is still tiresome in long calculations. A software package, called RACAH, has been developed at Canterbury. RACAH is a much more versatile and general version of the program which produced the tables of Butler (1981). We demonstrate, with a specific example, how useful RACAH is for simplifying general matrix elements to reduced matrix elements.

RACAH is not restricted to this problem however and contains the necessary structure for a broad range of uses. All point groups are recognised and the programming structure of RACAH is versatile enough to allow many open–shells, as we have seen in this application. All $3jm$, $6j$ and $9j$ can be calculated for all point groups, and the Wigner–Eckart Theorem can be used in collaboration with those coupling coefficients to reduce matrix elements. Specific information about the normalisation of the operators is not considered by the current version of RACAH. That is, the actual values of the reduced matrix elements of some operator cannot be obtained. Therefore the only restriction on the operators is that the group irrep labels associated with the operators can be specified.

The development of RACAH is an ongoing and long–term project (see Butler (1981)). The core development is at the stage where it should largely be driven by feedback from applied users. RACAH has been distributed to a number of such persons, who are finding it useful. Knowledge about what applications and capabilities users would like RACAH to have, would allow us to build into the core program the appropriate calculations relevant to other applications, and perhaps to develop libraries for special one–off calculations. Details about obtaining RACAH are given after the summary.

The approach we take to the analysis of Kerr rotation in $CrBr_3$, requires the calculation of matrix elements of spin–orbit operators, of known symmetry, between electron configurations with many open shells. From those the magnitudes of the spin–orbit coupling constants can be derived, the spin–orbit effect being the dominate cause of magneto–optical effects in ferromagnetic materials. Ferromagnetic materials with high magneto–optical effects have been applied to devices such as optical isolators, magnetic sensors and rewritable optical memories (Abe & Gomi 1990, Dillon 1990). In recent years there has been an increasing demand for materials with higher magneto–optical effects. This is therefore an example of practical significance.

The new aspects of this calculation are; the presence of RACAH to take the labour out of calculating the vector coupling coefficients (vcc's) (Butler 1981), and the way that choosing the right group chain to classify states reduces the calculation of matrix elements, even very complicated ones, to the calculation of vcc.

In one view, RACAH is just a convenient way of doing the tedious bits of calculating matrix elements. Thus many of the calculations in Piepho & Schatz (1983) are trivially reduced to finding values for the reduced matrix elements. The conceptual advantage of using RACAH is exactly analogous to the tensor calculus, and serves to unify all group theory calculations that arise in evaluating matrix elements. Contrary to the previous viewpoint, RACAH allows one to think in a structurally simple way *and* provides a means to calculate within that structure. RACAH allows the operators and symmetries of the physical problem to be retained throughout the calculation. The $6j$ and $9j$ that appear in more traditional reductions of matrix elements appear as special cases of $3jm$, whose labels are trivially constructed from those of the states and the operators.

In section B.2 we discuss the labelling of the cluster and the ground state configuration, and outline how RACAH recognises group chains. Section B.3 extends the group chain to allow such effects as trigonal distortion to be taken into account. Section B.4 demonstrates the transformation of the spin–orbit to a form compatible with the group chain we choose. In section B.5 we step through the calculation of a particular matrix element, utilising the Wigner–Eckart Theorem to its full potential.

The multi–centre reduced matrix elements, which we have derived by this stage are unable to be calculated by RACAH, so in section B.6 we give the results of reducing to single–center reduced matrix elements.

Section B.7 shows the results of applying RACAH to finding the relationship between matrix element and reduced matrix element, as examined in section B.5. Finally, bringing together the results of sections B.6 and B.7, we calculate the spin–orbit coupling coefficients.

Those spin–orbit coupling coefficients are required to investigate the Kerr–Rotation spectra of $CrBr_3$. This work will be followed by a calculation of the Kerr effect, again using a cluster approach.

B.1.1 The Butler irrep labelling scheme

The Butler notation, used extensively in both Butler (1981) and Piepho & Schatz (1983), is based on a simple numerical labelling scheme for irreps. The program RACAH takes advantage of this notation, while still recognising many other labelling schemes. See table B.1 for the relation between Schönflies and Butler irrep labels in the case of the groups O, and D_3. It is of particular importance to note that an S is prefixed to a number to indicate half integer, allowing RACAH to express fractional irrep labels. For example $s1 = \frac{3}{2}$ and $s5 = \frac{11}{2}$. This is particularly noticeable when dealing with SU_2 and SO_3. In this work we tend towards using the Schönflies notation which is more familiar to spectroscopists.

B.2 Labelling the cluster and the ground state configuration

The molecular orbitals which are largely of Br composition, are fully occupied in the clusters ground state. Those molecular orbitals with a mainly Cr composition are empty in the ground state, with the exception of the t_{2g} orbital, which is occupied by three electrons with parallel spins. High Kerr rotations have been observed (Jung 1965), and are attributed to the spin–orbit splitting of particular excited states. Those excited states arise from the transition of an electron in a t_{1u} or t_{2u} orbital to the e_g orbital, an molecular orbital which consists mainly of $3d$ orbitals of the chromium (Shinagawa et al. 1995). Since this transition represents a transition from a non–bonding π orbital, of mainly Br character, to an anti–bonding orbital, of mainly Cr character, it is known as a 'charge transfer' transition.

The ground state has the e_g shell empty and the various shells of the Br_6 that we shall consider, $t_{1u}^6(\rho)$ and $t_{2u}^6(\rho)$, full. So, with the 3 up–spin electrons in the t_{2g} shell the ground state has the configuration

$$(t_{2g}^3)\,(e_g^0)\,(t_{2u}^6)\,(t_{1u}^6)$$

Given that the octahedral field is "strong", the orbital parts of the chromium orbitals are classified using $O_h = O \times C_i$. Similarly the orbitals on the individual bromine atoms are classified using O_h. The atomic orbitals of the Cr^{3+} ion which contribute to the relevant molecular orbitals of the complex are the $3d$, $4s$ and the $4p$ orbitals. The electronic configurations of the complex are assumed to be given by a Linear Combination of Atomic Orbitals (LCAO).

The $4p$ orbitals on the single Br^- ions are first combined into molecular orbitals for the octahedral complex of six bromines. The symmetry types of the Br–molecular orbitals we obtain are given in table B.2. The third column of the table contains the linear combinations of the orbital spaces obtained by coupling the irreps of the permutation representation of O and the irrep of O given by the $4p$ orbitals on an individual bromine. The details of this combination process need not concern us at the moment, but they are important when we come to relate the reduced matrix elements of the molecular orbitals to the matrix elements of the bromide ions.

The Br_6 orbitals are characterised not only by the symmetry properties under the O_h group, but also by the extent to which they partake in the bonding of the bromides to the chromium. We have σ type bonding orbitals and π type anti–bonding orbitals. The σ and π molecular–orbitals are the only nontrivial linear combinations.

With the addition of spin our classifying group becomes $SU_2 \times O_h$.

We now want to obtain a labelling scheme for the excited states of the cluster. In the charge transfer states there are three open shells, two on the Cr centre and one on the Br_6 "molecule". The overall symmetry of the state of the cluster must be $SU_2 \times O_h$, before the inclusion of the trigonal distortion, and so we couple these three orbitals at the $SU_2 \times O_h$ level. Although we can couple the shells in any order

it is natural to couple the two Cr orbitals together first, and then couple the Br_6 orbital to the result. Thus our group chain currently looks like

$$\left\{\left((SU_2\times O_h)_{t_{2g}},\ (SU_2\times O_h)_{e_g}\right)\downarrow (SU_2\times O_h)_{\mathrm{Cr}},\ (SU_2\times O_h)_{\mathrm{Br_6}}\right\} \qquad \text{(B.1)}$$
$$\downarrow (SU_2\times O_h)_{\mathrm{Cluster}},$$

where $\downarrow$ denotes a branching. This completes the classification of states imposed by the terms in the Hamiltonian that have O_h symmetry. The remaining terms are the spin–orbit contribution, the trigonal term and the magnetic exchange interaction.

We consider two possible branching schemes, or chains, below the cluster term $(SU_2\times O_h)_{\mathrm{Cluster}}$. In each chain one of the perturbing terms is diagonal. The trigonal distortion term of the Hamiltonian will be diagonal in the scheme

$$(SU_2\times O_h)_{\mathrm{Cluster}}\downarrow {O^S}\times {O_h}^L\downarrow {D_3}^S\times {D_{3d}}^L\downarrow {C_3}^S\times {C_{3i}}^L\downarrow {C_3}^S\times {C_3}^L\downarrow {C_3}^J$$

and the spin–orbit interaction will be diagonal in

$$(SU_2\times O_h)_{\mathrm{Cluster}}\downarrow {O^S}\times {O_h}^L\downarrow {O_h}^J\downarrow {D_{3d}}^J\downarrow {C_{3i}}^J\downarrow {C_3}^J.$$

The inclusion of those branching schemes will be considered in section B.3, but first we demonstrate how RACAH recognises a branch.

B.2.1 Branching with RACAH

Once RACAH has been started our first action is to describe the group chain using the `branch` command. We do this first for the chain, in equation (B.1), down to $(SU_2\times O_h)_{\mathrm{Cluster}}$ using brackets and commas in exactly the way we have written the chain:

```
 Racah v3.1 Fri Apr 28 08:37:12 1995
>branch ((su2*oh, su2*oh) su2*oh, su2*oh) su2*oh (((su2 * oh),
(su2 * oh)) to (su2 * oh), (su2 * oh)) to (su2 * oh)
```

The output confirms we have entered the chain correctly and indicates where to put the irreps when we come to describe the states. The options for the chains below $(SU_2\times O_h)_{\mathrm{Cluster}}$ are entered thus

```
>branch su2*oh o*oh d3*d3d c3*c3i c3*c3 c3
(su2 to o, oh) to (o to d3, (o to d3, ci))
     to (d3 to c3, (d3 to c3, ci)) to (c3, c3i to c3) to c3
```

or

```
>branch (su2 o d3 c3, oh d3d c3i c3) c3
(su2 to o to d3 to c3, (o to d3, ci)
     to (d3 to c3, ci) to c3) to c3
```

for the scheme in which the trigonal term is diagonal. The second option branches the spin chain separately from the orbital chain, until they both reach C_3, at which point they are joined by a coupled branching. At the second level of this chain, the product of $O \times O_h$, there is an ambiguity about the branch to the O_h below. Depending on whether the product $O \times O_h$ is bracketed as $(O \times (O \times C_i))$ or $((O \times O) \times C_i)$ we have a different interpretation for the coupling. We need the later form, so that we can branch the SU_2 down to an O and then combine the product $O \times O$ into a single O by coupling them together. Two ways to implement such a scheme, within RACAH, are

```
>branch (su2*o, ci) (o*o, ci) (o, ci) d3d c3i c3
((su2 to o, o), ci) to ((o, o) to o, ci) to (o to d3, ci)
      to (d3 to c3, ci) to c3
```

and

```
>branch (su2*o o*o o d3 c3, ci) c3
((su2 to o, o) to o to d3 to c3, ci) to c3
```

It is both physically reasonably, and RACAH compatible, to drop the parity label at the earliest opportunity, thus obtaining a simpler branching

```
>branch su2*oh o*o o d3 c3
(su2 to o, oh to o) to o to d3 to c3
```

which we can take advantage of. Initially we will include explicit parity labels at the $O \times O_h$ level since RACAH is quite capable of dealing with them.

B.3 Extending the symmetry scheme

Although we are only concerned with calculating the spin–orbit coupling constant, and therefore do not need a definite symmetry scheme below the octahedral group (O^J), we would like to exhibit one that could be used in a calculation that went beyond spin–orbit effects, for instance taking into account the trigonal distortion of the lattice.

We choose a group chain to classify the states that reflects the environment of the Cr^{3+} ion. Since the point group symmetry of the Cr site is C_3, due to the trigonal distortion of the octahedral arrangement of bromines, the natural choice is the chain $O \supset D_3 \supset C_3$. Therefore the kets are essentially labelled with the following group structure

$$\{(SU_2\times O_h,\ SU_2\times O_h) \downarrow SU_2\times O_h,\ SU_2\times O_h\} \downarrow SU_2\times O_h \downarrow O\times O \downarrow O \downarrow D_3 \downarrow C_3,$$

for states with three open shells. The branching $SU_2 \times O_h \downarrow O \times O$ is a product branching of ${SU_2}^S \downarrow O^S$ and ${O_h}^L \downarrow O^L$, while $O^S \times O^L \downarrow O^J$ is a coupled branching.

By virtue of having only one open shell, the ground state of the cluster need not include labels for the closed shells t_{1u} and t_{2u}. Thus the ground state can be written in a simpler form, as

$$\left|t_{2g}^3\left({}^4A_{2g}\right) U'.A_2\ U'E''\tfrac{3}{2}\right\rangle$$

The excited states are referred to as 'charge transfer states' due to their connection with the ground state through the charge transfer transitions. The designations of these states, within the symmetry scheme given at the start of this section, are

$$\left|\mathcal{P}\left\{\left(t_{2g}^3\left({}^4A_{2g}\right),\ e_g\left({}^2E_g\right)\right){}^5E_g,\ t_{1u}^5\left({}^2T_{1u}\right)\right\}{}^4T_{2u}\ U'.T_{2u}\ r\ \lambda\ \mu\ l\right\rangle$$

and

$$\left|\mathcal{P}\left\{\left(t_{2g}^3\left({}^4A_{2g}\right),\ e_g\left({}^2E_g\right)\right){}^5E_g,\ t_{2u}^5\left({}^2T_{2u}\right)\right\}{}^4T_{2u}\ U'.T_{2u}\ r\ \lambda\ \mu\ l\right\rangle$$

for excitations from the t_{1u} and t_{2u} open shells respectively, and for the various values of r, λ, μ and l that occur. λ, μ and l are labels for the irreps of O, D_3 and C_3 respectively. r is a multiplicity label for the coupled branching $O^S \times O^L \downarrow O^J$. In these states the $\mathcal{P}$ (Piepho & Schatz 1983, section 19.7) indicates that the electrons in the separate shells are antisymmetrized, as well as those within the same shells.

B.4 The Spin–Orbit Hamiltonian

The matrix elements we seek are

$$\left\langle\mathcal{P}\left\{\left(t_{2g}^3\left({}^4A_{2g}\right),\ e_g\left({}^2E_g\right)\right){}^5E_g,\ t_{1u}^5\left({}^2T_{1u}\right)\right\}{}^4T_{2u}\ U'.T_{2u}\ r\ \lambda\ \alpha\ \mu\ l\right|$$
$$\mathcal{H}_{\rm so}\left|\mathcal{P}\left\{\left(t_{2g}^3\left({}^4A_{2g}\right),\ e_g\left({}^2E_g\right)\right){}^5E_g,\ t_{1u}^5\left({}^2T_{1u}\right)\right\}{}^4T_{2u}\ U'.T_{2u}\ r\ \lambda\ \alpha\ \mu\ l\right\rangle \quad \text{(B.2)}$$

where

$$\mathcal{H}_{\rm so} = \zeta_{t_{2g}}(\boldsymbol{S}\cdot\boldsymbol{L})_{t_{2g}} + \zeta_{e_g}(\boldsymbol{S}\cdot\boldsymbol{L})_{e_g} + \zeta_{t_{1u}}(\boldsymbol{S}\cdot\boldsymbol{L})_{t_{1u}}, \tag{B.3}$$

a sum of the spin–orbit operators for the electrons in the three open shells that are present. The spin–orbit operator for each shell contains a parameter or coupling constant, ζ, which depends on the particular radial character of that molecular orbital, and hence on which atomic orbitals it is a linear combination of.

B.4.1 Facing up to the group chain

It is more enlightening to denote the three operators in the sum by

$$\zeta_{t_{2g}}(\boldsymbol{S}\cdot\boldsymbol{L})_{t_{2g}}\otimes(\mathbf{1}\cdot\mathbf{1})_{e_g}\otimes(\mathbf{1}\cdot\mathbf{1})_{t_{1u}}, \qquad \zeta_{e_g}(\mathbf{1}\cdot\mathbf{1})_{t_{2g}}\otimes(\boldsymbol{S}\cdot\boldsymbol{L})_{e_g}\otimes(\mathbf{1}\cdot\mathbf{1})_{t_{1u}}$$
$$\textit{and}\quad \zeta_{t_{1u}}(\mathbf{1}\cdot\mathbf{1})_{t_{2g}}\otimes(\mathbf{1}\cdot\mathbf{1})_{e_g}\otimes(\boldsymbol{S}\cdot\boldsymbol{L})_{t_{1u}}$$

which is equivalent to the prior equation since the operators have trivial action on the spaces that they do not apply to.

To apply the full power of the Wigner–Eckart theorem (section B.5) we need to classify the operator $\mathcal{H}_{\rm so}$ using all groups of the group chain labelling the states. The set of three spin operators, $\{s_x, s_y, s_z\}$, forms a basis for the irrep 1 of SU_2, which branches uniquely to t_1 of O. The same analysis applies to the three orbital angular momentum operators, $\{l_x, l_y, l_z\}$, although there is a parity label present as well. For the lower part of the chain, $\mathrm{SU}_2{\times}\mathrm{O}_h \supset O{\times}\mathrm{O}_h \supset \mathrm{O}_h \supset O \supset \mathrm{D}_3 \supset \mathrm{C}_3$, the irrep labels for the spin–orbit operators are $|{}^3T_{1g}\ T_1.T_{1g}\ A_{1g}000|$. With the complete chain the labels for the t_{1u} term are

$$\zeta_{t_{1u}}\left[\left({}^1\!A_{1g},\ {}^1\!A_{1g}\right){}^1\!A_{1g},\ {}^3T_{1g}\right]{}^3T_{1g}\ T_1.T_{1g}\ A_1a_1.$$

There are similar expressions for the t_{2g} and e_g terms which differ only in the position of the ${}^3T_{1g}$ inside the nested brackets (and the ζ factor).

$$\zeta_{t_{2g}}\left[\left({}^3T_{1g},\ {}^1\!A_{1g}\right){}^3T_{1g},\ {}^1\!A_{1g}\right]{}^3T_{1g}\ T_1.T_{1g}\ A_1a_1$$

$$\zeta_{e_g}\left[\left({}^1\!A_{1g},\ {}^3T_{1g}\right){}^3T_{1g},\ {}^1\!A_{1g}\right]{}^3T_{1g}\ T_1.T_{1g}\ A_1a_1$$

We follow the conventions of Butler (1981) in defining the coupling of two operators. We adopt as a basis of the space of operators

$$\{s^{1\,T_1\,A_2\,0}, s^{1\,T_1\,e\,1}, s^{1\,T_1\,e\,-1}\} \quad \text{for} \quad \boldsymbol{S}, \tag{B.4}$$
$$\{l^{1^+\,T_{1g}\,T_1\,A_2\,0}, l^{1^+\,T_{1g}\,T_1\,e\,-1}, l^{1^+\,T_{1g}\,T_1\,e\,1}\} \quad \text{for} \quad \boldsymbol{L}, \tag{B.5}$$

and couple those bases using the coupling coefficients for the chain O $\supset$ D_3 $\supset$ C_3, treating the parity and SU_2 labels as parentage labels

$$(\boldsymbol{S}\otimes\boldsymbol{L})^{^3T_{1g}\ T_1.T_{1g}\ A_{1g}\ A_1\ A_1\ 0}=\sum_{\alpha,\beta}\langle T_1\alpha,\ T_1\beta|0\ 0\ 0\rangle\left(s^{T_1\alpha}\otimes l^{T_1\beta}\right). \tag{B.6}$$

Expanding the right hand side we obtain

$$\begin{aligned}(\boldsymbol{S}\otimes\boldsymbol{L})^{^3T_{1g}\ T_1.T_{1g}\ A_{1g}\ A_1\ A_1\ 0}=&\frac{1}{\sqrt{3}}\left(s^{T_11}\otimes l^{T_1-1}\right)-\frac{1}{\sqrt{3}}\left(s^{T_10}\otimes l^{T_10}\right)\\&+\frac{1}{\sqrt{3}}\left(s^{T_1-1}\otimes l^{T_11}\right)\end{aligned} \tag{B.7}$$

which differs from the expression we seek,

$$\mathcal{H}_{\rm so}=(s_x\otimes l_x)+(s_y\otimes l_y)+(s_z\otimes l_z) \tag{B.8}$$

in that it is expressed in a different basis. We follow Butler (1981) and Piepho & Schatz (1983) in relating the $\{x,y,z\}$ basis to the $\{T_11,T_1-1,T_10\}$ basis. We have

$$\begin{aligned}o^{T_11}&=\frac{1}{\sqrt{2}}o_x+\frac{i}{\sqrt{2}}o_y\\o^{T_1-1}&=-\frac{1}{\sqrt{2}}o_x+\frac{i}{\sqrt{2}}o_y\\o^{T_11}&=o_z\end{aligned} \tag{B.9}$$

which implies that

$$(\boldsymbol{S}\otimes\boldsymbol{L})^{^3T_{1g}\ T_1.T_{1g}\ A_{1g}\ A_1\ 0}=-\frac{1}{\sqrt{3}}\left((s_x\otimes l_x)+(s_y\otimes l_y)+(s_z\otimes l_z)\right). \tag{B.10}$$

Using this we transliterate $\mathcal{H}_{so}$ into a form that transforms under the same group chain as the states,

$$\begin{aligned}\mathcal{H}_{so}=-\sqrt{3}\Big[&\zeta_{t_{2g}}(\boldsymbol{S}\otimes\boldsymbol{L})^{\left[\left(^3T_{1g},\,^1A_{1g}\right)^3T_{1g},\,^1A_{1g}\right]^3T_{1g}\ T_1.T_{1g}\ A_{1g}A_1a_1}\\&+\zeta_{e_g}(\boldsymbol{S}\otimes\boldsymbol{L})^{\left[\left(^1A_{1g},\,^3T_{1g}\right)^3T_{1g},\,^1A_{1g}\right]^3T_{1g}\ T_1.T_{1g}\ A_{1g}A_1a_1}\\&+\zeta_{t_{1u}}(\boldsymbol{S}\otimes\boldsymbol{L})^{\left[\left(^1A_{1g},\,^1A_{1g}\right)^1A_{1g},\,^3T_{1g}\right]^3T_{1g}\ T_1.T_{1g}\ A_1a_1}\Big].\end{aligned} \tag{B.11}$$

Now that the spin–orbit Hamiltonian is in a compatible basis we can proceed

with the reduction of the matrix element using the Wigner–Eckart theorem. It is at this stage that $3jm$ (and other coefficients disguised as $3jm$) appear, and RACAH shows its worth.

B.5 Application of the Wigner–Eckart Theorem

In this section we apply the Wigner–Eckart theorem several times to the matrix elements we wish to calculate.

The Wigner–Eckart theorem (Butler 1981, equation (4.2.3)),

$$\langle x_1\lambda_1 l_1|\, T^{\lambda l}\,|x_2\lambda_2 l_2\rangle = \sum_r \begin{pmatrix} \lambda_1 \\ l_1 \end{pmatrix} \begin{pmatrix} \lambda_1^* & \lambda & \lambda_2 \\ l_1^* & l & l_2 \end{pmatrix}^r \langle x_1\lambda_1||\, T^{\lambda}\,||x_2\lambda_2\rangle_r \tag{B.12}$$

relates the matrix elements of some operator to a $3jm$ of the transforming group, multiplied by a normalising factor. This normalising factor is called a reduced matrix element. This reduced matrix element contains the properties of the operators, $T^{\lambda l}$, reduced by the extraction of their transformation properties. In many applications, states and operators transform according to irreps of groups in some chain, $G \supset H$. The Wigner–Eckart theorem may be applied to either group, and the reduced matrix elements with respect to each group may be related to each other. This allows, for example, octahedral reduced matrix elements to be related to SO_3 reduced matrix elements.

Before considering the t_{1u}–shell contribution to H_{so} we introduce some notation. Since we are dealing with matrix elements that are diagonal, except for the multiplicity label r, we denote the bra by $\langle *|$ on the understanding that it has the same labels as the ket, with the possible exception of the multiplicity label. Furthermore we use $(\boldsymbol{S}\otimes\boldsymbol{L})_{t_{1u}}$ to denote what would otherwise be written

$$\left[\left(1^0 1^{A_{1g}},\, 1^0 1^{A_{1g}}\right)^{^1\!A_{1g}},\ \boldsymbol{S}^1\boldsymbol{L}^{T_{1g}}\right]^{^3T_{1g}T_1.T_{1g}A_1a_1},$$

although we often superscript the last few labels so that we know how far back the operator has been reduced. Through the use of these expedients, and the Wigner–Eckart theorem, the t_{1u}–shell contribution to the matrix elements in (B.2) can be reduced to the $\mathrm{SU}_2\times\mathrm{O}_h$ level in one step, with the result

$$\left\langle *\right|\zeta_{t_{1u}}(\boldsymbol{S}\otimes\boldsymbol{L})_{t_{1u}}^{^3T_{1g}\,T_1.T_{1g}\,A_1a_1}\left|\left\{\left({}^4A_{2g},\ {}^2E_g\right)^5E_g,\ {}^2T_{1u}\right\}{}^4T_{2u}\ U'.T_{2u}\ r\ \lambda l\right\rangle =$$

$$\sum_s \begin{pmatrix} {}^4T_{2u}' \\ U'.T_{2u} \\ r' \\ \lambda \\ l \end{pmatrix} \begin{pmatrix} {}^4T_{2u} & {}^3T_{1g} & {}^4T_{2u} \\ U'.T_{2u} & T_1.T_{1g} & U'.T_{2u} \\ r' & 0 & r \\ \lambda & A_1 & \lambda \\ l^* & a_1 & l \end{pmatrix} s0 \qquad \text{(B.13)}$$

$$\times \left\langle * \middle\| \zeta_{t_{1u}} (\boldsymbol{S} \otimes \boldsymbol{L})^{\left[\left({}^1A_{1g}, {}^1A_{1g}\right)^1A_{1g}, {}^3T_{1g}\right]^3T_{1g}}_{t_{1u}} \middle\| \left\{ \left({}^4A_{2g}, {}^2E_g\right)^5E_g, {}^2T_{1u} \right\} {}^4T_{2u} \right\rangle .$$

This expression is analogous to equation (18.4.6) of Piepho & Schatz (1983). To see this clearly we use a relation between the $3jm$ of a coupled branching, $G{\times}G \downarrow G$, and a $9j$ for G.

$$\begin{pmatrix} \lambda_1\lambda_2 \\ r_1 \\ \lambda \end{pmatrix} \begin{pmatrix} \lambda_1^*\lambda_2^* & \kappa_1.\kappa_2 & \mu_1.\mu_2 \\ r_1 & t & r_2 \\ \lambda^* & \kappa & \mu \end{pmatrix} s_1 s_2 =$$

$$H(\lambda_1\lambda_2\lambda) H(\kappa_1\kappa_2\kappa) H(\mu_1\mu_2\mu) \left|\lambda\right|^{1/2} \left|\kappa\right|^{1/2} \left|\mu\right|^{1/2} \begin{Bmatrix} \lambda_1 & \lambda_2 & \lambda^* \\ \kappa_1^* & \kappa_2^* & \kappa \\ \mu_1^* & \mu_2^* & \mu \\ s_1 & s_2 & s \end{Bmatrix} \begin{matrix} r_1 \\ t \\ r_2 \end{matrix} \qquad \text{(B.14)}$$

Since, in the case we are considering, κ is restricted to A_1 we can, after cyclicly permuting the rows of the $9j$, apply equation (3.3.36) of Butler (1981), yielding a $6j$ plus phase and dimension factors:

$$\begin{pmatrix} U'.T_{2u} \\ r' \\ \lambda \end{pmatrix} \begin{pmatrix} U'.T_{2u} & T_1.T_{1g} & U'.T_{2u} \\ r' & 0 & r \\ \lambda & A_1 & \lambda \end{pmatrix} s0 \\ 0$$

$$= \left|\lambda\right| \begin{Bmatrix} U' & T_2 & \lambda \\ U' & T_2 & \lambda \\ T_1 & T_1 & A_1 \\ s & 0 & 0 \end{Bmatrix} \begin{matrix} r \\ r' \\ 0 \end{matrix}$$

$$= \left|\lambda\right|^{1/2} \left|T_1\right|^{-1/2} \{T_2\} \{T_2T_2T_1\} \{U'T_2\lambda\} \begin{Bmatrix} U' & U' & T_1 \\ T_2 & T_2 & \lambda \end{Bmatrix}_{r'r0s} \qquad \text{(B.15)}$$

Returning to the matrix element, (B.13), we factorise the $3jm$ and substitute the above expression involving the $6j$. Doing this the matrix element can be expressed as

$$\sum_s \left|\lambda\right|^{1/2} \left|T_1\right|^{-1/2} \{T_2\} \{T_2T_2T_1\} \{U'T_2\lambda\} \begin{Bmatrix} U' & T_2 & \lambda \\ T_2 & U' & T_1 \end{Bmatrix}_{s0rr'}$$

$$\times \begin{pmatrix} \frac{3}{2} \\ U' \end{pmatrix} \begin{pmatrix} \frac{3}{2} & 1 & \frac{3}{2} \\ U' & T_1 & U' \end{pmatrix}_s^0 \begin{pmatrix} \lambda \\ l \end{pmatrix} \begin{pmatrix} \lambda & A_1 & \lambda \\ l^* & a_1 & l \end{pmatrix}. \tag{B.16}$$

The last $3jm$ can be written as a $2jm$ times the square root of the dimension of l, one in this case, and divided by the square root of the dimension of λ (equation (3.3.8) of Butler (1981)). This means the last $2jm$ and $3jm$ become a simple $|\lambda|^{-1/2}$, which cancels one of the dimension factors at the beginning of the expression. The $2j$ phase $\{T_2\}$ is $+1$ because T_2 is a true irrep. Since the $SO_3 \downarrow O$ $2jm$ is unity, the only obstruction preventing favourable comparison of our expression with equation (18.4.6) of Piepho & Schatz (1983) is the dimension factor $|T_1|^{-1/2}$. This is explained by the different operators in the reduced matrix element. Since $s^1 u^{t_1} = (1/\sqrt{3})\zeta(\boldsymbol{S} \otimes \boldsymbol{L})$ the two expressions are indeed in agreement. ($|T_1| = 3$)

So the final form for this step of the reduction is either equation (B.13) or

$$\begin{aligned} &\left\langle * \middle| \zeta_{t_{1u}} (\boldsymbol{S} \otimes \boldsymbol{L})_{t_{1u}}^{{}^3T_{1g}\, T_1.T_{1g}\, A_1 a_1} \middle| \left\{ \left({}^4A_{2g},\ {}^2E_g \right) {}^5E_g,\ {}^2T_{1u} \right\} {}^4T_{2u}\ U'.T_{2u}\ r\ \lambda l \right\rangle = \\ &\sum_s |T_1|^{-1/2} \{T_2 T_2 T_1\} \{U' T_2 \lambda\} \begin{Bmatrix} U' & T_2 & \lambda \\ T_2 & U' & T_1 \end{Bmatrix} s 0 r r' \begin{pmatrix} \frac{3}{2} & 1 & \frac{3}{2} \\ U' & T_1 & U' \end{pmatrix}_s^0 \\ &\times \left\langle * \middle\| \zeta_{t_{1u}} (\boldsymbol{S} \otimes \boldsymbol{L})_{t_{1u}}^{\left[\left({}^1A_{1g},\, {}^1A_{1g} \right) {}^1A_{1g},\, {}^3T_{1g} \right] {}^3T_{1g}} \middle\| \left\{ \left({}^4A_{2g},\ {}^2E_g \right) {}^5E_g,\ {}^2T_{1u} \right\} {}^4T_{2u} \right\rangle. \end{aligned} \tag{B.17}$$

The next step in the reduction is very like the previous one, except that the group is not O but $SU_2 \times O_h$. Applying the Wigner–Eckart theorem to the partly reduced matrix element gives

$$\begin{aligned} &\left\langle * \middle\| \zeta_{t_{1u}} (\boldsymbol{S} \otimes \boldsymbol{L})_{t_{1u}}^{\left[\left({}^1A_{1g},\, {}^1A_{1g} \right) {}^1A_{1g},\, {}^3T_{1g} \right] {}^3T_{1g}} \middle\| \left\{ \left({}^4A_{2g},\ {}^2E_g \right) {}^5E_g,\ {}^2T_{1u} \right\} {}^4T_{2u} \right\rangle = \\ &\qquad \begin{pmatrix} {}^5E_g.{}^2T_{1u} \\ {}^4T_{2u} \end{pmatrix} \begin{pmatrix} {}^5E_g.{}^2T_{1u} & {}^1A_{1g}.{}^3T_{1g} & {}^5E_g.{}^2T_{1u} \\ {}^4T_{2u} & {}^3T_{1g} & {}^4T_{2u} \end{pmatrix} \\ &\qquad \times \left\langle * \middle\| \zeta_{t_{1u}} (\boldsymbol{S} \otimes \boldsymbol{L})_{t_{1u}}^{\left({}^1A_{1g},\, {}^1A_{1g} \right) {}^1A_{1g},\, {}^3T_{1g}} \middle\| \left({}^4A_{2g},\ {}^2E_g \right) {}^5E_g,\ {}^2T_{1u} \right\rangle. \end{aligned} \tag{B.18}$$

Because we are dealing with a direct product of three groups, SU_2, O and C_i, the $3jm$ and $2jm$ each factor into three pieces:

$$\begin{aligned} &\begin{pmatrix} {}^5E_g.{}^2T_{1u} \\ {}^4T_{2u} \end{pmatrix} \begin{pmatrix} {}^5E_g.{}^2T_{1u} & {}^1A_{1g}.{}^3T_{1g} & {}^5E_g.{}^2T_{1u} \\ {}^4T_{2u} & {}^3T_{1g} & {}^4T_{2u} \end{pmatrix} = \\ &\qquad \begin{pmatrix} 2.\frac{1}{2} \\ \frac{3}{2} \end{pmatrix} \begin{pmatrix} 2.\frac{1}{2} & 0.1 & 2.\frac{1}{2} \\ \frac{3}{2} & 1 & \frac{3}{2} \end{pmatrix} \begin{pmatrix} E.T_1 \\ T_2 \end{pmatrix} \begin{pmatrix} E.T_1 & A_1.T_1 & E.T_1 \\ T_2 & T_1 & T_2 \end{pmatrix} \\ &\qquad \times \begin{pmatrix} +.- \\ - \end{pmatrix} \begin{pmatrix} +.- & +.+ & +.- \\ - & + & - \end{pmatrix}. \end{aligned} \tag{B.19}$$

The irrep labels used for the parity group are $+$ and $-$, rather than the more common g and u respectively. Using (B.14) and equation (3.3.36) of Butler (1981) on each of the $2jm$–$3jm$ combinations, except for the parity piece which is equal to one, yields

$$\begin{pmatrix} {}^5E_g.{}^2T_{1u} \\ {}^4T_{2u} \end{pmatrix} \begin{pmatrix} {}^5E_g.{}^2T_{1u} & {}^1A_{1g}.{}^3T_{1g} & {}^5E_g.{}^2T_{1u} \\ {}^4T_{2u} & {}^3T_{1g} & {}^4T_{2u} \end{pmatrix} =$$
$$H\left(2\tfrac{3}{2}\tfrac{1}{2}\right) H\left(2\tfrac{3}{2}\tfrac{1}{2}\right) |2|^{-1/2} \left|\tfrac{3}{2}\right| \left\{\tfrac{3}{2}\right\} \left\{2\tfrac{3}{2}\tfrac{1}{2}\right\} \left\{\tfrac{3}{2}\tfrac{3}{2}1\right\} \begin{Bmatrix} \frac{1}{2} & \frac{1}{2} & 1 \\ \frac{3}{2} & \frac{3}{2} & 2 \end{Bmatrix}$$
$$\times |E|^{-1/2} |T_2| \{T_2\} \{ET_2T_1\} \{T_2T_2T_1\} \begin{Bmatrix} T_1 & T_1 & T_1 \\ T_2 & T_2 & E \end{Bmatrix}. \quad \text{(B.20)}$$

Factoring the reduced matrix element of the spin–orbit operator into a reduced matrix element of the unit operator, on the coupled e_g and t_{2g} orbitals (the chromium orbitals), and a reduced matrix element for the standard spin–orbit operator, on the t_1 orbital, we get

$$\left\langle * \middle\| \zeta_{t_{1u}} (\boldsymbol{S} \otimes \boldsymbol{L})^{({}^1A_{1g},\, {}^1A_{1g})\, {}^1A_{1g},\, {}^3T_{1g}}_{t_{1u}} \middle\| \left({}^4A_{2g},\ {}^2E_g\right) {}^5E_g,\ {}^2T_{1u} \right\rangle =$$
$$\left\langle \left({}^4A_{2g},\ {}^2E_g\right) {}^5E_g \middle\| \mathbf{1} \middle\| \left({}^4A_{2g},\ {}^2E_g\right) {}^5E_g \right\rangle$$
$$\times \left\langle t_{1u}^5 ({}^2T_{1u}) \middle\| \zeta_{t_{1u}} (\boldsymbol{S} \otimes \boldsymbol{L})^{{}^3T_{1g}}_{t_{1u}} \middle\| t_{1u}^5 ({}^2T_{1u}) \right\rangle. \quad \text{(B.21)}$$

The reduced matrix element of the unit operator is the square root of the dimension of the irrep we have reduced back to. Therefore we can write the reduced matrix element, in (B.13) and (B.17), as

$$\left\langle * \middle\| \zeta_{t_{1u}} (\boldsymbol{S} \otimes \boldsymbol{L})^{\left[({}^1A_{1g},\, {}^1A_{1g})\, {}^1A_{1g},\, {}^3T_{1g}\right] {}^3T_{1g}}_{t_{1u}} \middle\| \left\{ \left({}^4A_{2g},\ {}^2E_g\right) {}^5E_g,\ {}^2T_{1u} \right\} {}^4T_{2u} \right\rangle =$$
$$\left|\tfrac{3}{2}\right| |T_2| \left\{\tfrac{3}{2}\right\} \left\{2\tfrac{3}{2}\tfrac{1}{2}\right\} \left\{\tfrac{3}{2}\tfrac{3}{2}1\right\} \begin{Bmatrix} \frac{1}{2} & \frac{1}{2} & 1 \\ \frac{3}{2} & \frac{3}{2} & 2 \end{Bmatrix} \{ET_2T_1\} \{T_2T_2T_1\} \begin{Bmatrix} T_1 & T_1 & T_1 \\ T_2 & T_2 & E \end{Bmatrix}$$
$$\times \left\langle t_{1u}^5 ({}^2T_{1u}) \middle\| \zeta_{t_{1u}} (\boldsymbol{S} \otimes \boldsymbol{L})^{{}^3T_{1g}}_{t_{1u}} \middle\| t_{1u}^5 ({}^2T_{1u}) \right\rangle. \quad \text{(B.22)}$$

B.6 Multi–centre matrix elements

RACAH can calculate the factors that appear in the previous section, but we are faced with reducing the many–particle reduced matrix element to a one–particle matrix element ourselves. This involves the use of coefficients of fractional parentage which, at the moment, RACAH cannot calculate. We shall content our-

selves with quoting the result for this case, from Piepho & Schatz (1983):

$$\left\langle t_{1u}^5(^2T_{1u}) \middle\| \zeta_{t_{1u}}(\boldsymbol{S}\otimes\boldsymbol{L})^{^3T_{1g}}_{t_{1u}} \middle\| t_{1u}^5(^2T_{1u}) \right\rangle = -\left\langle \tfrac{1}{2}.t_{1u}(\pi) \middle\| \zeta_{t_{1u}}(\boldsymbol{S}\otimes\boldsymbol{L}) \middle\| \tfrac{1}{2}.t_{1u}(\pi) \right\rangle . \tag{B.23}$$

This naturally factors into a reduced matrix element for the spin and a reduced matrix element for the orbital angular momentum of an electron in the $t_{1u}(\pi)$ molecular orbital. The spin reduced matrix element is standard, but the orbital reduced matrix element involves considering many–centre integrals and is therefore more complicated. The required calculations were performed in Dillon, Kamimura & Remeika (1966), but required some corrections. The single–centre reduced matrix element for the $t_{1u}(\pi)$ molecular orbital is

$$\left\langle \tfrac{1}{2}.t_{1u}(\pi) \middle\| \zeta_{t_{1u}}(\boldsymbol{S}\otimes\boldsymbol{L}) \middle\| \tfrac{1}{2}.t_{1u}(\pi) \right\rangle = -\frac{3}{2}\zeta_{4p}^{\mathrm{Br}} . \tag{B.24}$$

We also require the reduced matrix elements of $\mathcal{H}_{\mathrm{so}}$ for the $t_{2u}(\pi)$, $t_{1u}(\sigma)$ molecular orbitals, and the t_{2g} and t_{1u} Cr orbitals.

$$\begin{aligned}
\left\langle \tfrac{1}{2}.t_{2u}(\pi) \middle\| \zeta_{t_{2u}}(\boldsymbol{S}\otimes\boldsymbol{L}) \middle\| \tfrac{1}{2}.t_{2u}(\pi) \right\rangle &= -\tfrac{3}{2}\zeta_{4p}^{\mathrm{Br}} \\
\left\langle \tfrac{1}{2}.t_{1u}(\sigma) \middle\| \zeta_{t_{1u}(\sigma)}(\boldsymbol{S}\otimes\boldsymbol{L}) \middle\| \tfrac{1}{2}.t_{1u}(\sigma) \right\rangle &= -\tfrac{1}{8}S\zeta_{4p}^{\mathrm{Br}} \\
\left\langle \tfrac{1}{2}.t_{2g} \middle\| \zeta_{t_{2g}}(\boldsymbol{S}\otimes\boldsymbol{L}) \middle\| \tfrac{1}{2}.t_{2g} \right\rangle &= -3\zeta_{3d}^{\mathrm{Cr}} \\
\left\langle \tfrac{1}{2}.t_{1u}^{\mathrm{Cr}} \middle\| \zeta_{t_{1u}}(\boldsymbol{S}\otimes\boldsymbol{L}) \middle\| \tfrac{1}{2}.t_{1u}^{\mathrm{Cr}} \right\rangle &= 3\zeta_{4p}^{\mathrm{Cr}}
\end{aligned}$$

S is related to the overlap between $p(\sigma)$ and $p(\pi)$ orbitals on neighbouring bromine ions.

B.7 The ins and outs of RACAH

After starting RACAH the first task is to describe the chain of groups that are used to classify states and operators (section B.2.1). Since the group $SO_3{\times}O_h \cong SU_2{\times}O_h$ occurs so often, we give it a shorter name before describing the branching.

```
Racah v3.1                                  Fri Dec 15 09:37:42 1995
>group groupname x so3*oh
x is so3 * oh
>branch ((x,x)x,x)x o*o o
((x, x) to x, x) to x to (so3 to o, oh to o) to o
>
```

Because the matrix elements do not depend on irrep labels lower than the octahedral group we do not take the chain any lower. The matrix element we want

to calculate, in equation (B.2), can be expressed as a sum over coefficients multiplying reduced matrix elements of the type found on the right hand side of (B.22). RACAH gives us the coefficients of the reduced matrix elements in this expression. The reduced matrix elements themselves are calculated using the procedure outlined in section B.6.

Now we ask for the Wigner–Eckart coefficients, with question marks in the place of irreps or multiplicities we wish to range freely. The output is such that, for example, 1/8.5#2.3 = $+\frac{1}{8\times5\sqrt{2\times3}}$

```
weme ((s1.~0+,s0.2+)2.2+,s0.1-)s1.~1- (s1 s1,~1- ~1) ?   %
%>((0.0+,0.0+)0.0+,1.1+)1.1+ (1 1,1+ 1) 0    %
%>((s1.~0+,s0.2+)2.2+,s0.1-)s1.~1- (s1 s1,~1- ~1) ?

(((s1.~0+, s0.2+) 2.2+, s0.1-) s1.~1-(s1 s1, ~1- ~1) s0 |
((0.0+, 0.0+) 0.0+, 1.1+) 1.1+(1 1, 1+ 1) 0, ((s1.~0+, s0.2+)
  2.2+, s0.1-) s1.~1-(s1 s1, ~1- ~1) s0) +  +1/8.5#2.3
(((s1.~0+, s0.2+) 2.2+, s0.1-) s1.~1-(s1 s1, ~1- ~1) \0 s1 |
((0.0+, 0.0+) 0.0+, 1.1+) 1.1+(1 1, 1+ 1) 0, ((s1.~0+, s0.2+)
  2.2+, s0.1-) s1.~1-(s1 s1, ~1- ~1) \0 s1) +  +1/4.3.5#3
(((s1.~0+, s0.2+) 2.2+, s0.1-) s1.~1-(s1 s1, ~1- ~1) \0 s1 |
((0.0+, 0.0+) 0.0+, 1.1+) 1.1+(1 1, 1+ 1) 0, ((s1.~0+, s0.2+)
  2.2+, s0.1-) s1.~1-(s1 s1, ~1- ~1) \1 s1) +  +1/4.3.5#3
(((s1.~0+, s0.2+) 2.2+, s0.1-) s1.~1-(s1 s1, ~1- ~1) \1 s1 |
((0.0+, 0.0+) 0.0+, 1.1+) 1.1+(1 1, 1+ 1) 0, ((s1.~0+, s0.2+)
  2.2+, s0.1-) s1.~1-(s1 s1, ~1- ~1) \0 s1) +  +1/4.3.5#3
(((s1.~0+, s0.2+) 2.2+, s0.1-) s1.~1-(s1 s1, ~1- ~1) \1 s1 |
((0.0+, 0.0+) 0.0+, 1.1+) 1.1+(1 1, 1+ 1) 0, ((s1.~0+, s0.2+)
  2.2+, s0.1-) s1.~1-(s1 s1, ~1- ~1) \1 s1) +  -1/8.3.5#3
(((s1.~0+, s0.2+) 2.2+, s0.1-) s1.~1-(s1 s1, ~1- ~1) ~s0 |
((0.0+, 0.0+) 0.0+, 1.1+) 1.1+(1 1, 1+ 1) 0, ((s1.~0+, s0.2+)
  2.2+, s0.1-) s1.~1-(s1 s1, ~1- ~1) ~s0) +  -1/8.3#2.3
```

This process is repeated for each state with each operator, using the following strings to represent the stated labels. The results are given in table B.3.

```
shell states.
eg    ((s1.~0+,0.0+)s1.~0+,0.0+)s1.~0+ (s1 s1,~0+ ~0) ?
t1u   ((s1.~0+,s0.2+)2.2+,s0.1-)s1.~1- (s1 s1,~1- ~1) ?
```

```
t2u   ((s1.~0+,s0.2+)2.2+,s0.~1-)s1.~1- (s1 s1,~1- ~1) ?
t2g^* ((1.~1+,0.0+)1.~1+,s0.~1-)s1.~1- (s1 s1,~1- ~1) ?

operator states.
t2g   ((1.1+,0.0+)1.1+,0.0+)1.1+ (1 1,1+ 1) 0
t1u   ((0.0+,0.0+)0.0+,1.1+)1.1+ (1 1,1+ 1) 0
eg    ((0.0+,1.1+)1.1+,0.0+)1.1+ (1 1,1+ 1) 0
```

B.7.1 The state energies

The matrices obtained by RACAH are not diagonal, and so we must find the eigenvalues of the two by two blocks to obtain the contribution of the spin–orbit interaction to the energy of these states. We multiply those values by the reduced matrix elements of section B.6 to give the energies of the various states.

Those state energies are given in table B.4. We use the notation $|t_{1u}s0\rangle$, for example, to represent the energy of the $s0$ projection state of the t_{1u} level. We give the energies in terms of the ζ's as well as the explicit values. The values of the free ζ parameters

$$\zeta_{3d}^{Cr} = 290 cm^{-1}$$
$$\zeta_{4p}^{Cr} = 50 cm^{-1}$$
$$\zeta_{4p}^{Br} = 2460 cm^{-1}$$

are taken from Dillon, Kamimura & Remeika (1966).

B.7.2 The spin–orbit coupling constant

The spin–orbit coupling constants are defined by

$$\lambda = -\frac{\langle {}^4T_2 \| \mathcal{H}_{so} \| {}^4T_2 \rangle}{\langle L \| L \| L \rangle \langle S \| S \| S \rangle} \tag{B.25}$$

where, for this case, $\langle L \| L \| L \rangle = -\sqrt{6}$ and $\langle S \| S \| S \rangle = \sqrt{S(S+1)(2S+1)}$.

In this case we need to calculate the reduced matrix elements for $\mathcal{H}_{so}$ as found on the left hand side of equation (B.22). We give below examples of how we would input requests to RACAH for the various factors appearing on the right hand side of that equation, and how RACAH returns the result. To the right we briefly explain each step.

```
>group su2                          Selecting a group.
su2

>irrep s1                          Obtaining information about
4   s1  s1    3     -   +4         and irrep, e.g. dimension=+4

>3j 2 s1 s0                        Asking for a 3j phase
2   s1  s0   +
>3j s1 s1 1
s1  s1  1    +

>6j s0 s0 1 s1 s1 2                Asking for a 6j
s0 s0 1   s1 s1 2  + +1/2#2.5
```

Putting those values together with equations (B.23) and (B.24) gives,

$$\lambda_{1u} = -\frac{1}{20}\zeta_{4p}^{\mathrm{Br}} \tag{B.26}$$

The complete set of spin–orbit coupling coefficients is given in table B.5.

B.8 Summary

We have demonstrated the power and convenience with which RACAH can calculate reduced matrix elements. Extensions of RACAH are planned to take in the simplification of the multi–center reduced matrix elements to single–center reduced matrix elements.

We have given the spin–orbit energies of the charge–transfer states, and the spin–orbit coupling constants associated with this. The results of this paper are being used to investigate the Kerr rotation of $CrBr_3$, an effect which hinges on the spin–orbit coupling.

A copy of RACAH can be obtained by emailing a message to:

`racah--help@phys.canterbury.ac.nz`

RACAH has been compiled and tested under MS–Dos, Unix and VMS.

Tab. B.1: Schönflies(S) and Butler(B) labelling for the irreps of O on the left, and D_3 on the right. The second label in the Butler columns is the form of the Butler notation that RACAH recognises.

S	B	S	B	S	B	S	B
A_1	0	A_2	$\tilde{0}$ or $\sim$0	A_1	0	E'	$\frac{1}{2}$ or s0
E	2	T_1	1	A_2	$\tilde{0}$ or $\sim$0	E	1
T_2	$\tilde{1}$ or $\sim$1	E'	$\frac{1}{2}$ or s0	E''	$\frac{3}{2}$ or s1 $-\frac{3}{2}$ or -s1		
E'	$\frac{\tilde{1}}{2}$ or $\sim$s0	U'	$\frac{3}{2}$ or s1				

Tab. B.2: Molecular orbitals for the six Br^- ions.

	Schönflies notation	Butler notation	Factorised states
σ–orbital	a_{1g}	0^+	$\|(1^-,1^-)0^+\rangle$
π–orbital	t_{1g}	1^+	$\|(1^-,1^-)1^+\rangle$
π–orbital	t_{2g}	$\tilde{1}^+$	$\left\|(1^-,1^-)\tilde{1}^+\right\rangle$
σ–orbital	e_g	2^+	$\|(1^-,1^-)2^+\rangle$
σ–orbital	t_{1u}	1^-	$1/\sqrt{3}\|(0^+,1^-)1^-\rangle - \sqrt{2}/\sqrt{3}\|(2^+,1^-)1^-\rangle$
π–orbital	t_{1u}	1^-	$\sqrt{2}/\sqrt{3}\|(0^+,1^-)1^-\rangle + 1/\sqrt{3}\|(2^+,1^-)1^-\rangle$
π–orbital	t_{2u}	$\tilde{1}^-$	$\left\|(2^+,1^-)\tilde{1}^-\right\rangle$

Tab. B.3: The output from RACAH.

t_{1u}	s0	\0 s1	\1 s1	~s0
s0	$\frac{1}{40\sqrt{6}}$	0	0	0
\0 s1	0	$\frac{1}{60\sqrt{3}}$	$\frac{1}{60\sqrt{3}}$	0
\1 s1	0	$\frac{1}{60\sqrt{3}}$	$-\frac{1}{120\sqrt{3}}$	0
~s0	0	0	0	$-\frac{1}{24\sqrt{6}}$

t_{2u}	s0	\0 s1	\1 s1	~s0
s0	$-\frac{1}{40\sqrt{3}}$	0	0	0
\0 s1	0	$-\frac{1}{60\sqrt{3}}$	$-\frac{1}{60\sqrt{3}}$	0
\1 s1	0	$-\frac{1}{60\sqrt{3}}$	$\frac{1}{120\sqrt{3}}$	0
~s0	0	0	0	$\frac{1}{24\sqrt{6}}$

t_{2g}^*	s0	\0 s1	\1 s1	~s0
s0	$\frac{1}{36}$	0	0	0
\0 s1	0	$\frac{1}{27\sqrt{2}}$	$\frac{1}{27\sqrt{2}}$	0
\1 s1	0	$\frac{1}{27\sqrt{2}}$	$-\frac{1}{54\sqrt{2}}$	0
~s0	0	0	0	$-\frac{5}{108}$

t_{2g}^*	s0	\0 s1	\1 s1	~s0
s0	$\frac{1}{18\sqrt{6}}$	0	0	0
\0 s1	0	$\frac{1}{27\sqrt{3}}$	$\frac{1}{27\sqrt{3}}$	0
\1 s1	0	$\frac{1}{27\sqrt{3}}$	$-\frac{1}{54\sqrt{3}}$	0
~s0	0	0	0	$-\frac{5}{54\sqrt{6}}$

Tab. B.4: State energy changes due to spin–orbit coupling.

State		$\sim(cm^{-1})$	$\sim$(eV)$\times 10^{-3}$
$\|t_{1u}\ s0\rangle$	$\frac{3}{80\sqrt{6}}\zeta_{4p}^{Br}$	37.7	4.7
$\|t_{1u}\ \backslash 0\ s1\rangle$	$\frac{3}{80\sqrt{3}}\zeta_{4p}^{Br}$	53.3	6.6
$\|t_{1u}\ \backslash 1\ s1\rangle$	$\frac{3}{40\sqrt{3}}\zeta_{4p}^{Br}$	106.5	13.2
$\|t_{1u}\sim s0\rangle$	$-\frac{1}{16}\zeta_{4p}^{Br}$	-153.8	-19.1
$\|t_{2u}\ s0\rangle$	$-\frac{3}{80\sqrt{6}}\zeta_{4p}^{Br}$	-37.7	-4.7
$\|t_{2u}\ \backslash 0\ s1\rangle$	$-\frac{3}{80\sqrt{3}}\zeta_{4p}^{Br}$	-53.3	-6.6
$\|t_{2u}\ \backslash 1\ s1\rangle$	$-\frac{3}{40\sqrt{3}}\zeta_{4p}^{Br}$	-106.5	-13.2
$\|t_{2u}\sim s0\rangle$	$\frac{1}{16}\zeta_{4p}^{Br}$	153.8	19.1
$\|t_{2g}^{*}\ s0\rangle$	$(2\zeta_{4p}^{Cr}-\sqrt{6}\zeta_{3d}^{Cr})\frac{\sqrt{5}}{72\sqrt{6}}$	-7.7	-0.95
$\|t_{2g}^{*}\ \backslash 0\ s1\rangle$	$(2\sqrt{5}\zeta_{4p}^{Cr}-\sqrt{3}\zeta_{3d}^{Cr})\frac{1}{72\sqrt{3}}$	-2.2	-0.27
$\|t_{2g}^{*}\ \backslash 1\ s1\rangle$	$(\sqrt{2}\zeta_{4p}^{Cr}-\sqrt{3}\zeta_{3d}^{Cr})\frac{\sqrt{5}}{54\sqrt{6}}$	-7.3	-0.91
$\|t_{2g}^{*}\sim s0\rangle$	$(10\sqrt{2}\zeta_{4p}^{Cr}-5\sqrt{6}\zeta_{3d}^{Cr})\frac{\sqrt{5}}{216\sqrt{6}}$	-12.0	-1.5

Tab. B.5: The spin–orbit coupling constants.

SO coupling constant	Value	(cm^{-1})
$\lambda_{1u}(\pi)$	$-\frac{1}{20}\zeta_{4p}^{Br}$	-123
$\lambda_{2u}(\pi)$	$\frac{1}{20}\zeta_{4p}^{Br}$	123
$\lambda_{1u}(\sigma)$	$\frac{1}{10}\|S\|\zeta_{4p}^{Br}$	$\|S\|246$
λ_{2g^*}	$\frac{1}{6}\left(\zeta_{4p}^{Cr}-\zeta_{3d}^{Cr}\right)$	-40

C. CHARGE TRANSFER TRANSITIONS IN CHROMIUM TRIHALIDES

Charge transfer transitions in chromium trihalides

K Shinagawa, H Sato†, H J Ross‡, L F McAven‡, and P H Butler‡

Department of Physics, Toho University, Funabashi-City, Chiba, 274 Japan
† Department of Information Science. Ochanomizu University, Bunkyo-ku, Tokyo 112, Japan
‡ Department of Physics and Astronomy, University of Canterbury, Private Bag 4800, Christchurch, New Zealand

The electronic states of chromium trihalides, CrM_3 (M=Cl, Br, I) are calculated by taking a USCF–X α–SW approach to an assumed $(CrM_6)^{3-}$ octahedral cluster model. It is found that there are three charge transfer (CT) transitions at the absorption edge. Those transitions are calculated as shifting to lower energies as the halide goes from chlorine to iodine, consistent with observation. In addition the transition energies obtained from Slater transition state calculations agree with the observed values. As a result, the transitions observed at the absorption band edge are assigned, in energy order, to the CT transitions: $4t_{1u}(np) \rightarrow 3e_g(3d)$ and $1t_{2u} \rightarrow 3e_g(3d)$ of π-type and $3t_{1u}(np) \rightarrow 3e_g(3d)$ of σ type. Combining this result with the signs of the spin-orbit constants for the CT states, the large Faraday and Kerr rotations observed at the absorption band edge in ferromagnetic $CrBr_3$ can be attributed to the two π-type CT transitions.

Published: J.Phys.:Condens. Matter **8** (1996) 8457-8463.

D. STUDYING SYMMETRIC GROUPS IN MATLAB

I have written a series of MATLAB scripts which are useful for studying symmetric groups. Those programs are related, with many calling others to perform calculations. Together they provide a useful collection of tools for studying, in MATLAB, representations of symmetric groups. An example of the flexibility is figure D.1, which has been generated using the following script.

```
p=[3 2 1];
[T,count]=tableau(p,perm(5));
[T,l]=sorttabs(T,p,2);
tabout(T,p);
```

On the next pages, we provide a non–exhaustive list of the scripts. In particular some scripts were modified to perform equivalent purposes for the Hecke algebras, which we studied to a much lesser extent than the symmetric group.

run:: This initialisation package prepares some of the necessary transformation coefficient matrices.

QmatS3:: Contains all of the representation matrices for S_3.

QmatS4:: Contains all of the representation matrices for S_4.

QmatS5:: Contains all of the representation matrices for S_5.

Chenmats:: Contains all of the transformation matrices given by Chen, Collinson & Gao (1983). This was used as a basis for testing our results.

get3mats:: Generates all the representation matrices for S_3.

get4mats:: Generates all the representation matrices for S_4.

get5mats:: Generates all the representation matrices for S_5.

get6mats:: Generates all the representation matrices for S_6.

get7mats:: Generates all the representation matrices for S_7.

Fig. D.1: First letter ordered tableaux for labelling the basis vectors of the irrep [3 2 1]

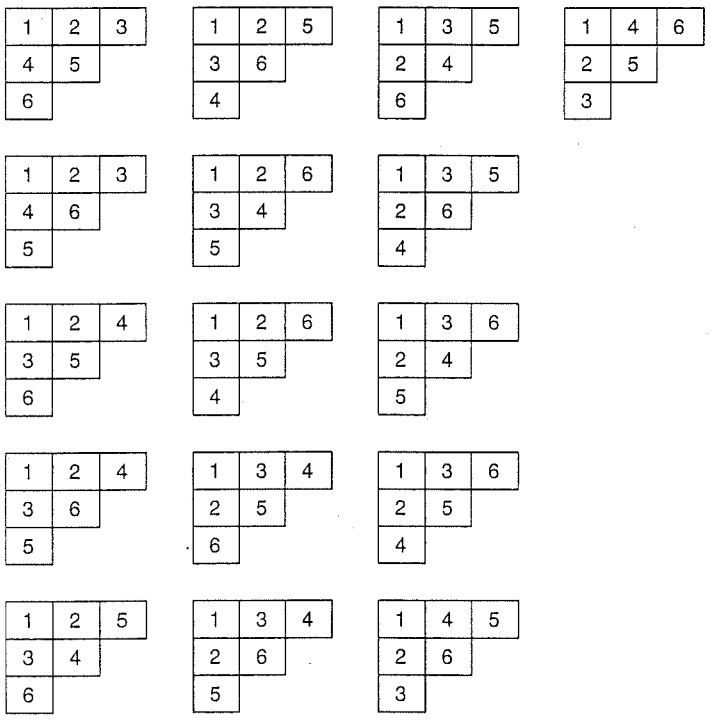

get8mats:: Generates all the representation matrices for S_8.

get9mats:: Generates all the representation matrices for S_9.

[C]=cycles(p,a):: For a permutation p, expressed in vector format, the cycle decomposition is generated in C. If a=1 the correct format for a cycle will also be printed to the screen.

[out]=difftab(T1,T2,a,b):: Checks if swapping the positions of the labels a and b in the tableau T1 generates the tableau T2.

[out]=fact(a,b):: Calculates factorials. Changing the second variable differentiates between $a!$ and $(a/2)!$ functions.

[string]=gen_str_mat(p,t):: Expresses the representation matrix for the permutation p and partition t in terms of transposition matrices. For example, the command, gen_str_mat([4 2 1 3 5],[3 2]) outputs the required decomposition as the string M32p42135=M32p14*M32p34.

[M]=genmat(p,k,L):: Given the irrep p, this program generates the matrix for the adjacent transposition (k,k+1). L is the set of permutations on (n-1) objects.

[weight]=hook(T,a,b):: Returns the hook length from a to b in the tableau T.

[out]=isin(a,T):: Checks if the label a appears in the tableau T.

[out]=isrepeat(T):: Checks if any element in the tableau T is repeated. Returns 1 if it is repeated, otherwise 0.

mat2tex(A,'file'):: Converts a matrix A into latex format in 'file'.tex. Overwrites existing file with the same name.

[sym]=YYsym(T):: Returns the standard Young-Yamanouchi symbol for a tableau T associated with permutations on n objects.

[R]=box_remove(T,l):: Given a tableau T and label l contained in T, this function returns the tableau R given by removing the box containing l from the tableau. *Jeu de taquin* is used where necessary to give the appropriate standard tableau. l can be larger than the number of boxes in the tableau, since some boxes may already have been removed.

[out]=checktab(T,p):: Checks if the tableau T is standard and without repeated values.

[L]=parts(n,m,X):: Returns the list of partitions of n. If the partitions of m are known and are listed in X, the program will use those partitions.

[L]=perm(n):: Returns the ordered list of permutations of length n on n objects.

[a,b,c,d]=simple(x):: Converts a number x into the form $\frac{a\sqrt{b}}{b\sqrt{d}}$, a common form for symmetric group matrix entries.

[n]=sizepart(p):: Checks the partition and returns the n of which the p is a partition.

[p,n]=sizetab(T):: Returns the particular partition p and n value for a tableau, without validating the tableau.

[N,l]=sorttabs(T,p,f):: Sorts the set of tableaux in T into an order based on the Young–Yamanouchi symbols. The set of ordered tableaux is returned in N, with l recording the list of associated Young–Yamanouchi symbols. The type of ordering is fixed by f, and includes last letter and first letter. The standard adopted by us is first letter, corresponding to f=2.

[X,Y]=tab2tab(T,a):: A size a for the first part of a split basis is entered along with a tableau T. The pair of tableaux obtained by removing the last n-a and first a is returned. Those tableaux label a basis vector in the $S_n \supset S_a \times S_{n-a}$ basis.

[T,count]=tableau(p,L):: Produces the set of standard tableaux, in standard order, for a given partition p. L is the set of permutations of n-1 objects.

tabout(T,p):: T can be a single tableau or a set of tableaux. With the partition p specified, a picture of the tableaux is produced.

E. OTHER PROJECTS

In my research I have brushed against other problems which I consider interesting. This appendix contains brief discussions on a number of areas requiring further study. I also include some details, in the first section, of an Honours project which I co–supervised with Dr. M. F. Reid.

E.1 Bipolar expansions.

The states of quantum mechanical systems are often known to have well defined angular momentum, that is well defined transformation properties with respect to the standard angular momentum (rotation) group SO_3. The matrix elements used to calculate the effect of interactions upon such states are easily calculated if the operator, or function describing the interaction, also has well defined angular momentum properties. Spherical harmonic operators have well defined angular momentum properties. Because the set of spherical harmonic operators provide an orthonormal basis for 3–space, functions (in 3–space) can be usefully expanded in terms of them. Then matrix elements of the function are written as a sum over matrix elements of spherical harmonic operators.

A well known example is the expansion of $1/r$, in terms of spherical harmonics. This is a physically relevant function, since it appears in, for example, the Coulomb interaction between electrons about a single centre. The expansion is,

$$r_{12}^{-1} = \sum_k (-1)^k \sqrt{\frac{(2k+1)!}{(2k)!}} \left(\frac{r_>^k}{r_<^{k+1}} \mathbf{C}_>^{(\mathbf{k})} . \mathbf{C}_<^{(\mathbf{k})} \right), \tag{E.1}$$

where we use $r_>$ and $r_<$ to denote the radial distance of the electrons farthest from and closest to the nuclei respectively.

Where one has many–atom molecules, expanding wavefunctions about a single centre may be clumsy, or unhelpful. Other methods become more useful. For example, it is often useful to study a diatomic molecular in bipolar coordinates, where we express the wavefunction as a sum over products of spherical harmonic functions centred on the two nuclei (see figure E.1).

Dr. Reid and I proposed a fourth year (honours) project, to investigate delta and exchange interactions using bipolar expansions. This project was carried out

by Jonathon Whittle in 1996 (Whittle 1996), and was misleadingly titled *Investigations with Bipolar Expansions into delta and exchange interactions.* Misleadingly, because although we aimed towards an investigation of the interactions, the project focused on the expansions themselves, which were found to require further study.

A major proportion of Jonathon's time was spent calculating bipolar expansions for functions of the form $r^{-j-1}\mathrm{C}^{(j)}$. Judd (1975) had previously calculated the expansion for non–overlapping wavefunctions, but we considered the general case, which additionally includes the partially and totally overlapping wavefunctions. We also carried out some bipolar expansions for the more general function $r_{12}^{(-j-1)}C_m^{(j)}$. Expansions of delta functions, useful for some correlation crystal field calculations (McAven, Reid & Butler 1996), were obtained.

E.1.1 Results

The polar expansion, equation (E.1), is separated into two regions by the greater than, less than conditions on the electron radii. Similarly the bipolar expansions are also divisible into distinct cases. The standard division of regions (Judd 1975) is presented in a Buehler–Hirschfelder diagram (see figure E.2). Judd described the solution in region I only.

We found that the solutions in regions II and II' could be expressed as one equation, using lesser than and greater than symbols as used in the polar expansion. The condition for the combined region then becomes,

$$r_{AB} + r_< < r_> \,, \tag{E.2}$$

where $r_<$ and $r_>$ are distinct r_{1A} and r_{2B}. Clearly the regions II and II' given in figure E.2 satisfy this condition. The expansion for those combined regions is then,

$$r_{12}^{-1} = \sum_k \sum_{l=k} (-1)^l \sqrt{\frac{(2l+1)!}{(2l-2k+1)!(2k)!}} \frac{r_<^k r_{AB}^{l-k}}{r_{1A}^{l+1}} (\mathrm{C}_>^{(l)} \mathrm{C}_<^{(k)})^{l-k} \cdot \mathrm{C}_{AB}^{(l-k)} \,. \tag{E.3}$$

Region III was more difficult however and a complete solution was not found. However we did show that the solutions holding in region II and II' also hold in parts of region III. A new description for the regions was introduced, in which they are taken to be dependent on the radial parameters. Region A was defined to be where the region I type solution holds; regions B and B' where region II and II' solutions hold respectively; and region C where neither A nor B/B' holds.

We observed numerically that regions II/II' and III sometimes overlap. Furthermore sometimes A and B/B' overlap. We developed some MATLAB scripts, which were used to confirm numerically our expansions. It was interesting to note

Fig. E.1: Electrons 1 and 2 with respect to centres A and B.

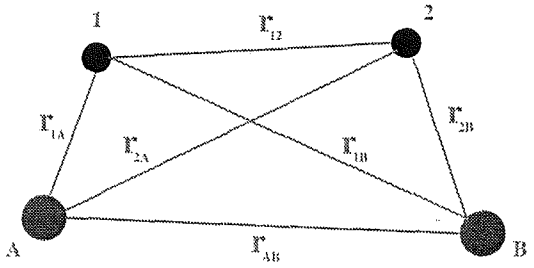

Fig. E.2: The Buehler–Hirschfelder diagram.

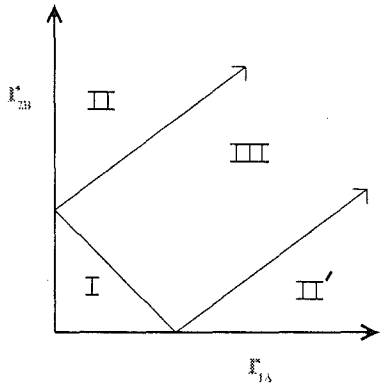

region I $r_{1A} + r_{2B} < r_{AB}$

region II $r_{AB} + r_{2B} < r_{1A}$

region II' $r_{AB} + r_{1A} < r_{2B}$

region III $|r_{1A} - r_{2B}| < r_{AB} < r_{1A} + r_{2B}$

Fig. E.3: Region I — non–overlapping wavefunctions.

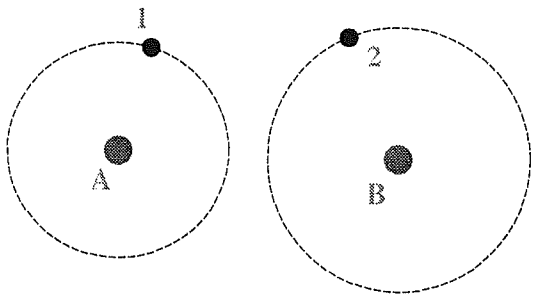

Fig. E.4: Region II and II' — completely overlapping wavefunctions.

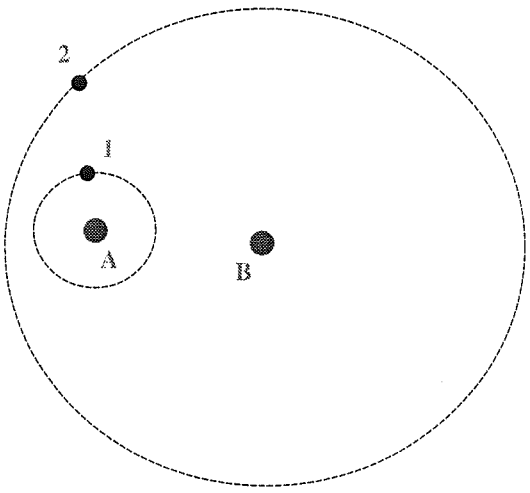

Fig. E.5: Region III — partially overlapping wavefunctions.

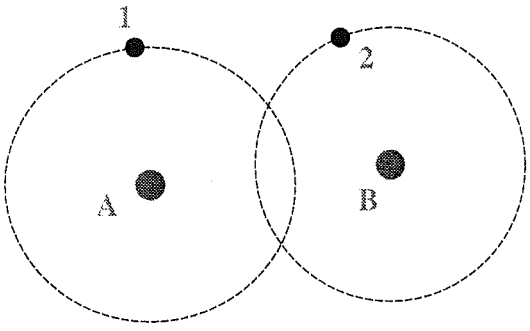

that when more than one solution appeared to give the correct result, one would generally converge faster. Perhaps the other solutions were only valid for a finite number of terms, before divergence. We did not have time to investigate intensively, but it is an issue which needs closer scrutiny.

We found that the expansions for the more general $r_{12}^{(-j-1)}C_m^{(j)}$ expansions also appeared to obey our modified Buehler–Hirschfelder diagram.

This project leaves several issues open for further research.

- ◇ Having obtained the bipolar expansions, one could use them in investigations of delta and exchange interactions.
- ◇ The solution for region C has not been obtained.
- ◇ The question remains as to whether the apparently overlapping solutions are actually both correct in some regions, and why one should be converging faster otherwise.
- ◇ Both the overlapping of regions, and the definition of regions, need to be considered in a physical manner, in addition to the mathematical approach taken above.

E.2 Hyperspherical harmonics

Originally, we proposed this problem, rather than the one discussed in the previous section. I reproduce the original proposal here, since the investigation is still to be carried out.

Investigations with hyperspherical harmonics into delta and exchange interactions in many–body systems

The most common approaches to the many particle Schrödinger equation involve the use of approximations, particularly the Born–Oppenheimer to separate the motion of nuclei from the motion of electrons, and the Hartree–Fock approximation which reduces a many–electron equation to a single–electron equation. Correlation effects are added by means of a configuration interaction calculation. But very large numbers of configurations are required to adequately describe the correlation effects.

Rather than making those approximations to the N particle Schrödinger equation, it is sometimes useful to try and solve it directly in a space of dimension $3N$. It is natural in trying to solve such a system that one should make use of hyperspherical harmonics, the generalisation of the familiar spherical harmonics in three dimensions.

First, it will be necessary to find or derive an expression for the d–dimensional delta function in terms of hyperspherical harmonics. Following this, the form of an exchange–type interaction should be investigated. Extensive use of harmonic polynomials, the Gegenbauer polynomials in particular, will be necessary. Work by Avery, Judd and others provides a basis for the necessary formalism.

References

- John Avery *Hyperspherical Harmonics*, 1989.
- John Avery in *Conceptual Trends in Quantum Chemistry*, under the heading *Hyperspherical Harmonics; some properties and applications*, 1994.
- Brian Judd *Angular momentum theory for diatomic molecules*, 1975.
- References listed in those books above, particularly the first two.

E.3 Reduction spectra via domino tableaux.

Assoc. Prof. P. H. Butler and I proposed this project in 1997 for the honours students. (No one took up the project.). I reproduce the proposal here.

Reduction spectra of fully paired symmetric tensors using domino tableaux

Irreducible tensors have been used for some time in the analysis of many physical systems (Jerphagnon, Chemla & Bonneville 1978). The number of independent components in a tensor may be catalogued according to rank, associated with the number of indices, and symmetries on those indices. Tensors can be decomposed into irreducible tensor parts with well defined angular momentum (SO_3) properties.

For example, a rank two tensor can be expressed as the sum of a symmetric tensor and an antisymmetric tensor. The antisymmetric part transforms as an object with angular momentum 1 (3 cpts), whereas the symmetric part contains components transforming as 2 and 0 (5+1 cpts).

We are particularly interested in what we shall call fully paired symmetric tensors. We write a general tensor as $T_{a_1 a_2 a_3 \cdots a_{2n}}$, and define a paired symmetric tensor to be invariant under the following exchange of indices,

$$a_i \leftrightarrow a_{i+1} \qquad \forall\, i \text{ odd} \tag{E.4}$$

$$(a_i a_{i+1}) \leftrightarrow (a_j a_{j+1}) \qquad \forall\, i, j \text{ odd} \tag{E.5}$$

so that the symmetry of the indices may be written as $((12)(34)(56)\ldots(2n-1)(2n))$.

Although it is possible to calculate the reduction spectra for those tensors of a given rank, and results for up to four have been given, there is no general formula. There is however a formula for reduction of tensors satisfying the first of the conditions (Mikhailov 1977). Those two tensor types are related by the plethysm operation (Wybourne 1970), which gives the different symmetry components of a product. When only (E.4) hold, we would consider the product $(2 \oplus 0)^{\otimes n}$ within SO_3, since it is the nth power of a fully symmetric rank two tensor. The fully symmetric part of this product satisfies equation (E.5) and corresponds to our fully paired symmetric tensors. The plethysm operation is complicated however.

Combinatorial techniques, notably those using tableaux, are providing increasingly significant insights into group theory, particularly of the very combinatorially accessible permutation groups (Hamel et al. 1996, McAven, Hamel & Butler 1998, McAven & Butler 1998). A recent advance (Carré & LeClerc 1995) makes use of domino tableaux to decompose particular squares into symmetric and antisymmetric components. Tableaux could provide a means for calculating the reduction spectra of tensors.

Although formulas exist for tensors of certain symmetries, in particular the type satisfying equation (E.4), we would like to be able to re–derive those formulas using tableaux methods. Having done this, we would like to use the concept of domino tableaux to extend those formulas to the fully paired symmetric tensors.

E.4 Double cosets and transformation coefficients

The transformation coefficients of symmetric and unitary groups are known to be linked by Schur–Weyl duality (Elliott, Hope & Jahn 1954, Kramer 1968, Vanagas 1971, Haase & Butler 1984*a*, Haase & Butler 1984*b*). During the 1970s, and early to mid 1980s, Sullivan attempted to calculate the symmetry and unitary group transformation coefficients by carrying out extensive investigations of the relationships between them. His approach depended heavily on the use of double cosets. Sullivan (1972, 1973a,b, 1975a,b, 1976, 1978a,b,c, 1980a,b, 1985). built on the work of Kramer (1967, 1968) and Kramer & Seligman (1969), who gave links between coefficients and the double coset matrix elements.

Although double cosets gain a mention in some modern group theory texts, the treatment tends to be very brief. Robinson (1996) fills half of page 12, Rotman (1995) relegates double cosets to an exercise for the reader (2.27, p.31), and Alperin & Bell (1995) also only lightly touches on them (p. 31). Robinson states, "There is a partition of the group into double cosets which is occasionally useful".

In spite of those sparse references, double cosets have been found to be useful in a number of fields. Ruch & Klein (1983) review the use of double cosets in chemistry and physics. They discuss (p.449) the use of double cosets, "as a mathematical tool suitable for a conceptual analysis of classifying structures". To date, the applications tend to have been chemical in nature, relating particularly to the classification of sterioisomers (Klein & Cowley 1978) and chemical reactions (McLarnan 1983). Double cosets have also been used to calculate $3jm$ for point groups (Zhang & Li 1986). This list is far from exhaustive but it the use of double cosets is certainly not widespread.

Double cosets were introduced by Frobenius (1887), as a generalisation of the common coset. Let G be a group, and H and K subgroups of G. H and K need not be distinct. Then the double coset of $g \in G$ with respect to H and K is defined as,

$$HgK = \{hgk : h \in H, k \in K, g \in G, \} \ . \tag{E.6}$$

This can be thought of as being similar to the right coset of H in the (left coset of K in G), or alternately as similar to the left coset of K in the (right coset of H in G). This is not rigorous however, since neither gK or Hg need be groups.

Sullivan was unable to obtain general solutions for the double coset matrix elements, and his work has largely gone uncited in the literature. Several techniques for calculating significant coefficients of S_n have since been developed (chapters 3, 4 and 5). It is therefore possible now to work backwards, using some of Kramer's and Sullivan's results, to obtain results for double coset matrix elements. This will improve understanding of the double cosets themselves and, more significantly, improve the understanding of the role they play in split and other non–standard symmetric group.

E.5 Non–trivially zero CFP's: calculation by multiplicity separation

Many group theoretical or related spectroscopic coefficients vanish without apparent reason. Much effort has been put into explaining those anomalies (Judd & Wadzinski 1967, Judd & Lister 1990, Judd & Lister 1991, Van der Jeugt 1992, Judd & Lister 1993*a*, Judd & Lister 1993*b*, Raynal et al. 1993, Vanden Berghe 1994). Biedenharn & Louck (1981, Topic 10) also make a systematic study of non–trivial zeros in $3jm$ and $6j$ zeros. In obtaining results about the vanishing coefficients, a variety of techniques are employed. The zeros can be related to roots of special polynomials, and hypergeometric series are often seen to be relevant. Judd's quarklike structure provides useful selection rules, but doesn't appear to explain everything. A unifying structure would certainly be helpful.

For a specific case I propose the following line of reasoning.

We know that f–shell coefficients of fractional parentage (cfps) can be written as a sum over products of $3jm$ between adjacent groups in the chain $U_{14} \supset Sp_{14} \supset SU_2^S \times \{SO_7 \supset G_2 \supset SO_3^L\}$. However, are the cfps independent of the choices of $6j$ at the group levels between U_{14} and $SO(3)$?

If they are independent, as I suspect they must be, then the cfps must presumably be consistent with any valid $6j$ choices for those intermediate groups. Thus the values of terms in each sum of products representing a cfp might be different, although the result must be the same of course. Some of the choices might make it clear that a particular cfp must vanish, because a $3jm$ upon which it depends can be chosen, via the $6j$, to be zero, for example. Similarly, where two cfps are the same, it might be possible to see this more clearly by choosing a different primitive $6j$ set.

It may be that this approach could also provide insight into the vanishing of other matrix elements.

E.6 More for RACAH

Shinagawa has proposed a number of other problems which need analysis of the type performed in chapters 7 and 8.

I quote Shinagawa's comments on those problems.

> A new problem is to clarify the magneto–optical properties of Bi–substituted magnetic garnets. These garnets show very large Faraday rotation in the visible wavelength region and have been used as optical isolators, magnetic sensors, etc. However, the mechanism of the large Faraday rotation has not been clarified yet. I think that the charge transfer transitions of t_{1u}^n to t_{2g}^* and t_{2u}^n to t_{2g}^* for an octahedral Fe^{3+}–O cluster, and t_1^n to e^* and t_2^n to e^* for a tetrahedral Fe^{3+}–O one should be responsible for the large Faraday rotation, as shown in our work on the $CrBr_3$. The reason is that the spin–orbit constant of a 6p electron is known to be larger than that of a 2p electron by an order of magnitude, so the spin–orbit constant of 2p electrons are effectively enhanced by the mixing of 6p orbitals of Bi ions incorporated in the dodecahedral sites (Y^{3+} sites in YIG). So, the work we have to do is to calculate the spin–orbit constants of the excited $[t_{2g}^{*4}e_g^{*2}](t_{1u}^5$ or $t_{2u}^5)^2\ {}^6T_{1g}$ and $[t_2^{*3}e^{*3}](t_1^5$ or $t_2^5)\ {}^6T_2$ states. I have calculated those by hand as shown in separate notes following the Piepho and Schatz's "Group Theory in Spectroscopy". So, I would like to check the results with RACAH.
>
> In addition, another problem is to clarify the magneto–optical properties of Co^{2+}–substituted magnetic garnets. In this case, a large Faraday rotation was observed in the near infrared region. It has been known that this rotation originates from ${}^4A_2$ to ${}^4T_1$ crystal field transition in Co^{2+} at the tetrahedral sites. To clarify the mechanism, we also have to calculate the spin–orbit constants of the $(t_2^4e^3)^4T_1$ and $(t_2^5e^2)^4T_1$ excited states. I have calculated those constants by hand as shown in separate notes. These constants have been calculated by Professor Tanabe in Suppl. Prog. Theor. Phys. 14 (1960) 17. However, the sign of the nondiagonal matrix element is different from my result. So, I would like to check the sign with RACAH.

Those problems should provide a good test for RACAH version 4.

E.7 The theory of transformation coefficients

We can reformulate the Racah-Wigner algebra, from irreducible representations up, in terms of transformation coefficients. Symmetrised coefficients, such as $3jm$ and $6j$, are related to their counterparts, vector coupling (vcc) and recoupling coefficients (rcc) respectively. The Biedenharn-Elliott Sum Rule (BES), the Wigner relation, Racah-Back Coupling (RBC) and Orthonormality, can be similarly reformulated. We can prove that simply defined sets of vccs and rccs are trivial.

This braket formalism is built into the new RACAH. Although we have made considerable advances on the algorithmic structure and recursion formalism we have yet to write up this work. This work is to be completed in 1998, in a continuing collaboration with Dr. Searle, Dr. Ross and Assoc.Prof. Butler. The motivation for the work essentially lies in the work of Ross (1997).

There are many interesting questions still to be answered in this project.

E.8 A new SU_2 $6j$ identity?

Early to mid 1996 I was in contact with Professor Lionel Bréhamet of the Centre d'Etudes Nucléaires de Saclay, France. In particular, he asked me to read a preprint of his, with the working title: *How any $SU(2)$ tensor operator commutes with the iterated–angular–momenta reveals and unknown $6j$ identity exchanging spins.*[1]

Of particular interest to Bréhamet was an SU_2 $6j$ identity which appeared distinct from others identities, such as the Biedenharn–Elliott sum rule. Unsure of this distinction however, he asked if I could derive the formula using known identities.

The form of the identity is improved if one defines w–$6j$,

$$\left\{ \begin{array}{ccc} j_1 & j_2 & j_3 \\ j_4 & j_5 & j_6 \end{array} \right\} = \Delta(j_1 j_2 j_3)\Delta(j_1 j_5 j_6)\Delta(j_4 j_2 j_6)\Delta(j_4 j_5 j_3) \tag{E.7}$$

$$\times \left\{ \begin{array}{ccc} j_1 & j_2 & j_3 \\ j_4 & j_5 & j_6 \end{array} \right\}_w , \tag{E.8}$$

where

$$\Delta(j_1 j_2 j_3) = \left[\frac{(j_1 + j_2 - j_3)!(j_1 - j_2 + j_3)!(-j_1 + j_2 + j_3)!}{(j_1 + j_2 + j_3 + 1)!} \right]^{1/2} . \tag{E.9}$$

The identity is then

$$\frac{t!(j_1 + j_3 - t)!}{(j_1 + j_3 + t + 1)!} \left\{ \begin{array}{ccc} j_1 & t & j_3 \\ j & j' & j \end{array} \right\}_w \tag{E.10}$$

$$(-1)^{t+j_1-j_3} \sum_{m=|j_1-j_3|}^{m=\inf(t,2j')} \frac{m!(j_1 + j_3 - m)!}{(t-m)!(j_1 + j_3 + m + 1)!} \left\{ \begin{array}{ccc} j_1 & m & j_3 \\ j' & j & j' \end{array} \right\}_w .$$

While unable to derive this result by means other than that provided in the preprint, I confirmed the result numerically for spin values up to 10. In investigating this identity, I found many related $6j$ identities which may be more accessible to independent derivations. In addition to making further attempts at deriving this formula it would be helpful to test its applicability to other groups, specifically point groups. The technique used in the derivation of Bréhamet suggests it may well be isolated to SU_2 $6j$, probably with generalisations to SU_n $6j$.

[1] *How an $SU(2)$ tensor operator commuting with the iterated–angular–momenta reveals an unknown $6j$ identity exchanging spins*

E.9 Generating representations of S_n

As we discussed in section 3.2, there are various common representations of the symmetric groups. Wu & Zhang (1994) point out that "the evaluation of the orthogonal representation is a bottleneck in the SGA[2] and the UGA[3]". Wu & Zhang (1994) improve upon previous approaches with a technique which is equally efficient for arbitrary permutations, as it is for adjacent transpositions, which is the only one directly accessible to the approach of Hamermesh (1962). This improved technique is also applicable to deriving representation matrices for the normal and semi–normal representations.

Other techniques have been developed independently over the last few years (Sarma, Ahsan & Rettrup 1996, Rettrup & Pauncz 1996). Those improve upon a useful technique proposed by Rettrup (1986) for particular coupling schemes. They generate the natural representations of S_n using spin eigenfunctions, obtained with the aid of projection operators. This graphical technique is closely tied to the analysis of many–particle systems.

Other research, by Garsia & McLarnan (1988), has concentrated on transformations between the natural and Kazhdan–Lusztig representations of S_n. In this work, they have given a combinatorial recipe for generating the natural representations of S_n. This recipe appears to be similar, if not identical, to that of Wu & Zhang (1994), although no reference is given within. More interestingly there are therefore at least two techniques for calculating the normal representation matrices. The approaches of Garsia & McLarnan (1988) and Wu & Zhang (1994) appear much simpler, and could be used to improve the understanding of the spin functions used by Rettrup (1986) and others.

If nothing else, further investigation of the equivalence or correlation between the different approaches is needed. Even if Wu & Zhang (1994) and Garsia & McLarnan (1988) are identical, the language is different and an interpretation of the distinctions would prove useful. Either way, one would expect that the derivations by Wu & Zhang (1994) of the orthogonal, natural and semi–normal representations could be given a rigorous combinatorial structure.

[2] Symmetric Group Approach
[3] Unitary Group Approach

F. GLOSSARY

We list here a few notational definitions.

$\forall i$	for all i		§2.1
$g \in G$	g is an element of G		§2.1
$H \subset G$	H is a subgroup of G		§2.1
$G \supset H$	H is a subgroup of G		§2.1
$G \sim H$	G and H are isomorphic		§2.1
$G \rightarrow H$	G is homomorphic to H		§2.1
δ_{ij}	Kronecker delta	$\delta_{ij} = \begin{cases} 1 & \text{if } i = j, \\ 0 & \text{otherwise.} \end{cases}$	
$0_n \equiv 0$	$n \times n$ Zero matrix	$\{0_n\}_{ij} = 0$	
$I_n \equiv 1$	$n \times n$ Identity matrix	$\{I_n\}_{ij} = \delta_{ij}$	
†	Hermitian conjugate	$A^\dagger = (A^t)^*$	
*	Complex conjugation	$(a + ib)^* = (a - ib)$	
^{t}	Transpose	$\{A^t\}_{ij} = A_{ji}$	
σ_i	Generator of S_n	$\sigma_i = (i, i+1)$	§3.1
O_n	Orthogonal group		§6.2
S_n	Symmetric group		§3.1
Sp_{2n}	Symplectic group		§6.2
U_n	Unitary group		§6.2
$\dim(A)$	Dimension of A		
irrep	Irreducible representation		§2.3
orthogonal	$OO^t = 1$		
rep	representation		§2.3
unitary	$UU^\dagger = 1$		
$\otimes$	outer product		5.1

The spectroscopic notation for the angular momentum l values is,

$$\begin{array}{cccccccccc} l = & 0 & 1 & 2 & 3 & 4 & 5 & 6 & 7 & \ldots \\ & s & p & d & f & g & h & i & k & \ldots . \end{array} \tag{F.1}$$

The first four labels arise from the nature of observations on the spectral emissions from electrons in those orbitals (Whitten, Gailey & Davis 1988). Late in the nineteenth century, Rydberg (Sternberg 1994, p.397) distinguished series associated with the first three: sharp, principle, and diffuse. The lines of the principle series were seen mostly in the ultra–violet, but the name comes from the first li-

nes, which are usually the most intense in the visible region. In 1908 Bergmann introduced a fourth series, the fundamental, usually in the infrared.

BIBLIOGRAPHY

Abe, M. & M. Gomi. 1990. "??" *J. Magn. Mat.* 84:222.

Abel, N. H. 1826. "Démonstration de l'impossibilité de la résolution algébrique des équations générales qui passent le quatriéme degré." *J.reine angew.Math.* 1:65–84.

Alperin, J. L. & Rowen B. Bell. 1995. *Groups and Representations*. Number 162 *in* "Graduate texts in mathematics" Springer.

Antoci, S. & L. Mihich. 1978. "Determination of the self–consistent band structure of $CrCl_3$, $CrBr_3$, $NiCl_2$ and $NiBr_2$ by the intersecting–spheres model." *Physical Review B* 18(10):5768–5774.

Argyres, Petros N. 1955. "Theory of the Faraday and Kerr effects in ferromagnetism." *Physical Review* 97:334–345.

Ballhausen, C. J. & H. B. Gray. 1964. *Molecular Orbital Theory*. New York: W A Benjamin.

Beck, Bleicher & Crowe. 1969. *Excursions into Mathematics*. New York: Worth Publishers.

ben Gershon, Levi. 1321. "Maaser Hoshev.".

Bergdolt, G. 1995. "Tilted irreducible representations of the symmetric group." *Computer Physics Communications* 86:97–104.

Bermudez, V. M. & D. S. McClure. 1979*a*. "Spectroscopic studies of the two–dimensional magnetic insulators chromium trichloride and chromium tribromide–I." *J.Phys. Chem. Solids* 40:129–147.

Bermudez, V. M. & D. S. McClure. 1979*b*. "Spectroscopic studies of the two–dimensional magnetic insulators chromium trichloride and chromium tribromide–II." *J.Phys. Chem. Solids* 40:149–173.

Bethe, H. A. 1929. "Term separation in crystals." *Ann.Physik* 3(2):133–208.

Bickerstaff, R. Paul, Philip H. Butler, M. B. Butts, Richard W. Haase & Michael F. Reid. 1982. "$3jm$ and $6j$ tables for some bases of SU_6 and SU_3." *J.Phys.A:Math. Gen.* 15:1087–117.

Biedenharn, L. C. & H. van Dam, eds. 1965. *Quantum Theory of Angular Momentum.* New York: Academic Press.

Biedenharn, L. C. & J. D. Louck. 1981. *The Racah–Wigner Algebra in Quantum Theory.* Vol. 9 of *Encyclopedia of mathematics and its applications* United States of America: Addison–Wesley.

Burdick, Gary W., C. K. Jayasankar, F. S. Richardson & Michael F. Reid. 1994. "Energy–level and line–strength analysis of optical transitions between Stark levels in Nd^{3+} : $Y_3Al_5O_{12}$." *Physical Review* 50(22):16309–16325.

Butler, Philip H. 1975. "Coupling coefficients and tensor operators for chains of groups." *Philos. Trans. R. Soc. London* 277:545–585.

Butler, Philip H. 1976. "Calculation of j and jm symbols for arbitrary groups II. An alternate procedure for angular momentum." *Int. J. Quantum Chem.* X:599–613.

Butler, Philip H. 1981. *Point Group Symmetry Applications : Methods and Tables.* New York: Plenum Press.

Butler, Philip H. & A. M. Ford. 1979. "Special symmetries of jm and j symbols." *J.Phys.A:Math. Gen.* 12:1357–1365.

Butler, Philip H., A. M. Ford & Michael F. Reid. 1983. "Symmetry–adapted functions: molecular vibrations." *J. Phys. B* 16:967–974.

Butler, Philip H. & Associates. 1995. "The program RACAH v3.1.". Department of Physics and Astronomy, University of Canterbury, New Zealand.

Butler, Philip H. & Brian G. Wybourne. 1976. "Calculation of j and jm symbols for arbitrary groups I. Methodology." *Int. J. Quantum Chem.* X:581–598.

Butler, Philip H. & Hughan J. Ross. 1990. The Racah–Wigner technology, How do you calculate what you need? In *Symmetry and Structural Properties of Condensed Matter*, ed. W. Florek, T. Lulek & M. Mucha. Singapore: World Scientific pp. 192–206.

Cardano, G. 1545. "Ars Magna.".

Carré, Christophe & Bernard LeClerc. 1995. "Splitting the square of a Schur function into its symmetric and antisymmetric parts." *Journal of Algebraic Combinatorics* 4:201–231.

Carricaburu, B., J. Ferre, R. Mamy, I. Pollini & J. Thomas. 1986. "Optical and electron energy loss experiments in ionic $CrCl_3$ crystals." *J.Phys.C:Solid State Phys.* 19:4985–4997.

Cartan, E. J. 1894. Sue la Structure des Groupes de Transformations Finis et Continus PhD thesis Faculté des sciences de Paris.

Cassels, J. M. 1982. *Basic Quantum Mechanics.* Second ed. Macmillan Press.

Chen, Jin-Quan, D. F. Collinson & Mei-Juan Gao. 1983. "Transformation coefficients of symmetric groups." *J.Math.Phys.* 24(12):2695–2705.

Chen, Jin-Quan & Mei-Juan Gao. 1982. "A new approach to permutation group representation." *J.Math.Phys.* 23(6):928–943.

Cobb, C. G., V. Jaccarino, J. P. Remeika, R. Silberglitt & H. Yasuoka. 1971. "Field dependence of the magnetisation and spin–wave correlations in ferromagnetic $CrBr_3$." *Physical Review B* 3:1677–1688.

Coleman, A. John. 1997. "Groups and Physics – Dogmatic opinions of a senior citizen." *Notices of the American Mathematical Society* 44(1):8–17.

Condon, E. U. & G. H. Shortley. 1935. *The Theory of Atomic Spectra.* Cambridge: Cambridge University Press.

Condon, E. U. & G. H. Shortley. 1967. *The Theory of Atomic Spectra.* Cambridge: Cambridge University Press.

Condon, E. U. & H. Ödabaşi. 1980. *Atomic Structure.* Cambridge University Press.

Cornwell, J. F. 1984. *Group Theory in Physics.* Vol. 1–2 London: Academic.

Davis, H. L. & A. Narath. 1964. "Spin–wave renormalization applied to ferromagnetic $CrBr_3$." *Physical Review* 134(2A):A433–A441.

Derome, J-R. & W. T. Sharp. 1965. "Racah algebra for an arbitrary group." *J.Math.Phys.* 6:1584–1590.

Derome, Jean-Robert. 1966. "Symmetry Properties of the 3j-Symbols for an Arbitrary Group." *Journal of Mathematical Physics* 7(4):612–615.

Descartes, Renè. 1637. "La Gèomètrie.". English translation: *The Geometry*, Dover, New York, 1954.

Dillon, J. F. 1990. "??" *J. Magn. Mat.* 84:213.

Dillon, J. F., H. Kamimura & J. P. Remeika. 1966. "Magneto–optical properties of ferromagnetic chromium trihalides." *J.Phys.Chem.Solids* 27:1531–1549.

Edmonds, A. R. 1965. *Angular Momentum in Quantum Mechanics.* Princeton: Princeton University Press.

Elliott, J. P., J. Hope & H. A. Jahn. 1954. "Theoretical studies in nuclear structure IV. Wave functions for the nuclear p–shell; Part B $\langle p^n | p^{n-2} p^2 \rangle$ fractional parentage coefficients." *Phil.Trans.R.Soc. A* 246:241–279.

Elliott, J. P. & P. G. Dawber. 1979*a*. *Symmetry in Physics: Further Applications.* Vol. 2 Macmillan Press.

Elliott, J. P. & P. G. Dawber. 1979*b*. *Symmetry in Physics: Principles and Simple Applications.* Vol. 1 Macmillan Press.

Fano, U. & G. Racah. 1959. *Irreducible Tensorial Sets.* New York: Academic.

Frobenius, G. F. 1887. "??" *J.reine angew.Math.* 101:273.

Galois, Evariste. 1846. "Œuvres mathématiques d'Évariste Galois." *Journal de mathématiques pures et appliquées* 11:381–444.

Garsia, A.M. & T.J. McLarnan. 1988. "Relations between Young's natural and the Kazhdan–Lusztig representations of S_n." *Advances in Mathematics* 69:32–92.

Goudsmit, S. & R. F. Bacher. 1934. "Atomic Energy Relations. I." *Phys.Rev* 46:948–969.

Griffith, J. S. 1962. *The Irreducible Tensor Method for Molecular Symmetry.* Englewood Cliffs, NJ: Wesley.

Guizetti, G., L. Nosenzo, I. Pollini, E. Reguzzoni, G. Samoggia & G. Spinolo. 1976. "Reflectance and themoreflectance studies of $CrCl_3$, $CrBr_3$, $NiCl_2$ and $NiBr_2$ crystals." *Physical Review B* 14(10):4622–4629.

Haase, Richard W. & Philip H. Butler. 1984*a*. "Coupling, subduction and induction transformations for group representations." *J.Phys.A:Math. Gen.* 17:47–59.

Haase, Richard W. & Philip H. Butler. 1984*b*. "Symmetric and Unitary group representations: I. Duality Theory." *J.Phys.A:Math. Gen.* 17:61–74.

Haase, Richard W. & Philip H. Butler. 1985. "Algebraic formulas for some non–trivial U_n $6j$ symbols and $U_{mn} \supset U_m \times U_n$ $3jm$ symbols." *J. Math. Phys.* 26:1493–1510.

Hamel, A. M., L. F. McAven, H. J. Ross & P. H. Butler. 1996. "Transformations between Young–Yamanouchi and dual bases of the symmetric group." *J.Phys.A:Math.Gen.* 29(18):5935–5944.

Hamermesh, M. 1962. *Group Theory and Its Application to Physical Problems.* Addison–Wesley Series in Physics Reading, Massachusetts: Addison–Wesley.

Harrison, Walter A. 1980. *Electronic Structure and the Properties of Solids: The Physics of the Chemical Bond.* United States of America: W H Freeman and Company.

Haüe, R-J. 1784. "Essai d'une théorie sur la structure des cristaux." Paris.

Haüe, R-J. 1822. "Traité de Crystallographie." three volumes, Paris.

Horie, H. 1964. "Representations of the symmetric group and the fractional parentage coefficients." *Journal of the Physical Society of Japan* 19(10):1783–1799.

Jahn, H. A. 1954. "Direct evaluation of fractional parentage coefficients using Young operators. General theory and $\langle 4|2,2\rangle$ coefficients." *Phys.Rev.* 96(4):989–995.

Janssen, T. 1973. *Crystallographic Groups.* Amsterdam: North–Holland Publishing Company.

Jerphagnon, J., D. Chemla & R. Bonneville. 1978. "The description of the physical properties of condensed matter using irreducible tensors." *Advances in Physics* 27(4):609–650.

Johnson, K. H. & F. C. Smith. 1972. "Chemical bonding of a molecular transition–metal ion in a crystalline environment." *Phys. Rev. B* 5:831–843.

Judd, Brian R. 1963. *Operator Techniques in Atomic Spectroscopy.* United States of America: McGraw–Hill Book Company.

Judd, Brian R. 1975. *Angular Momentum Theory for Diatomic Molecules.* New York: Academic Press.

Judd, Brian R. 1977. "Ligand field theory for actinides." *The Journal of Chemical Physics* 66(7):3163–3170.

Judd, Brian R. 1978. *Ligand polarizations and lanthanide ion spectra.* Vol. 79 of *Lecture Notes in Physics* Berlin: Springer–Verlag pp. 417–419.

Judd, Brian R. & G. M. S. Lister. 1984. "Laporte–Platt degeneracies and delta–function interactions." *J.Phys.B:At.Mol.Phys.* 17:3637–3643.

Judd, Brian R. & G. M. S. Lister. 1990. "Unexpected relations between spectroscopic coefficients for f electrons." *J.Phys.B:At.Mol.Opt.Phys.* 23:1733–1747.

Judd, Brian R. & G. M. S. Lister. 1991. "Selection rules in the atomic f shell from quarklike substructures." *Physical Review Letters* 67(13):1720–1722.

Judd, Brian R. & G. M. S. Lister. 1993*a*. "Relating Slater–Racah bases to a quark–like formalism for the atomic f shell." *J.Phys.B:At. Mol. Opt. Phys.* 26:193–203.

Judd, Brian R. & G. M. S. Lister. 1993*b*. "Selection rules for some three–electron operators in the atomic f shell." *J.Phys.B:At. Mol. Opt. Phys.* 26:3177–3188.

Judd, Brian R. & H. T. Wadzinski. 1967. "A class of null spectroscopic coefficients." *Journal of Mathematical Physics* 8(10):2125–2130.

Jung, Wun. 1965. "Dielectric constant and magneto–optical Kerr rotation of ferromagnetic chromium tribromide above the absorption band edge." *Journal of Applied Physics* 36(8):2422–2426.

Kaplan, Il'iâ Grigor'evich. 1961. "The transformation matrix for the permutation group and the construction of coordinate wave functions for a multishell configuration." *Zh.Eksp.Teor.Fiz.* 41:560. [*Sov. Phys. JETP* **14** (1962) 401–407].

Kaplan, Il'iâ Grigor'evich. 1975. *Symmetry of Many–Electron Systems*. Vol. 34 of *Physical Chemistry* Academic Press. Translated by H. Gerratt from the Russian version of 1969.

Kittel, C. 1986. *Introduction to Solid State Physics*. Sixth ed. John Wiley and Sons.

Klein, D. J. & A. H. Cowley. 1978. "Permutational isomerism with bidentate ligands and other constraints." *J.Am.Chem.Soc.* 100:2593–2599.

Knuth, Donald E. 1973. *The Art of Computer Programming*. Addison–Wesley Series: in Computer Science and Information Processing Addison–Wesley Publishing Company sections 5.1.4–5.2 pp. 48–73.

Kooy, H. J. 1994. Two–body Operators in Rare Earth Spectroscopy. PhD thesis University of Hong Kong.

Kooy, H. J. & Mike. F. Reid. 1993. "Two–body operators for the f shell." *J. Alloys and Compounds* 193:197–202.

Kramer, P. 1967. "Orbital fractional parentage coefficients for the harmonic oscillator shell model." *Zeitschrift für Physik* 205:181–198.

Kramer, P. 1968. "Recoupling coefficients of the symmetric group for shell and cluster model configurations." *Zeitschrift für Physik* 216:68–83.

Kramer, P. & T. H. Seligman. 1969. "Studies in the nuclear cluster model. (II). Two–cluster configurations." *Nuclear Physics* A136:545–563.

Kukulin, V. I., Yu. F. Smirnov & L. Majling. 1967. "??" *Nucl.Phys.A* 103:681.

Lagrange, J. L. 1771. "Réflexions sur la résolution algébrique des équations." *Nouv.Mém.Acad.Berlin* .

Larsson, S. & J. W. D. Connolly. 1974. "??" *J.Chem.Phys.* 60:1514.

Li, C. L. & Michael F. Reid. 1990. "Correlation–crystal–field analysis of the $^2H(2)_{11/2}$ multiplet of Nd^{3+}." *Phys.Rev.B* 42(4):1903–1909.

Littlewood, D. E. & A. R. Richardson. 1934. "Group characters and algebra." *Phil. Trans. A* 233:99–141.

Lo, T. S. 1993. Two–body Operators and Correlation Crystal Field Models. Master's thesis University of Hong Kong.

Lo, T. S. & Michael F. Reid. 1993. "Group–theoretical analysis of correlation crystal–field models." *J. Alloys and Compounds* 193:180–182.

Lützen, J. 1982. *The Prehistory of the Theory of Distributions.* Vol. 7 of *Studies in the History of Mathematics and Physical Sciences* New York: Springer–Verlag.

Macdonald, Ian Grant. 1979. *Symmetric Functions and Hall Polynomials.* Clarendon Press, Oxford University Press.

Mattheiss, L. F. 1969. "Band structure and Fermi surface of ReO_3." *Physical Review* 181:987–1000.

McAven, L. F., A. M. Hamel & P. H. Butler. 1998. "Multiplicity separation in symmetric group transformation coefficients.". Submitted for refereeing.

McAven, L. F. & P. H. Butler. 1998. "Split–standard transformation coefficients: The block selective conjecture.". Nearing completion.

McAven, Luke F., Hughan J. Ross, Kiminari Shinagawa & Philip H. Butler. 1998. "The Kerr magneto–optic effect in ferromagnetic $CrBr_3$ and $CrCl_3$.". To be submitted.

McAven, Luke F., Michael F. Reid & Philip H. Butler. 1996. "Transformation properties of the delta function model of correlation crystal fields." *J.Phys.B:At.Mol.Opt.Phys.* 29(8):1421–1431.

McClure, D. S. 1959. *Electronic Spectra of Molecules and Ions in Crystals.* Vol. 8—9 of *Solid State Reprints edited by F Seitz and D Turnball* New York: Academic Press.

McLarnan, T. J. 1983. "The enumeration of reaction pathways using Burnside's Lemma." *Theoret.Chim.Acta* 63:195–207.

Mikhailov, V. V. 1977. "Addition of arbitrary number of identical angular momenta." *J.Phys.A:Math.Gen.* 10(2):147–153.

Mirman, R. 1987*a*. "Expansion of symmetric group products and states." *Can.J.Phys.* 65:185–192.

Mirman, R. 1987*b*. "Tensors of symmetric and unitary groups." *Can.J.Phys.* 65:193–197.

Mirman, R. 1995*a*. *Group Theoretical Foundations of Quantum Mechanics.* Nova Science Publishers, Inc.

Mirman, R. 1995*b*. *Group Theory: An Intuitive Approach.* Nova Science Publishers, Inc.

Nosenzo, L., G. Samoggia & I. Pollini. 1984. "Effect of magnetic ordering on the optical properties of transition–metal halides: $NiCl_2$, $NiBr_2$, $CrCl_3$, $CrBr_3$." *Physical Review B* 29(6):3607–3616.

Nowick, Arthur S. 1995. *Crystal Properties Via Group Theory.* Cambridge: Cambridge University Press.

Ogilvie, J. F. 1994. The Nature of the Chemical Bond 1993: There are no such things as orbitals! In *Conceptual Trends in Quantum Chemistry*, ed. E. S. Kryachko & J. L. Calais. Kluwer Academic Publishers.

Osborne, M. R. 1985. *Finite Algorithms in Optimization and Data Analysis.* Wiley Series in Probability and Mathematical Statistics John Wiley & Sons.

Pan, Feng & Jin-Quan Chen. 1993. "Irreducible representations of Hecke algebras in the non–standard basis and subduction coefficients." *J.Phys.A:Math. Gen.* 26:4299–4310.

Perkins, P. G. & J. J. P. Stewart. 1980. "Cluster model for solids." *J.Chem.Soc.Faraday II* 76:520—533.

Pickover, Clifford A. 1997. *The Loom of God: Mathematical Tapestries at the Edge of Time.* Plenum Press.

Piepho, Susan B. & Paul N. Schatz. 1983. *Group Theory in Spectroscopy : With Applications to Magnetic Circular Dichroism.* Wiley–Interscience Monographs in Chemical Physics Wiley–Interscience.

Pierloot, K. & L. G. Vanquickenbourne. 1990. "The ligand field spectrum of the hexaflurochromate(III) anion: An *ab initio* study including correlation effects." *J.Chem.Phys.* 93(6):4154–4163.

Pollini, I., J. Thomas, B. Carricaburu & R. Mamy. 1989. "Optical and electron energy loss experiments in ionic $CrBr_3$ crystals." *J.Phys.:Condens.Matter* 1:7695–7704.

Racah, G. 1942*a*. "Theory of Complex Spectra. I." *Physical Review* 61:186–197. Reprinted in Biedenharn & van Dam (1965, pp. 134–145).

Racah, G. 1942*b*. "Theory of Complex Spectra. II." *Physical Review* 62:438–462. Reprinted in Biedenharn & van Dam (1965, pp. 146–170).

Racah, G. 1943. "Theory of Complex Spectra. III." *Physical Review* 63(9 and 10):367–382. Reprinted in Biedenharn & van Dam (1965, pp. 171–186).

Racah, G. 1949. "Theory of Complex Spectra. IV." *Physical Review* 76(9):1352–1365. Reprinted in Biedenharn & van Dam (1965, pp. 187–200).

Raynal, Jacques, J. Van der Jeugt, K. Srinivasa Rao & V. Rajeswari. 1993. "On the zeros of $3j$ coefficients: polynomial degree versus recurrence order." *J.Phys.A:Math.Gen.* 26:2607–2623.

Reid, Michael F. 1987. "Correlation crystal field analyses with orthogonal operators." *J.Chem.Phys.* 87(5):2875–2884.

Rettrup, Sten. 1986. "Direct evaluation of spin representation matrices and ordering or permutation–group elements." *International Journal of Quantum Chemistry* XXIX:119–128.

Rettrup, Sten & Ruben Pauncz. 1996. "Representations of the symmetric group generated by projected spin functions: A graphical approach." *International Journal of Quantum Chemistry* 60:91–98.

Robinson, Derek J.S. 1996. *A Course in the Theory of Groups.* Number 80 *in* "Graduate Texts in Mathematics" second ed. Berlin: Springer–Verlag.

Robinson, G. de B. 1938. "On the representations of S_n, I." *Amer.J.Math.* 60:745–760.

Rosen, Joe. 1995. *Symmetry in Science.* Springer–Verlag.

Ross, H. J. 1994. Private communication.

Ross, Hughan J. 1997. The Racah–Wigner Calculus PhD thesis Department of Physics and Astronomy, University of Canterbury.

Ross, Hughan J., Luke F. McAven, Kiminari Shinagawa & Philip H. Butler. 1996. "Calculating spin–orbit matrix–elements with RACAH." *J.Comp.Phys.* 128(2):331–340.

Rotman, Joseph J. 1995. *An Introduction to the Theory of Groups.* Number 148 *in* "Graduate texts in mathematics" fourth ed. Springer-Verlag.

Ruch, Ernst & Douglas J. Klein. 1983. "Double cosets in chemistry and physics." *Theoret.Chim.Acta* 63:447–472.

Ruffini, P. 1799. *"Teoria generale delle quazioni in cui si dimostra impossibile la soluzione algebraica delle equazioni generali di grade superiore al quarto.".*

Rutherford, D. E. 1948. *Substitutional Analysis.* Edinburgh University Press.

Sarma, C. R. 1981. "Permutation group and interacting subsystems of particles." *J.Phys.A:Math. and Gen.* 14:565–573.

Sarma, C. R., M. A. H. Ahsan & Sten Rettrup. 1996. "A graphical approach to permutation group representations for many–electron systems." *International Journal of Quantum Chemistry* 58:637–643.

Schützenbeger, M P. 1963. "Quelques remarques sur une construction de Schensted." *Math Scand.* 12:117–128.

Schützenbeger, M. P. 1977. *Combinatoire et Représentation du Groupe Symétrique.* Vol. 579 of *Lecture Notes in Math.* Springer–Verlag chapter title 'La correspondance de Robinson', p. 59.

Schwartz, K. 1972. "Optimization of the statistical exchange parameter α for the free atoms H through Nb." *Phys. Rev. B.* 5:2466–2468.

Searle, Barry G. 1988. Calculation of $6j$ Symbols PhD thesis University of Canterbury, New Zealand.

Searle, Barry G. & Philip H. Butler. 1988*a*. "Calculation of primitive 6–j symbols." *J.Phys.A:Math. Gen.* 21:3041–50.

Searle, Barry G. & Philip H. Butler. 1988*b*. "Recursive calculation of transformation factors in terms of primitive factors." *J.Phys A:Math. Gen.* 21:1977–81.

Senechal, Marjorie. 1990. *Crystalline Symmetries: an Informal Mathematical Introduction.* IOP Publishing Ltd.

Shinagawa, K. 1996. Manual calculation of the spin–orbit coupling coefficients of chromium tribromide.

Shinagawa, K., T. Suzuki, T Saito & T. Tsushima. 1995. "Magnetic Kerr effect and charge transfer transitions in ferromagnetic chromium tribromide." *Journal of Magnetism and Magnetic Materials* 140–144:171–172.

Shinagawa, Kiminari, H. Sato, Hughan J. Ross, Luke F. McAven & Philip H. Butler. 1996. "Charge transfer transitions in chromium trihalides." *Journal of Physics: Condensed Matter.* 8(44):8457–8463.

Shinagawa, Kiminari, K. Tamanoi, T. Saito, Y. Aman, K. Sato & T. Tsushima. 1988. "Cotton–Mouton effect of Co^{2+} substituted magnetic garnets." *Journal de Physique* 49(C8 no.12):959–960.

Silver, B. L. 1976. *Irreducible Tensor Methods: An Introduction for Chemists.* New York: Academic Press.

Slater, J. C. 1929. "The theory of complex spectra." *Phys.Rev.* 34:1293–1322.

Slater, J. C. 1951. "Magnetic effects and the Hartree–Fock equation." *Phys. Rev.* 82:538–541.

Slater, J. C. & G. F. Koster. 1954. "Simplified LCAO method for the periodic potential problem." *Phys.Rev.* 94:1498–1524.

Slater, John C. 1979. *The Calculation of Molecular Orbitals.* Wiley–Interscience.

Stancu, Fl. 1996. *Group Theory in Subnuclear Physics.* Number 19 *in* "Oxford Studies in Nuclear Physics" Oxford Science Publications.

Sternberg, S. 1994. *Group Theory and Physics.* Cambridge University Press.

Stewart, James J. P. 1998. "Symmetry groups for unit cells in solids." *Journal of Computational Chemistry* 19(2):168–180.

Sullivan, J. J. 1972. "Permutation symmetry and the N–electron problem." *Physical Review A* 5(1):29–37.

Sullivan, J. J. 1973*a*. "Evaluation of the S_n content of GL(n): $Gl(n) \supset S_n$." Louisiana State University in New Orleans: . preprint.

Sullivan, J. J. 1973*b*. "Nth rank tensor representations of U(n) symmetry adapted to subgroups of the symmetric group S_N." *J.Math.Phys.* 14(3):387–395.

Sullivan, J. J. 1975*a*. "Double coset analysis for symmetry adapting Nth rank tensors of U(n) to its unitary subgroups." *J.Math.Phys.* 16(4):756–760.

Sullivan, J. J. 1975*b*. "Orthonormality properties of double coset matrix elements." *J.Math.Phys.* 16(9):1707–1709.

Sullivan, J. J. 1976. Racah coefficients and the symmetric group. In *International Symposium on Mathematical Physics*. International Symposium on Mathematical Physics Mexico City: pp. 0–14.

Sullivan, J. J. 1978*a*. "On labelling the basis in GL(n) and identifying the Racah algebra with S_N." Louisiana State University in New Orleans: . preprint.

Sullivan, J. J. 1978*b*. "Recoupling coefficients of the general linear group in bases adapted to shell theories." *J.Math.Phys.* 19(8):1681–1687.

Sullivan, J. J. 1978*c*. "Recoupling coefficients of the symmetric group involving outer plethysms." *J.Math.Phys.* 19(8):1674–1680.

Sullivan, J. J. 1980*a*. "Generalized back coupling rules for the Racah algebra of Gl_n." *J.Math.Phys.* 21(2):227–233.

Sullivan, J. J. 1980*b*. "A phase convention for the general Racah algebra of U_n." Louisiana State University in New Orleans: . preprint.

Sullivan, J. J. 1985. "Character constraints on duality." Louisiana State University in New Orleans: . preprint.

Suryanarayana, C. & M. K. Rao. 1982. "A note on the transformation coefficients between the standard and non–standard representations." *J.Phys.A:Math. Gen.* 15:2013–2016.

Tanabe, Y. & S. Sugano. 1954*a*. "??" *J.Phys.Soc.(Japan)* 9:753.

Tanabe, Y. & S. Sugano. 1954*b*. "??" *J.Phys.Soc.(Japan)* 9:766.

Thomas, Glânffrwd P. 1974. Baxter algebras and Schur functions PhD thesis University College of Swansea.

Thomas, Glânffrwd P. 1977. "On a construction of Schützenberger." *Discrete Math.* 17:107–118. Have copy.

Van der Jeugt, J. 1992. "Tensor product of group representations and structural zeros of Racah coefficients." *J.Math.Phys* 33(7):2417–2421.

Vanagas, V. V. 1971. *Algebraic Methods in Nuclear Theory*. Mintis: Vilnius. (in Russian).

Vanden Berghe, G. 1994. "Structural zeros of Racah coefficients and exceptional Lie algebras." *J.Math.Phys.* 35(1):508–516.

Vandermonde, A.-T. 1771. "Mémoire sur la résolution algébrique des équations.".

Weyl, H. 1928. *Gruppentheorie und Quantenmechanik.* Leipzig: Verlag von S. Hirzel.

Weyl, H. 1946. *The Classical Groups: Their Invariants and Representations.* Vol. 1 of *Princeton Mathematical Series* second ed. United States of America: Princeton University Press.

Whitten, Kenneth W., Kenneth D. Gailey & Raymond E. Davis. 1988. *General Chemistry: With Qualitative Analysis.* Saunders College Sunburst Series third ed. United States of America: Saunders College Publishing.

Whittle, Jonathon. 1996. "Investigations with Bipolar Expansions into Delta and Exchange Interactions." University of Canterbury, New Zealand: . Undergraduate project report.

Wigner, E. P. 1959. *Group theory and its application to quantum mechanics of atomic spectra.* London: Academic Press. Translated and modified from the original German, *Gruppentheorie und ihre Andwendung auf die Quantenmechanik der AtomSpektren* Vieweg, Braunschwieg, 1931.

Wigner, Eugene P. 1940. "On the matrices which reduce the Kronecker products of representations of S.R. groups." Published with modifications in Biedenharn & van Dam (1965, pp. 87–133).

Wu, Wei & Qian-Er Zhang. 1992. "An efficient algorithm for evaluating the standard Young–Yamanouchi orthogonal representation with two–column Young tableaux for symmetric groups." *J.Phys.A:Math. Gen.* 25:3737–3747.

Wu, Wei & Qian-Er Zhang. 1994. "The orthogonal and the natural representation for symmetrical groups." *Int. J. Quantum Chem.* 50:55.

Wybourne, Brian G. 1970. *Symmetry Principles and Atomic Spectroscopy: with an appendix of tables by P. H. Butler.* United States of America: Wiley–Interscience. Translated into Russian by V.V.Tolmachev, Moscow(1973).

Wybourne, Brian G. 1974. *Classical Groups for Physicists.* United States of America: John Wiley and Sons.

Yamanouchi. 1937. "??" *Proc.Phys.–Math. Soc. Jpn.* 18:623.

Young, Alfred. 1977. *The Collected Papers of Alfred Young.* University of Toronto Press.

Zhang, Qian-Er & Xiangzhu Li. 1986. "Double coset for symmetry orbitals." *Int.J.Quant.Chem.* 29:293–303.